RESISTANCE NETWORKS AS A MODEL FOR CONDUCTION ON THE NANO-SCALE

A THESIS IN
Physics

Presented to the Faculty of the University
of Missouri-Kansas City in partial fulfillment of
the requirements for the degree

MASTER OF SCIENCE

by
BENJAMIN ASHLEY WALKER

B.S. Computer Science, University of Missouri-Kansas City, 2004
Kansas City, Missouri

Kansas City, Missouri
2011

RESISTANCE NETWORKS AS A MODEL FOR CONDUCTION

ON THE NANO-SCALE

Ben Walker, Candidate for the Master of Science Degree

University of Missouri-Kansas City, 2010

ABSTRACT

In this thesis, we calculate transport properties of amorphous materials in one, two, and three dimensions. We take into account site disorder, manifest as a random variation of the locations of atomic species. We employ a resistor network model as a theoretical framework for calculating transport characteristics.

The numerical calculations we employ are based on an iterative algorithm used as an improvement over the direct solution of the relevant linear systems. The Monte Carlo calculations are used to validate analytical perturbative treatment valid in the bulk limit.

In approaching random resistor networks, we discuss and apply a paradigm based on the connectivity of nodes instead of mesh currents where the applicability is limited to a specific set of geometries. We argue that this perspective is very useful in strongly disordered systems, especially for three-dimensional cases.

APPROVAL PAGE

The faculty listed below, appointed by the Dean of the College of Arts and Sciences, have examined a thesis titled, "Resistance Networks as a Model for Conduction on the Nano-Scale", presented by Benjamin Ashley Walker, candidate for the Master of Science degree, and certify that in their opinion it is worthy of acceptance.

Supervisory Committee

Donald Priour, Ph.D., Committee Chair
Department of Physics

Anthony Caruso, Ph.D.
Department of Physics

Wai-Yim Ching, Ph.D.
Department of Physics

CONTENTS

ILLUSTRATIONS

TABLES

Tables Page

CHAPTER 1

INTRODUCTION

"…Into a thousand parts divide one man and make imaginary puissance; Think when we talk of horses, that you see them printing their proud hoofs I' the receiving earth; For 'tis your thoughts that now must deck our kings, carry them here and there; jumping o'er times, turning the accomplishments of many years into an hour glass…"
-William Shakespeare, King Henry V

1.1: Preliminary Remarks

The great bard of England has suggested that the use of a compact cast of actors on a narrow stage faces a daunting task if the canvas is as broad as the epic conflict between two nations. Similarly, theoretical physics finds no mean challenge in giving a cogent description of systems as intricate and diverse as the materials one examines in condensed matter physics. Single atoms are finite, and have energy levels and other physical characteristics that emerge, with some assistance from modern computational devices from a solution of the Schrödinger equation.

Nevertheless, when a hoste of more than a few hundred atoms are joined together, nontrivial properties may emerge which are not seen in the individual atomic components. As an example, carbon is a relatively simple atom, and the six electrons determine its chemical characteristics that each single carbon atom possesses. Moreover, among the six electrons which are bound to each carbon species, two are even more tightly bound, and the 1s core electrons are involved to only a limited extend in chemical processes.

Hence, one might say that to a great extent the chemistry of carbon is determined by but four electrons. Certainly, one is aware that the properties of carbon-based compounds are as complex as they are diverse. Even elemental carbon exists in allotropic forms with characteristics so distinct from one another as to seem to be different materials altogether. Diamond and graphite are two salient examples, and even at a superifical level significant contrasts are evident.

Diamond is among the hardest materials known, due in large measure to the fact that a single crystal, easily visible to the human eye, may be viewed as a giant macroscopic carbon molecule held tightly together by covalent bonds among the atomic species. Diamond, though resplendently transparent to radiation in the optical range, does not permit an electrical current to flow in the absence of dopants due to a large band gap.

On the other hand, graphite is a very soft material, quite opaque in the bulk, and may be regarded as made up of individual monolayers loosely held together by Van der Waals interactions, and in the modern laboratory easily dislodged. The individual layers, made up of carbon atoms arranged in a two-dimensional honeycomb lattice, are as mechanically robust as bulk graphite is soft, and are under consideration for use as semiconductor substrates that ultimately may supplant silicon. Just as individually simple species such as carbon may join together and exhibit much richer behavior, theoretical constructs also may have simple characteristics when broken down to individual components while more complicated characteristics emerge on a larger scale.

Resistor networks are such an example. Simple networks consisting of a handful of resistive elements are often relegated to their native habitat, the second semeseter of a

first year college physics course. The arrangements most often considered in the undergraduate classroom are resistor networks assembled in two-dimensional geometries. Often, such configurations are comprised of one or more square loops, where the resistors double as line segments defining the square networks. However, in more complicated situations such as those that we examine, nontrivial characteristics emerge not seen in simple networks on a small scale. For very large random resistor networks where there us a broad stochastic variation in the resistive elements comprising the network, the transport characteristics may be governed by the traits of a phase transition known as a percolation transition. In such strongly disorderd systems, the current follows an irregular and convoluted path, much as a bolt of lightning picks a haphazardly jagged course across the sky.

1.1.1: the Use of Mesh Currents in the Simple Case

In simple two-dimensional geometries, the resistor networks may be presented in conjunction with two rules. The first, which we'll revisit in multiple ways and from multiple perspectives in this dissertation, is an expression of local charge conservation often called Kirchhoff's First Rule in the contrext of electrical circuit problems. Conceptually, the charge conservation constraint, expressed at a node on junction in a circuit, is easy to grasp intuitively. If at any point, there is a current imbalance, charge will accumulate and ultimately will counteract the imbalance. This characteristic is a direct consequence of local charge conservation.

Hence, at steady state, there are two conditions that cannot under any circumstances hold. First, there may not be an indefinite influx of current into a node in a circuit. Second, it is not possible to have a net flow of current out of an individual site.

Instead, the total of the currents entering and departing must be zero, so that a steady state accumulation on depletion of charge does not occur. This precept is also known as Kirchhoff's First Rule in discussions of circuit analysis [1]. The very name "circuits" suggests the form of Kirchhoff's Second Rule, which sometimes is also called the "Loop Rule" [1].

The loop rule, as the name implies, is most readily brought to bear in situations for which the network geometry is easily decomposed into discrete loops. The loop rule exploits the fact that an electrostatic potential is a conservative field, so the net changes in the potential as one moves about the loop (except in the case that a voltage source such as a battery is incorporated in the loop) will vanish. A mesh current formalism is compatible with the loop rule, and the analysis of a circuit in terms of mesh currents affords an elegant and efficient solution in cases where the lattice is conveniently decomposed into individual loops. The square lattice with connections only among nearest neighbors is a canonical example of a situation where one profits by operating in terms of mesh currents.

1.1.2: Situations that are not Amenable to Mesh Current Analysys

Although the decomposition of currents in a network into circulating loops of current provides a succinct solution when mesh current analysis is a viable technique, there are many situations in which the network isnot readily broken apart into discrete loops. In such a circumstance, the mesh current paradigm would be difficult to bring to bear.

One situation that certainly may frustrate the decomposition into loops would be the case, even in two dimensions, where nodes in a resistor network are connected to

many other sites with conductive links. An extreme case would be a scenario where in a large square lattice, each site is joined to every other site with a resistor spanning the distance between sites. Certainly, there would in such a situation be a maddening array of wire radiating in countless directions, and the prospect of analyzing the circuit characteristics in terms of individual loops would be a daunting one indeed.

Nevertheless, even a much simpler connectivity scheme where sites in a square lattice are connected to the four nearest neighbors as well as the four next-nearest neighbors would frustrate an analysis in terms of mesh currents. A fundamental difficulty associated with analysis involving loops is the fact that loops are nonlocal, and are difficult to describe in a compact way in a general lattice geometry.

1.1.3: The Node Connectivity Paradigm

Whereas there are many situations in which visualizing a lattice in terms of constituent loops is a difficult task, the node-connectivity scheme is easy to implement, because one need only understand the local characteristics of a node. By "local characteristics", we mean the list of all neighbors a site is linked to as well as the resistances of the wires that join the site under consideration to the neighboring nodes. If the local structure of each site is recorded in this fashion, all of the transport characteristics may be described in terms of this connectivity pattern. This holds true whether sites are connected only to nearest neighbors, or in an extended scheme in which a node in the resistor network is connected to many other nodes much farther away than the small cluster of nearest neighbors.

As we consider in this dissertation, the node-connectivity picture may be used in a variety of ways to calculate all observables of interest for a specific resistor network,

regardless of its intricacy. As we will see, there are three fundamental ingredients needed to approach an arbitrary network and understand its charateristics with regard to charge transport.

I. The node connectivity scheme is specified for each site in the lattice

II. Ohm's Law is utilized. Consider two nodes i and j where the site potentials are, respectively, V_i and V_j. If the resistor connecting i and j has a value R_{ij}, then the current which is set up between the two sites is given by

$$I_{ij} = \frac{\Delta V_i - \Delta V_j}{R_{ij}}$$

III. The centerpiece of the node-connectivity perspective, and what transforms it into a technique for quantitative calculations is the local charge conservation constraint, where we insist for a given site that no net current either depart from or enter the node under consideration.

Amorphous materials present many interesting challenges in materials science. To model how charge propagates through an amorphous material, it's advantageous to use a network of randomly-placed resistors. For the 2D case, calculating the amount of current flowing through each resistor can be done numerically using linear solvers. However, the 3D case is far less trivial. Specifically, an iterative solution can be achieved by the temporary violation and ultimate restoration of Kirchoff's Laws of current conservation. This process is an algorithm that leads to a successively improved result for the node potential. The refinement is achieved in a steady fashion, as each site is visited in succession to cancel currents departing from or entering the node. Proceeding in this fashion is analogous to attempting to remove a ripple in a carpet by stepping on it. However, in our case, the process is sound because the "ripple"

systematically becomes smaller, diminishing exponentially with the nuymber of "stomps". It is also possible to construct a system of sparse linear equations that can be solved efficiently using what's called the conjugate-gradient algorithm.

1.1 The Node-Conductivity Method

A simple manifestation of the Node-Conductivity Picture is the Wheatstone bridge. The following configuration of resistors is taken into consideration:

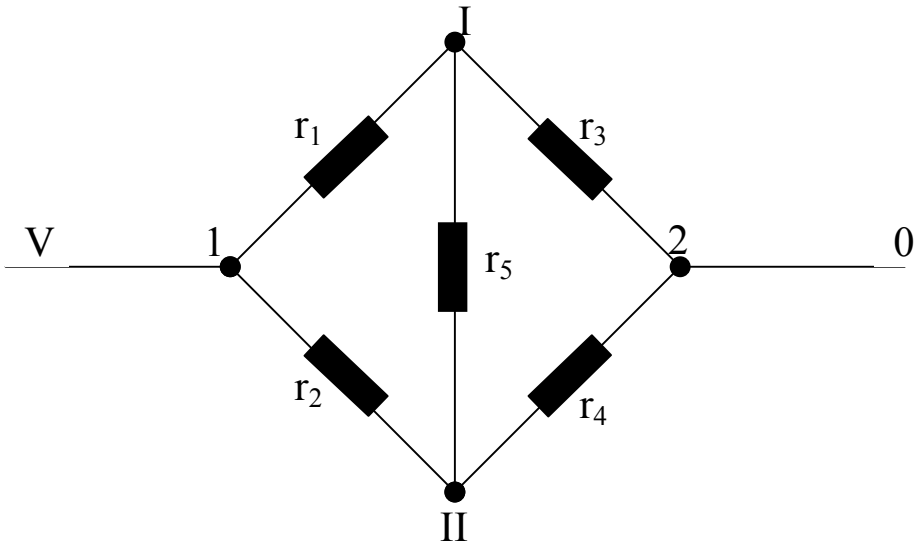

Figure 1: Wheatstone Bridge Configuration

The voltage across nodes I and II is unknown. The first step in the procedure is to calculate the currents that locally satisfy Ohm's Law, with the initial condition

$$V_I = V_{II} = 0$$

The system will have the following configuration:

$$V_1 = V$$
$$V_2 = 0$$
$$V_I^0 = V_{II}^0 = 0$$
$$i_{II}^I = i_0^I = i_0^{II} = 0$$

Initially, nonzero currents are only present on the links between nodes 1 and I and 1 and II. Ohm's Law is used to determine these currents.

$$i_{1I}^{0} = \frac{V}{r_1}$$
$$i_{1II}^{0} = \frac{V}{r_2}$$

Current conservation must be enforced. To achieve this, voltage shifts at nodes I and II will be introduced. These voltages are ΔV^I and ΔV^{II}. Of course, current in the first node must be conserved. Consequently, the charge flux into the first node is

$$i_{1II}^{0} + i_{II,I}^{0} + i_{2I}^{0} = \frac{V}{r_1}$$

and the flux out of I is initially zero. However, this local charge non-conservation may be remedied by activating ΔV^I in this context. Therefore, the charge flux out will be of the form

$$\Phi^{out} = \frac{\Delta V^I}{r_1} + \frac{(\Delta V^I - \Delta V^{II})}{r_5} + \frac{\Delta V^I}{r_3}$$

$$= \Delta V^I \left[\frac{1}{r_1} + \frac{1}{r_5} + \frac{1}{r_3} \right] - \frac{\Delta V^{II}}{r_5}.$$

Equating the two equations, we find

$$\Phi^{out} = \Phi^{in} = \Delta V^I \left[\frac{1}{r_1} + \frac{1}{r_5} + \frac{1}{r_3} \right] - \Delta V^{II} \left[\frac{1}{r_5} \right] = \frac{V}{r_1}$$

Similarly, we examine the second node, node II.

$$\Phi^{in} = \frac{V}{r_2}$$

Activating ΔV^{II} leads to an expression of the form

$$\Phi^{out} = \Phi^{in} = \frac{V}{r_2} = \Delta V^{II}\left[\frac{1}{r_2} + \frac{1}{r_5} + \frac{1}{r_4}\right] - \frac{\Delta V^{I}}{r_5},$$

thereby giving us a system of equations to be solved for V^I and V^{II}. Though tedious, this system will solve them in full generality without a great deal of effort. Furthermore, one finds the following:

$$\Delta V^{I}\left[r_5 r_3 + r_1 r_5 + r_1 r_3\right] - \Delta V^{II}\left(r_1 r_3\right) = V\left(r_3 r_5\right)$$
$$\Delta V^{II}\left[r_5 r_4 + r_2 r_5 + r_2 r_4\right] - \Delta V^{I}\left(r_2 r_4\right) = V\left(r_4 r_5\right)$$

Having each resistor be identical forms the simple case. This leads to the following:

$$3r^2\Delta V^{I} - \Delta V^{II} r^2 = Vr^2 \Rightarrow 3\Delta V^{I} - \Delta V^{II} = V$$
$$3r^2\Delta V^{II} - \Delta V^{I} r^2 = Vr^2 \Rightarrow 3\Delta V^{II} - \Delta V^{I} = V$$
$$\therefore \left(3\Delta V^{I} - \Delta V^{II}\right) + 3\left(3\Delta V^{II} - \Delta V^{I}\right) = V + 3V = 4V \cdot$$
$$= 8\Delta V^{II} = 4V \Rightarrow \Delta V^{II} = \frac{V}{2}$$

Similarly,

$$3\Delta V^{I} = V + \frac{V}{2} = \frac{3V}{2} \Rightarrow \Delta V^{I} = \frac{V}{2}$$

This symmetry is significant.

This encapsulates the analytical scheme that yields the set of linear equations, which in turn determine the value of the voltage shifts. From this, the overall conductance and resistance of the system can be calculated. However, it becomes quite inconvenient to solve large sets of linear equations; it's computationally expensive. It becomes imperative to develop an iterative technique. In this case, only the lattice connectivity need be known.

In this dissertation we will use iterative algorithms in conjunction with the current conservation condition. On the one hand, we will use computer simulations to calculate the currents and node voltages in large-scale random resistor networks. On the other hand, we also will use the same fundamental ideas to carry out analytical calculations in closed form, which we validate with the numerical simulations.

1.2: Comments as to Structuring of the Thesis

In this dissertation, we consider a sequence of topics designed to successively improve our understanding of resistor networks and the condensed matter systems they are at times used to represent. We will see that the charge conservation condition is not merely a physical constraint, but a point of departure for a variety of methods for obtaining physical observables in a quantitative fashion.

In Chapter 2, we develop the node-connectivity perspective by examining finite sized simple examples. In the course of our study of a few small resistor networks, the technique for relating the potential at a given node to those of the neighboring nodes is refined, polished, and articulated in a concise and succinct manner, leading to a compact expression based on charge conservation and the node connectivity point of view.

In Chapter 3, we introduce the Fourier variables that are imployed elsewhere in the dissertation to useful effect to obtain closed form expressions for transport characteristics of random resistor networks. Our principal aim for Chapter 3, however, is to consider current injection scenarios and to show that there are theoretical intricacies of the current injection scenario that limit its utility as an analytical technique.

In Chapter 4, we describe and apply an iterative numerical technique for calculating transport characteristics. The charge conservation condition and the node-

connectivity point of view are at the heart of the iterative scenario. We consider an instance of bond disorder, finding the bulk conductivity to be robust with respect to the introduction of mild, and even moderate, disorder.

In Chapter 5, we examine lattices with a variety of geometries and hopping schemes in the variable range hopping picture. Although the calculations make no attempt to take into account disordering influences, we later see through explicit calculation that many systems are robust with respect to mild disorder.

In Chapter 6, we use a one-dimensional system with nearest neighbor connectivity as a prototype for the development of an analytical technique for calculating the bulk conductivity that we subsequently apply to systems in two and three dimensions. We validate the method in the one-dimensional case where simply summing resistances provides an independent way to check the extent to which the iterative technique is yielding the correct results order by order in the perturbing influence. We also review the machinery used to construct Padé approximants. The latter are used in this thesis to extend the validity of a perturbative series beyond the regime where it normally would be applicable.

In Chapter 6, we use in a broad sense the analytical formalism validated in the one-dimensional case, but we consider bond disordered two-dimensional systems. We pursue the calculation of the perturbative series to third order, and we evaluate the results by comparison with conductivity data gleaned from direct numerical simulation. Also in the context of the numerical calculations, we examine the extent to which strong disorder may mimic the characteristics of critical behavior in the vicinity of a percolation transition. In particular, we consider the degree to which the computational cost of the

calculation may be used as a gauge of the closeness of a resistor network to critical behavior at the percolation phase transition.

In Chapter 8, we extend the analytical perturbative treatment to three-dimensional bond disordered systems. As square symmetry proves useful in the theoretical calculations in the two-dimensional context, we find that cubic symmetry may be systematically exploited for the calculation in three dimensions to obtain the conductance to third order in the perturbing influence responsible for random disorder.

Additionally, the calculations in Chapter 8 are extended to a three-dimensional case representing variable range hopping in the absence of chemical disorder, but with positional disorder taken into account.

CHAPTER 2

AN APPLICATION OF CHARGE CONSERVATION AND NODE CONNECTIVITY

2.1: Preliminary Comments Regarding Conservation Rules

We'll now consider more complicated resistor networks and we will give attention to specific examples.

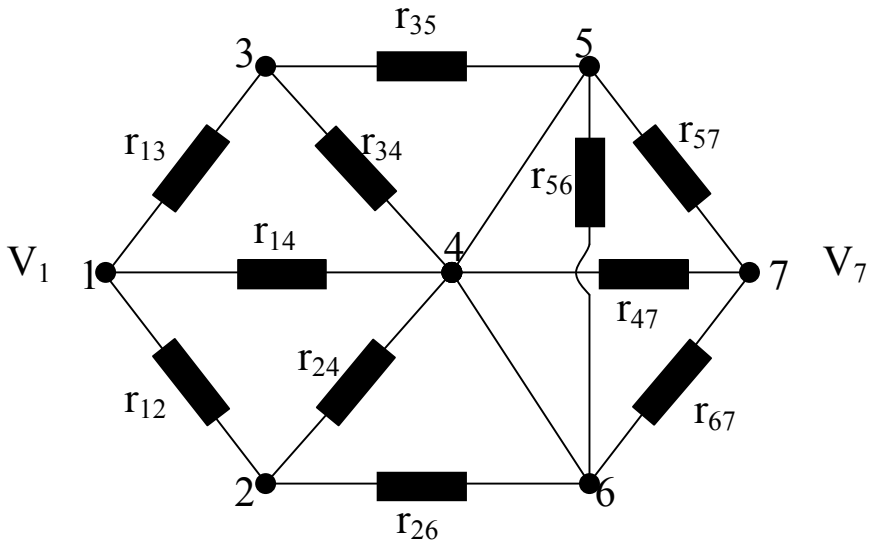

Figure 2: A random network of resistances with an irregular connectivity pattern for the nodes

Here, it's advantageous to work in terms of the connectivity scheme, rather than dealing with mesh currents. This logic will carry through to the three dimensional case, where application of the mesh current method is difficult or impossible.

Figure 2 shows 7 nodes that are connected to each other. A voltage V is applied at node 1; let the voltage at node 7 be zero $(V_7 = 0)$. The potential at the remaining five nodes $\{V_2, V_3, V_4, V_5, V_6\}$ is unknown, but can be determined using the iterative scheme.

The connectivity of each node in the lattice must be taken into consideration, as current flow greatly depends on this as current flows through the system. Node 1 is

connected by resistors $\{r_{13}, r_{14}, r_{12}\}$ to nodes 2, 3, and 4. We first set the potential at the undetermined nodes (2 through 6) to zero. The currents are simply determined by Ohm's Law, but current conservation is not yet satisfied. This requires the voltage at each undetermined node be adjusted until local charge conservation isn't violated. Each time the nodes are visited, the required voltage change decreases, hence the iterative nature of this approach. Each sweep through the lattice repairs errors from the previous iteration, but will introduce inaccuracies as well.

2.2: Concrete Examples of Simple Resistor Networks

Let's first consider a simple square lattice as shown below:

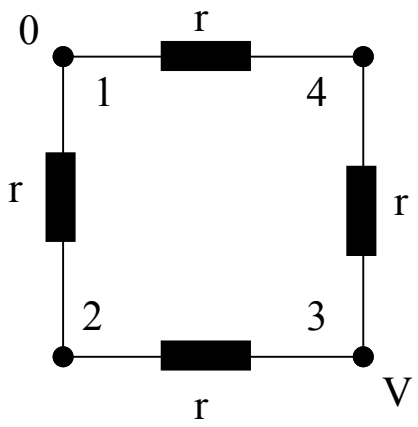

Figure 3: A simple square resistor array

Initially, a voltage V is activated at node 3, while the voltages at nodes 1, 2, and 4 are zero. Although zero initially, the voltages at nodes 1, 2, and 4 will shift later.

Now the iterations will be performed. We see that current will accumulate at node 2; this current flows from node 3, and has a value of $\frac{V_3 - V_2}{r} = \frac{V}{r}$. On the other hand, $\frac{V_2 - V_1}{r} = 0$, and there is no current flowing from node 2, which violates current

conservation. The potential at node 2 needs to be adjusted to compensate for this. This results in the activation of a voltage ΔV_2.

The current flowing into node 2 will be $\frac{V}{r}$, and the current flowing out to nodes 2 and 3 will be $\frac{\Delta V_2}{r}$. For node 2, this will partially cancel the current entering from node 3. The charge flux is equalized by choosing ΔV_2 such that

$$\frac{V}{r} = \frac{\Delta V_2}{r} + \frac{\Delta V_2}{r} = \frac{2\Delta V_2}{r}$$
$$\Delta V_2 = \frac{V}{r}$$

where $\frac{V}{r}$ is the flux entering and $\frac{\Delta V_2}{r} + \frac{\Delta V_2}{r}$ is the flux departing. Similarly, we'll consider node 4.

If a voltage $\Delta V_4 = \frac{V}{2}$ is activated, the charge flux imbalance will be corrected. In this unique example, the first sweep solved the problem, so additional iterations aren't needed.

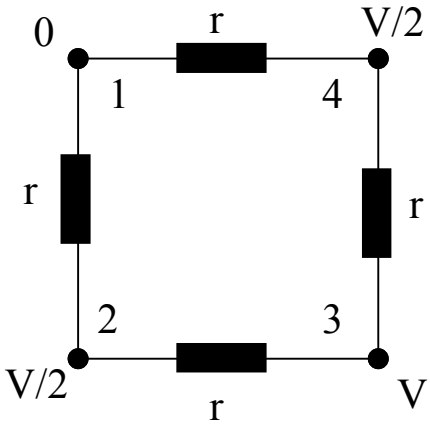

Figure 4: a four-node square resistor array with a potential difference imposed across the diagonal

The current flowing from node 3 to nodes 4 and 2 is $\frac{V}{r}$, therefore the resistance of a square with voltages applied to diagonally opposite node is simply r, which follows from Ohm's Law ($V = IR$).

We'll now consider a more streamlined approach: operating in terms of imposed voltages. This will lead us to the conclusion that we've been dealing with discretized versions of Laplace's Equation. Previously, the calculations had been done in terms of currents; we can now dispense with the intermediate calculation of currents that are set up by boundary voltage. We may use the iterative technique developed previously, or we may set up a set of linear equations that can be solved using Gaussian elimination, as well as with a method known as the conjugate gradient algorithm for sparse systems. First, we'll develop the formal equations and find the solution for a few special cases. Next, the iterative technique will be examined.

As always, charge conservation must be satisfied. We'll consider a set of nodes i where the total number of nodes is equal to n. The following are examples:

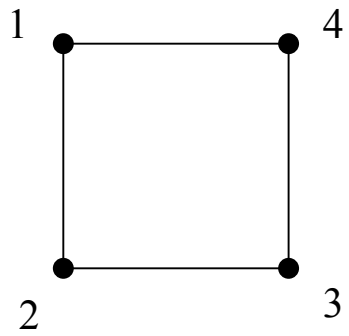

Figure 5: A simple resistor network with four nodes and four links

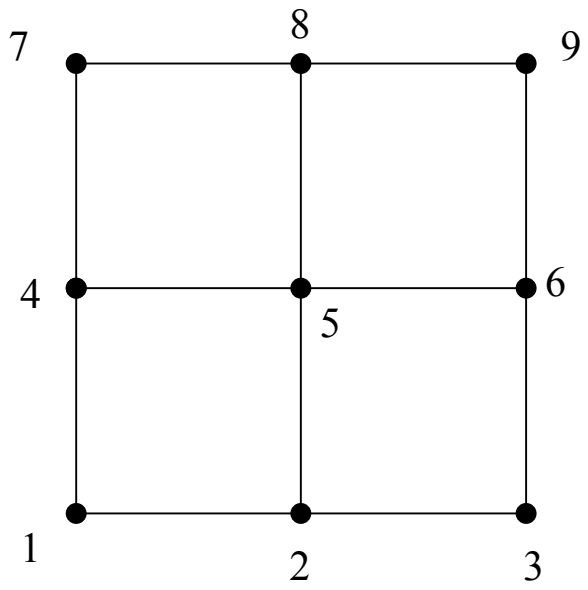

Figure 6: A 3x3 square network with nearest neighbor connections only

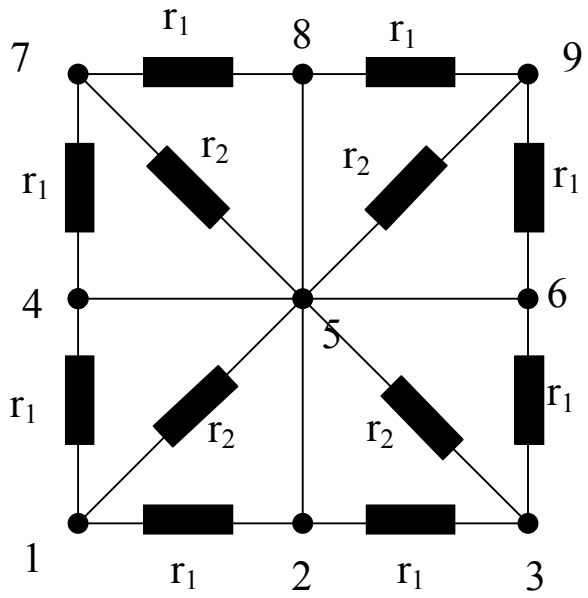

Figure 7: A 3x3 square network with connections extended to next-nearest neighbors

The number of nodes is the same in the last two figures ($n = 9$), but the connectivity schemes of the two figures are quite different.

2.3: The Charge Conservation Condition in the General Case

Some nodes ($V_{j1}, V_{j2}, ...V_{jm}$) have present potentials that cannot be changed, but we are able to change the potentials on the remaining nodes. This is done in such a way so as to enforce current conservation at each node. Once again, we must insist on the condition $\Phi_{in} = \Phi_{out}$. Each of these are calculated in terms of the voltages of node i and the surrounding nodes k to which it is connected. Displayed in **Figure 8** are six such nodes.

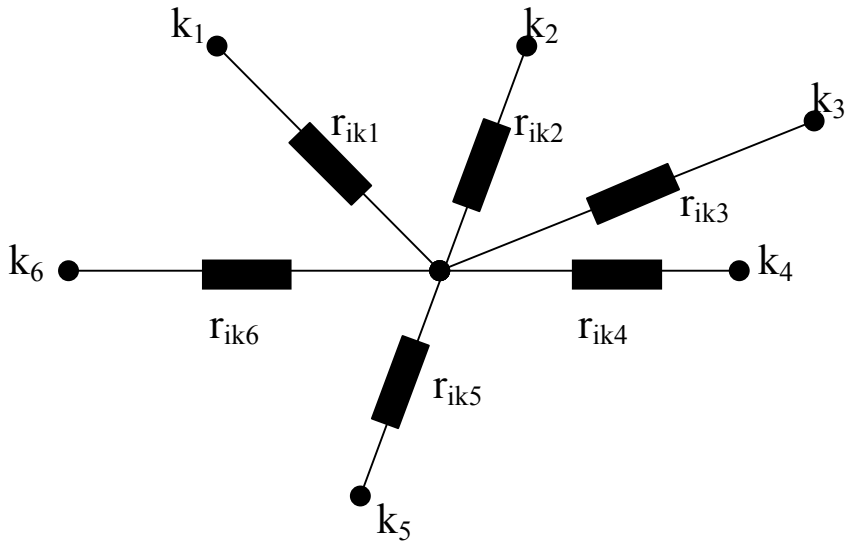

Figure 8: A single node with an intricate connectivity pattern

Now we'll determine the relationship between V_i and $\{V_{k_1}, V_{k_2}, V_{k_3}, V_{k_4}, V_{k_5}, V_{k_6}\}$.

The net current will therefore be

$$\left[\frac{(V_i - V_{k_1})}{r_{ik_1}} + \frac{(V_i - V_{k_2})}{r_{ik_2}} + \frac{(V_i - V_{k_3})}{r_{ik_3}} + \frac{(V_i - V_{k_4})}{r_{ik_4}} + \frac{(V_i - V_{k_5})}{r_{ik_5}} + \frac{(V_i - V_{k_6})}{r_{ik_6}}\right].$$

This quantity must vanish, such that

$$0 = (V_i)\left[\frac{1}{r_{ik_1}} + \frac{1}{r_{ik_2}} + \frac{1}{r_{ik_3}} + \frac{1}{r_{ik_4}} + \frac{1}{r_{ik_5}} + \frac{1}{r_{ik_6}}\right] - \left[\frac{V_{k_1}}{r_{ik_1}} + \frac{V_{k_2}}{r_{ik_2}} + \frac{V_{k_3}}{r_{ik_3}} + \frac{V_{k_4}}{r_{ik_4}} + \frac{V_{k_5}}{r_{ik_5}} + \frac{V_{k_6}}{r_{ik_6}}\right]$$

$$V_i \sum_{l=1}^{6}\left[\frac{1}{r_{ik_l}}\right] = \sum_{l=1}^{6}\frac{V_{k_l}}{r_{ik}},$$

which yields

$$V_i = \frac{\sum_{l=1}^{6}\frac{V_{k_l}}{r_{ik_l}}}{\sum_{l=1}^{6}\frac{1}{r_{ik_l}}}.$$

The system of equations for the voltages at the nodes is constructed in this way. This is a more streamlined approach because the intermediate current calculation can be avoided.

2.4: Concrete Examples Examined in Terms of the Streamlined Formalism

2.4.1: Two Simple Cases

Now let us solve the equations for two special cases.

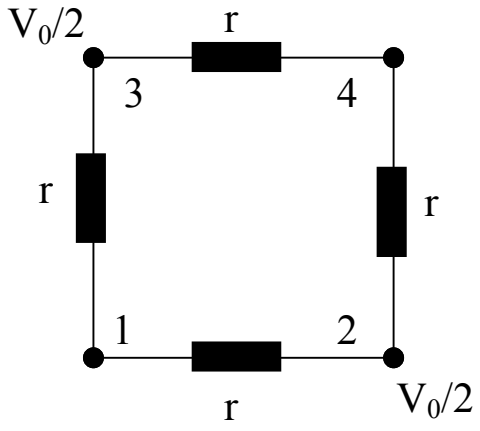

Figure 9: A 2x2 network biased along the digaonal

We'll consider the square arrangement in **Figure 9** with a voltage $\frac{V_0}{2}$ applied to node 3, and a voltage $\frac{-V_0}{2}$ applied to node 2. At node 4 the current is

$$V_4\left(\frac{1}{r}+\frac{1}{r}\right)=\frac{V_0}{2}\left(\frac{1}{r}\right)-\frac{V_0}{2}\left(\frac{1}{r}\right)=0$$

so that $V_4=0$. Similarly,

$$V_1\left(\frac{1}{r}+\frac{1}{r}\right)=\frac{V_0}{r}\left(\frac{1}{r}\right)-\frac{V_0}{2}\left(\frac{1}{r}\right)=0$$

so that $V_1=0$.

A similar approach can be used for a more complicated situation.

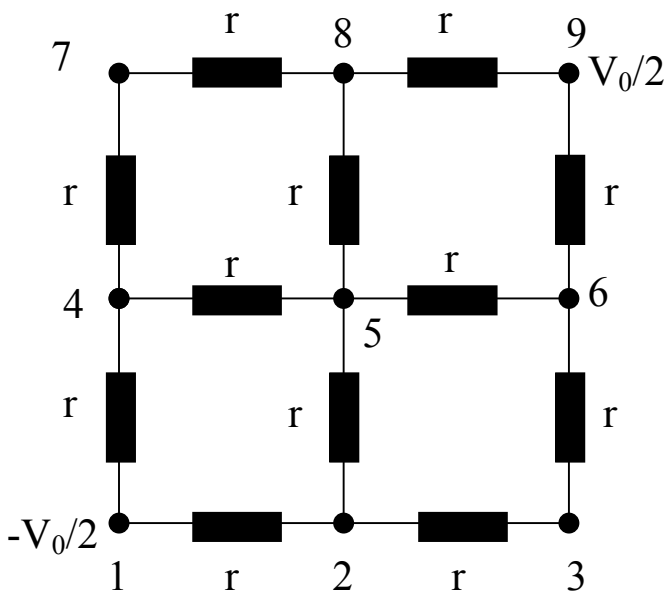

Figure 10: A diagonally biased 3x3 resistor network

A voltage V_0 is applied across the entire grid. To emphasize symmetry, we choose $\frac{V_0}{2}$ and $\frac{-V_0}{2}$ at the contacts since the voltage is known up to a constant. Now set up the potentials for the remaining nodes. At node 2, we see that

$$V_2\left[\frac{1}{r}+\frac{1}{r}+\frac{1}{r}\right]=\frac{V_1}{r}+\frac{V_5}{r}+\frac{V_3}{r}$$
$$3V_2=V_1+V_5+V_3$$
$$V_2=\frac{1}{3}\left[V_3+V_5-\frac{V_0}{2}\right]$$

For node 3, we find that

$$V_3\left[\frac{1}{r}+\frac{1}{r}\right]=\frac{V_2}{r}+\frac{V_6}{r}=\frac{1}{2}\left[V_2+V_6\right]$$

For node 4, the corresponding expression is the following:

$$V_4=\frac{1}{3}\left[V_7+V_5+V_1\right]=\frac{1}{3}\left[V_7+V_5-\frac{V_0}{2}\right]$$

For node 5, the expression is the following:

$$V_5=\frac{1}{4}\left[V_2+V_4+V_6+V_8\right]$$

For node 6, the expression is the following:

$$V_6=\frac{1}{3}\left[V_3+V_5+V_9\right]=\frac{1}{3}\left[V_3+V_5+\frac{V_0}{2}\right]$$

Likewise, for nodes 7 and 8 we have the following expressions:

$$V_7=\frac{1}{2}\left[V_4+V_8\right]$$
$$V_8=\frac{1}{3}\left[V_7+V_5+V_9\right]=\frac{1}{3}\left[V_7+V_5+\frac{V_0}{2}\right]$$

Using symmetry, we can make simplifications. We know that $V_7=V_3$, $V_6=V_8$, and $V_2=V_4$. This leads to the following substitutions:

$$V_2=\frac{1}{3}\left[V_3+V_5-\frac{V_0}{2}\right]$$

$$V_3=\frac{1}{2}\left[V_2+V_6\right]$$

$$V_6 = \frac{1}{3}\left[V_3 + V_5 + \frac{V_0}{2}\right]$$

$$V_5 = \frac{1}{4}\left[V_2 + V_4 + V_6 + V_9\right] = \frac{1}{2}\left[V_2 + V_6\right]$$

We now have four equations and four unknowns, as opposed to the previous situation in which we had seven equations and seven unknowns. Furthermore, we know that the diagonal spanning nodes 1 and 9 is a nodal line. This means that $V_7 = V_5 = V_3 = 0$. Therefore, we know that

$$V_2 = \frac{-1}{3}\left(\frac{V_0}{2}\right) = \frac{-V_0}{6}$$

$$V_6 = \frac{V_0}{6}$$

Now all the potential values are known. The figure is therefore redrawn with the voltages indicated in the appropriate locations.

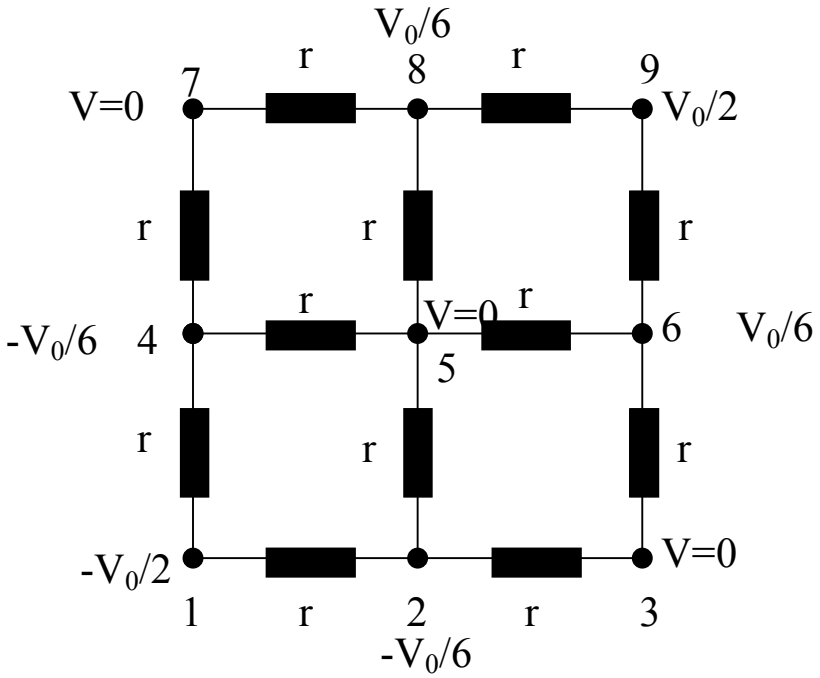

Figure 11: A diagonally biased 3x3 resistor network with node voltages indicated

The equivalent resistance needs to be determined. We begin to do this by calculating the current flowing into node 1 and emerging from node 9. The current flowing from node 1 to node 2 is $\left(\frac{-V_0}{6}+\frac{V_0}{2}\right)\frac{1}{r}=\frac{V_0}{3r}$. Similarly, the current that flows from node 1 to node 4 is $\frac{V_0}{3r}$. The total current is $I_{total}=\frac{2V_0}{3r}$, so the equivalent resistance is

$$R_{eq}=\left(\frac{I_{total}}{\Delta V}\right)^{-1}=\left[\frac{\left(\frac{2V_0}{3r}\right)}{V_0}\right]^{-1}=\frac{3}{2}r$$

2.4.2: A Sixteen Node Lattice with a Diagonal Potential Bias

To conclude to two-dimensional case we can examine an even larger mesh, where Kirchoff's law and symmetry arguments can once again be employed to calculate voltages at each node.

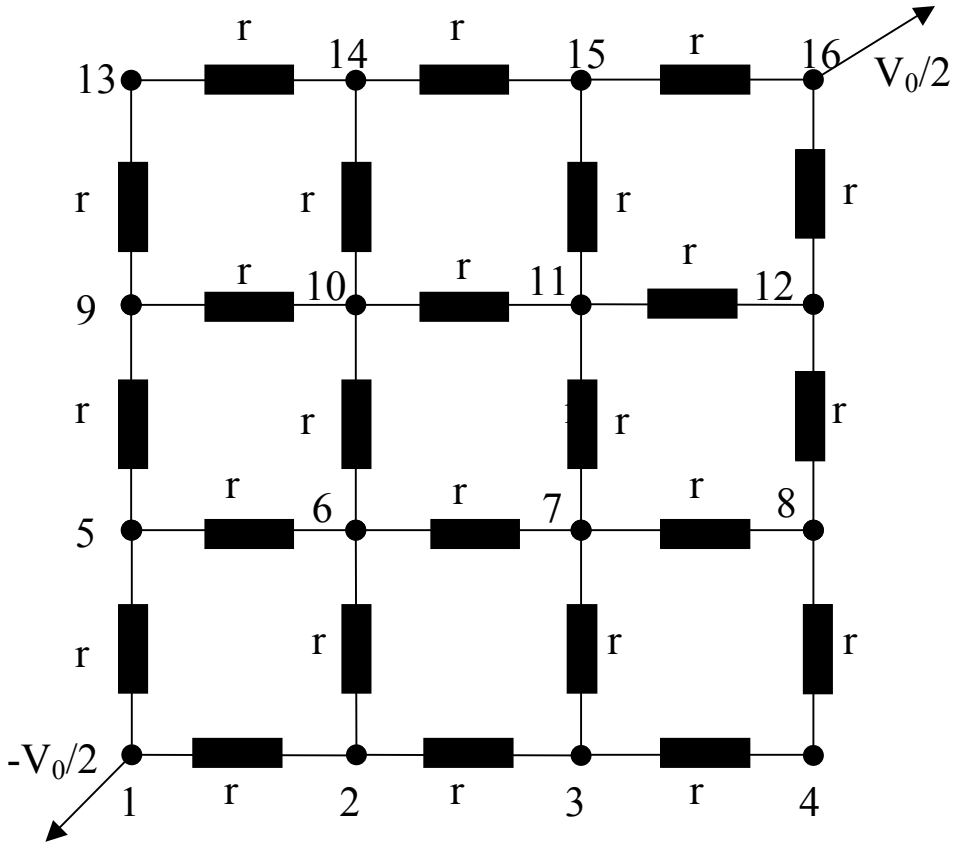

Figure 12: A 4x4 resistor network

There are sixteen nodes in this mesh, but symmetry properties can greatly simplify the calculation. Firstly, we can see that $V_1 = V_{16} = \frac{-V_0}{2}$. From symmetry, we also know that $V_5 = V_2$, $V_9 = V_3$, $V_{13} = V_4$, $V_{14} = V_8$, and $V_{15} = V_{12}$. Just as in the previous example, a diagonal nodal line spans nodes 4, 7, 10, and 13. This means that $V_4 = V_7 = V_{10} = V_{13} = 0$. The modified figure is shown below:

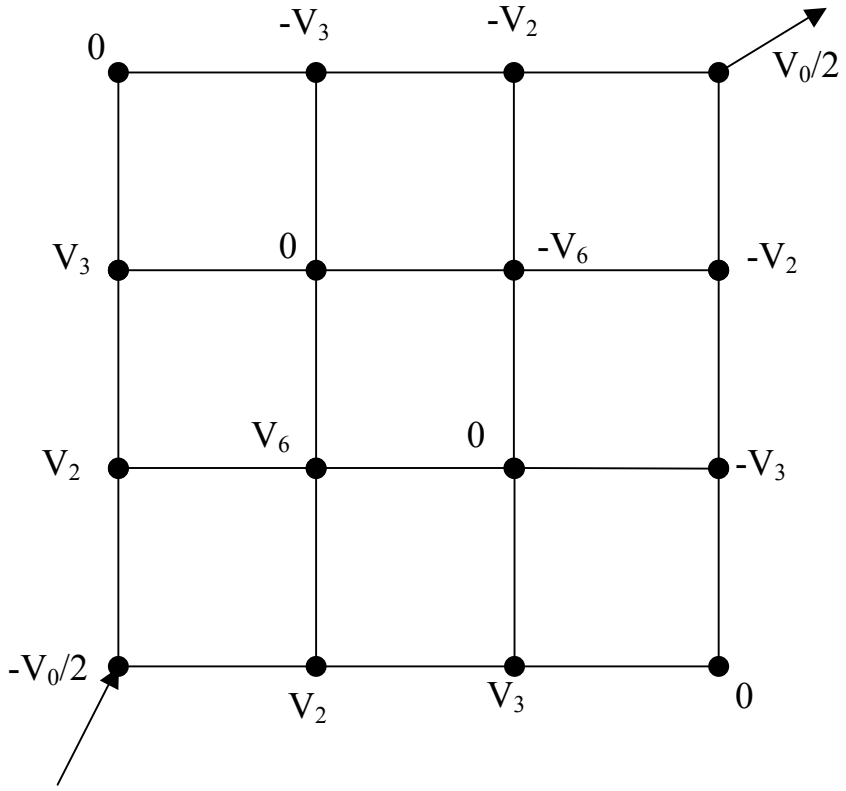

Figure 13: A 4x4 resistor network with diagonal antisymmetry and bilateral symmetry constraints implemented

Across the nodal line we know that $V_3 = -V_8$, $V_6 = -V_{11}$, $V_9 = -V_{14}$, $V_2 = -V_8$, and $V_5 = -V_{15}$. This leaves V_2, V_3, and V_6 to calculate using symmetry properties.

$$V_6 = \frac{1}{2}V_2$$
$$V_3 = \frac{V_2}{3}$$
$$V_2 = \frac{1}{3}\left[V_6 + V_3 - \frac{V_0}{2}\right]$$

Via substitution, we see that

$$V_2 = \frac{1}{3}\left[\frac{V_2}{2} + \frac{V_2}{3} - \frac{V_0}{2}\right]$$
$$\frac{13}{6}V_2 = \frac{-1}{2}V_0$$

Therefore we can find the three voltages:

$$V_2 = \frac{-3}{13}V_0$$
$$V_3 = \frac{-V_0}{13}$$
$$V_6 = \frac{-3}{26}V_0$$

The mesh then takes the following form:

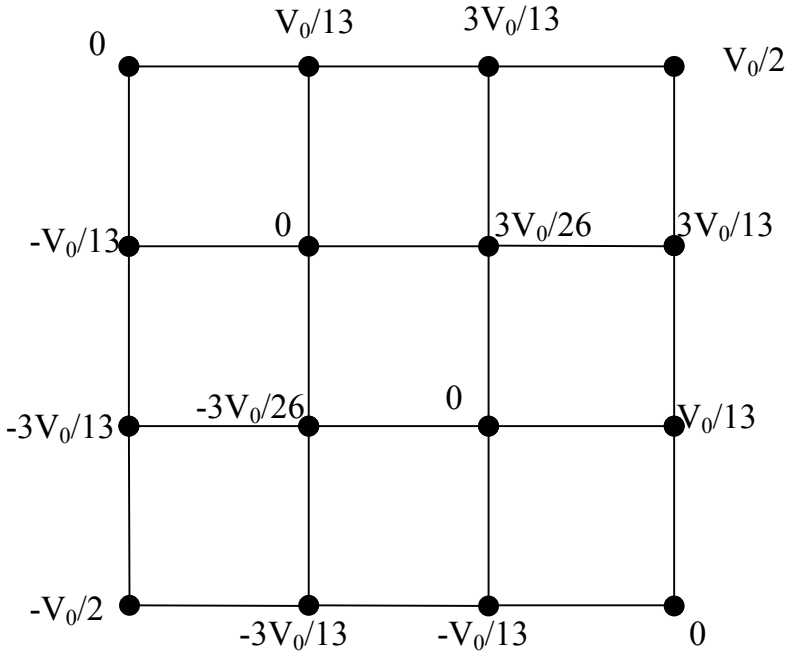

Figure 14: A 4x4 resistor network with node voltage indicated

The total current is $I_{total} = \frac{V_0}{r}\left[2\left(\frac{1}{2} - \frac{3}{13}\right)\right] = \frac{V_0}{r}\left(1 - \frac{6}{13}\right) = \frac{V_0}{r}\left(\frac{7}{13}\right)$. The equivalent resistance is therefore:

$$R_{eq} = \frac{\Delta V}{I_{total}} = \frac{V_0}{\frac{7}{13}V_0\frac{1}{r}} = \frac{13}{7}r$$

2.5: Summary and Comments on Results

In this Chapter, we have labored to develop a more concise formulation of the charge conservation rule in order to express it cleanly and crisply as a relationship among neighboring potentials. We have seen by explicit consideration of several concrete examples that all pertinent information that may be determined from a resistor network is governed and determined by the voltages at the lattice nodes.

We have also seen that symmetry principles (e.g. bilateral symmetry and antisymmetry across a diagonal) may work to our advantage and facilitate the calculation. We ultimately will apply symmetry principles in a grander way to fashion an analytical technique.

CHAPTER 3

PERIODIC RESISTOR NETWORKS WITH CURRENT INJECTED AT SPECIFIC NODES

3.1: General Comments About Current Injection Scenarios

Now the case of infinite lattices will be examined. The equivalent resistance of such infinite systems will be calculated using translational invariance. Fourier variables will be used to perform this calculation on periodic square and cubic lattices. Although we examine the current injection scenario, we do so for the sake of providing a comprehensive treatment of phenomena in resistor networks. In fact, we ultimately will settle on a method which does not involve the manipulation of voltages at specific sites in the lattice, since doing so introduces significant theoretical intricacies and thereby frustrates obtaining close form results. Nevertheless, in Chapter 3 the reader is afforded a glimpse of the Fourier variables and the orthogonality principle that facilitates Fourier analysis and respresents the essence of its utility. We also see in action the use of square symmetry, which we use again in similar ways later in this dissertation.

3.2: One-Dimensional Geometries

3.2.1: The Periodic Boundary Conditions

It's important to find the conditions for potentials for a large periodic lattice. Excluding nodes in which the potential is imposed, the charge conservation rule can be applied-that the charge flux entering a node is equal to the charge flux departing from the node. To begin, a periodic linear array will be examined:

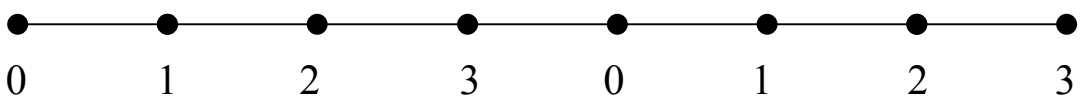

Figure 15: A periodic one-dimensional resistor array

Figure 15 shows the labeling scheme employed. Four distinct nodes are displayed, 0 through 3, with the pattern repeating. More generally, for n nodes, the labeling would begin at 0 and end at $n-1$.

3.2.2: Application of the Charge Conservation Condition

In some parts of the circuit the node voltages will not be specified in advance. The conditions on these node voltages are such that local charge conservation must hold.

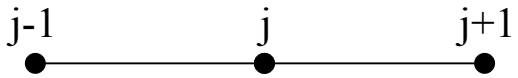

Figure 16: Illustration of the connectivity scheme for the one-dimensional system

In **Figure 16**, the focus is on the node labeled "j". Since charge flux must balance, we know that

$$\left[\frac{-V_{j+1}+V_j}{r}+\frac{V_j-V_{j-1}}{r}\right]=0.$$

If the currents to the left and right are both zero, we know that

$$2V_j-V_{j+1}-V_{j-1}=0.$$

This is the one-dimensional discrete version of the Laplacian Equation $\nabla^2\Phi=0$.

3.2.3: Introducing the Fourier Variables

Fourier variables will be used here to facilitate the calculation. Periodicity and translational invariance conditions suggest that the following relation should be employed:

$$V_j = \sum_{k=0}^{n-1} a_k e^{\frac{2\pi i k j}{n}}.$$

The Fourier components respect the periodicity of the system.

Now the current conservation formalism will be implemented in a way that makes contact with the current sources. This will be done using the Kronecker Delta notation such that we specify the injected current at various points. This current is given by

$$\frac{V_{j+1} - V_j}{r} + \frac{V_{j-1} - V_j}{r} = \frac{1}{r}\left[V_{j+1} + V_{j-1} - 2V_j\right] = \sum_{j'} I_{j'}\delta_{jj'}$$

In terms of Fourier variables,

$$\frac{1}{r}\left[V_{j+1} + V_{j-1} - 2V_j\right] = \frac{1}{r}\left[\sum_{k=0}^{n-1} a_k e^{\frac{2\pi i(j+1)}{n}} + \sum_{k=0}^{n-1} a_k e^{\frac{2\pi i(j-1)}{n}} - 2\sum_{k=0}^{n-1} a_k e^{\frac{2\pi i j}{n}}\right]$$

Furthermore:

$$\sum_{k=0}^{n-1} a_k e^{\frac{2\pi i j k}{n}}\left(e^{\frac{2\pi i k}{n}} + e^{\frac{-2\pi i k}{n}} - 2\right) = r\sum_{j'} I_{j'}\delta_{jj'}$$

$$= \sum_{k=0}^{n-1} 2a_k e^{\frac{2\pi i j k}{n}}\left(\cos\left[\frac{2\pi k}{n}\right] - 1\right) = r\sum_{j'} I_{j'}\delta_{jj'}$$

3.2.4: The Orthogonality Condition for the Fourier Variables

Next, the idea is to multiply both sides of this expression by $e^{\frac{2\pi i j k'}{n}}$ and sum over all values of the position index variable j. Only certain values of k' will yield a nonzero result, so this will be used to uniquely calculate the Fourier coefficients a_k. The result can be exploited for the partial summation of geometric series, which holds that

$\sum_{m=0}^{n-1} z = \frac{1 - z^n}{1 - z}$, so

$$\sum_{j=0}^{n-1}\left[\sum_{k=0}^{n-1}2a_k\left(\cos\left[\frac{2\pi k}{n}-1\right]\right)e^{\frac{2\pi ij(k+k')}{n}}\right]=r\sum_{j,j'}I_{j'}\delta_{jj'}e^{\frac{2\pi ijk'}{n}}$$
$$=\sum_{k=0}^{n-1}\left[2\sum_{j=0}^{n-1}e^{\frac{2\pi ij(k+k')}{n}}\right]\left[a_k\left(\cos\left(\frac{2\pi k}{n}\right)-1\right)\right]=r\sum_{j'}I_{j'}e^{\frac{2\pi ij'k'}{n}}$$

Let's consider the summation

$$\sum_{j=0}^{n-1}e^{\frac{2\pi ij(k+k')}{n}}=\frac{1-e^{2\pi ij(k+k')}}{1-e^{\frac{2\pi i(k+k')}{n}}}$$

The denominator vanishes in all cases, but the result is undefined when the denominator vanishes. This case needs to be examined closely, where $1-e^{\frac{2\pi i(k+k')}{n}}=0$. From Euler's Formula, this would mean that $k+k'=mn$ where m is an integer. The simplest choice is to let $m=0$ so that $k=-k'$. The same would be true if $k=n-k'$, and only this case is compatible with the summation over k. Then we find that

$$\sum_{k=0}^{n-1}\left(2\sum_{j=0}^{n-1}e^{\frac{2\pi ij(k+k')}{n}}\right)\left(a_k\left[\cos\left(\frac{2\pi k}{n}\right)-1\right]\right)=r\sum_{j'}I_{j'}e^{\frac{2\pi ij'k'}{n}}$$
$$=\sum_{k=0}^{n-1}\delta_{k(n-k')}\left(2\sum_{j=0}^{n-1}e^{\frac{2\pi ij(k+k')}{n}}\right)\left(a_k\left[\cos\left(\frac{2\pi k}{n}\right)-1\right]\right)=2na_{n-k'}\left[\cos\left(\frac{2\pi[n-k']}{n}\right)-1\right]$$

The expression for the Fourier coefficient is then

$$a_{n-k'}=\left(\frac{r}{2n}\right)\frac{\sum_{j'=0}^{n-1}I_{j'}e^{\frac{2\pi ij'k'}{n}}}{\cos\left(\frac{2\pi k'}{n}\right)-1}$$

where the appropriate trigonometric identities have been used.

3.2.5: The Current Injection Condition

Now a case will be examined where a current I_0 is injected at the point $j' = 0$ and withdrawn at the point $j' = n - 1$. We obtain

$$a_{n-k'} = \left(\frac{rI_0}{2n}\right)\frac{1 - e^{\frac{-2\pi ik'}{n}}}{\cos\left(\frac{2\pi k'}{n}\right) - 1}$$

where we have used the face that $e^{\frac{2\pi i(n-1)k'}{n}} = e^{-\frac{2\pi ik'}{n}}$.

Now, the case where $n = 3$ will be considered. As previously, the Fourier coefficients will be calculated.

$$a_{[3-1]} = a_2 = \left(\frac{rI_0}{6}\right)\frac{\left[1 - e^{\frac{-2\pi i}{3}}\right]}{\left[\cos\left(\frac{2\pi}{3}\right) - 1\right]} = \left(\frac{rI_0}{6}\right)\left(-1 - \frac{i}{\sqrt{3}}\right)$$

Noting that $e^{\frac{6\pi i}{3}} = e^{2\pi i} = 1$, it simplifies to the following expression:

$$a_1 = \left(\frac{rI_0}{6}\right)\left(\frac{1 - e^{\frac{2\pi i}{3}}}{\cos\left(\frac{-2\pi}{3}\right) - 1}\right) = \left(\frac{rI_0}{6}\right)\left(-1 + \frac{i}{\sqrt{3}}\right).$$

Now the voltages can be calculated. Summing the Fourier components and letting $a_0 = 0$, one finds that $V_j = \sum_{k=0}^{n-1} a_k e^{\frac{2\pi ijk}{n}}$.

$$V_0 = \left(a_1 + a_2\right) = \left(\frac{rI_0}{6}\right)(-2) = \frac{-I_0 r}{3}$$

$$V_1 = a_1 e^{\frac{2\pi i}{3}} + a_2 e^{\frac{-2\pi i}{3}} = \left(\frac{rI_0}{6}\right)\left(-1 + \frac{i}{\sqrt{3}}\right)\left(\frac{-1}{2} + \frac{\sqrt{3}}{2}i\right) + \left(\frac{rI_0}{6}\right)\left(-1 - \frac{i}{\sqrt{3}}\right)\left(\frac{-1}{2} - \frac{\sqrt{3}}{2}i\right)$$

V_2 is calculated in a similar way.

$$V_2 = a_1 e^{\frac{-2\pi i}{3}} + a_2 e^{\frac{2\pi i}{3}} = \frac{rI_0}{3}$$

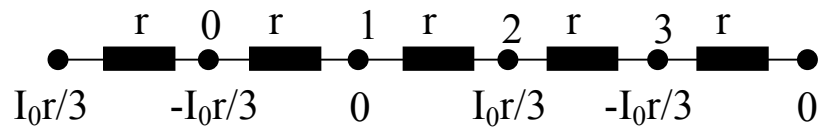

Figure 17: A periodic one-dimensional resistor array with a three-node supercell

Now the current fluxes will be calculated. For point 0, $\Phi = \frac{I_0}{3} + \frac{2I_0}{3} = I_0$. For point 1 the flux vanishes. For point 3, $\Phi = \frac{I_0}{3} + \frac{2I_0}{3} = I_0$. Therefore, everything is developing as predicted.

3.3: Two-Dimensional Geometries

Here the two dimensional prototype will be examined. This result will be pertinent to more complicated lattice structures of higher dimensionalities. The treatment here will bear similarities to the approach for the one-dimensional system. As previously, we will operate in terms of Fourier coefficients.

3.3.1: The Charge Conservation Condition for the Square Lattice

In the two-dimensional system, Kirchoff's Law forbids the accumulation of charge. Again, this current conservation condition serves as a foundation for our calculation.

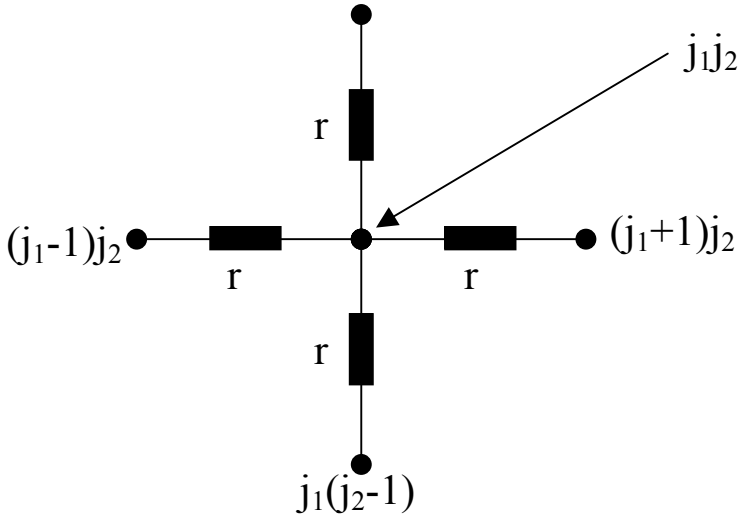

Figure 18: The nearest neighbor connectivity scheme illustrated for the two-dimensional resistor network

Using **Figure 18** as an example, we know from Kirchoff's Law that

$$\frac{1}{r}\left[V_{j_1,j_2} - V_{j_1,j_2+1}\right] + \frac{1}{r}\left[V_{j_1,j_2} - V_{j_1-1,j_2}\right] + \frac{1}{r}\left[V_{j_1,j_2} - V_{j_1+1,j_2}\right] + \frac{1}{r}\left[V_{j_1 j_2} - V_{j_1,j_2-1}\right] = 0$$

$$\frac{1}{r}\left[4V_{j_1 j_2} - V_{j_1(j_2+1)} - V_{j_1(j_2-1)} - V_{(j_1+1)j_2} - V_{(j_1-1)j_2}\right] = 0.$$

This is the discrete form of the Laplacian Equation in two dimensions.

In some cases, current will be injected into a node; this is signified with the Kronecker Delta symbol. Then, we operate in terms of the Fourier components appropriate for two-dimensional systems. We find that

$$\frac{1}{r}\left[4V_{j_1,j_2} - V_{j_1,j_2+1} - V_{j_1,j_2-1} - V_{j_1-1,j_2} - V_{j_1+1,j_2}\right] = I_{j_1,j_2}$$

where I_{j_1,j_2} is the current flow from a particular node, and eventually the Kronecker Delta formalism will be applied when the number of sites of nonzero flux is reduced by two.

3.2.2: Introducing the Fourier Variables in Two Dimensions

In terms of Fourier components, we have $V_{j_1 j_2} = \sum_{k_1=0}^{n-1}\sum_{k_2=0}^{n-1} a_{k_1 k_2} e^{\frac{2\pi i}{n}(k_1 j_1 + k_2 j_2)}$, where the indices k_1 and k_2 are integer values.

Now, this relation is inserted into the Helmholtz Equation. The Helmholtz Equation is the version of Laplace's Equation generalized to allow for nonzero fluxes into and out of nodes. Once again, orthogonality of the Fourier elements will be used to calculate the Fourier coefficients. We start with

$$I_{j_1,j_2} = \frac{1}{r}\left[4V_{j_1,j_2} - V_{j_1,j_2+1} - V_{j_1,j_2-1} - V_{j_1+1,j_2} - V_{j_1-1,j_2}\right].$$

$$I_{j_1,j_2} = \frac{1}{r}\left[\begin{array}{l} 4\sum_{k_1,k_2} a_{k_1 k_2} e^{\frac{2\pi i}{n}(k_1 j_1 + k_2 j_2)} - \sum_{k_1,k_2} a_{k_1 k_2} e^{\frac{2\pi i}{n}(k_1 j_1 + k_2 [j_2+1])} - \sum_{k_1,k_2} a_{k_1 k_2} e^{\frac{2\pi i}{n}(k_1 j_1 + k_2 [j_2-1])} - \sum_{k_1,k_2} a_{k_1 k_2} e^{\frac{2\pi i}{n}(k_1 [j_1+1] + k_2 j_2)} \\ - \sum_{k_1,k_2} a_{k_1 k_2} e^{\frac{2\pi i}{n}(k_1 [j_1-1] + k_2 j_2)} \end{array}\right]$$

$$I_{j_1,j_2} = \frac{1}{r}\sum_{k_1,k_2} a_{k_1 k_2} e^{\frac{2\pi i}{n}(k_1 j_1 + k_2 j_2)}\left[4 - e^{\frac{2\pi i}{n}k_2} - e^{\frac{-2\pi i}{n}k_2} - e^{\frac{2\pi i}{n}k_1} - e^{\frac{-2\pi i}{n}k_1}\right]$$

$$I_{j_1,j_2} = \frac{1}{r}\sum_{k_1,k_2} a_{k_1 k_2} e^{\frac{2\pi i}{n}(k_1 j_1 + k_2 j_2)}\left[4 - 2\cos\left(\frac{2\pi k_2}{n}\right) - 2\cos\left(\frac{2\pi k_1}{n}\right)\right]$$

Multiplying both sides by the Fourier element $e^{\frac{2\pi i}{n}(k_1' j_1 + k_2' j_2)}$ will reveal the orthogonality condition. The factor $\left[4 - 2\cos\left(\frac{2\pi k_2}{n}\right) - 2\cos\left(\frac{2\pi k_1}{n}\right)\right]$ is the discrete version of the Laplacian operator in Fourier space. This term is "local", meaning that in Fourier space there is no connection among the coefficients corresponding to distinct wave numbers. In analogy with the one-dimensional case, we find

$$a_{[n-k_1'][n-k_2']} = \frac{\frac{r}{n^2}\sum_{j_1=0}^{n-1}\sum_{j_2=0}^{n-1}\left(I_{j_1 j_2} e^{\frac{2\pi i}{n}[k_1' j_1 + k_2' j_2]}\right)}{4 - 2\cos\left[\frac{2\pi k_1'}{n}\right] - 2\cos\left[\frac{2\pi k_2'}{n}\right]}$$

3.3.3: Current Injection in the Case of the Square Lattice

Now an example will be examined. A large lattice with a current source and sink at adjacent nodes is shown in **Figure 19**:

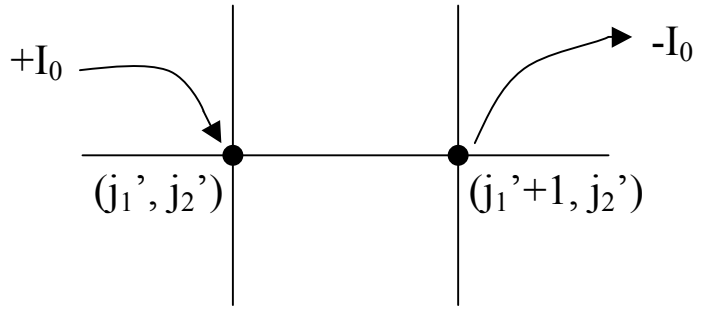

Figure 19: The current injection scenario with source and drain separated by a single resistance link

From this, we see that $I_{j_1 j_2} = I_0\left(\delta_{j_1 j_1'}\delta_{j_2 j_2'} - \delta_{j_1[j_1'+1]}\delta_{j_2 j_2'}\right)$.

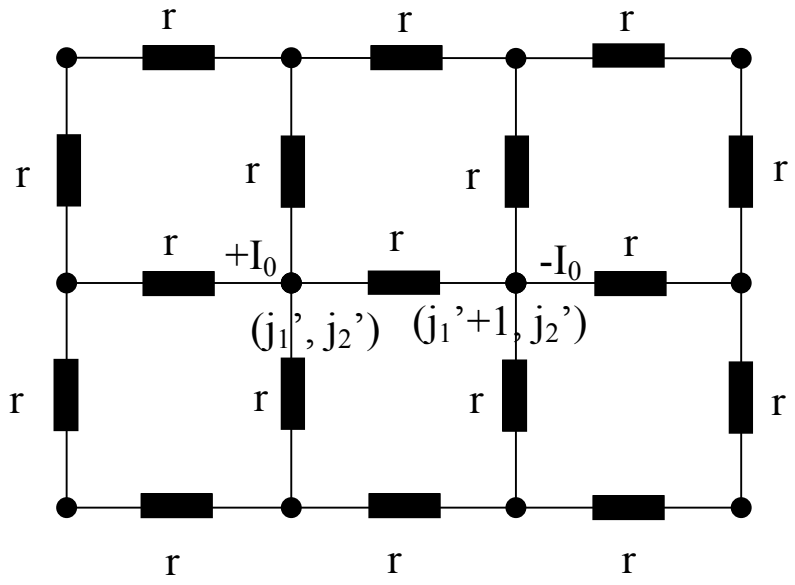

Figure 20: Illustration of the current source and current sink

From this source and sink configuration, we find that

$$a_{[n-k_1'][n-k_2']} = \frac{\frac{r}{n^2}\sum_{j_1=0}^{n-1}\sum_{j_2=0}^{n-1}\left(e^{\frac{2\pi i}{n}[k_1' j_1 + k_2' j_2]} I_0\left[\delta_{j_1 j_1'}\delta_{j_2 j_2'} - \delta_{j_1[j_1'+1]}\delta_{j_2 j_2'}\right]\right)}{4 - 2\cos\left(\frac{2\pi k_1'}{n}\right) - 2\cos\left(\frac{2\pi k_2'}{n}\right)}$$

$$= \frac{\frac{I_0 r}{n^2} e^{\frac{2\pi i}{n}[k_1' j_1' + k_2' j_2']}\left(1 - e^{\frac{2\pi i k_1'}{n}}\right)}{4 - 2\cos\left(\frac{2\pi k_1'}{n}\right) - 2\cos\left(\frac{2\pi k_2'}{n}\right)} = a_{[n-k_1'][n-k_2']}$$

This provides the means to calculate the voltages on nodes $[j_1', j_2']$ and $[(j_1'+1), j_2']$, which in turn will allow for the calculation of the potential difference and equivalent resistance with the help of the following expression:

$$R_{eq} = \frac{\Delta V}{I_0}$$

Again, we note that $a_{0,0} = 0$.

The voltage at (j_1', j_2') is given by $V_{j_1' j_2'} = \sum_{k_1 k_2} a_{k_1 k_2} e^{\frac{2\pi i}{n}[k_1 j_1' + k_2 j_2']}$. This sum may be rewritten in order to simplify its evaluation. Particularly, the indices can be relabeled such that

$$k_1 = n - k_1' \text{ and } k_2 = n - k_2'$$

Then $k_1' = n - k_1$ and $k_2' = n - k_2$.

Hence,

$$a_{[n-k_1'][n-k_2']} = \frac{\frac{I_0 r}{n^2} e^{\frac{2\pi i}{n}[(n-k_1)j_1' + (n-k_2)j_2']}\left(1 - e^{\frac{2\pi i[n-k_1]}{n}}\right)}{4 - 2\cos\left(\frac{2\pi[n-k_1]}{n}\right) - 2\cos\left(\frac{2\pi[n-k_2]}{n}\right)}$$

$$= \frac{\frac{I_0 r}{n^2} e^{\frac{-2\pi i}{n}[k_1 j_1' + k_2 j_2']}\left(1 - e^{\frac{-2\pi i k_1}{n}}\right)}{4 - 2\cos\left(\frac{2\pi k_1}{n}\right) - 2\cos\left(\frac{2\pi k_2}{n}\right)} = a_{k_1 k_2}$$

This will be used to calculate the potential at $[j_1', j_2']$ and $[j_1'+1, j_2']$. Noting that in general $V_{j_1 j_2} = \sum_{k_1=0}^{n-1}\sum_{k_2=0}^{n-1} a_{k_1 k_2} e^{\frac{2\pi i}{n}[k_1 j_1 + k_2 j_2]}$, we see that

$$V_{j_1' j_2'} = \sum_{k_1=0}^{n-1}\sum_{k_2=0}^{n-1} \frac{I_0 r}{n^2} \frac{\left(1 - e^{\frac{-2\pi i k_1}{n}}\right)}{\left[4 - 2\cos\left(\frac{2\pi k_1}{n}\right) - 2\cos\left(\frac{2\pi k_2}{n}\right)\right]}$$

and

$$V_{j_1'+1, j_2'} = \sum_{k_1=0}^{n-1}\sum_{k_2=0}^{n-1} \frac{\frac{I_0}{n^2} r\left(e^{\frac{2\pi i k_1}{n}} - 1\right)}{\left[4 - 2\cos\left(\frac{2\pi k_1}{n}\right) - 2\cos\left(\frac{2\pi k_2}{n}\right)\right]}$$

where cancellation in the exponent has been performed. So the potential difference has the form

$$\left(V_{j_1'+1,j_2} - V_{j_1'j_2}\right) = \Delta V = \left(\frac{rI_0}{n^2}\right)\sum_{k_1=0}^{n-1}\sum_{k_2=0}^{n-1}\left[\frac{2\cos\left(\frac{2\pi k_1}{n}\right)-2}{2\cos\left(\frac{2\pi k_1}{n}\right)+2\cos\left(\frac{2\pi k_2}{n}\right)-4}\right]$$

This is leading up to the exact calculation of the resistance.

3.3.4: Applying Square Symmetry

The dummy indices for the ΔV expression may be exchanged to write

$$\Delta V = \left(\frac{rI_0}{n^2}\right)\sum_{k_1=0}^{n-1}\sum_{k_2=0}^{n-1}\left[\frac{2\cos\left(\frac{2\pi k_2}{n}\right)-2}{2\cos\left(\frac{2\pi k_1}{n}\right)+2\cos\left(\frac{2\pi k_2}{n}\right)-4}\right]$$

Combining the two ΔV expressions ultimately yields

$$2\Delta V = \left(\frac{rI_0}{n^2}\right)\sum_{k_1=0}^{n-1}\sum_{k_2=0}^{n-1}\left[\frac{2\cos\left(\frac{2\pi k_2}{n}\right)+2\cos\left(\frac{2\pi k_1}{n}\right)-4}{2\cos\left(\frac{2\pi k_1}{n}\right)+2\cos\left(\frac{2\pi k_2}{n}\right)-4}\right]$$

As $n \to \infty$ the expression yields $2\Delta V = I_0 r \Rightarrow \Delta V = \frac{I_0 r}{2}$. So $\frac{\Delta V}{I_0} = r_{eq} = \frac{1}{2}r$. Applying similar logic yields that in three dimensions, $r_{eq} = \frac{r}{3}$. So in general, one finds (e.g. for a hypercubic lattice) that $r_{eq} = \frac{r}{d}$.

3.3.5: The Continuum Limit and Lattice Green's Function

Now a very large lattice will be examined by making n very large.

$$V_{j_1' j_2'} = \sum_{k_1=0}^{n-1}\sum_{k_2=0}^{n-1}\frac{I_0 r}{n^2}\frac{\left(1-e^{\frac{-2\pi i k_1}{n}}\right)}{\left[4-2\cos\left(\frac{2\pi k_1}{n}\right)-2\cos\left(\frac{2\pi k_2}{n}\right)\right]}$$

Let us define $\tilde{k}_1 = \frac{2\pi k_1}{n}$ and $\tilde{k}_2 = \frac{2\pi k_2}{n}$. One then finds that

$$V_{j_1' j_2'} = \sum_{\tilde{k}_1}\sum_{\tilde{k}_2}\frac{I_0 r}{n^2}\frac{\left(1-e^{-i\tilde{k}_1}\right)}{\left[4-2\cos\left(\tilde{k}_1\right)-2\cos\left(\tilde{k}_2\right)\right]}$$

Shifts in the $\tilde{k}_1$ and $\tilde{k}_2$ indices will become smaller and smaller where $\tilde{\Delta}k_1 = \frac{2\pi}{n}$ and $\tilde{\Delta}k_2$ are the separations between adjacent $\tilde{k}_1$ and $\tilde{k}_2$ numbers. Ultimately, the expression becomes an integral, so we find that

$$V_{j_1' j_2'} = \frac{I_0 r}{n^2}\sum_{\tilde{k}_1}\sum_{\tilde{k}_2}\frac{\left(1-e^{-i\tilde{k}_1}\right)\tilde{\Delta}k_1\tilde{\Delta}k_2}{\left[4-2\cos\left(\tilde{k}_1\right)-2\cos\left(\tilde{k}_2\right)\right]}\frac{1}{\tilde{\Delta}k_1}\frac{1}{\tilde{\Delta}k_2}$$

$$\Rightarrow \frac{I_0 r}{n^2}\int_0^{2\pi}\int_0^{2\pi}\frac{\left(1-e^{-i\tilde{k}_1}\right)d\tilde{k}_1 d\tilde{k}_2}{\left[4-2\cos\left(\tilde{k}_1\right)-2\cos\left(\tilde{k}_2\right)\right]}\left(\frac{n^2}{4\pi^2}\right)$$

$$= \frac{I_0 r}{4\pi^2}\int_0^{2\pi}\int_0^{2\pi}\frac{\left(1-e^{-i\tilde{k}_1}\right)d\tilde{k}_1 d\tilde{k}_2}{\left[4-2\cos\left(\tilde{k}_1\right)-2\cos\left(\tilde{k}_2\right)\right]}$$

Notably the result doesn't depend on the size of the lattice.

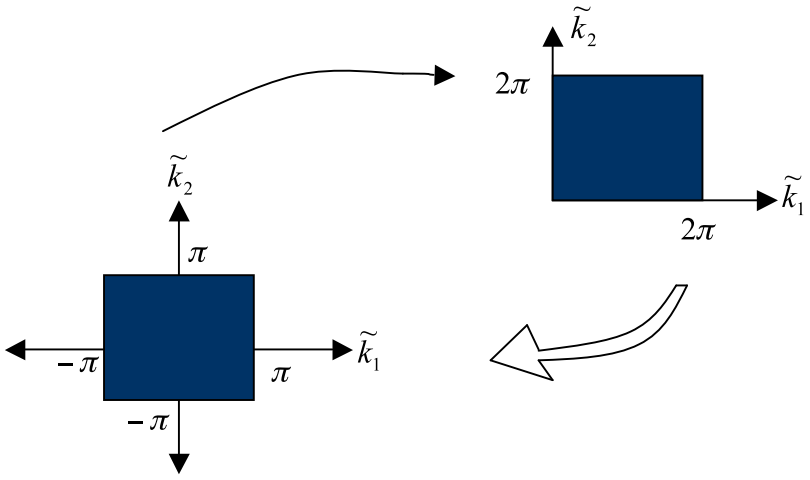

Figure 21: Illustration of the recentering of the domain of integration

Without altering the result, the region of integration may be shifted to better exploit symmetries of the integrand. So $V_{j_1' j_2'} = \frac{I_0 r}{4\pi^2}\int_{-\pi}^{\pi}\int_{-\pi}^{\pi}\frac{\left(1-e^{-i\tilde{k}_1}\right)d\tilde{k}_1 d\tilde{k}_2}{\left[4-2\cos\left(\tilde{k}_1\right)-2\cos\left(\tilde{k}_2\right)\right]}$.

Since $e^{-i\tilde{k}_1} = \cos\left(\tilde{k}_1\right) + i\sin\left(\tilde{k}_1\right)$, we know from symmetry arguments that the imaginary term vanishes upon integration. Thus

$$V_{j_1' j_2'} = \frac{I_0 r}{4\pi^2}\int_{-\pi}^{\pi}\int_{-\pi}^{\pi}\frac{\left(1-\cos\left[\tilde{k}_1\right]\right)d\tilde{k}_1 d\tilde{k}_2}{\left[4-2\cos\left(\tilde{k}_1\right)-2\cos\left(\tilde{k}_2\right)\right]}$$

Discretion must be exercised when evaluating this integral. Using contour integration techniques, at least one of the integrals may be evaluated, but ultimately the calculation is nontrivial. This expression is an example of a lattice Green's function. Lattice Green's functions are interesting in their own right, and have been the object of theoretical study [2].

There are significant analytical difficulties in calculating currents and potentials in the presence of localized current sources. For this reason, in subsequent discussion we

dispense with currents injected or withdrawn at specific sites. In the manner, we will be able to consider the case of interest, a bulk system subject to a global potential difference. We have discussed the case where the current sources are separated only by a single resistor link. However, the calculation is more intricate. An elegant and quite readable discussion of this more general situation may be found in the relatively recent literature [3].

CHAPTER 4

ITERATIVE ALGORITHM FOR THE NUMERICAL CALCULATIONS OF TRANSPORT CHARACTERISTICS

4.1: The Advantage of Periodic Boundary Conditions

We found in the previous chapter that the consideration of specific current cources is not without significant challenges in the theoretical analysis. Additionally, the use of individual locations where current is injected is an artifice not generally appropriate to the bulk system where it is difficult to access specific lattice sites. Consequently, we seek a different approach and we use periodic boundary conditions for the potentials of the lattice nodes.

The use of periodic boundary conditions is a departure from the methods most often described in the literature where, e.g., a certain percentage of the nodes in proximity ot the anode and cathode plates are used as current injection sites, as illustrated below.

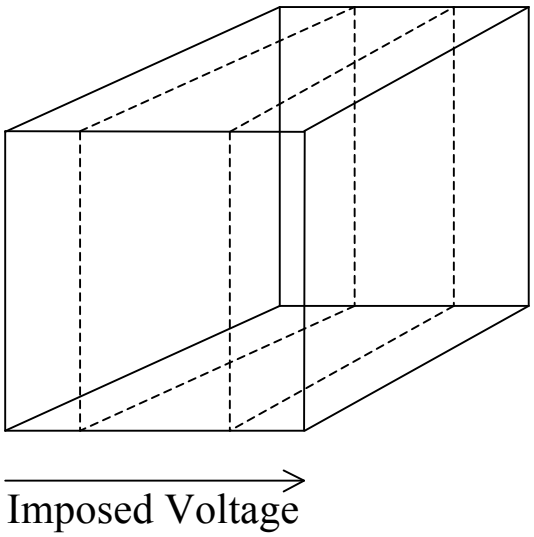

Figure 22: General scheme for a three-dimensional geometry which encorporates electrode zones, to the left and right of the central portion marked with dashed lines

In some cases, the “electrode region” may correspond to 5% of the nodes closest to the anode plate as well as 5% of the nodes closest to the cathode plate. However, in this manner we again have an artificial situation where specific voltages are applied to individual sites. Moreover, there are subtleties to work out such as what portion of the sites in the lattice is given over to be a part of the electrodes. These concerns are peculiar to the specific experimental arrangement and geometry, and they do not correspond to bulk material characteristics.

Our program, however, is to work out the bulk characteristics to the extent possible without committing ourselves to a particular setup. We hope to operate in the context of the thermodynamic limit, which is another label ascribed to the condition of having the system size so large that, practically speaking, the system is infinite in size. What this means is that any transport characteristic we wish to computeis not influenced to a significant degree by the size of the system.

An appropriate question to ask is how relevant is the thermodynamic limit for samples which may be prepared for analysis in experiment? Consider a very small sample a single micron (one thousandth of a millimeter) on a side. Such an object will be so small that a billion cubic micrometer samples would fit in a volume the size of a sugar cube. Nevertheless, for the purpose of calculating a variety of physical quantities, the cubic micrometer sample may be considered to be a “bulk” system, as we shall consider.

For many purposes, a measure of the extent to which the bulk limit has been reached is the total number of particles contained in the system. Let us suppose that each atom occupies a cubic region three Angstroms or 0.3 nanometers on a side. Then to find

the number of particles contained in the sample under consideration, we must divide its volume by the volume of the 27 cubic Angstrom cell. One finds in this specific instance that the total number of atoms is given by

$$N = \frac{10^{-6} \times 10^{-6} \times 10^{-6}}{9 \times 10^{-10} \times 10^{-10} \times 10^{-10}} \approx 1.1 \times 10^{11}$$

So despite the small physical size of the sample, there are more than one hundred billion atoms contained in its volume. This is more than the number of neurons contained in a human brain, and certainly exceeds what may feasibly be examined in a contempory computer similation. Thus, we see that for many scenarios, the thermodynamic limit is an appropriate assumption.

4.2: The Periodic Boundary Conditions

For the boundary conditions, we must proceed carefully to impose periodicity for the physical observables while also maintaining a potential difference V_0 maintained along one of the Cartesian axes. In this hypothesis, we will invariably impose the potential bias in the x-direction, for the purpose of the numerical calculations.

To set up the periodic boundary conditions, we ascribe to each node in the lattice a potential value $V_{i,j,k}$. Suppose that the geometry is cubic and each of the entries i, j, and k run from zero to $n-1$. We have standard periodicity in the j and k indices since no potential is imposed in either the y or z-directions. Thus, in the computer calculations we will need to insist that

$$V_{i,j+n,k} = V_{i,j,k}$$

as well as

$$V_{i,j,k+n} = V_{i,j,k}$$

In the i indices, we have a periodicity condition that is modified by the presence of a potential gradient in the direction of the x-axis. To set up a "down-hill" potential to push carriers in the x-direction, we use the condition

$$V_{i+n,j,k} = V_{i,j,k} - V_0$$

These periodic boundary conditions implemented in the manner described here are not generally used in the literature. Nonetheless, we argue that the use of periodicity is prudent for a variety of reasons.

4.3: Implementing the Numerical Calculations

4.3.1: The Essential Features of an Iterative Algorithm

Our numerical approach is fundamentally an iterative paradigm. What this means is we begin with an initial guess for the solution for the potential, and by a sequence of successive refinements we approach the correct solution. Thus, as the figure indicates, an iterative process has a cyclical character where the iterative refinement process is repeated many times.

An important part of the iterative process is a gauge to indicate if a suitable level of convergence has been accomplished in the calculations. In this vein, we will calculate a residual quantity to evaluate the degree to which a solution has been refined, and to halt the iterative sequence when the desired threshold has been reached.

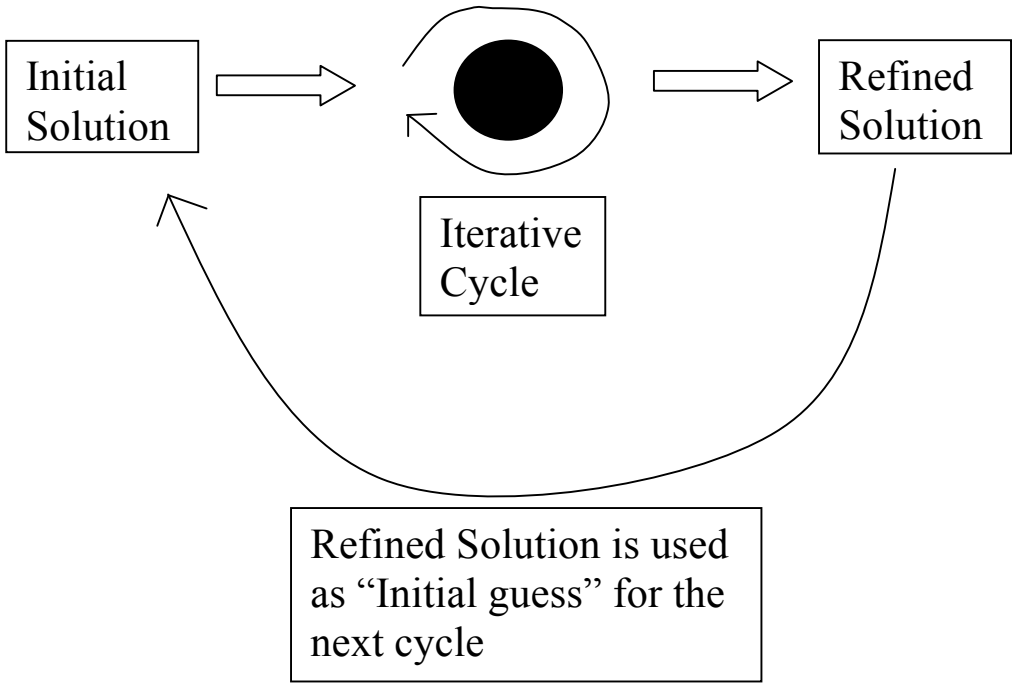

Figure 23: A schematic rendtion of the iterative calculations

4.3.2: The Charge Conservation Constraint as a Computational Tool

The charge conservation condition, also known as Kirchhoff's first rule, stipulates that the currents that enter a node must be equal to those receding outward from the node. The point is to avoid a current imbalance, which would lead to an accumulation of charge. However, the principle that forbids the pile-up of charge carriers also has a much more profound purpose, in that it provides a quantitative tool which may be systematically applied to calculate the node voltages, which govern every characteristic of the system which we may wish to interrogate.

Let us now formally express the iterative scheme in terms of matrix algebra. Although our notation makes no reference to any specific geometry, it nevertheless is general and may readily be specialized to any dimensionality of scheme for the connectivity of the nodes. We consider a case in which there are N nodes indexed by the

label i. In principal each node contained in the system may be connected to every other node in the system, though in practice schemes such as the Variable Range Hopping (VRH) picture will confine the conductive links to a small number of neighboring nodes close to the node i under consideration.

Now, let us restate the current conservation condition for the node i. One has

$$0 = \sum_{j \neq i} \frac{V_i - V_j}{R_{ij}}$$

where Ohm's Law has been used to calculate the current in links connecting the node i with the node j. Now, having expressed the current conservation condition, we have all that is required to explicitly describe the iterative machinery to be used in the numerical calculations.

Let us first solve for the voltage V_i in terms of the potentials V_j at the neighboring nodes. One finds that

$$V_i = \frac{\sum_{j \neq i} \frac{V_j}{R_{ij}}}{\sum_{j \neq i} R_{ij}^{-1}}$$

Now, in an iterative calculation our aim is to express the new potential values in terms of an older set of values. Then, our expression becomes

$$V_i^{NEW} = \frac{\sum_{j \neq i} \frac{V_j^{OLD}}{R_{ij}}}{\sum_{j \neq i} R_{ij}^{-1}}$$

The general strategy, then, is to express the new revised potentials in terms of a previous set of nodal voltages. As we continue with the iterative refinements, potential is redistributed about the lattice in such a way as to ultimately satisfy charge conservation at

each node in the lattice under consideration. The principal merit of this method is its ease of implementation. We are achieving the solution of a linear system of equations without formally invoking a matrix, which has its own advantages in situations where memory is a scarce commodity.

This method also encapsulates a vital piece of intuition, the connectivity of the lattice. One need only care about the scheme of connecting each node to its neighbors in order to solve the problem. Thus, in situations where the use of mesh currents is hampered by irregular or intricate lattice geometries, a technique which focus on individual nodes and the ways in which they are connected to their neighbors encounters relatively little difficulty.

4.3.3: Comments on Alternative Iterative Methods

Finally, we mention that there are techniques of solution that proceed more rapidly than the method that we have described. However, for reasons that we now summarize, the alternative approaches are more of a technical challenge to implement. Moreover, the method that we have described yields convergent results reasonably rapidly for systems typically of interest on modern computational platforms. In particular, we find we are able to examine sufficiently large systems that finite size effects do not play a significant role in our numerical Monte Carlo calculations.

With regard to the alternative methods of solution, in the case of large lattices where nodes are linked only to close neighbors, the task of calculating the resistances at the nodes is mathematically the same as solving a linear system of the form $\hat{A}\vec{x} = \vec{b}$ where $\vec{x}$ represents the voltages at the nodes, $\vec{b}$ is a constant vector, and the matrix $\hat{A}$ is specified by the connectivity scheme particular to the lattice under consideration. In

regular lattices, or any system where the bond resistances are identical, the conjugate gradient algorithm provides a robust way to hasten the rate of convergence. However, in situations of interest to us, it is most often the case that the relevant matrix is not symmetric, and the conjugate gradient method is not directly applicable.

In lieu of the ocnjugate gradient technique, one would instead use the Biconjugate Gradient method [4]. The biconjugate gradient technique is fashioned expressly to address cases in which the matrix for the linear system is not symmetric. However, the technical intricacies associated with the boconjugate gradient method are more formidable than those of its simpler counterpart. In addition, the stability of the biconjugate gradient approach is in general more difficult to guarantee than the conjugate gradient technique, where a robust convergence is assured in most reasonable situations.

4.3.4: Assessing the Convergence of the Iterative Calculations

An important consideration in executing the iterative cycles we have described to determine voltages at the lattice nodes is the appropriate criterion to use to halt the calculations and emerge with a set of node voltages which is accurate to within the bounds of a per-determined tolerance. One possible candidate to use as a gauge of the progress of the convergence of the calculation would be to use the magnitude of successive changes in the node potentials, and to cease the sequence of iterations if the shifts decrease below a certain threshold.

However, the method of monitoring changes in the potentials V_i between cycles is not objective in a physical sense, and is instead subject to dynamics of the calculation which may be unrelated to the actual degree wo which the solution has been refined. An example which we treat later in this thesis is the case of critical slowing down which may

occur in the civinity of a percolation transition, a type of phase transition observed in random resistor networks under certain conditions.

4.3.4.1: Defining the Residual Quantity

We sish to objectively specify the extent of convergence, and we do so with a physically significant residual quantity. A requirement that we have frequent occasion to visit is the condition that currents at the nodes should be balanced to prevent an accumulation of charge at the junction. As a consequence, the extent to which current is not balanced may be utilized as a quantitative measure of the degree to which there remain inaccuracies in the V_i values produced by the iterative cycles. To this end, we define

$$r \equiv \frac{1}{N}\sum_{i=1}^{N}|I_i|$$

where we are calculating the average of the absolute magnitude of the total current either flowing into or departing from the node labeled i.

It is wise to calculate absolute values in order to avoid obtaining a spuriously low value due to cancellations among terms in the sum. In terms of expressions we have discussed previously, the residual quantity has the form

$$r = \frac{1}{N}\sum_{i=1}^{N}\left|\sum_{j=1}^{N}\frac{V_i - V_j}{R_{ij}}\right|$$

In the numerical calculations which we report on, we insist that the mean residual index r converge to within one part in 10^8 before halting the iterative cycles.

4.3.4.2: Implementing Random Disorder

To examine how r converges, we consider a square lattice where each node is connected by resistive links to four nearest neighbors. However, while the lattice

geometry is regular, we introduce an element of disorder by perturbing the resistances of the links from their native values, taken initially to be identical. In particular, a resistance with the random perturbation incorporated appears as

$$r = r_0\left(1 + \frac{\varepsilon}{2} y\right)$$

where ε is a number somewhat less than 1, and y is a random number selsected with uniform probability between the bounds 1- and +1. The statement that one must be "objective" in choosing a random number may seem self-contradicting, but it nonetheless is a valid notion in the snese that we would prefer a stochastic influence not to be "biased" in any external manner.

An excellent random number generator, which we have made use of for the purpose of the numerical calculations described in this thesis, is the Mersenne Twister algorithm. A principal advantage of the Twister is a very long period of erpetition, so that for practical purposes the sequence of random numbers does not repeat itself and introduce spurious effects. In addition, the Mersenne Twister has passed vigorous statistical tests that check for correlations among successively generated random numbers.

4.3.4.3: Computational Cost and System Size

First, it is instructive to examine the computational cost (in terms of the total number of iterations needed to achieve a convergence threshold) with respect to the size of the system, and the graph shown below displays results for the two-dimensional alttices under consideration.

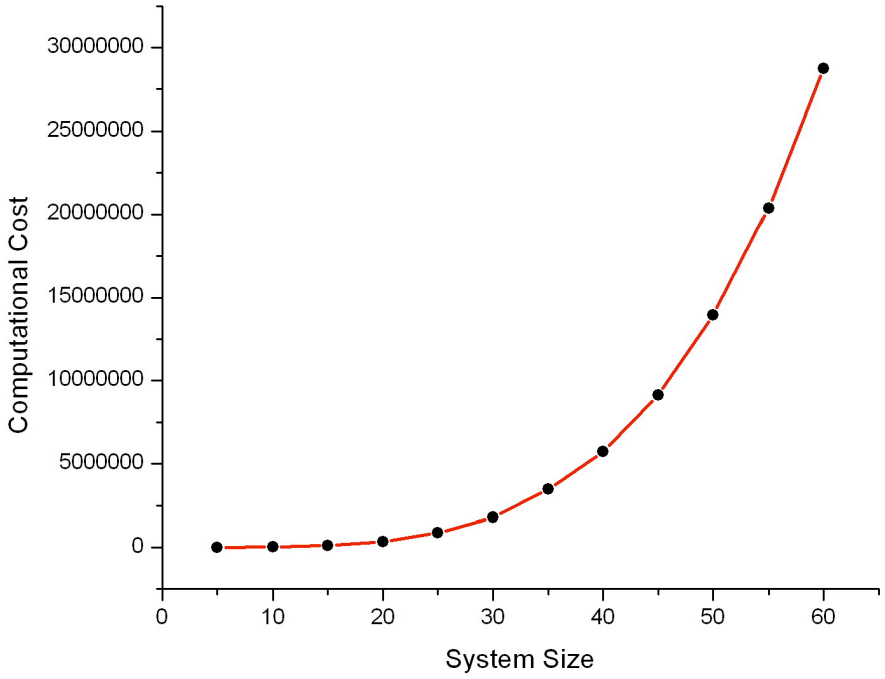

Graph 1: Raw computational cost graphed with respect to system size for a two-dimensional bond disordered case; the computational cost is specified as the number of iterations needed for convergence

The results shown in the preceding graph are drawn directly from numerical calculations that we have performed for specific systems and configurations of disorder. To highlight salient trends, it is often worthwhile to plot logarithms on one or more axes. If a power law scaling is anticipated, logarithms on both axes will yield an asymptotically linear graph, precisely the behavior which we see in the graph below where the horizontal axis is the base ten of the size of the system while the vertical axis indicates the base ten logarithm of the number of iterations needed to achieve convergence.

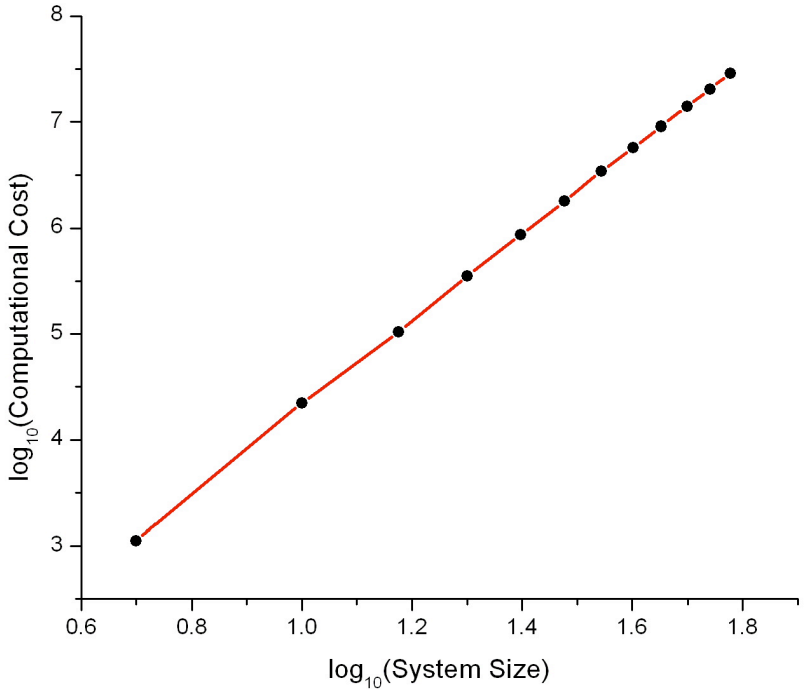

Graph 2: A base ten log-log graph of computational cost with respect to system size for a bond disordered two-dimensional system, where computational cost is the number of iterations needed for convergence

We discern from the results that the computational cost increases as a power law in the size of the square lattice, and fortunately does not rise more dramatically (e.g. at a exponential rate in the system size).

4.3.4.4: The Variation of the Residual Quantity with the Number of Iterations

It is also useful to examine how the convergence, as quantified by the residual number, progresses with the number of iterations for a system of a specific size. In the graph shown below, traces are shown for several system sizes. The residual quantity, rendered as the mean of the absolute magnitude of the current entering or departing from the nodes, decreases rapidly with the number of iterative cycles and hence it is appropriate to use the base ten logarithm for the vertical axis.

Several features are immediately evident. First, the traces have a primarily linear profile. The graph is semi-logarithmic, and in such a situation a linearly decreasing in a quantity is a hallmark of an exponentially rapid decrease along the abscissa, which in the present is the number of iterations. Another salient characteristic is the difference of the slopes of the three traces corresponding to the three distinct system sizes under consideration. The monotonic decrease in the slope is a direct consequence of the fact that the computational burden increases with increasing system size.

Finally an additional feature of note is the fact that for each of the linear curves, the downward trajectory is ultimately interrupted by the arrival at a base line (in the vicinity of 10^{-17}) beyond which no further decrease of the residual parameter r is witnessed. The barrier is a consequence of the finite level of occuracy of even the double precision afforded by FORTRAN acting in conjunction with rounding errors that finally hinder further convergence. What, nevertheless, is encouraging is the fact that for a diverse set of systems, the greatest extent of convergence possible is quite similar and considerably exceeds the $r = 10^{-8}$ standard which we adopt in this work.

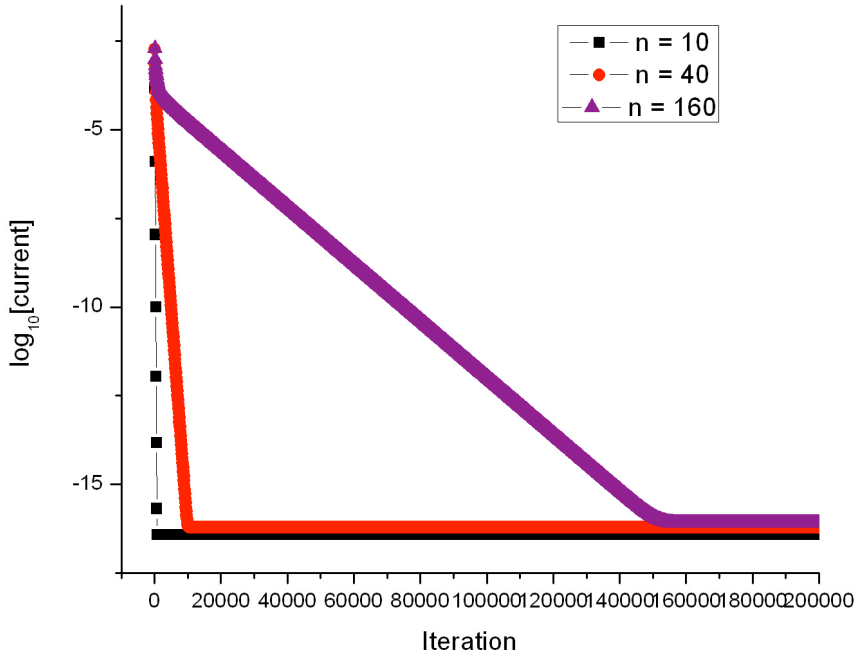

Graph 3: Semi-logarithmic graph of the residual nodal current flux with respect to the number of iterations for several system sizes

4.3.4.5: Results of the Calculations and Robustness with respect to Disorder

Having examined the convergence characteristics, it is also appropriate that we examine someof the physics contained in the disordered model. Accordingly, we calculate and display the forward currents as a function of the parameter ε controlling the strength of the perturbation. The values of ε which we examine range from 0.0 to 2.0, and the system is a square lattice containing 10,000 individual nodes in a 100x100 geometry.

Two features of the first graph are immediately evident. First, even for values of ε on the order of unity, the conductance changes very little, and certainly there is no

evident first order contribution. Another important characteristic is the smoothness of the curve. Although each point corresponds to a distinct realization of disorder, the points nevertheless lie on a smooth line and thereby reveal a global trend which transcends individual configurations of disorder, and which corresponds to a bulk characteristic.

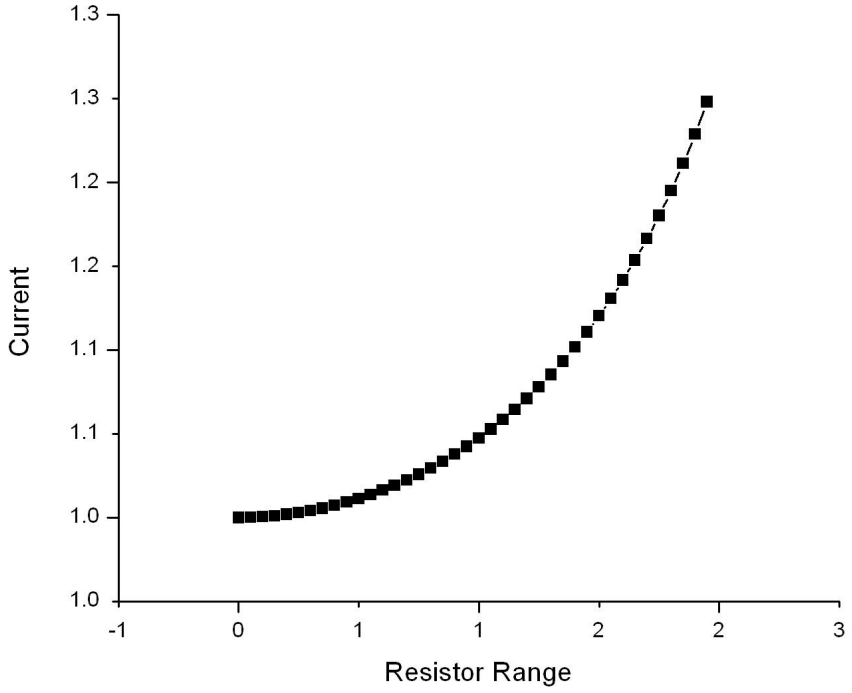

Graph 4: Mean forward current plotted with respect to the resistor range for a two-dimensional bond disordered network

The divergence of the trace in the graph is a consequence of the fact that we are degrading resistances as often as we are augmenting the values of the link resistances. Initially, the net effect is quite subtle because the effects of increased and decreased resistances oppose each other. Eventually, however, the resistive links with significantly diminished resistance prevail and to some degree short the system out, leading to the divergence in the current.

Another way to probe the effect of disorder is to calculate the standar deviation of the current to gain an idea of the extent to which the current fluctuates about a mean value. The results may be seen in the graph below, and one again sees a very slow rise in the fluctuations about the mean. Although we are calculating a quantity that owes itself entirely to the disordering influence (i.e. the standard deviation would vanish in the absence of a random perturbation), the smoothness of the curve again speaks to the fact that the bulk limit has been achieved to a suitable extent.

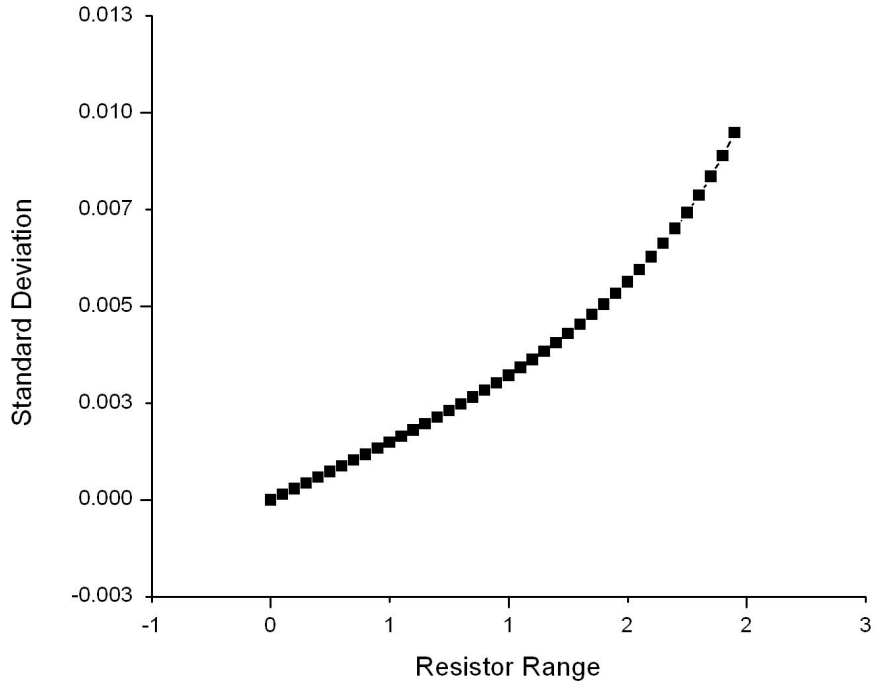

Graph 5: Standard deviation of forward current plotted with respect to resistor range for a 100x100 two-dimensional disordered system

In summary, one sees that the current values remain essentially uniform, even amid considerable disorder.

CHAPTER 5

A RESISTOR NETWORK MODEL FOR TRANSPORT CHARACTERISTICS IN REGULAR LATTICES

5.1: The Variable Range Hopping Picture

Resistor networks have been reviewed and studied theoretically as entities of interest in their own right. Here we will use our experience with resistor networks to calculate the transport properties of amorphous materials. We make use of the resistor network model used as a theoretical treatment for charge transport in systems with a significant component of disorder. In the analysis we employ a result treats the connections between active sites as resistor links [5]. The result is developed from a theoretical analysis from Miller and Abrahams [6].

Consider a set of sites i and j in a disordered lattice. The conductance is given by

$$G_{ij} = G_0 e^{\left[\frac{-2d_{ij}}{a} - \frac{|E_i|+|E_j|+|E_i-E_j|}{k_B T}\right]}.$$

To determine the resistance, one takes the reciprocal and finds that

$$R_{ij} = R_0 e^{\left[\frac{2d_{ij}}{a} + \frac{|E_i|+|E_j|+|E_i-E_j|}{k_B T}\right]},$$

since $R_0 \equiv G_0^{-1}$.

This expression has two important features. First, there is the dependence on the physical separation between sites that asymptotically decays exponentially in the separation between the sites in the case of the conductance. This exponential decay is a result of the nature of the overlap among wave functions, which we take to be

exponentially decaying. For a characteristic length scale, one uses "$\frac{a}{2}$", which is related to the Bohr radius of hydrogenic atoms, where one also has an exponential fall-off.

The second important consideration is "chemical disorder", manifest as variations in the local site energy (E_i and E_j for the sites "i" and "j" in the present context) which often have a random component in amorphous materials. In addition to chemical disorder, we will also examine the effects of site disorder which is a consequence of random displacements in the positions of the atoms comprising the amorphous material.

In this chapter, we will first examine and perform calculations for the iso-energetic case for which chemical disorder is absent. In this manner, we will discern the effect of deviations in the atomic positions from locations in a perfect crystal lattice. "Iso-energetic" pertains to the case in which each of the site energies are the same.

5.2: Specializing to the Iso-energetic Regime

In the iso-energetic regime, we will be able to consider the effect of positional disorder on transport characteristics. The procedure will involve steadily increasing the magnitude of deviations from the crystal coordinates of a pristine atomic lattice. The shifts δ_i will be introduced at random for each i^{th} atom. The task will involve the minimization of finite size effects to the extent possible, so we sill consider as large systems as may be achieved.

We will operate in two and three dimensions, and in both cases we will apply different potentials to opposite faces of the system. The situation for the two dimensional case is illustrated in **Figure 24**, where the pristine and disordered cases are depicted in juxtaposition.

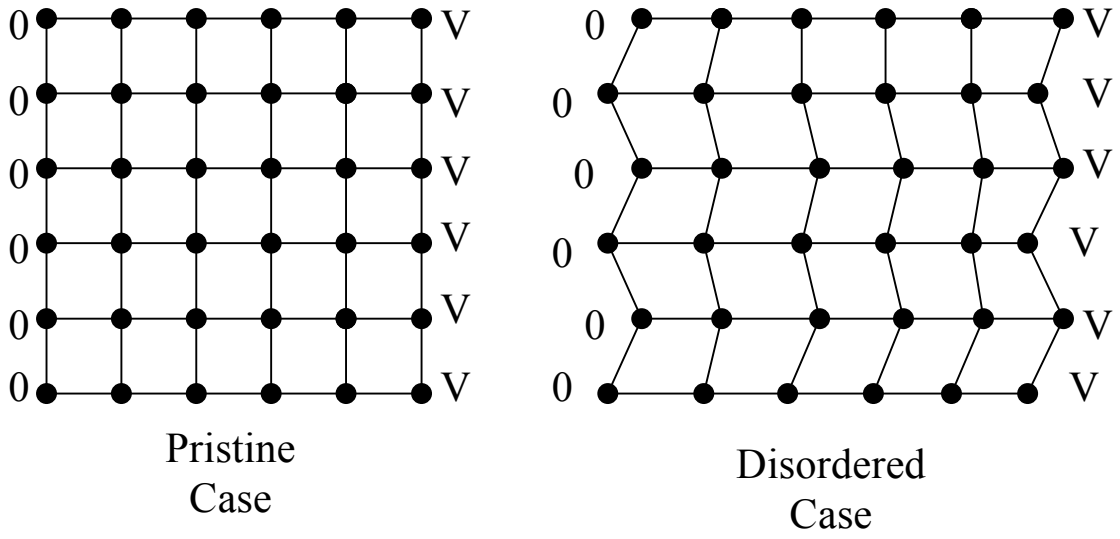

Figure 24: Illustration of how a regular unperturbed lattice is affected by the presence of positional disorder

Although there are deviations from the square lattice positions in the case on the right, the potential difference is held constant by fixing the potentials of the points on the left to "0" Volts and the points on the right to "V" volts. In what follows, we will consider the special case of regular crystal lattices in one, two, and three dimensions. The results of the calculations in this context will be relevant for lattices other than the pristine case since, as we have seen, transport characteristics may be robust with respect to the introduction of moderate levels of disorder.

5.3: Calculating the Conductance of Resistor Networks in One-dimensional Geometries

Let us now examine a periodic system and impose a potential difference across the lattice. The one-dimensional system will be considered first. This calculation is simplified by the absence of current sources, which required considerable mathematical formulation.

In this one-dimensional case, we'll examine a set of nodes connected only to nearest neighbors, as shown in **Figure 25**:

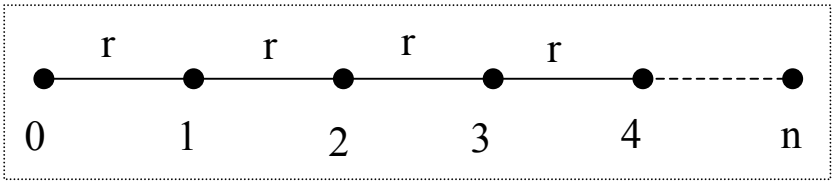

Figure 25: Illustration of one-dimensional regular lattice

Though all physical observables will be identical at every point on the lattice, the potential will vary linearly with the lattice coordinate i. Hence $V_{i+n} = V_i + V_0$, where V_0 is the imposed potential difference. We will see that the correct form to employ for the potential is $V_i = -\frac{iV_0}{n}$. As we'll see, the actual resistance depends on the connectivity of the nodes.

5.3.1: The Circumstance of Connections among Nearest Neighbors

We'll examine the case in which the lattice nodes are bound only to the nearest neighbors. Again, we utilize the form $V_i = -\frac{iV_o}{n}$ for the potential at any given location in the lattice. Again, the one-dimensional case is considered here. The current which exists at node i in the positive direction will be $\frac{\Delta V_{i,i+1}}{r} = \frac{V_0}{nr}$, so the resistance is $\frac{V_0}{i} = nr = R_{nearest\ neighbor}$. This result isn't surprising, however the simplicity of the calculation is an important issue in this context.

5.3.2: An Extended Connectivity Scheme and an Exact Result

Now, we'll examine the case in which the nearest neighbor connectivity is relaxed. We first examine a general scheme where the (monotonically decreasing) resistances are indexed as r_i. In **Figure 26**, r_1 represents the resistance between adjacent nodes and r_2 represents the resistance between non-adjacent nodes.

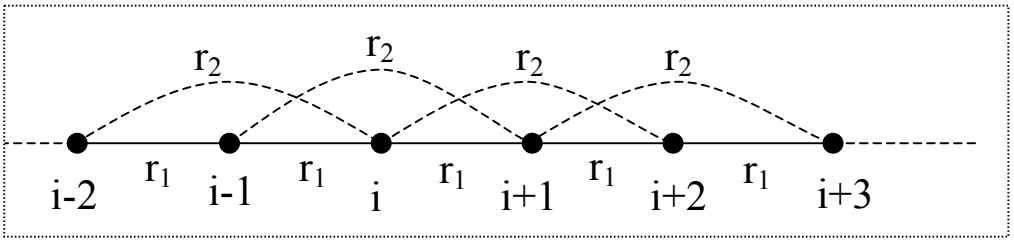

Figure 26: One-dimensional resistor network with connectivity extended beyond nearest neighbors

Again, we'll calculate the current which flows in the forward direction.

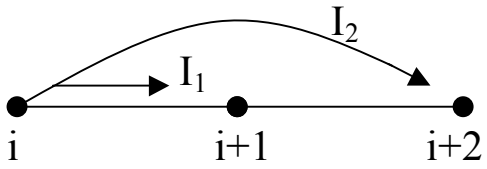

Figure 27: Illustration of contributions to the forward current in an extended scheme

The current flowing from i to $i+1$ will be $\frac{\Delta V_{i,i+1}}{r} = \frac{V_0}{nr_1} = I_1$. Noting that $\Delta V_{i,i+2} = 2V_0$, we see that the current flowing forward will be $I_2 = \frac{2V_0}{nr_2}$.

We proceed in a similar way to calculate additional currents, finding that in general $I_m = \frac{mV_0}{nr_m}$. So the total current moving forward is given by

$$I_\Sigma = I_1 + I_2 + I_3 + ... = \sum_{j=1}^{\infty} I_j .$$

We then see that $I_\Sigma = \sum_{j=1}^{\infty} I_j$, and we find that $I_\Sigma = \sum_{j=1}^{\infty} \frac{jV_0}{nr_j}$. So the total resistance is given by

$$R_\Sigma = \frac{V_0}{I_\Sigma} = \frac{V_0}{\sum_{j=1}^{\infty} \frac{jV_0}{nr_j}} = \frac{n}{\sum_{j=1}^{\infty} \frac{j}{r_j}}$$

So the total resistance still scales as n, but with a pre-factor $\rho = \left(\sum_{j=1}^{\infty} \frac{j}{r_j} \right)^{-1}$.

Now a situation will be considered in which the resistance scales exponentially with the physical separation between nodes i and j such that

$$r_{ij} = r_0 e^{f\alpha d_{ij}} .$$

The reciprocal of the factor f is

$$f^{-1} = \sum_{j=1}^{\infty} \frac{j}{r_j}$$

$$= \sum_{j=1}^{\infty} \frac{j}{r_0} e^{-\alpha j}$$

This sum may be calculated with the aid of

$$-\frac{d}{d\alpha} \left[\sum_{j=1}^{\infty} \frac{e^{-\alpha j}}{r_0} \right] = +\sum_{j=1}^{\infty} \frac{j e^{-\alpha j}}{r_0}$$

We also know from the geometric series

$$\sum_{j=0}^{\infty} r^j = \frac{1}{1-r} \, (where \, |r| < 1),$$

that we can evaluate the sum. The result is

$$\sum_{j=1}^{\infty} \frac{e^{-\alpha j}}{r_0} = e^{-\alpha} \sum_{j=0}^{\infty} \frac{e^{-\alpha j}}{r_0}$$

$$= \frac{e^{-\alpha}}{r_0} \frac{1}{1-e^{-\alpha}}$$

Differentiating this gives

$$-\frac{d}{d\alpha}\left(\sum_{j=1}^{\infty} \frac{e^{-\alpha j}}{r_0}\right) = -\frac{d}{d\alpha}\left[\frac{e^{-\alpha}}{r_0} \frac{1}{1-e^{-\alpha}}\right]$$

$$= \frac{e^{-\alpha}}{r_0} \frac{1}{1-e^{-\alpha}} + \frac{e^{-\alpha}}{r_0} \frac{1}{1-e^{-\alpha}} e^{-\alpha}$$

$$= \frac{e^{-\alpha}}{r_0\left(1-e^{-\alpha}\right)^2}$$

$$= f^{-1}$$

Therefore the resistance of the system taken as a whole is $nf = nr_0 e^{\alpha}\left(1-e^{-\alpha}\right)^2$. If we suppose that $\alpha << 1$ so that we my use $e^{\alpha} = 1 + \alpha + ...$ and $e^{-\alpha} = 1 - \alpha + ...$ to obtain

$$R_{\alpha}^{\ n} = nr_0\left[1 + \alpha + ...\right]\left[\alpha - ...\right]^2 = nr_0\alpha^2$$

to first order in the decay constant α. Thus, a less stringent exponential cutoff encourages transmission of current and lowers the resistance.

5.4: Calculating the Conductance of Two-Dimensional Networks

Now we'll consider square resistance arrays and endeavor to evaluate the resistance. We'll examine the nearest neighbor case first.

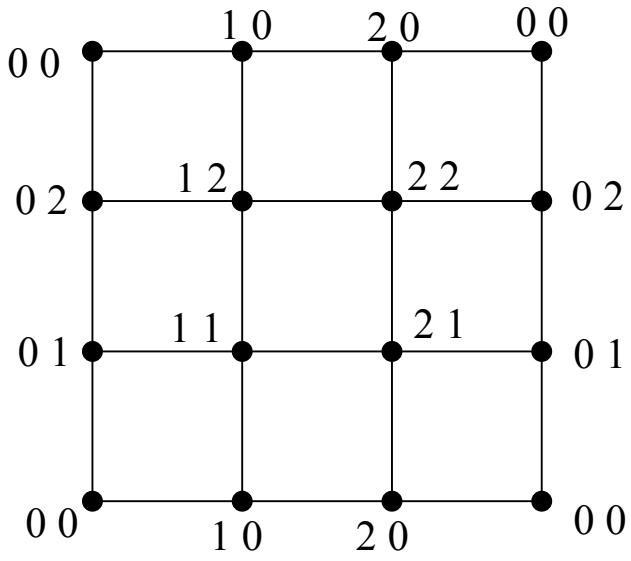

Figure 28: Two-dimensional resistor network with periodic boundary conditions and node labeling scheme

Figure 28 shows the labeling scheme. We'll impose the potential from left to right. Therefore, we set $V_{00} = V_{01} = V_{02} = ... = V_0$. On the right side, we set $V_{N0} = V_{N1} = V_{N2} = ... = V_{NN} = 0$. This condition is successfully implemented in the context of a periodic system by using $V_{ij} = \frac{V_0}{n} i$ so that the condition arises where one has a steadily increasing potential in the "x" direction.

5.4.1: The Current in the Nearest Neighbor Case

Now we endeavor to calculate the conductance (reciprocal of the resistance) of the system. As previously, this is achieved by calculating the total current that flows through the system.

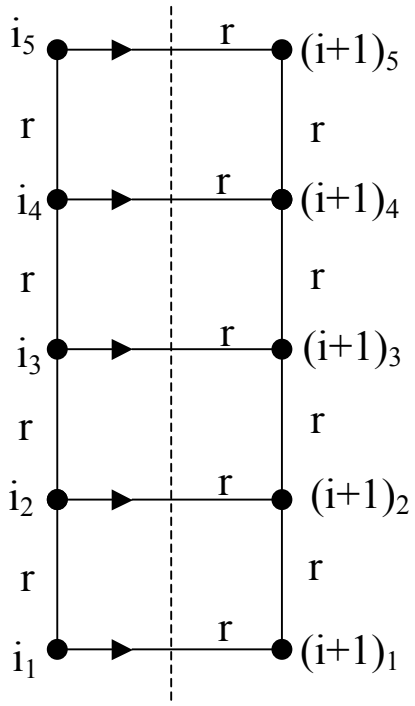

Figure 29: Cross-section of a two-dimensional network. The dashed line is used as a reference point in the calculation of the total current

The current may be calculated by determining the charge flux through the dashed line in **Figure 29**. This current is the sum of the individual currents, which, for the nearest neighbor system, are $(n)\frac{V_o}{r} = \frac{V_0}{r}$. The total resistance is $\frac{V_0}{V_0/r} = r$. The conductance is the reciprocal $\frac{1}{r}$.

5.4.2: The Extended Scheme in the Two-Dimensional Case

As done previously, we will examine an extended scheme for the one-dimensional case. Again, we consider an exponentially decaying coupling.

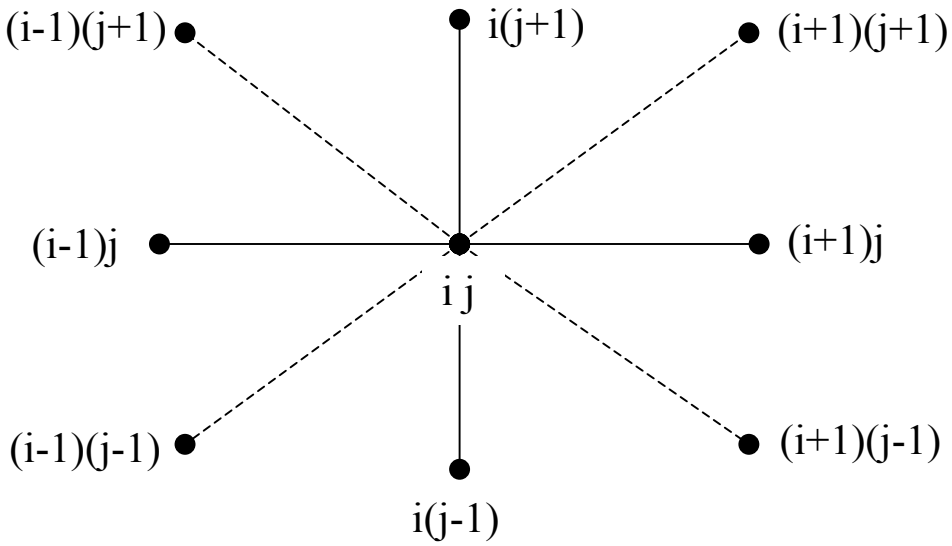

Figure 30: Connectivity pattern of a single node in a two-dimensional lattice with connections to next-nearest neighbors

Figure 30 shows and example of nearest and next nearest neighbors. The interaction is $e^{-\alpha\Delta s}$, where Δs is the spacing between points in the two dimensional lattice. The same relation as before holds for the resistance between two points on the lattice.

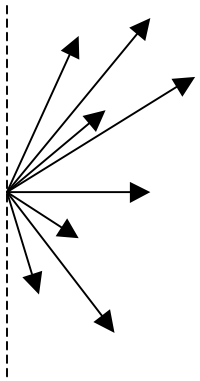

Figure 31: Illustration of charge fluxes from a single node with connections extended to many neighbors

The summation takes the form $\sum_{i=1}^{\infty}\sum_{j=-\infty}^{+\infty} j_{ij}{}^{x}$ where $j_{ij}{}^{x}$ is the current that flows forward to the point indexed as "ij". Our task will be to calculate the $j_{ij}{}^{x}$ values within our framework.

5.4.2.1: Calculating Current in a Two Dimensional Regular Lattice with Extended Connectivity

Here we continue our examination of current in a two dimensional regular lattice in the iso-energetic case. We'd determined that the total current would be $J_{total} = \sum_{i=1}^{\infty}\sum_{j=-\infty}^{+\infty} j_{ij}{}^{x}$ from a single point where the individual component currents may be calculated by appealing to the Cartesian formula for distances in two dimensions.

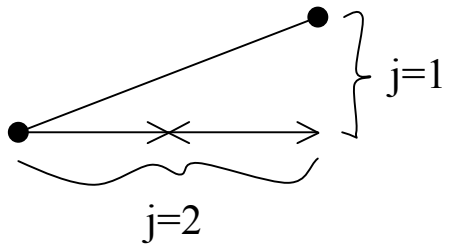

Figure 32: A link spanning non-nearest neighbor nodes in the two-dimensional pattern

In **Figure 32**, the distance to the point $i = 2; j = 1$ is given by the Cartesian relation $r_{ij} = \sqrt{i^2 + j^2} = \sqrt{5}$ in the units under consideration.

However, it would be prudent to operate in terms of the lattice constant a. In terms of the lattice constant, the length r_{ij} is instead given by $r_{ij} = \sqrt{(ia)^2 + (ja)^2} = a\sqrt{i^2 + j^2}$. The potential difference over the length r_{ij} is given by

$\Delta V_{ij} = \frac{V_0}{n} i$. The resistance in the conducting element to the point ij is $R_{ij} = R_0 e^{+\frac{r_{ij}}{l}}$

where we have used the localization length l in lieu of the constant α.

Assembling the aforementioned relations in terms of the lattice parameters, we solve for the individual currents $j_{ij}{}^{x}$:

$$j_{ij}{}^{x} = \frac{\Delta V_{ij}}{R_{ij}}$$

as one finds from Ohm's Law. Hence, $j_{ij}{}^{x} = \frac{V_0}{R_0 n} i e^{-\frac{r_{ij}}{l}} = \frac{V_0 i}{R_0 n} e^{-\frac{a}{l}\sqrt{i^2 + j^2}}$. Then the total current moving forward from a particular point is given by $j_{total}{}^{x} = \sum_{i=1}^{\infty} \sum_{j=-\infty}^{+\infty} \frac{V_0 i}{R_0 n} e^{-\frac{a}{l}\sqrt{i^2 + j^2}}$.

Then for the entire system, we have to take into consideration that each slice will cut across n sites in the $n \times n$ system we now examine. Hence, we see that the total current in the square system is given by

$$J_{total}{}^{x} = \sum_{i=1}^{\infty} \sum_{j=-\infty}^{+\infty} \frac{V_0 i}{R_0} e^{\left[\frac{-a}{l}\sqrt{i^2 + j^2}\right]} \text{ (i).}$$

It is crucial for us to have $na \to l$, so the system length at width na should considerably exceed the length l. We always assume that we are operating in this limit.

5.4.2.2: The Limit of Strong Localization

In what follows, we examine the limiting cases. First we consider the circumstance in which the localization length l is considerably smaller than the lattice constant a so that $l << a$. In such a situation, the exponential scaling of the formula for the inter-site resistances R_{ij} will suppress all but the contributions that involve nearest neighbors.

For the considered square lattice, the absolute nearest neighbor is the site directly in front of the lattice site under consideration. This condition is shown in **Figure 33**.

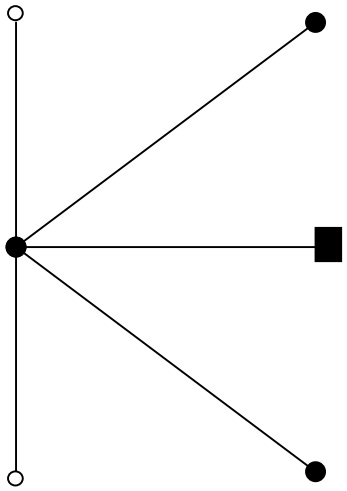

Figure 33: Scheme used in calculating the forward-directed current with connectivity extended to next-nearest neighbors in two dimensions

The square point is the nearest neighbor, and it corresponds to the coordinate $[i = 1; j = 0]$. The points marked by open circles are situated either immediately above or below the primary site for which the forward charge flux is calculated. Since the potential difference vanishes for all sites where $j = 0$, there isn't a nonzero current going to the lattice nodes immediately above or below, or indeed in the same column as the primary lattice point. Thus, returning to the exact formula $J_{total}{}^{x} = \sum_{i=1}^{\infty} \sum_{j=-\infty}^{+\infty} \frac{V_0 i}{R_0} e^{-\frac{a}{l}\sqrt{i^2 + j^2}}$ we see that we have the nearest neighbor case $J_{total}{}^{x} = \frac{V_0}{R_0} e^{-\frac{a}{l}}$. The exponential variation of the current is now readily apparent.

In some situations, such as when anisotropy is considered, it will be useful to include next-nearest neighbors as well. The next-nearest neighbors correspond to the coordinates $[i=1;j=1]$ and $[i=1;j=-1]$, and are illustrated as closed circles in **Figure 35**. Hence, with next-nearest neighbors incorporated, the forward current takes the form

$$J_{total}{}^{x} = \frac{V_0}{R_0} e^{-\frac{a}{l}} + \frac{4V_0}{R_0} e^{-\frac{a}{l}\sqrt{2}}$$

$$= \frac{V_0}{R_0} e^{-\frac{a}{l}} \left[1 + 4e^{-\frac{a}{l}(\sqrt{2}-1)} \right]$$

which will yield a more refined result that will be of relevance when we investigate anisotropic characteristics of various lattice geometries.

5.4.2.3: The Case of a Large Localization Length l

Here we examine the case of a very large localization length, such that $l >> a$ and the granularity of the lattice will be much less readily evident. Calculating $J_{total}{}^{x}$ with the aid of the general summation formula would be extremely difficult. As a general practice, incorporating neighbors typically involves including lattice sites where the length r_{ij} satisfies $r_{ij} \le 5l$. This truncation of the sum will yield an accurate result.

In this way we consider the exponential decay of the conductances R_{ij}^{-1} in the distance r_{ij} to be an inherently finite ranged charge transport linkage. But in the case of $l >> a$, the sum goes over to an integral in a manner that we now directly examine. As stated earlier, an exact expression for the forward current flow in the square sample has the form $J_{total}{}^{x} = \sum_{i=1}^{\infty} \sum_{j=-\infty}^{+\infty} \frac{V_0 i}{R_0} e^{-\frac{a}{l}\sqrt{i^2+j^2}}$. This summation may be represented as a Reimann sum in the limit that $l >> a$. In this way we find that the current is given by

$$J_{total}{}^{x} = a^{-2}\sum_{i=1}^{\infty}\sum_{j=-\infty}^{+\infty}\frac{V_0 i}{R_0}e^{-\frac{a}{l}\sqrt{i^2+j^2}}a^2$$

$$= \frac{a^{-2}V_0}{R_0}\int_0^{\infty}\int_{-\infty}^{+\infty} ie^{-\frac{a}{l}\sqrt{i^2+j^2}}\,dxdy$$

Conversion of the summation to a continuum integral is accomplished by expressing the indices "i" and "j" in terms of the appropriate "x" and "y" coordinates. Since $x = ai$ and $y = aj$, we find that the integral expression is

$$J_{total}{}^{x} = a^{-2}\frac{V_0}{R_0}\int_0^{\infty}\int_{-\infty}^{+\infty}\frac{x}{a}e^{-\frac{1}{l}\sqrt{x^2+y^2}}\,dxdy$$

Noting that in polar coordinates $r = \sqrt{x^2+y^2}$ and $x = r\cos\phi$ we will switch to the polar system to facilitate evaluation of the integral.

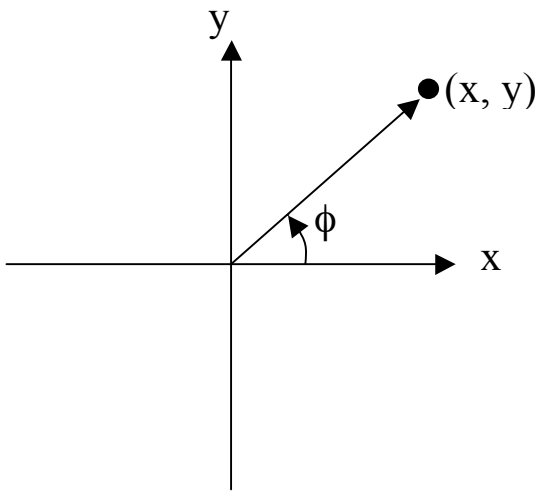

Figure 34: Illustration of the Polar Coordinate System

$$J_{total}{}^{x} = \frac{V_0}{R_0 a^3}\int_0^{\infty}\int_{-\pi/2}^{\pi/2} r^2 e^{-\frac{r}{l}}\cos(\phi)\,drd\phi$$

Fortunately the two integrations decouple, allowing for easy evaluation of the angular and radial integrals. So we find that

$$J_{total}{}^{x} = \frac{V_0}{R_0 a^3}\left[\int_0^\infty e^{-\frac{r}{l}} r^2 dr\right]\left[\int_{-\pi/2}^{\pi/2} \cos\phi d\phi\right]$$

For the angular integral, we have

$$\int_{-\pi/2}^{\pi/2} \cos\phi d\phi = \sin\phi\Big|_{-\pi/2}^{\pi/2} = 2$$

We must calculate $\int_0^\infty r^2 e^{-\frac{r}{l}} dr$ for the radial integral. To accomplish this, we'll consider the case $\int_0^\infty e^{-\alpha u} du = -\frac{1}{\alpha} e^{-\alpha u}\Big|_0^\infty = \frac{1}{\alpha}$. Given this result, we'll differentiate both sides with respect to α. One finds

$$-\frac{1}{\alpha^2} = -\int_0^\infty u e^{-\alpha u} du$$

After a second differentiation, we obtain a result of interest:

$$\frac{2}{\alpha^3} = \int_0^\infty u^2 e^{-\alpha u} du$$

With this, the double integral can now be evaluated, yielding $J_{total}{}^{x}$. We have

$$J_{total}{}^{x} = \frac{V_0}{R_0 a^3}\left[\int_0^\infty e^{-\frac{r}{l}} r^2 dr\right]\left[\int_{-\pi/2}^{\pi/2} \cos\phi d\phi\right]$$

$$= \left(4\frac{V_0}{R_0}\right)\left(\frac{l}{a}\right)^3$$

So the result for the forward current will be confined between two analytical results. For $l << a$, $J_{total}{}^{x} = \frac{V_0}{R_0} e^{-\frac{a}{l}}$ and for $l >> a$, $J_{total}{}^{x} = \frac{4V_0}{R_0}\left(\frac{l}{a}\right)^3$.

5.4.3: Exploring the Implications of Anisotropy in a 2D Resistor Network

Thus far, we have examined cases in which the potential is not applied along the axis of symmetry. In generalizing the case in which the potential is applied along the x axis, we obtain a potential that changes linearly along both the x and y axes. A potential that possesses this form is $V = \frac{-V_{0x}}{n} i + \frac{-V_{0y}}{n} j$. **Figure 35** illustrates this geometry.

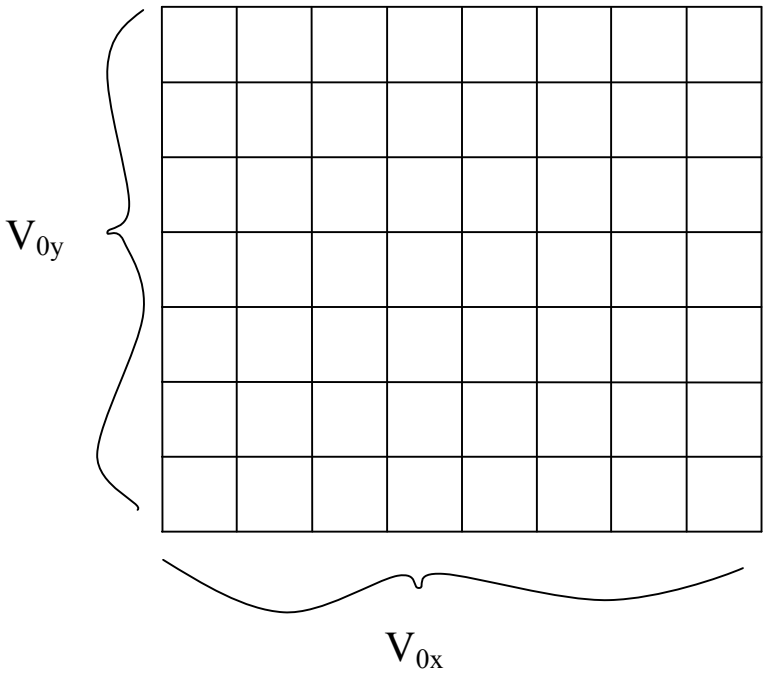

Figure 35: Illustration of the x and y components of the imposed potential bias

The objective now is to calculate the current set up in this configuration. An important question we will attempt to answer is whether the current set up will flow in the same direction as the applied voltage. Although one could readily calculate the currents flowing in the links, the question we set out to answer here exists at a broader scale.

We need to calculate the total current flowing in order to determine the conductance (or resistance) of the entire system. Insights gained during this process will be pertinent when considering the amorphous case where random displacements are introduced in the site positions. To evaluate the current, we must calculate and sum the charge flux through each point in the lattice. Therefore, we will return to the square lattice and calculate the current flowing through the system.

For now, we will focus on the average charge flux per node. We now examine the square lattice in which the applied voltage is not along the axis of symmetry.

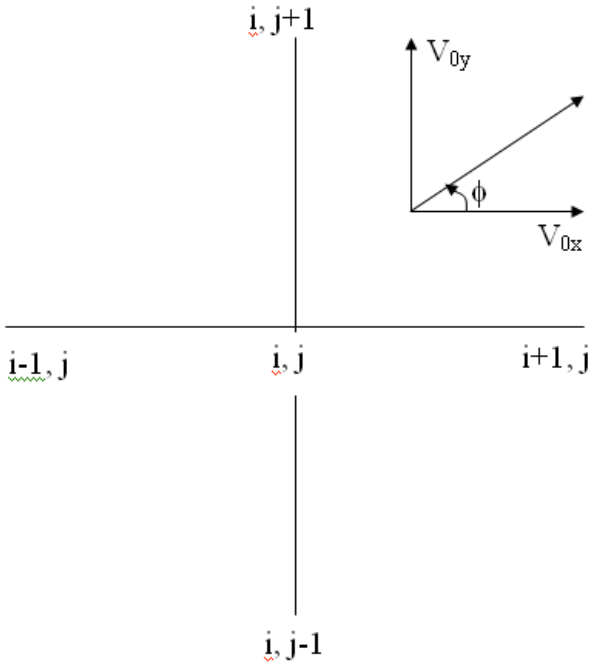

Figure 36: Illustration of a voltage bias not imposed by a symmetric axis

Figure 36 shows such a situation. The angle of the applied voltage my be readily calculated using the following relation:

$$\cos\phi = \frac{V_{0x}}{\sqrt{{V_{0x}}^2 + {V_{0y}}^2}}, \quad \sin\phi = \frac{V_{0y}}{\sqrt{{V_{0x}}^2 + {V_{0y}}^2}}.$$

A pertinent problem to solve is how to calculate the voltages given a particular angle ϕ. Given the overall applied voltage magnitude, the result will be $V_{0x} = V_0 \cos\phi$ and $V_{0y} = V_0 \sin\phi$.

5.4.3.1: The Isotropy Issue in the Nearest Neighbor Case

Now we'll calculate the flux from a node along with the degree of anisotropy for a particular localization length l. Ohm's law and the voltage formula $V_{ij} = \frac{-V_{0x}}{n} i - \frac{V_{0y}}{n} j$ will suffice. An important question is what the current in the x and y directions will be. The goal now is to calculate the current component-wise, which must be done carefully.

For both the x and y components, we must sum over all the surrounding neighbors, though when the localization length l is small we merely need to include the four nearest neighbors. Firstly, we'll consider an example in order to highlight a salient conceptual issue. When calculating the pieces of current, we must take into account the direction in which the current flows. For example, consider a potential with only an x component with no voltage gradient imposed in the y direction. Due to the symmetry of the square lattice, we could easily choose the point $[0,0]$ as the site under consideration, as shown in **Figure 37**.

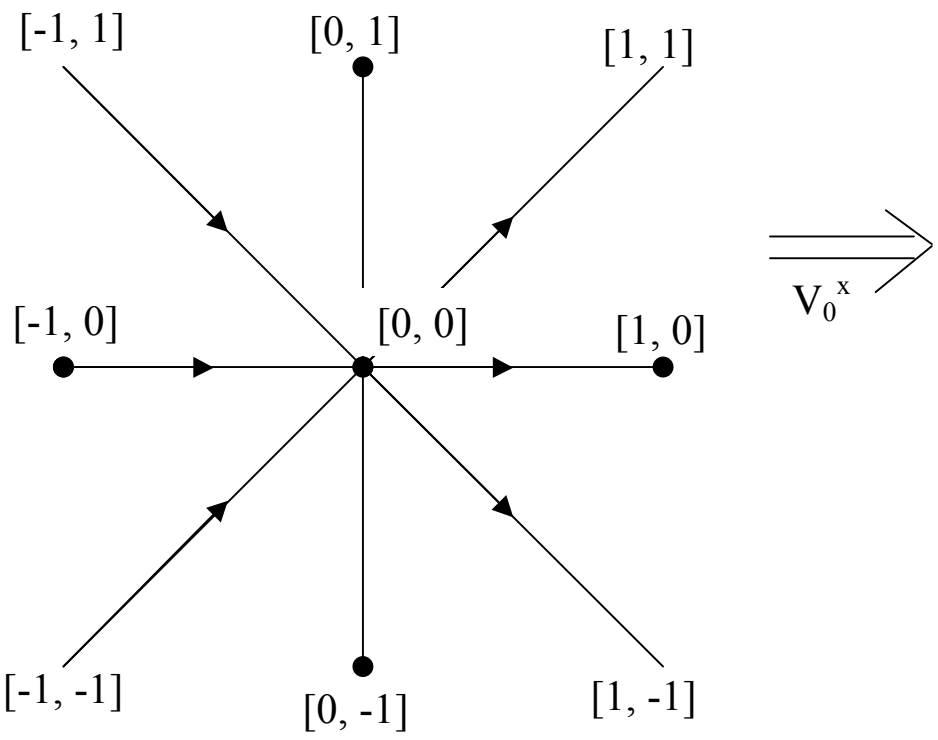

Figure 37: Illustration of current flows set up by a bias in the x-direction

Since the potential is imposed in the x direction, the current will flow to neighbors in the way depicted in **Figure 37**. In the x direction one sees a steady movement with charge born systematically to the right. In the y direction the currents sum to zero, and there is no movement of charge upward or downward. To take this into account, we must carefully consider the direction of the current for each link between nodes.

For the nearest neighbor case we'll calculate the current flux for the site indexed as $[0,0]$. We consider the most general case where there is both a V_{0x} and V_{0y} in the system. For the x direction one has

$$I_x^{\Sigma} = \frac{1}{2}\left[\frac{V_{0x}}{n} r_{10}^{-1} + \frac{V_{0x}}{n} r_{10}^{-1}\right]$$

where the first term comes from the link connecting $[-1,0]$ to $[0,0]$, and the second term comes from the link connecting $[1,0]$ to $[0,0]$.

Now we examine the nearest neighbor situation now with a voltage directed in an arbitrary direction. First we calculate the current flowing in the x direction, then we consider the y direction. As stated earlier, the direction of the current must be considered carefully. Starting with examining site $[0,0]$, from symmetry we see that the current flow magnitude and direction from each site in the lattice will be identical since there is no preferred site in the square lattice.

The goal is to find the current flow from $[0,0]$ to $[1,0]$. This is the following:

$$I_{10} = \frac{V_{0x} e^{-a/l}}{nr_0}$$

The current I_{-10} will have the same magnitude but opposite sign:

$$I_{-10} = \frac{-V_{0x} e^{-a/l}}{nr_0}$$

Thus, the total current in the x direction is

$$\frac{1}{2}\left(\frac{V_{0x}}{nr_0} e^{-a/l} + \frac{V_{0x}}{nr_0} e^{-a/l}\right) = \frac{V_{0x}}{nr_0} e^{-a/l}$$

$$= I_{nn}{}^{x}$$

where the "nn" subscript means "nearest neighbor". Current for the y direction is handled in a similar fashion.

$$I_{01} = \frac{V_{0y}}{nr_0} e^{-a/l}, \quad I_{0,-1} = \frac{-V_{0y}}{nr_0} e^{-a/l}$$

So the total flux in the y direction is given by

$$I_{nn}{}^{y} = \frac{V_{0y}}{nr_0} e^{-a/l}$$

in the context of the nearest neighbor treatment. Employing polar coordinates, we see that

$$I_{nn}{}^{x} = \frac{V_0}{nr_0} e^{-a/l} \cos\phi$$
$$I_{nn}{}^{y} = \frac{V_0}{nr_0} e^{-a/l} \sin\phi$$

and the nearest neighbor case is seen to be isotropic if one calculates the magnitude of the current as a function of the polar angle. This yields the following result:

$$I(\phi) = \frac{V_0}{nr_0} e^{-a/l}$$

Obviously, there is no variation with respect to ϕ, so the current magnitude does not depend on the direction of the imposed voltage.

5.4.3.2: Investigating Isotropy in the Next-Nearest Neighbor Case

Now we will examine the next-nearest neighbors case and check to see of isotropy remains intact. Just as there were four nearest neighbors, there are four next-nearest neighbors. While the distance to the nearest neighbors was a, the distance to the next-nearest neighbors is $\sqrt{2}a$. For the x direction, the current set up by V_{0x} is given by

$$I_{10}{}^{x} = -I_{01}{}^{x} = \frac{V_{0x}}{nr_0} e^{-a/l}$$

as shown previously. Now onto consider the next-nearest neighbors. To the point $[1,1]$ the current in the x direction is $\frac{1}{2}\frac{V_{0x}}{nr_0} e^{-\frac{\sqrt{2}a}{l}} + \frac{1}{2}\frac{V_{0y}}{nr_0} e^{-\frac{\sqrt{2}a}{l}}$. To the point $[1,-1]$ the current in the x direction is $\frac{1}{2}\frac{V_{0x}}{nr_0} e^{-\frac{\sqrt{2}a}{l}} - \frac{1}{2}\frac{V_{0y}}{nr_0} e^{-\frac{\sqrt{2}a}{l}}$.

The current also flows to the points $[-1,1]$ and $[-1,-1]$. For $[-1,1]$ the current flowing from the point $[0,0]$ is given by

$$I_{[-1,1]}{}^{x} = -\frac{1}{2}\frac{V_{0x}}{nr_0}e^{-\frac{\sqrt{2}a}{l}} - \frac{1}{2}\frac{V_{0y}}{nr_0}e^{-\frac{\sqrt{2}a}{l}}$$

To calculate the total current flowing to the next-nearest neighbors set up in the x direction, we use the following:

$$I_{nnn}{}^{x} = \left[I_{[1,1]}{}^{x} + I_{[1,-1]}{}^{x} - I_{[-1,1]}{}^{x} - I_{[-1,-1]}{}^{x}\right]$$

$$= \frac{2V_{0x}}{nr_0}e^{-\frac{\sqrt{2}a}{l}}$$

So we have a cancellation of the currents set up by the y component $\frac{V_{0y}}{n}$ of the applied potential. By symmetry, we know that the current $I_{nnn}{}^{y}$ is given by

$$I_{nnn}{}^{y} = \frac{2V_{0y}}{nr_0}e^{-\frac{\sqrt{2}a}{l}}$$

Here we have exploited the geometric symmetry of the square lattice with respect to rotations by $\frac{\pi}{2}$. The total current in the x direction is given by

$$I^{x} = I_{nn}{}^{x} + I_{nnn}{}^{x}$$

$$= \frac{V_{0x}}{nr_0}\left[e^{-\frac{a}{l}} + 2e^{-\frac{\sqrt{2}a}{l}}\right]$$

Similarly, for the y direction we know that

$$I^{y} = I_{nn}{}^{y} + I_{nnn}{}^{y}$$

$$= \frac{V_{0y}}{nr_0}\left[e^{-\frac{a}{l}} + 2e^{-\frac{\sqrt{2}a}{l}}\right]$$

This shows that the current is indeed isotropic if contributions up to and including the current flows to next-nearest neighbors are taken into consideration. An angular variant of the current is given by

$$\frac{V_0}{nr_0}\left[e^{-\frac{a}{l}}+2e^{-\frac{\sqrt{2}a}{l}}\right]$$

5.4.3.3: The Isotropy Calculation for a Coupling Scheme which Encompasses all Neighbors

Now, a more general case in the context of the square lattice will be examined. We'll take all sets of neighbors into consideration, so we will construct a general sum which we will not truncate for the moment. To set up this sum, we proceed carefully and first examine current fluxes only in sites contained within the first Cartesian quadrant, as seen in **Figure 38**.

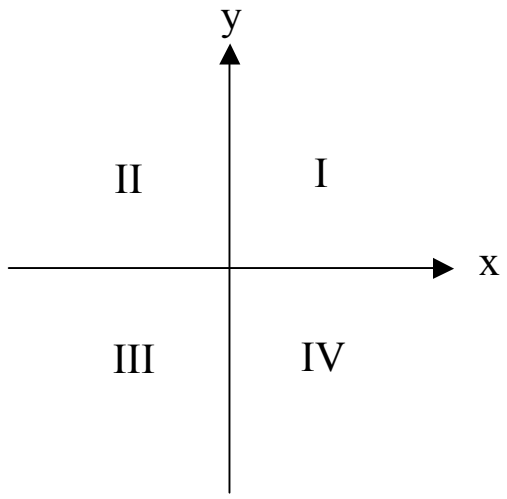

Figure 38: Convention for dividing the two-dimensional Cartesian system into quadrants

This means that the ordered pairs $[i,j]$ will be positive. First, the flow set up in the x direction needs to be determined. The contribution from ${V_0}^x$ is given by $\frac{1}{2}\sum_{i=1}^{\infty}\sum_{j=0}^{\infty}\frac{{V_0}^x}{nR_{ij}}i$, where the point $[0,0]$ is excluded from the sum. R_{ij} is the resistance of the "wire" extending to the point $[i,j]$ and is given by $R_{ij}=r_0e^{r_{ij}/l}$ where $r_{ij}=a\sqrt{i^2+j^2}$. So now we have

$$I_{{V_0}^x}{}^x=\frac{1}{2}\sum_{i=1}^{\infty}\sum_{j=1}^{\infty}\frac{{V_0}^x i}{nr_0}e^{\frac{-\sqrt{i^2+j^2}a}{l}}$$

Similarly the contribution due to the potential in the y direction will be

$$I_{{V_0}^y}{}^x=\frac{1}{2}\sum_{i=1}^{\infty}\sum_{j=1}^{\infty}\frac{{V_0}^y i}{nr_0}e^{\frac{-\sqrt{i^2+j^2}}{l}}$$

We will show that only the contribution due to ${V_0}^x$ will survive when we take the presence of other quadrants of the lattice into consideration.

Quadrant I:

$$I_I{}^x=\frac{1}{2}\sum_{i=1}^{\infty}\sum_{j=1}^{\infty}\frac{e^{-\frac{a}{l}\sqrt{i^2+j^2}}}{nr_0}\left({V_0}^x i+{V_0}^y j\right)$$

Quadrant II:

$$I_{II}{}^x=\frac{1}{2}\sum_{i=1}^{\infty}\sum_{j=1}^{\infty}\frac{e^{-\frac{a}{l}\sqrt{i^2+j^2}}}{nr_0}\left(-{V_0}^x i+{V_0}^y j\right)$$

Quadrant III:

$$I_{III}{}^x=\frac{1}{2}\sum_{i=1}^{\infty}\sum_{j=1}^{\infty}\frac{e^{-\frac{a}{l}\sqrt{i^2+j^2}}}{nr_0}\left(-{V_0}^x i-{V_0}^y j\right)$$

Quadrant IV:

$$I_{IV}{}^{x} = \frac{1}{2}\sum_{i=1}^{\infty}\sum_{j=1}^{\infty}\frac{e^{-\frac{a}{l}\sqrt{i^2+j^2}}}{nr_0}\left(V_0{}^{x}i - V_0{}^{y}j\right)$$

It's clear that the sum will cancel contributions from $V_0{}^{y}$ and will be strictly proportional to $V_0{}^{x}$. We then have

$$I_{Interior}{}^{x} = \left[I_I{}^{x} - I_{II}{}^{x} - I_{III}{}^{x} + I_{IV}{}^{x}\right]$$

$$= \frac{2}{nr_0}\sum_{i=1}^{\infty}\sum_{j=1}^{\infty}V_0{}^{x}ie^{-\frac{a}{l}\sqrt{i^2+j^2}}$$

We should also take into account contributions from the x axis. The result is

$$I_{Border}{}^{x} = \sum_{i=1}^{\infty}(2)\frac{1}{2nr_0}V_0{}^{x}ie^{-\frac{a}{l}i}$$

Ultimately we see that

$$I_{\Sigma}{}^{x} = \frac{1}{nr_0}\left[2\sum_{i=1}^{\infty}\sum_{j=1}^{\infty}V_0{}^{x}ie^{-\frac{a}{l}\sqrt{i^2+j^2}} + \sum_{i=1}^{\infty}V_0{}^{x}ie^{-\frac{a}{l}i}\right]$$

$$= I_{Border}{}^{x} + I_{Interior}{}^{x}$$

$$= \frac{V_0{}^{x}}{nr_0}\sum_{i=1}^{\infty}\left[2\sum_{j=1}^{\infty}e^{-\frac{a}{l}\sqrt{i^2+j^2}} + e^{-\frac{a}{l}i}\right]$$

Similarly, direct calculation or symmetry arguments will show that

$$I_{\Sigma}{}^{y} = \frac{V_0{}^{y}}{nr_0}\sum_{j=1}^{\infty}j\left[2\sum_{i=1}^{\infty}e^{-\frac{a}{l}\sqrt{i^2+j^2}} + e^{-\frac{a}{l}j}\right]$$

so that $I_{\Sigma}{}^{x}$ and $I_{\Sigma}{}^{y}$ both contain a prefactor multiplied by the appropriate component of the applied potential. Relabeling the dummy indices, it can be shown that the prefactors are the same for the x and y components of the current. Thus, the total current

magnitude is not dependent upon the angle of the applied voltage, so the current flow in the system is indeed isotropic in the general case. The current magnitude will be

$$I_{\Sigma} = \frac{V_0}{nr_0}\sum_{j=1}^{\infty} j\left[2\sum_{i=1}^{\infty} e^{-\frac{a}{l}\sqrt{i^2+j^2}} + e^{-\frac{a}{l}j}\right]$$

5.5: The Three Dimensional Regular Cubic Lattice

To complete our discussion of regular lattices, we consider the case of the three-dimensional lattice, as shown in **Figure 39**.

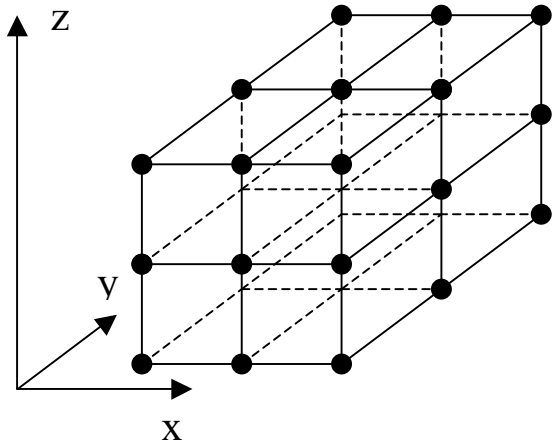

Figure 39: Illustration of a portion of a three-dimensional cubic lattice with Cartesian axes depicted for reference

The potential V_0 is applied along the x axis of the cubic system such that $V_{ijk} = \frac{V_0 i}{n}$.

Now we consider a single point in the lattice, for example a location (i,j,k). A pertinent question to answer is what the current flowing forward from such a location is.

5.5.1: The Next-Nearest Neighbor Case in the Cubic Lattice

First, we consider a very small localization scale l such that one only need take into consideration the nearest neighbors. We find that for ijk the relevant neighbors are

$[i+1, j, k]$ so that only one among the six neighbors in the cubic lattice is forward facing.

The current flowing in the link is $\frac{V_0}{nr_0} e^{-\frac{a}{l}}$. In one single face, the total forward current is

$$\frac{V_0}{nr_0} e^{-\frac{a}{l}} n^2 = \frac{V_0}{nr_0} e^{-\frac{a}{l}}$$

Figure 40 shows the geometry of such a situation.

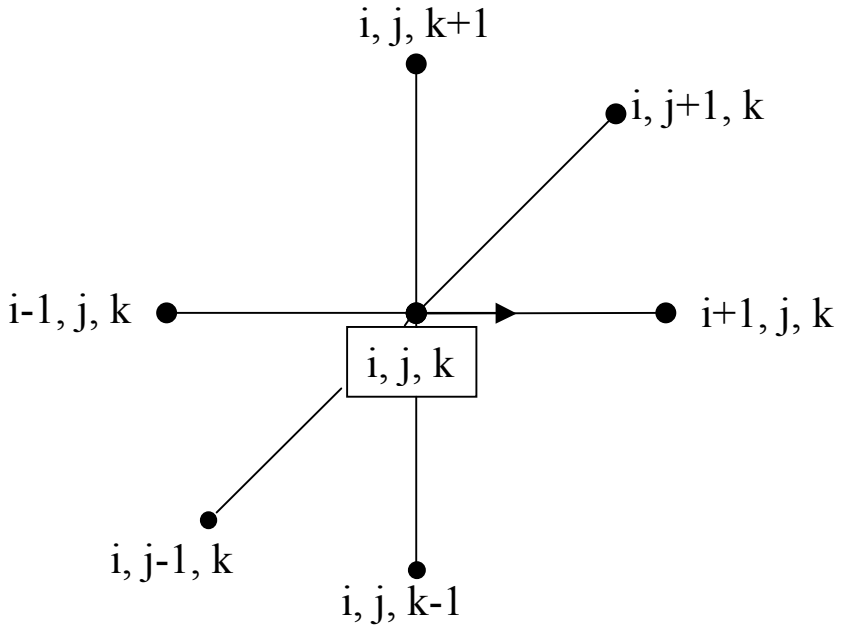

Figure 40: Perspective illustration of the nearest neighbor connection scheme in the three-dimensional cubic lattice

In the three-dimensional system the current will grow linearly in the size of the system as

$$I_{\Sigma} = \frac{nV_0}{r_0} e^{-\frac{a}{l}}$$

The total effective resistance proceeds from Ohm's Law, and has the form

$$R_{eq} = \frac{V_0}{I_{\Sigma}} = \frac{r_0}{n} e^{\frac{a}{l}}$$

5.5.2: The Extended Coupling Scheme for the Cubic Geometry

Beyond the nearest neighbors, the resistance will still decrease with the size of the system. However, the prefactor will be altered. We will now calculate this prefactor. The total current that flows in the forward direction will now have the form

$$I_{ijk} = \sum_{\Delta i=1}^{\infty} \sum_{\Delta j=-\infty}^{+\infty} \sum_{k=-\infty}^{+\infty} \frac{V_0}{n r_{\Delta i \Delta j \Delta k}}$$

for a single point (i, j, k). Using the symmetry of the cubic lattice we know that we should obtain the same result at each site in the cubic lattice for the forward flowing current. One finds

$$I_{\Delta i \Delta j \Delta k} = \sum_{\Delta i=1}^{\infty} \sum_{\Delta j=-\infty}^{+\infty} \sum_{k=-\infty}^{+\infty} \frac{V_0^{\Delta i}}{n r_0} e^{-\frac{r_{\Delta i \Delta j \Delta k}}{l}}$$

$$= \frac{V_0}{n r_0} \sum_{\Delta i=1}^{\infty} \sum_{\Delta j=-\infty}^{+\infty} \sum_{k=-\infty}^{+\infty} \Delta i e^{-\frac{a}{l}\sqrt{\Delta i^2 + \Delta j^2 + \Delta k^2}}$$

since in the three dimensional Cartesian system on has $r_{\Delta i \Delta j \Delta k} = a\sqrt{\Delta i^2 + \Delta j^2 + \Delta k^2}$ for the distance between two points.

This formula is correct in all regimes for the localization parameter l, but it is particularly useful in the intermediate regime where $a \sim l$. We obtained a simple result when $a >> l$. We also obtain a compact result when $l >> a$, and again the summation goes over to a Riemann sum and a volume integral. So we obtain:

$$I_{\Delta i \Delta j \Delta k} = \frac{V_0}{n r_0} \sum_{\Delta i=1}^{\infty} \sum_{\Delta j=-\infty}^{+\infty} \sum_{\Delta k=-\infty}^{+\infty} \Delta i e^{-\frac{a}{l}\sqrt{\Delta i^2 + \Delta j^2 + \Delta k^2}}$$

$$= \frac{V_0 a^{-4}}{nr_0} \sum_{\Delta i=1}^{\infty} \sum_{\Delta j=-\infty}^{+\infty} \sum_{\Delta k=-\infty}^{+\infty} a\Delta i e^{-\frac{a}{l}\sqrt{\Delta i^2+\Delta j^2+\Delta k^2}} a^3$$

$$= \frac{V_0 a^{-4}}{nr_0} \sum_{\Delta i=1}^{\infty} \sum_{\Delta j=-\infty}^{+\infty} \sum_{\Delta k=-\infty}^{+\infty} a\Delta i e^{-\frac{1}{l}\sqrt{a^2\Delta i^2+a^2\Delta j^2+a^2\Delta k^2}} a^3$$

$$= \frac{V_0 a^{-4}}{nr_0} \int_0^{\infty} \int_{-\infty}^{+\infty} \int_{-\infty}^{+\infty} x e^{-\frac{1}{l}\sqrt{x^2+y^2+z^2}} dxdydz$$

$$= \frac{V_0 a^{-4}}{nr_0} \int_0^{\infty} \int_0^{\pi} \int_{-\pi/2}^{\pi/2} \left(r\sin\theta\cos\phi\right) e^{-\frac{r}{l}} \left(r^2\sin\theta\right) drd\theta d\phi$$

Switching to spherical coordinates will aid in the evaluation of this integral, as illustrated in **Figure 41**.

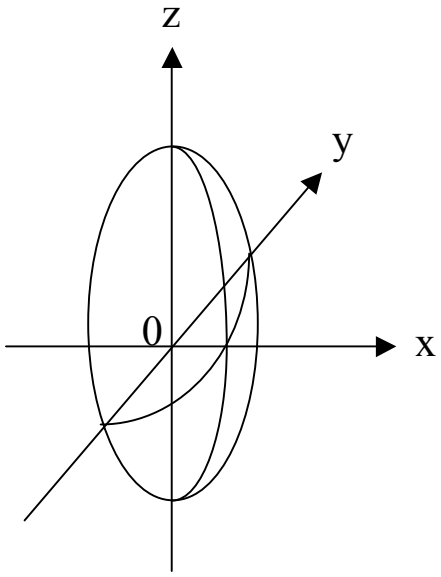

Figure 41: Spherical polar system superimposed on three-dimensional Cartesian axes

$$I_{\Delta i\Delta j\Delta k} = \frac{V_0 a^{-4}}{nr_0} \int_0^{\infty} \int_0^{\pi} \int_{-\pi/2}^{\pi/2} r^3 e^{-\frac{r}{l}} \cos\phi \sin^2\theta drd\theta d\phi$$

$$= \frac{V_0 a^{-4}}{nr_0} \int_0^{\infty} r^3 e^{-\frac{r}{l}} dr \int_0^{\pi} \sin^2\theta d\theta \int_{-\pi/2}^{\pi/2} \cos\phi d\phi$$

This decoupling of the integrals allows for their easy evaluation individually. We find that for the angular integrals $\int_0^{\pi} \sin^2\theta d\theta = \frac{\pi}{2}$ while $\int_{-\pi/2}^{\pi/2} \cos\phi = 2$. To evaluate the site current we evaluate the radial integral using the following property:

$$-\frac{d^3}{d\alpha^3}\int_0^{\infty} e^{-\alpha r} dr = \int_0^{\infty} r^3 e^{-\alpha r} dr$$

$$= -\frac{d^3}{d\alpha^3}\left[\frac{1}{\alpha}\right]$$

$$= \frac{6}{\alpha^4}$$

Hence, we see that the integral $\int_0^{\infty} r^3 e^{-\frac{r}{l}} dr = 6l^4$. So we see that

$$I_{\Delta i \Delta j \Delta k} = \frac{V_0 a^{-4}}{n r_0}\int_0^{\infty}\int_0^{\pi}\int_{-\pi/2}^{\pi/2} r^3 e^{-\frac{r}{l}} \cos\phi \sin^2\theta dr d\theta d\phi$$

$$= \frac{V_0 a^{-4}}{n r_0}\left(\frac{\pi}{2}\right)(2)\left(6l^4\right)$$

$$= 6\frac{\pi V_0}{n r_0}\left(\frac{l}{a}\right)^4$$

So the total current flowing is given by the expression

$$I_{\Delta i \Delta j \Delta k} = \frac{6\pi V_0 n}{r_0}\left(\frac{a}{l}\right)^4$$

Therefore the total equivalent resistance is given by the expression

$$R_{eq} = \frac{r_0}{6\pi n}\left(\frac{a}{l}\right)^4$$

CHAPTER 6

INTRODUCTION OF DISORDER: AN ANALYTICAL PERTURBATIVE CALCULATION IN ONE DIMENSION

In this treatment we hold the site energies constant and implement site disorder by introducing perturbations in the site positions. The computations will be amenable to numerical calculations. The goal is to study the effect of positional disorder on transport characteristics. Additionally, following the formalism of Pike and Seager and Miller and Abrahams, our model is mapped onto the task of calculating the transport characteristics of a random resistor network with an extended scheme.

Our goal is to introduce site disorder, but to exert control over the average magnitude of the positional perturbations. In this way, we will govern the strength of the perturbations and systematically study the effect of various disorder strengths on the sample conductivity.

We will eventually consider systems in two and three dimensions, though for now our focus is the one-dimensional case. Preliminarily, we expect that three-dimensional systems will be more robust with respect to disorder than the characteristics of two-dimensional geometries where disorder fluctuations have a more significant impact. When disorder, especially strong disorder are examined, calculations will always depend on the specific characteristics of the configuration of disorder for the individual system.

It is our program to make statements about the bulk limit where the system is so large that the individual disorder details average out, and the thermodynamic limit is obtained. One way to achieve the approximate bulk limit would be to perform disorder averaging by calculating conductances for a large number of systems, then averaging the

results. However, if one is able to study a large enough system, there will be little variation in the characteristics with respect to charge transport from one realization of disorder to another. This phenomenon is known as self-averaging, and this will be exploited in the numerical calculations we describe in this Master's Dissertation.

6.1: The One-Dimensional Case: A variable Range Hopping Picture

Another salient advantage of the one-dimensional case is the prospect of making analytical statements. Particularly simple is the case in which couplings are limited to nearest neighbors. A salient point is the characteristic of local charge conservation that prevents the accumulation of carriers at a lattice node. In fact, in terms of a specific system configuration with site positions subject to random perturbations in position, we may immediately record a valid expression for the total resistance and thus the current that flows through the entire system.

6.1.1: The Regular Unperturbed One-Dimensional Lattice

Let us consider a specific case to see how the transport characteristics are influenced with the introduction of site disorder. First, we'll examine a regular system where the nodes are equidistantly separated by a distance a, as shown in **Figure 42**.

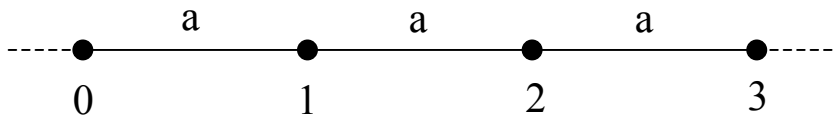

Figure 42: Unperturbed one-dimensional resistor network

Figure 42 shows a system containing four site members and a finite example of the pristine case with no disorder incorporated. For the regularly spaced system, we may

graph the potential, which varies linearly since drops across the resistors are identical, as shown in **Figure 43**.

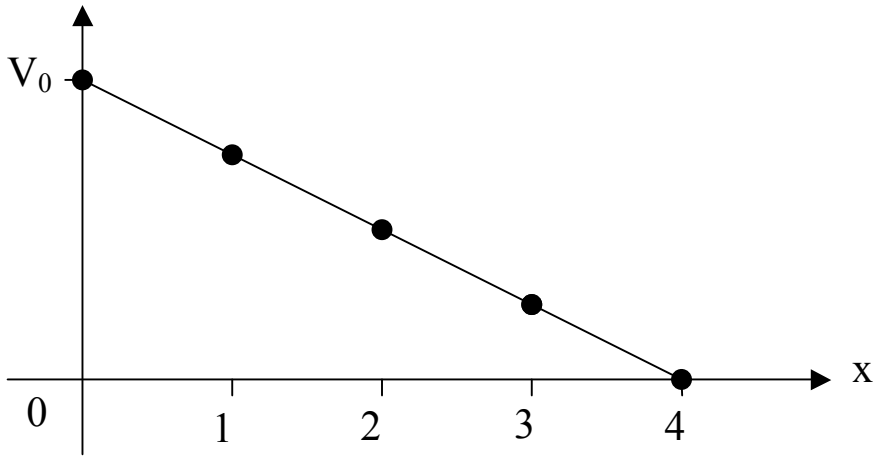

Figure 43: Graph of the node voltages for the unperturbed one-dimensional system

Since each gap is the same, they are equal to $\frac{V_0}{n} = \frac{V_0}{4}$. Since each resistance is $r_0 e^{\frac{a}{l}}$, the current flowing through the links is

$$\frac{\Delta V}{r} = \frac{V_0}{4r_0} e^{-\frac{a}{l}}$$

$$= \frac{V_0}{nr_0} e^{-\frac{a}{l}} \quad \text{(for the general case)}$$

So we see that even for the regular case, the current flowing is inversely proportional to the size of the system. Equivalently, the equivalent resistance grows linearly in the system size n. Our central task for the one-dimensional system is to learn if an average R_{eq} scales linearly or if it grows more rapidly. We will ask this question for a variety of coupling schemes, including the exponential dependence suggested by Pike and Seager.

6.1.2: Introducing Perturbations in the One-Dimensional Geometry

Now we consider a perturbed version of the preceding system where no disorder was present. Consider a system as shown in **Figure 44** where positional disorder has been introduced.

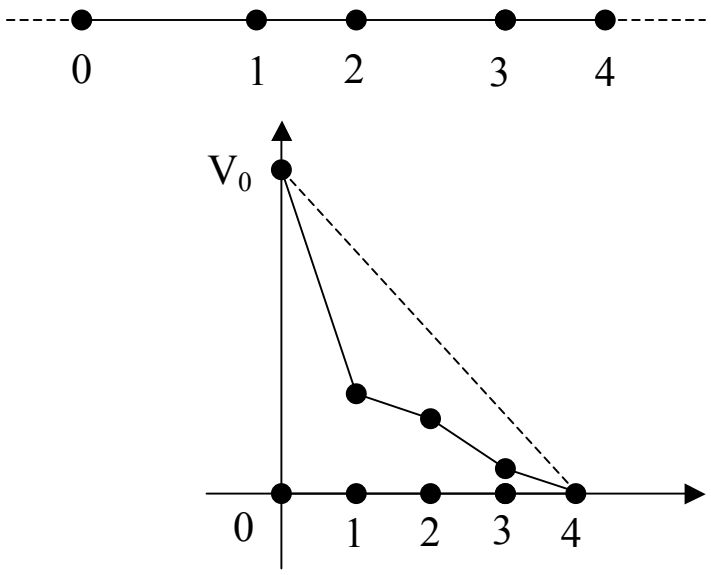

Figure 44: Above: Illustration of a one-dimensional resistor array with positional disorder. Below: graph of the voltages of the perturbed one-dimensional system; the horizontal axis is the node index number

From this graph it's obvious that introducing positional disorder disrupts the linearity of the voltage trace. The points are uniformly dispersed and hence not rendered to scale in a spatial sense. The more abrupt drops occur where intermodal gaps are especially large and, hence, where the corresponding resistances and the associated voltage drops are particularly large.

For the two-dimensional situation we may record a formula for the potential drop in terms of the flowing current. In this manner, we may glean the current itself in terms of the applied potential V_0. Therefore we have

$$V_0 = \sum_{i=0}^{n-1} I r_{i[i+1]}$$

$$= I \sum_{i=0}^{n-1} r_{i[i+1]}$$

So $I = \dfrac{V_0}{\sum_{i=0}^{n-1} r_{i[i+1]}}$ for the flowing current.

It is then our goal to gain an understanding of the characteristics of the equivalent resistance, which is simply the sum of the resistances in the system supercell.

$$R_{eq} = \sum_{i=0}^{n-1} r_{i[i+1]}$$

6.1.2.1: Introducing the Iso-Energetic Variable Range Hopping Picture

Consider the particle locations x_i. In the absence of a perturbation, the coordinates are $x_i = ia$ for a particular node. However, if we introduce the shifts in a random fashion, the new altered node locations are given by

$$x_i = ai + \delta_i$$

So if the resistance varies exponentially in the separation as

$$r_{i,i+1} = r_0 e^{\frac{1}{l}(x_{i+1} - x_i)}$$

$$= r_0 e^{\frac{a}{l}} e^{\frac{1}{l}[\delta_{i+1} - \delta_i]}$$

This formula reduces to the pristine formula $r_0 e^{\frac{a}{l}}$ if no perturbations are introduced.

A Taylor series expansion will permit us to determine the effect of the perturbations to various orders in the perturbation strength. For example, we specify that $\delta_i = \varepsilon y_i$ where y_i is a random variable with a value uniformly chosen between -1 and $+1$. In terms of these variables, the resistance is given by

$$r_{i,i+1} = r_0 e^{\frac{a}{l}} e^{\frac{1}{l}\varepsilon[y_{i+1}-y_i]}$$

We have introduced a perturbative parameter ε which may be manipulated in a systematic way to calculate a perturbative series for the shifts in the equivalent resistance.

Our goal is to identify specific trends in the system size n. First, we note that $e^n = 1 + n + \frac{1}{2}n^2 + \frac{1}{6}n^3 + \frac{1}{24}n^4 + ...$ via the Taylor Series expansion. It is worth noting that we want to calculate the mean total resistance, $\langle R_{eq} \rangle$. This will be done by averaging individually over each of the $[n]$ random variables y_i.

$$R_{eq} = \sum_{i=0}^{n-1} r_0 e^{\frac{a}{l}} e^{\frac{\varepsilon}{l}[y_{i+1}-y_i]}$$

$$= r_0 e^{\frac{a}{l}} \sum_{i=0}^{n-1} e^{\frac{\varepsilon}{l}[y_{i+1}-y_i]}$$

6.1.2.2: Evaluating the First Order Contribution

To start with, we expand to first order in ε. The result is

$$R_{eq} \approx r_0 e^{\frac{a}{l}} \sum_{i=0}^{n-1} \left[1 + \frac{\varepsilon}{l}(y_{i+1} - y_i) + ... \right]$$

$$= \left[r_0 e^{\frac{a}{l}} n \right] + r_0 e^{\frac{a}{l}} \left(\frac{\varepsilon}{l} \right) \sum_{i=0}^{n-1} (y_{i+1} - y_i) + O\left(\frac{\varepsilon}{l} \right)^2$$

Now to consider a concrete example in which only four nodes are present with $[n = 4]$. We also assume periodic boundary conditions such that $y_n = y_0$. To a first order approximation in ε we have

$$R_{eq} = \left[r_0 n e^{\frac{a}{l}} \right] + r_0 e^{\frac{a}{l}} \left(\frac{\varepsilon}{l} \right) [y_4 - y_3 + y_3 - y_2 + y_2 - y_1 + y_1 - y_0]$$

$$= \left[r_0 n e^{\frac{a}{l}} \right] + r_0 e^{\frac{a}{l}} \left(\frac{\varepsilon}{l} \right) \left[y_4 - y_0 \right]$$
$$= \left[r_0 n e^{\frac{a}{l}} \right] + 0 + 0 \left(\frac{\varepsilon}{l} \right)^2$$
$$= \left[r_0 n e^{\frac{a}{l}} \right]$$

Since $y_4 = y_0$, all contributions to a first order term mutually cancel. Therefore, there are no first order contributions so we see that $R_{eq} = r_0 e^{\frac{a}{l}} n$ to first order. Being that first order contributions are absent, we consider that the one-dimensional systems are robust with respect to random shifts in position. This tolerance of random shifts in the nodal positions is due to the fact that moving one node causes one resistance link to become longer, while another becomes shorter. Hence, the changes tend to cancel with no contribution to the total resistance at the first order level.

6.1.2.3: Including Second Order Contributions

Next we consider the case of second and higher order contributions. To second order in ε, on has

$$R_{eq} = r_0 e^{\frac{a}{l}} \sum_{i=0}^{n-1} e^{\frac{a}{l}[y_{i+1} - y_i]}$$
$$= \left[n r_0 e^{\frac{a}{l}} \right] + r_0 e^{\frac{a}{l}} \left(\frac{\varepsilon}{l} \right) \sum_{i=0}^{n-1} \left(y_{i+1} - y_i \right) + \frac{1}{2} r_0 e^{\frac{a}{l}} \left(\frac{\varepsilon}{l} \right)^2 \sum_{i=0}^{n-1} \left(y_{i+1} - y_i \right)^2$$

Then one finds

$$\left\langle R_{eq} \right\rangle = \left[n r_0 e^{\frac{a}{l}} \right] + \frac{r_0}{2} e^{\frac{a}{l}} \left(\frac{\varepsilon}{l} \right)^2 \sum_{i=0}^{n-1} \left\langle \left({y_{i+1}}^2 + {y_i}^2 - 2 y_{i+1} y_i \right) \right\rangle$$
$$= {R_{eq}}^0 + \frac{r_0}{2} e^{\frac{a}{l}} \left(\frac{\varepsilon}{l} \right)^2 \left\langle \sum_{i=0}^{n-1} {y_{i+1}}^2 + \sum_{i=0}^{n-1} {y_i}^2 - 2 \sum_{i=0}^{n-1} y_{i+1} y_i \right\rangle$$

Before calculating the average over all possible disorder configurations, a couple things bear mentioning. First, we notice from the periodicity condition that $\sum_{i=0}^{n-1} y_i^{\,2} = \sum_{i=0}^{n-1} y_{i+1}^{\,2}$. So up to second order in $\frac{\varepsilon}{l}$ on has for a particular realization of disorder that

$$\left\langle R_{eq} \right\rangle = R_{eq}^{\,0} + \frac{r_0 e^{\frac{a}{l}}}{2}\left(\frac{\varepsilon}{l}\right)^2 \left[2\sum_{i=0}^{n-1} y_i^{\,2} - 2\sum_{i=0}^{n-1} y_{i+1} y_i \right]$$

$$= R_{eq}^{\,0} + \left\langle r_0 e^{\frac{a}{l}}\left(\frac{\varepsilon}{l}\right)^2 \left[\sum_{i=0}^{n-1} y_i^{\,2} - \sum_{i=0}^{n-1} y_i y_{i+1} \right] \right\rangle$$

$$= R_{eq}^{\,0} + r_0 e^{\frac{a}{l}}\left(\frac{\varepsilon}{l}\right)^2 \left\langle \sum_{i=0}^{n-1} y_i^{\,2} - \sum_{i=0}^{n-1} y_i y_{i+1} \right\rangle$$

Linearity of the averaging allows for separation of the terms in angle brackets so they can be considered individually. One has

$$\left\langle R_{eq} \right\rangle = n r_0 e^{\frac{a}{l}} + r_0 e^{\frac{a}{l}}\left(\frac{\varepsilon}{l}\right)^2 \left\{ \left\langle \sum_{i=0}^{n-1} y_i^{\,2} \right\rangle - \left\langle \sum_{i=0}^{n-1} y_i y_{i+1} \right\rangle \right\}$$

Furthermore, we know from the linearity of the mean that $\left\langle \sum_{i=0}^{n-1} y_i^{\,2} \right\rangle = \sum_{i=0}^{n-1} \left\langle y_i^{\,2} \right\rangle$. The task is now reduced to calculating an average of the form $\left\langle y_j^{\,2} \right\rangle$. This average has the form

$$\left\langle y_j^{\,2} \right\rangle = \frac{\int_{-1}^{+1} \left[y_j \right]^2 dy_j}{\int_{-1}^{+1} dy_j}$$

$$= \frac{1}{2}\int_{-1}^{+1} \left[y_j \right]^2 dy_j$$

$$= \frac{1}{3}$$

Hence, we see that $\sum_{i=0}^{n-1}\left\langle y_i^{\,2}\right\rangle = \frac{n}{3}$. Now we'll consider the second of the sums

$\left\langle \sum_{i=0}^{n-1} y_i y_{i+1} \right\rangle = \sum_{i=0}^{n-1}\left\langle y_i y_{i+1}\right\rangle$. We now need to calculate an average of the form $\left\langle y_j y_{j+1}\right\rangle$. The result is

$$\left\langle y_j y_{j+1}\right\rangle = \frac{\int_{-1}^{+1}\int_{-1}^{+1} y_j y_{j+1} dy_j dy_{j+1}}{\int_{-1}^{+1}\int_{-1}^{+1} dy_j dy_{j+1}}$$

The integrations decouple in the following way:

$$\left\langle y_j y_{j+1}\right\rangle = \frac{\left(\int_{-1}^{+1} y_j dy_j\right)\left(\int_{-1}^{+1} y_{j+1} dy_{j+1}\right)}{\left(\int_{-1}^{+1} dy_j\right)\left(\int_{-1}^{+1} dy_{j+1}\right)}$$

The integrands are both zero, so the average vanishes, yielding

$$\left\langle y_j y_{j+1}\right\rangle = 0$$

The equivalent resistance may be calculated to second order in the perturbing influence $\left(\frac{\varepsilon}{l}\right)$ as

$$\left\langle R_{eq}\right\rangle = r_0 e^{\frac{a}{l}} n\left[1 + \frac{1}{3}\left(\frac{\varepsilon}{l}\right)^2\right]$$

So the contributions so far will scale as n. Hence, the increase in resistance does not appear to be hastened in the expansion of the sample size n.

6.1.2.4: Incorporating Third and Higher Order Effects

Now we will calculate the third order terms. One finds that the third order piece in $\left(\frac{\varepsilon}{l}\right)$ has the form

$$r_0 e^{\frac{a}{l}} \sum_{i=0}^{n-1} \left(\frac{\varepsilon}{l}\right)^3 \frac{1}{6}\left[y_{i+1} - y_i\right]^3 = \frac{r_0 e^{\frac{a}{l}}}{6}\left(\frac{\varepsilon}{l}\right)^3 \sum_{i=0}^{n-1}\left[{y_{i+1}}^3 - 3{y_{i+1}}^2 y_i + 3y_{i+1}{y_i}^2 - {y_i}^3\right]$$

$$= \frac{r_0 e^{\frac{a}{l}}}{6}\left(\frac{\varepsilon}{l}\right)^3 \sum_{i=0}^{n-1}\left[\left({y_{i+1}}^3 - {y_i}^3\right) + 3\left(y_{i+1}{y_i}^2 - {y_{i+1}}^2 y_i\right)\right]$$

In the sum, both cubic terms vanish outright with no averaging needed. The third order piece then takes the form $\frac{r_0}{2} e^{\frac{a}{l}}\left(\frac{\varepsilon}{l}\right)^3 \sum_{i=0}^{n-1}\left(y_{i+1}{y_i}^2 - {y_{i+1}}^2 y_i\right)$. The ensemble averaged contribution will take the form

$$\frac{r_0}{2} e^{\frac{a}{l}}\left(\frac{\varepsilon}{l}\right)\sum_{i=0}^{n-1}\left(\left\langle y_{i+1}{y_i}^2\right\rangle - \left\langle {y_{i+1}}^2 y_i\right\rangle\right)$$

The task now is to calculate each of these expectation values.

$$\left\langle y_{j+1}{y_j}^2\right\rangle = \frac{\int_{-1}^{+1}\int_{-1}^{+1} y_{j+1}{y_j}^2 dy_{j+1}dy_j}{\int_{-1}^{+1}\int_{-1}^{+1} dy_{j+1}dy_j}$$

Once again, the integrals decouple, yielding

$$\left\langle y_{j+1}{y_j}^2\right\rangle = \frac{\int_{-1}^{+1} y_{j+1}dy_{j+1}\int_{-1}^{+1}{y_j}^2 dy_j}{\int_{-1}^{+1} dy_{j+1}\int_{-1}^{+1} dy_j}$$

The first integral in the numerator vanishes, so one has $\left\langle y_{j+1}{y_j}^2\right\rangle$ and $\sum_{i=0}^{n-1}\left\langle y_{i+1}{y_i}^2\right\rangle = 0$.

Similarly, one also finds that $\sum_{i=0}^{n-1} -\left\langle {y_{i+1}}^2 y_i\right\rangle = 0$. Therefore, we conclude that the third order contribution vanishes.

Now we will calculate the fourth order contribution. The term will be of the form

$$\frac{1}{24}\left(r_0 e^{\frac{a}{l}}\right)\left(\frac{\varepsilon}{l}\right)^4 \sum_{i=0}^{n-1}\left(y_{i+1} - y_i\right)^4 = \frac{1}{24} r_0 e^{\frac{a}{l}}\left(\frac{\varepsilon}{l}\right)^4 \sum_{i=0}^{n-1}\left({y_{i+1}}^4 - 4{y_{i+1}}^3 y_i + 6{y_{i+1}}^2 {y_i}^2 - 4y_{i+1}{y_i}^3 + {y_i}^4\right)$$

When we calculate the ensemble average, we will need to evaluate five terms. However, we've established that the second and fourth terms vanish due to the presence of odd powers which will ultimately contribute to a zero average. Furthermore, by virtue of periodicity, we know that $\sum_{i=0}^{n-1} {y_i}^4 = \sum_{i=0}^{n-1} {y_{i+1}}^4$. Thus, the quantity now becomes

$$\frac{1}{24} r_0 e^{\frac{a}{l}\left(\frac{\varepsilon}{l}\right)^4} \left[2\sum_{i=0}^{n-1} \left\langle {y_i}^4 \right\rangle + 6\sum_{i=0}^{n-1} \left\langle {y_{i+1}}^2 {y_i}^2 \right\rangle \right] = \frac{r_0 e^{\frac{a}{l}\left(\frac{\varepsilon}{l}\right)^4}}{12} \left[\sum_{i=0}^{n-1} \left\langle {y_i}^4 \right\rangle + 3\sum_{i=0}^{n-1} \left\langle {y_{i+1}}^2 {y_i}^2 \right\rangle \right]$$

The first term gives

$$\left\langle {y_i}^4 \right\rangle = \frac{\int_{-1}^{+1} {y_j}^4 dy_j}{\int_{-1}^{+1} dy_j} = \frac{1}{5}$$

Next we calculate $\left\langle {y_{j+1}}^2 {y_j}^2 \right\rangle$. The result is

$$\left\langle {y_j}^2 {y_{j+1}}^2 \right\rangle = \frac{\int_{-1}^{+1}\int_{-1}^{+1} {y_j}^2 {y_{j+1}}^2 dy_j dy_{j+1}}{\int_{-1}^{+1}\int_{-1}^{+1} dy_j dy_{j+1}}$$

$$= \frac{\left[\int_{-1}^{+1} {y_j}^2 dy_j\right]\left[\int_{-1}^{+1} {y_{j+1}}^2 dy_{j+1}\right]}{\left[\int_{-1}^{+1} dy_j \int_{-1}^{+1} dy_{j+1}\right]}$$

As shown in the above step, the integrals decouple. Noting that $\int_{-1}^{+1} {y_j}^2 dy_j = \frac{2}{3}$, we see that

$$\left\langle {y_j}^2 {y_{j+1}}^2 \right\rangle = \frac{1}{9}$$

Thus the fourth order term becomes

$$\frac{r_0 e^{\frac{a}{l}\left(\frac{\varepsilon}{l}\right)^4}}{12} \left[\sum_{i=0}^{n-1} \left\langle {y_i}^4 \right\rangle + 3\sum_{i=0}^{n-1} \left\langle {y_{i+1}}^2 {y_i}^2 \right\rangle \right] = \frac{2nr_0}{45} e^{\frac{a}{l}\left(\frac{\varepsilon}{l}\right)^4}$$

Up to fourth order, we have $\left\langle R_{eq} \right\rangle = nr_0 e^{\frac{a}{l}} \left[1 + \frac{1}{3}\left(\frac{\varepsilon}{l}\right)^2 + \frac{2}{45}\left(\frac{\varepsilon}{l}\right)^4 + ... \right]$. Now it becomes advantageous to calculate higher order terms. We will use Padé analysis to extend the scope of applicability of the perturbative series and efficiently obtain accurate results. One finds that

$$\left\langle \frac{r_0 e^{\frac{a}{l}}}{120} \sum_{i=0}^{n-1} \left(y_{i+1} - y_i \right)^5 \right\rangle \left(\frac{\varepsilon}{l}\right)^5 = \frac{r_0 e^{\frac{a}{l}}}{120} \left(\frac{\varepsilon}{l}\right)^5 \sum_{i=0}^{n-1} \left\langle \left(y_{i+1} - y_i \right)^5 \right\rangle$$

$$= \frac{r_0 e^{\frac{a}{l}}}{120} \left(\frac{\varepsilon}{l}\right)^5 \sum_{i=0}^{n-1} \left\langle {y_{i+1}}^5 - 5{y_{i+1}}^4 y_i + 10{y_{i+1}}^3 {y_i}^2 - 10{y_{i+1}}^2 {y_i}^3 + 5 y_{i+1} {y_i}^4 - {y_i}^5 \right\rangle = 0$$

Since all terms involve a single displacement raised to an odd power, they will be as often positive as negative under the configuration average, and there is no net contribution.

Thus, we will focus on the sixth order term for the next non-zero contribution. One finds that for the sixth order case

$$\left\langle \frac{r_0 e^{\frac{a}{l}}}{720} \sum_{i=0}^{n-1} \left(y_{i+1} - y_i \right)^6 \right\rangle \left(\frac{\varepsilon}{l}\right)^6 = \frac{r_0 e^{\frac{a}{l}}}{720} \left(\frac{\varepsilon}{l}\right)^6 \sum_{i=0}^{n-1} \left[\begin{array}{l} \left\langle {y_{i+1}}^6 \right\rangle - 6\left\langle {y_{i+1}}^5 y_i \right\rangle + 15\left\langle {y_{i+1}}^4 {y_i}^2 \right\rangle - 20\left\langle {y_{i+1}}^3 {y_i}^3 \right\rangle + 15\left\langle {y_{i+1}}^2 {y_i}^4 \right\rangle \\ -6\left\langle y_{i+1} {y_i}^5 \right\rangle + \left\langle {y_i}^6 \right\rangle \end{array} \right]$$

Noting that terms with odd displacement powers will vanish after averaging over disorder leads to

$$\frac{r_0 e^{\frac{a}{l}}}{720} \left(\frac{\varepsilon}{l}\right)^6 \sum_{i=0}^{n-1} \left[\left\langle {y_{i+1}}^6 \right\rangle + 15\left\langle {y_{i+1}}^4 {y_i}^2 \right\rangle + 15\left\langle {y_{i+1}}^2 {y_i}^4 \right\rangle + \left\langle {y_i}^6 \right\rangle \right]$$

After exploiting the periodicity condition and combining terms, one now has

$$\frac{r_0 e^{\frac{a}{l}}}{720}\left(\frac{\varepsilon}{l}\right)^6 \sum_{i=0}^{n-1}\left[2\left\langle {y_i}^6\right\rangle + 15\left\langle {y_{i+1}}^4 {y_i}^2\right\rangle + 15\left\langle {y_{i+1}}^2 {y_i}^4\right\rangle\right]$$

Now to evaluate the terms contained in the summation.

$$\left\langle {y_j}^6\right\rangle = \frac{\int_{-1}^{+1} {y_j}^6 dy_j}{\int_{-1}^{+1} dy_j} = \frac{1}{7}$$

Furthermore, we find that

$$\left\langle {y_{j+1}}^4 {y_j}^4\right\rangle = \frac{\int_{-1}^{+1}\int_{-1}^{+1} {y_{j+1}}^4 {y_j}^4 dy_j dy_{j+1}}{\int_{-1}^{+1}\int_{-1}^{+1} dy_j dy_{j+1}}$$

$$= \frac{\int_{-1}^{+1} {y_{j+1}}^4 dy_{j+1}\int_{-1}^{+1} {y_j}^2 dy_j}{\int_{-1}^{+1} dy_j \int_{-1}^{+1} dy_{j+1}} = \frac{1}{15}$$

Using the same reasoning we find that $\left\langle {y_{j+1}}^2 {y_j}^4\right\rangle = \frac{1}{15}$. We can now evaluate the sixth order term, which will be

$$\frac{r_0 e^{\frac{a}{l}}}{720}\left(\frac{\varepsilon}{l}\right)^6 \sum_{i=0}^{n-1}\left[2\left\langle {y_i}^6\right\rangle + 15\left\langle {y_{i+1}}^4 {y_i}^2\right\rangle + 15\left\langle {y_{i+1}}^2 {y_i}^4\right\rangle\right] = \frac{r_0 e^{\frac{a}{l}}}{315}\left(\frac{\varepsilon}{l}\right)^6 n$$

So to the sixth order, the perturbative series has the form

$$\left\langle R_{eq}\right\rangle = \left(n r_0 e^{\frac{a}{l}}\right)\left[1 + \frac{1}{3}\left(\frac{\varepsilon}{l}\right)^2 + \frac{2}{45}\left(\frac{\varepsilon}{l}\right)^4 + \frac{1}{315}\left(\frac{\varepsilon}{l}\right)^6 + \ldots\right]$$

It is still beneficial to calculate additional higher order terms. In calculating these higher order terms, we take note of the fact that $\left\langle y_i\right\rangle^M = \frac{\int_{-1}^{+1} {y_i}^M dy_i}{\int_{-1}^{+1} dy_i} = \left(\frac{1}{M+1}\right)$ to facilitate the calculations. So the eighth order term is given by

$$\left\langle \frac{r_0 e^{\frac{a}{l}}}{40{,}320}\sum_{i=0}^{N-1}\left(y_{i+1}-y_i\right)^8 \right\rangle \left(\frac{\varepsilon}{l}\right)^8 = \left(\frac{\varepsilon}{l}\right)^8 \frac{r_0 e^{\frac{a}{l}}}{8!}\sum_{i=0}^{N-1}\left\langle \begin{matrix} y_i{}^8 - 8y_i{}^7 y_{i+1} + 28y_i{}^6 y_{i+1}{}^2 - 56y_i{}^5 y_{i+1}{}^3 + 78y_i{}^4 y_{i+1}{}^4 - 56y_i{}^3 y_{i+1}{}^5 \\ +28y_i{}^2 y_{i+1}{}^6 - 8y_i y_{i+1}{}^7 + y_i{}^8 \end{matrix} \right\rangle$$

After eliminating the odd powers of y_i we find

$$\left(\frac{\varepsilon}{l}\right)^8 \frac{r_0 e^{\frac{a}{l}}}{8!}\sum_{i=0}^{N-1}\left[\begin{matrix} \left\langle y_i{}^8 \right\rangle + 28\left\langle y_i{}^6 \right\rangle\left\langle y_{i+1}{}^2 \right\rangle + 70\left\langle y_i{}^4 \right\rangle\left\langle y_{i+1}{}^4 \right\rangle \\ +28\left\langle y_i{}^2 \right\rangle\left\langle y_{i+1}{}^6 \right\rangle + \left\langle y_i{}^8 \right\rangle \end{matrix} \right] = \left(\frac{\varepsilon}{l}\right)^8 \frac{r_0 e^{\frac{a}{l}}}{8!}\sum_{i=0}^{N-1}\left[2\left\langle y^8 \right\rangle + 56\left\langle y^6 \right\rangle\left\langle y^2 \right\rangle + 70\left\langle y^4 \right\rangle\left\langle y^4 \right\rangle\right]$$

where the right side of the equation exploits the periodicity characteristic. Thus we have for the eighth order term

$$\left(\frac{\varepsilon}{l}\right)^8 \frac{Nr_0}{8!} e^{\frac{a}{l}}\left[\frac{2}{9} + 56\left(\frac{1}{7}\right)\left(\frac{1}{3}\right) + 70\left(\frac{1}{25}\right)\right] = Nr_0\left(\frac{\varepsilon}{l}\right)^8 \frac{2}{14{,}175}$$

It becomes clear that the higher order terms rapidly diminish. Hence, the equivalent resistance is of the form

$$\left\langle R_{eq} \right\rangle = \left(Nr_0 e^{\frac{a}{l}}\right)\left[1 + \frac{1}{3}\left(\frac{\varepsilon}{l}\right)^2 + \frac{2}{45}\left(\frac{\varepsilon}{l}\right)^4 + \frac{1}{315}\left(\frac{\varepsilon}{l}\right)^6 + \frac{2}{14{,}175}\left(\frac{\varepsilon}{l}\right)^8 + O\left(\frac{\varepsilon}{l}\right)^{10}\right]$$

The total current is calculated by dividing the total potential difference V_0 by the total resistance $\left\langle R_{eq} \right\rangle$. This yields

$$I = \frac{V_0}{Nr_0} e^{\frac{-a}{l}}\left[1 + a_2\left(\frac{\varepsilon}{l}\right)^2 + a_4\left(\frac{\varepsilon}{l}\right)^4 + a_6\left(\frac{\varepsilon}{l}\right)^6 + a_8\left(\frac{\varepsilon}{l}\right)^8\right]^{-1}$$

where the coefficients are $a_2 = \frac{1}{3}$, $a_4 = \frac{2}{45}$, $a_6 = \frac{1}{315}$, and $a_8 = \frac{2}{14{,}175}$. This series may be inverted with the aid of formalism given elsewhere [arxiv:0902.4675(math-ph)]. We may conveniently calculate the reciprocal of the series. One will find

$$I = \frac{V_0}{Nr_0} e^{-\frac{a}{l}} \left(\begin{array}{l} 1 + \left(\frac{\varepsilon}{l}\right)^2 \left[a_2 d_1\right] + \left(\frac{\varepsilon}{l}\right)^4 \left[d_1 a_4 + \frac{1}{2} d_2 a_2{}^2 \right] + \left(\frac{\varepsilon}{l}\right)^6 \left[d_1 a_6 + d_2 a_4 a_2 + \frac{1}{3!} d_3 a_2{}^3 \right] \\ + \left(\frac{\varepsilon}{l}\right)^8 \left[d_1 a_8 + d_2 a_6 a_2 + \frac{1}{2} d_2 a_4{}^2 + \frac{1}{2} d_3 a_4 a_2{}^2 + \frac{1}{4!} d_4 a_2{}^4 \right] \end{array} \right)$$

where the derivatives are $d_1 = -1$, $d_2 = 2$, $d_3 = -6$, and $d_4 = 24$.

$$I = \frac{V_0}{Nr_0} \left(1 + b_2 \left[\frac{\varepsilon}{l}\right]^2 + b_4 \left[\frac{\varepsilon}{l}\right]^4 + b_6 \left[\frac{\varepsilon}{l}\right]^6 + b_8 \left[\frac{\varepsilon}{l}\right]^8 + \ldots \right)$$

The individual coefficients are given by

$$b_2 = d_1 a_2 = -\frac{1}{3}$$

$$b_4 = \left[d_1 a_4 + \frac{1}{2} d_2 a_2{}^2 \right] = -a_4 + a_2{}^2 = -\frac{2}{15} + \frac{1}{9} = \frac{1}{15}$$

$$b_6 = \left[d_1 a_6 + d_2 a_4 a_2 + \frac{1}{6} d_3 a_2{}^3 \right] = -a_6 + 2a_4 a_2 - a_3{}^3 = \frac{-1}{315} + \frac{4}{135} - \frac{1}{27} = \frac{-2}{189}$$

$$b_8 = \left[d_1 a_8 + d_2 a_6 a_2 + \frac{1}{2} d_2 a_4{}^2 + \frac{1}{2} d_3 a_4 a_2{}^2 + \frac{1}{24} d_4 a_2{}^4 \right] = \frac{-2}{14{,}175} + \frac{2}{945} + \frac{4}{2025} - \frac{2}{135} + \frac{1}{81} = \frac{1}{675}$$

6.1.2.5: Padé Analysis of the Perturbative Series

Padé analysis provides a way to account accurately and compactly for the characteristics of the function represented by the series. The Padé approximant has the form $P_M^N(x) = \frac{\alpha_0 + \alpha_1 x + \ldots + \alpha_N x^N}{1 + \beta_1 x + \ldots + \beta_M x^M}$ which will be used to represent a series of the form $S(x) = c_0 + c_1 x + \ldots + c_{N+M} x^{N+M}$. To obtain a unique set of coefficients for the approximant, we impose the condition that the number of "α" and "β" coefficients be the same as the total number of "c" coefficients. The advantage to using the Padé approximant is its ability to take into account singular behavior by virtue of zeros in the denominator of the approximant.

To calculate the currents, we will construct $P_1^1(x)$ and $P_2^2(x)$ where $x \equiv \left(\frac{\varepsilon}{l}\right)^2$ is used for the parameter of the perturbation. First we will construct the general case, then we will specialize to the case of interest, the one-dimensional perturbed chain. The goal is to compare the Padé approximant by comparing the values of $P_1^1\left(\frac{\varepsilon}{l}\right)$ and $P_2^2\left(\frac{\varepsilon}{l}\right)$ as ε ranges from 0 to $\frac{a}{2}$. This range encompasses the full range from an ordered crystalline system to an amorphous medium where the sites are randomly distributed.

Calculation of $P_1^1(x)$

One starts with $P_1^1(x) = \frac{\alpha_0 + \alpha_1 x}{1 + \beta_1 x}$. There are three unknown coefficients, so we use the condition

$$\frac{\alpha_0 + \alpha_1 x}{1 + \beta_1 x} = c_0 + c_1 x + c_2 x^2$$

Which leads to

$$\alpha_0 + \alpha_1 x = \left(1 + \beta_1 x\right)\left(c_0 + c_1 x + c_2 x^2\right)$$

Order by order in x, we equate coefficients on both sides of the equation. One finds

$$\begin{aligned} \alpha_0 &= c_0 \\ \alpha_1 &= \left(c_1 + \beta_1 c_0\right) \\ 0 &= \left(\beta_1 c_1 + c_2\right) \end{aligned}$$

So $\beta_1 = \frac{-c_2}{c_1}$ and $\alpha_1 = c_1 - \frac{c_0 c_2}{c_1} = \frac{1}{c_1}\left(c_1^{\,2} - c_0 c_2\right)$. So it becomes clear that

$$P_1^1(x) = \frac{\alpha_0 + \alpha_1 x}{1 + \beta_1 x}$$

$$= \left(\frac{c_1 c_0 + x\left[{c_1}^2 - c_0 c_2 \right]}{c_1 - c_2 x} \right)$$

Calculation of $P_2^2(x)$

Here we calculate $P_2^2(x)$ in the general case. One has

$$P_2^2(x) = \frac{\alpha_0 + \alpha_1 x + \alpha_2 x^2}{1 + \beta_1 x + \beta_2 x^2}$$

$$= c_0 + c_1 x + c_2 x^2 + c_3 x^3 + c_4 x^4$$

Using the same logic as in calculating $P_1^1(x)$ gives

$$\alpha_0 + \alpha_1 x + \alpha_2 x^2 = \left(1 + \beta_1 x + \beta_2 x^2\right)\left(c_0 + c_1 x + c_2 x^2 + c_3 x^3 + c_4 x^4\right)$$

Again, we equate the coefficients of x order by order. The result is

$$\begin{aligned}
\alpha_0 &= c_0 \\
\alpha_1 &= \left(c_0 \beta_1 + c_1\right) \\
\alpha_2 &= \left(c_0 \beta_2 + c_1 \beta_1 + c_2\right) \\
0 &= \left(c_1 \beta_2 + c_2 \beta_1 + c_3\right) \\
0 &= \left(c_2 \beta_2 + c_3 \beta_1 + c_4\right)
\end{aligned}$$

To calculate the "β" coefficients the lower two equations will be used. Kramer's rule permits one to write

$$\beta_1 = \frac{\begin{vmatrix} -c_3 & c_1 \\ -c_4 & c_2 \end{vmatrix}}{\begin{vmatrix} c_2 & c_1 \\ c_3 & c_2 \end{vmatrix}} = \frac{\left(c_4 c_1 - c_3 c_2\right)}{\left({c_2}^2 - c_1 c_3\right)}$$

β_2 is calculated the same way

$$\beta_2 = \frac{\begin{vmatrix} c_2 & -c_3 \\ c_3 & -c_4 \end{vmatrix}}{\begin{vmatrix} c_2 & c_1 \\ c_3 & c_2 \end{vmatrix}} = \frac{{c_3}^2 - c_2 c_4}{\left(-c_1 c_3 + {c_2}^2\right)}$$

α_1 and α_2 are obtained via back substitution.

$$\alpha_1 = c_0\beta_1 + c_1$$

$$= \frac{c_0\left(c_4c_1 - c_3c_2\right) + c_1{c_2}^2 - {c_1}^2c_3}{{c_2}^2 - c_1c_3}$$

$$\alpha_2 = \frac{c_0\left({c_3}^2 - c_2c_4\right) + \left(c_4{c_1}^2 - c_1c_2c_3\right) + \left({c_2}^3 - c_1c_2c_3\right)}{{c_2}^2 - c_1c_3}$$

Despite the difficulty in calculating the "α" and "β" coefficients for $P_2^2(x)$, we may still obtain specific formulas for the current for the perturbed one-dimensional system.

We first calculate $P_1^1(x)$

$$P_1^1(x) = \frac{\alpha_0 + \alpha_1 x}{1 + \beta_1 x} = \frac{\alpha_0 + \alpha_1\left[\frac{\varepsilon}{l}\right]^2}{1 + \beta_1\left[\frac{\varepsilon}{l}\right]^2}$$

for the primary series

$$S\left(\left[\frac{\varepsilon}{l}\right]\right) = 1 + \frac{-1}{3}\left[\frac{\varepsilon}{l}\right]^2 + \frac{1}{15}\left[\frac{\varepsilon}{l}\right]^4$$

The merit of considering $P_1^1\left(\left[\frac{\varepsilon}{l}\right]\right)$ lies mainly in the fact that we need only examine contributions up to fourth order in the parameter $\frac{\varepsilon}{l}$ specifying the strength of the perturbation. Specifically, we have

$$P_1^1\left(\left[\frac{\varepsilon}{l}\right]^2\right) = \frac{1 - \frac{2}{15}\left(\frac{\varepsilon}{l}\right)^2}{1 + \frac{1}{5}\left(\frac{\varepsilon}{l}\right)^2}$$

It can be shown via direct calculation that this approximant yields the correct series expansion up to fourth order in $\left(\frac{\varepsilon}{l}\right)$.

Now we need to calculate $P_2^2\left(\left[\frac{\varepsilon}{l}\right]^2\right)$. We find that

$$\alpha_0 = 1 \qquad \beta_1 = \frac{3}{13}$$
$$\alpha_1 = -\frac{4}{39} \qquad \beta_2 = \frac{59}{495}$$
$$\alpha_2 = \frac{17}{4095}$$

so that $P_2^2\left(\left[\frac{\varepsilon}{l}\right]^2\right) = \left[\frac{1 - \frac{4}{39}\left(\frac{\varepsilon}{l}\right)^2 + \frac{17}{4095}\left(\frac{\varepsilon}{l}\right)^4}{1 + \frac{3}{13}\left(\frac{\varepsilon}{l}\right)^2 + \frac{59}{4095}\left(\frac{\varepsilon}{l}\right)^4}\right]$ which we have directly verified as providing the correct series up to eighth order in $\left(\frac{\varepsilon}{l}\right)$.

We now examine the relative performance of the approximants by preparing graphs where ε ranges from 0 to 0.5 for various values of the localization scale l. These are shown in **Graphs 6** and **7** for the cases $l = 0.5$, $l = 1.0$, and $l = 2.0$. The dashed line indicates the $P_1^1\left(\left[\frac{\varepsilon}{l}\right]^2\right)$ curve while the solid line corresponds to $P_2^2\left(\left[\frac{\varepsilon}{l}\right]^2\right)$.

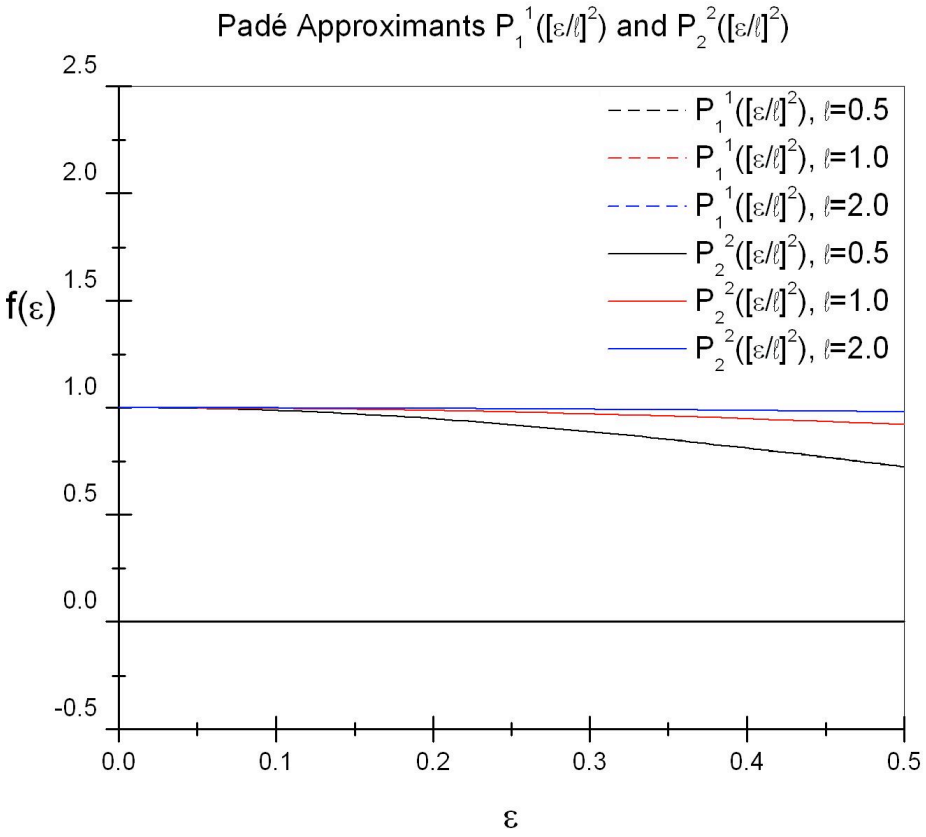

Graph 6: Graph of Padé Approximants with respect to the perturbing influence ε. The currents correspond to various values of the localization length l expressed in units of lattice constants. The dashed lines are for simpler approximants calculated from the fourth order series, and the solid lines are for approximants calculated for the eighth order series.

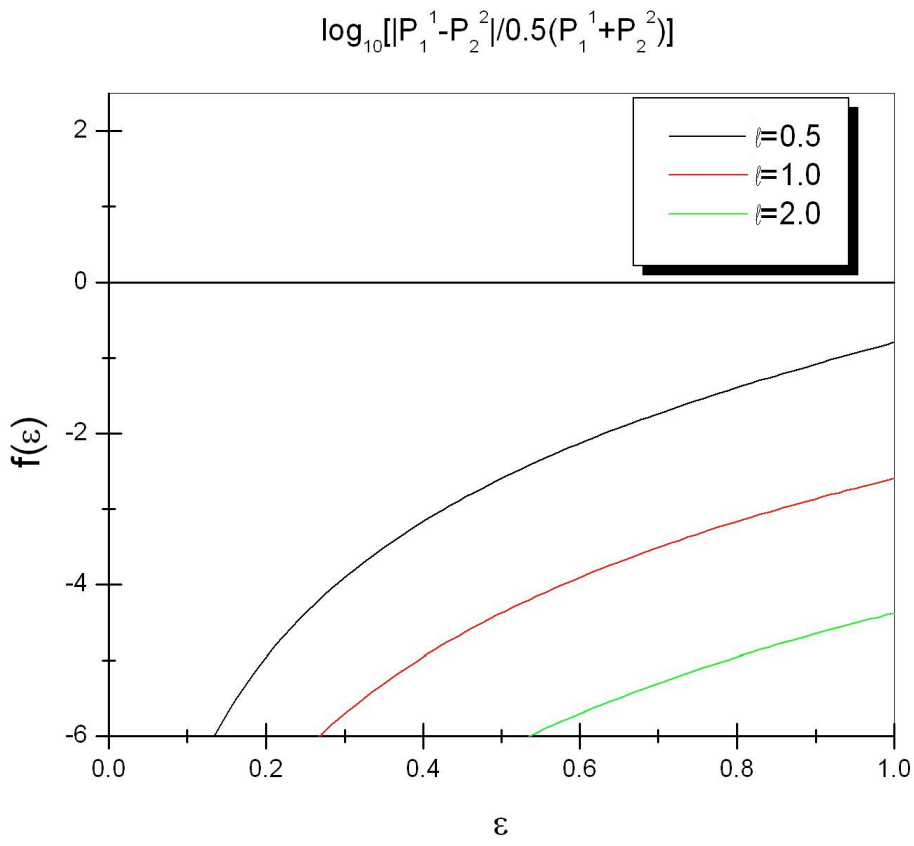

Graph 7: Base ten logarithmic graph showing the relative discrepancy among the approximants calculated for the fourth and eighth order series. The traces are for various localization lengths, expressed in units of lattice constants.

From the figures it's clear that the approximants provide very similar results and overlap quite strongly. Specifically, the difference in the traces for $l = 1$ is only a few parts in 100,000 even for $\left(\frac{\varepsilon}{l}\right)$ as high as 0.50. Furthermore, we see that even in the case of the shortest decoy length $l = 0.5$ (where $\left(\frac{\varepsilon}{l}\right)^2$ may attain the value of 1.0), the difference is at most a few tenths of a percent. This serves as strong justification for

using the approximant $P_1^1\left(\left[\frac{\varepsilon}{l}\right]^2\right)$, which is based on a series calculated up to fourth order in $\left(\frac{\varepsilon}{l}\right)$.

In this vein, it will be our aim in future considerations to take into account contributions up to fourth order with no need to examine the sixth and eighth order terms. Our early success is a primary motivation for following this course. So we will obtain the perturbative series to fourth order in the perturbing parameter $\left(\frac{\varepsilon}{l}\right)$ and then compute $P_1^1\left(\left[\frac{\varepsilon}{l}\right]^2\right)$.

6.2: A Generalized Recursive Perturbative Calculation of Transport Characteristics

Now our goal is to return to the same systems, and again craft a perturbative analysis, but do so in a way more easily generalized to two and three-dimensional systems.

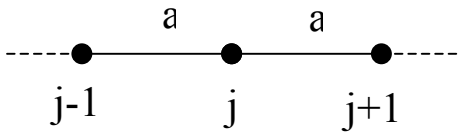

Figure 45: The lattice structure near node j for the one-dimensional system

Again, we start with current conservation. Between nodes i and $i+1$, the current is given by

$$I_{j;j+1} = \frac{V_j - V_{j+1}}{R_{j;j+1}}$$

where $R_{j;j+1}$ is the resistance between the nodes j and $j+1$. The principle fo charge conservation requires that we posit

$$I_{j;j+1} = I_{j-1;j} = \frac{V_j - V_{j+1}}{R_{j;j+1}} = \frac{V_{j-1} - V_j}{R_{j-1;j}}$$

6.2.1: Introducing Potential and Resistance Shifts

Normally, in the pristine system with no perturbations imposed, we would find

$$I_{j;j+1} = I_{j;j-1} = \frac{V_0}{NR_0} e^{-\frac{a}{l}}$$

However, the link resistances will be altered when we introduce shifts in position x_i. This means that for example,

$$R_{j;j} = R_0 e^{\frac{a}{l}} e^{\frac{x_{j+1} x_j}{l}}$$

So in terms of the shifts we calculate that

$$I_{j;j+1} = \frac{\left(\frac{1}{N} V_0 + \Delta V_j - \Delta V_{j+1}\right)}{R_0} e^{-\frac{a}{l}} e^{\frac{1}{l}\left[x_j - x_{j+1}\right]}$$

$$I_{j-1;j} = \frac{\left(\frac{1}{N} V_0 + \Delta V_{j-1} - \Delta V_j\right)}{R_0} e^{-\frac{a}{l}} e^{\frac{1}{l}\left[x_{j-1} - x_j\right]}$$

Equating these two equations and eliminating common factors gives

$$\left[\frac{1}{N} V_0 + \Delta V_j - \Delta V_{j+1}\right] e^{\frac{1}{l}\left[x_j - x_{j+1}\right]} = \left[\frac{1}{N} V_0 + \Delta V_{j-1} - \Delta V_j\right] e^{\frac{1}{l}\left[x_{j-1} - x_j\right]}$$

Subsequent calculations will be facilitated if we use

$$e^{\frac{1}{l}\left[x_j - x_{j+1}\right]} \equiv 1 + \lambda_j = 1 + \left\{\frac{1}{l}\left(x_j - x_{j+1}\right) + \frac{1}{2l^2}\left(x_j - x_{j+1}\right)^2 + \ldots\right\}$$

So the perturbations are

$$\lambda_j = \frac{1}{l}\left(x_j - x_{j+1}\right) + \frac{1}{2l^2}\left(x_j - x_{j+1}\right)^2 + \ldots$$

and thus we see that λ_j is on the order of $\frac{1}{l}\left(x_j - x_{j+1}\right)$ and is "small" in the same sense.

In the more advanced stages of perturbative analysis, we will replace λ_j with the expression particular to the perturbation we have in mind. In the present example, we will ultimately expand $\left\{e^{\frac{1}{l}\left(x_j - x_{j+1}\right)} - 1\right\}$ and then average over the x_j variables. As before, we use $x_j = \varepsilon_j y_j$ where y_j is a random variable which ranges between -1 and $+1$ while ε_j is a quantity to parameterize the strength of the perturbation. We assume that ε is "small" and in a typical case one could assume that $\frac{\varepsilon}{a} << 1$. Nevertheless, Padé analysis will aid in extending the calculation to cases in which ε may approach unity, corresponding generally to a strongly disordered lattice.

6.2.2: Applying Fourier Analysis

We begin the perturbative analysis by introducing Fourier variables. We use the results from Chapter 2, where Fourier analysis was used to consider the effect of localized current sources. The expression enforcing charge conservation is

$$\begin{aligned}\left[\frac{1}{N}V_0 + \Delta V_j - \Delta V_{j+1}\right]e^{\frac{1}{l}\left(x_j - x_{j+1}\right)} &= \left[\frac{1}{N}V_0 + \Delta V_{j-1} - \Delta V_j\right]e^{\frac{1}{l}\left(x_{j-1} - x_j\right)} \\ &= \left[v_0 + \Delta V_j - \Delta V_{j+1}\right]\left(1 + \lambda_j\right) \\ &= \left[v_0 + \Delta V_j - \Delta V_{j-1}\right]\left(1 + \lambda_{j-1}\right)\end{aligned}$$

where we have used the label $v_0 = \frac{V_0}{N}$. After simplification and some erarrangement, we have

$$2\Delta V_j - \Delta V_{j+1} - \Delta V_{j-1} = v_0\left(\lambda_{j-1} - \lambda_j\right) + \Delta V_{j-1}\lambda_{j-1} + \Delta V_{j+1}\lambda_j - \Delta V_j\lambda_{j-1} - \Delta V_j\lambda_j$$

On the left side of this equation is a discretized Laplacian, while the right side has a term on the order of $\Delta V \times \lambda$. The latter may be seen to be on the order of λ^2, and it will support an iterative procedure to set up a perturbative series in terms of the Fourier variables.

We begin with

$$\Delta V_j = \sum_{k=0}^{N-1} \Delta V_k e^{\frac{2\pi i j k}{N}}$$
$$\lambda_j = \sum_{k=0}^{N-1} \lambda_k e^{\frac{2\pi i j k}{N}}$$

We now have

$$2\Delta V_j - \Delta V_{j+1} - \Delta V_{j-1} = 2\sum_{k=0}^{N-1} \Delta V_k e^{\frac{2\pi i j k}{N}} - \sum_{k=0}^{N-1} \Delta V_k e^{\frac{2\pi i j k}{N}} e^{\frac{2\pi i k}{N}} - \sum_{k=0}^{N-1} \Delta V_k e^{\frac{2\pi i j k}{N}} e^{\frac{-2\pi i k}{N}}$$

$$= \sum_{k=0}^{N-1} \Delta V_k e^{\frac{2\pi i j k}{N}} \left(2 - e^{\frac{2\pi i k}{N}} - e^{\frac{-2\pi i k}{N}}\right)$$

$$= v_0\left(\lambda_{j-1} - \lambda_j\right) + \left[\Delta V_{j-1}\lambda_{j-1} + \Delta V_{j+1}\lambda_j - \Delta V_j\lambda_{j-1} - \Delta V_j\lambda_j\right]$$

$$= v_0 \sum_{k=0}^{N-1} \lambda_k e^{\frac{2\pi i j k}{N}} \left(e^{\frac{-2\pi i k}{N}} - 1\right) + \left[\begin{array}{l} \left(\sum_{k=0}^{N-1} \Delta V_k e^{\frac{2\pi i j k}{N}} e^{\frac{-2\pi i k}{N}}\right)\left(\sum_{k'=0}^{N-1} \lambda_{k'} e^{\frac{2\pi i j k'}{N}} e^{\frac{-2\pi i k'}{N}}\right) \\ + \left(\sum_{k=0}^{N-1} \Delta V_k e^{\frac{2\pi i j k}{N}} e^{\frac{2\pi i k}{N}}\right)\left(\sum_{k'=0}^{N-1} \lambda_{k'} e^{\frac{2\pi i j k'}{N}}\right) \\ - \left(\sum_{k=0}^{N-1} \Delta V_k e^{\frac{2\pi i j k}{N}}\right)\left(\sum_{k'=0}^{N-1} \lambda_{k'} e^{\frac{2\pi i j k'}{N}} e^{\frac{-2\pi i k'}{N}}\right) \\ - \left(\sum_{k=0}^{N-1} \Delta V_k e^{\frac{2\pi i j k}{N}}\right)\left(\sum_{k'=0}^{N-1} \lambda_{k'} e^{\frac{2\pi i j k'}{N}}\right) \end{array}\right]$$

Combining sums in the last term on the right leads to a more compact result, and we find

$$\sum_{k=0}^{N-1} \Delta V_k \left(2 - e^{\frac{2\pi i k}{N}} - e^{\frac{-2\pi i k}{N}}\right) e^{\frac{2\pi i j k}{N}} = \sum_{k=0}^{N-1} \Delta V_k e^{\frac{2\pi i j k}{N}} \left(2 - 2\cos\left[\frac{2\pi k}{N}\right]\right)$$

$$= v_0 \sum_{k=0}^{N-1} \lambda_k e^{\frac{2\pi i j k}{N}} \left(e^{\frac{-2\pi i j k}{N}} - 1 \right) + \left(\sum_{k=0}^{N-1} \Delta V_k e^{\frac{2\pi i j k}{N}} \right) \left(\sum_{k'=0}^{N-1} \lambda_{k'} e^{\frac{2\pi i j k'}{N}} \right) \begin{bmatrix} e^{\frac{-2\pi i}{N}(k+k')} \\ +e^{\frac{2\pi i k}{N}} \\ -e^{\frac{-2\pi i k'}{N}} - 1 \end{bmatrix}$$

Now we proceed by selecting out an individual Fourier component. This is accomplished by multiplying $e^{\frac{2\pi i j}{N}(N-k'')}$ and summing on both sides over the position index j. The result will be

$$\Delta V_{k''} \left(2 - 2\cos\left[\frac{2\pi k''}{N} \right] \right) = v_0 \lambda_{k''} \left(e^{\frac{-2\pi i k''}{N}} - 1 \right) + \sum_{k=0}^{N-1} \sum_{k'=0}^{N-1} \Delta V_k \lambda_{k'} \left(e^{\frac{-2\pi i}{N}[k+k']} + e^{\frac{2\pi i k}{N}} - e^{\frac{-2\pi i k'}{N}} - 1 \right) \delta_{k''[k+k']}$$

The Kronecker Delta symbol $\delta_{k''[k+k']}$ allows us to collapse one of the sums. With $k' = k'' - k$, one finds that

$$\Delta V_{k''} \left(2 - 2\cos\left[\frac{2\pi k''}{N} \right] \right) = v_0 \lambda_{k''} \left(e^{\frac{-2\pi i k''}{N}} - 1 \right) + \sum_{k=0}^{N-1} \Delta V_k \lambda_{k''-k} \left(e^{\frac{-2\pi i k''}{N}} + e^{\frac{2\pi i k}{N}} - e^{\frac{-2\pi i}{N}(k-k'')} - 1 \right)$$

To solve for $\Delta V_{k''}$ one would need to divide by the factor $\left(2 - 2\cos\left[\frac{2\pi k''}{N} \right] \right)$, feasible only for the finite wave number case in which $k'' \neq 0$. However, we may avert this difficulty if we remember that one may set $\Delta V_0 = 0$ since only differences in the potential shifts have a physical effect.

6.2.3: The Bare Propagator and a Recursive Iterative Procedure

We define an expression $g_k^0 \equiv \left(e^{\frac{2\pi i k}{N}} - 1 \right)$, which is similar to the formalism used in many-body treatments. In terms of g_k^0,

$$\left(2 - 2\cos\left[\frac{2\pi k''}{N} \right] \right) = \left(e^{\frac{2\pi i k''}{N}} - 1 \right) \left(e^{\frac{-2\pi i k''}{N}} - 1 \right) = g_{k''}^0 g_{-k''}^0$$

We also use the following expression:

$$e^{\frac{-2\pi ik''}{N}} + e^{\frac{2\pi ik}{N}} - e^{\frac{2\pi i}{N}(k-k'')} - 1 = -\left(e^{\frac{-2\pi ik''}{N}} - 1\right)\left(e^{\frac{2\pi ik}{N}} - 1\right)$$

$$= -g^0_{-k''} g^0_k$$

The expression for the potential shifts becomes

$$\Delta V_{k''} g^0_{k''} g^0_{-k''} = v_0 \lambda_{k''} g^0_{-k''} - \sum_{k=1}^{N-1} \Delta V_k \lambda_{k''-k} g^0_{-k''} g^0_k$$

When $k'' \neq 0$, we may solve for $\Delta V_{k''}$ with $\Delta V_{k''} = \frac{1}{g^0_{k''}}\left(v_0 \lambda_{k''} - \sum_{k=1}^{N-1} \Delta V_k \lambda_{k''-k} g^0_k\right)$.

It is important to note that the summations in Fourier space do not include a zero wave number term, since we have determined that $\Delta V_0 = 0$. For the sake of future convenience, we relabel the dummy indices. The result is

$$\Delta V_k = \frac{1}{g^0_k}\left(v_0 \lambda_k + \sum_{k_1=0}^{N-1} \Delta V_{k_1} \lambda_{k-k_1} g^0_{k_1}\right)$$

6.2.3.1: Obtaining and Expressing the General Perturbative Series

Now we recursively substitute the formula for ΔV_k into the second term in the curved braces. One finds

$$\Delta V_k = \frac{1}{g^0_k}\left(v_0 \lambda_k + \sum_{k_1=1}^{N-1}\left[\frac{1}{g^0_{k_1}}\left\{v_0 \lambda_{k_1} + \sum_{k_2=1}^{N-1} \Delta V_{k_2} \lambda_{k_1-k_2} g^0_{k_2}\right\}\right] \lambda_{k-k_1} g^0_{k_1}\right)$$

After algebraic manipulation, the expression becomes

$$\Delta V_k = \frac{1}{g^0_k}\left(v_0 \lambda_k - \sum_{k_1=1}^{N-1} v_0 \lambda_{k_1} \lambda_{k-k_1} - \sum_{k_1=1}^{N-1}\sum_{k_2=1}^{N-1} \Delta V_{k_2} \lambda_{k_1-k_2} \lambda_{k-k_1} g^0_{k_2}\right)$$

With subsequent iterations implemented in a similar recursive way, one finds

$$\Delta V_k = \frac{v_0}{g_k^0}\left(\lambda_k - \sum_{k_1=1}^{N-1}\lambda_{k_1}\lambda_{k-k_1} + \sum_{k_1=1}^{N-1}\sum_{k_2=1}^{N-1}\lambda_{k_2}\lambda_{k_1-k_2}\lambda_{k-k_1} - \sum_{k_1=1}^{N-1}\sum_{k_2=1}^{N-1}\sum_{k_3=1}^{N-1}\lambda_{k_3}\lambda_{k_2-k_3}\lambda_{k_1-k_2}\lambda_{k-k_1} + \ldots\right)$$

and a pattern emerges where subsequent terms are readily obtained.

6.2.4: Calculating the Current

The current between the links is an important physical quantity, and it is most convenient for us to calculate the mean current. The current between the nodes j and $j+1$ was previously determined to be

$$I_{j;j+1} = \frac{1}{R_0}\left(v_0 + \Delta V_j - \Delta V_{j+1}\right)e^{-\frac{a}{l}}e^{\frac{1}{l}\left[x_j - x_{j+1}\right]}$$

$$= \frac{1}{R_0}\left(v_0 + \Delta V_j - \Delta V_{j+1}\right)e^{-\frac{a}{l}}\left(1+\lambda_j\right)$$

Now we sum over each of the sites in the one-dimensional lattice and divide by the total number N. The result is

$$\bar{I} = \frac{e^{-\frac{a}{l}}}{NR_0}\sum_{j=0}^{N-1}\left(v_0 + \Delta V_j - \Delta V_{j+1}\right)\left(1+\lambda_j\right)$$

$$= \frac{e^{-\frac{a}{l}}}{R_0}v_0 + \frac{e^{-\frac{a}{l}}}{NR_0}v_0\sum_{j=0}^{N-1}\lambda_j + \frac{e^{-\frac{a}{l}}}{NR_0}\sum_{j=0}^{N-1}\lambda_j\left(\Delta V_j - \Delta V_{j+1}\right)$$

where we have exploited the periodicity condition to eliminate terms and produce a more compact result.

6.2.4.1: Calculating the First Order Contribution to the Current

The task now is to evaluate the last term on the right side that involves ΔV terms. Since the latter have been calculated in Fourier space, we will need to exercise caution. First, we need to convert the expression $\bar{I}$ from a sum in real space to a sum in reciprocal

space. To accomplish this we use the "Fourier trick" which was applied in the case of Chapter 2. One has, for example

$$\lambda_j = \sum_{k=0}^{N-1} \lambda_k e^{\frac{2\pi i j k}{N}}$$

Multiplying by $e^{\frac{-2\pi i k'}{N} j}$ and summing over the position index j gives

$$\sum_{j=0}^{N-1} \lambda_j e^{\frac{-2\pi i k' j}{N}} = \sum_{j=0}^{N-1}\sum_{k=0}^{N-1} \lambda_k e^{\frac{2\pi i j}{N}(k-k')}$$

The right side of the equation has a sum that will collapse since the sum over j vanishes unless $k = k'$, enabling us utilize the Kronecker Delta $\delta_{kk'}$. One has

$$\sum_{j=0}^{N-1} \lambda_j e^{\frac{-2\pi i k' j}{N}} = \sum_{k=0}^{N-1}\sum_{j=0}^{N-1} \lambda_k \delta_{kk'} = N\lambda_{k'}$$

So that $\lambda_{k'} = \frac{1}{N}\sum_{j=0}^{N-1} \lambda_j e^{\frac{-2\pi i k' j}{N}}$. In s similar fashion $\Delta V_{k'} = \frac{1}{N}\sum_{j=0}^{N-1} \Delta V_j e^{\frac{-2\pi i j k'}{N}}$. It will be advantageous to be able to make the transition from λ_j to λ_k and vice versa.

6.2.4.2: Calculating Second and Higher Order Contributions to the Current

We now give close consideration to the term $\frac{e^{-\frac{a}{l}}}{NR_0}\sum_{j=0}^{N-1} \lambda_j \left[\Delta V_j - \Delta V_{j+1}\right]$. One finds that

$$\frac{e^{-\frac{a}{l}}}{NR_0}\sum_{j=0}^{N-1} \lambda_j \left[\Delta V_j - \Delta V_{j+1}\right] = \frac{e^{-\frac{a}{l}}}{NR_0}\sum_{j=0}^{N-1}\left(\sum_{k=0}^{N-1} \lambda_k e^{\frac{2\pi i j k}{N}}\right)\left(\sum_{k'=0}^{N-1} \Delta V_{k'}\left[1 - e^{\frac{2\pi i k'}{N}}\right] e^{2\pi i j k'}\right)$$

$$= \frac{e^{-\frac{a}{l}}}{NR_0}\sum_{j=0}^{N-1}\sum_{k=0}^{N-1}\sum_{k'=0}^{N-1} \lambda_k \Delta V_{k'} e^{\frac{2\pi i j}{N}[k+k']}\left(1 - e^{\frac{2\pi i k'}{N}}\right)$$

The sum over j will lead to a Kronecker Delta symbol. By setting $k = -k'$, we collapse the sum over k and we obtain

$$\frac{e^{-\frac{a}{l}}}{NR_0}\sum_{j=0}^{N-1}\lambda_j\left(\Delta V_j - \Delta V_{j+1}\right) = \frac{e^{-\frac{a}{l}}}{NR_0}\sum_{k'=0}^{N-1}\lambda_{-k'}\Delta V_{k'}\left(1 - e^{\frac{2\pi i k'}{N}}\right)$$

$$= \frac{e^{-\frac{a}{l}}}{NR_0}\sum_{k'=1}^{N-1}\lambda_{-k'}\Delta V_{-k'}\left(1 - e^{\frac{2\pi i k'}{N}}\right)$$

where the sum over Fourier indices begins with "1" since $\Delta V_0 = 0$. Changing the dummy indices and using the previously obtained formula for ΔV_k gives

$$\frac{e^{-\frac{a}{l}}}{NR_0}\sum_{j=0}^{N-1}\lambda_j\left(\Delta V_j - \Delta V_{j+1}\right) = \frac{-e^{-\frac{a}{l}}}{R_0}v_0\sum_{k=1}^{N-1}g_k^0\lambda_{-k}\Delta V_k\frac{1}{g_k^0}\left(\lambda_k - \sum_{k_1=1}^{N-1}\lambda_{k_1}\lambda_{k-k_1} + \sum_{k_1=1}^{N-1}\sum_{k_2=1}^{N-1}\lambda_{k_2}\lambda_{k_1-k_2}\lambda_{k-k_1} - \ldots\right)$$

where we have used the fact that $1 - e^{\frac{2\pi i k}{N}} = -g_k^0$.

With the aid of $V_k = \frac{1}{N}\sum_{j=0}^{N-1}V_j e^{\frac{-2\pi i j k}{N}}$ we will be able to operate in terms of the λ_j quantities for which the characteristics are understood. One then sees that

$$\frac{e^{-\frac{a}{l}}}{NR_0}\sum_{j=0}^{N-1}\lambda_j\left(\Delta V_j - \Delta V_{j+1}\right) = \frac{-v_0 e^{-\frac{a}{l}}}{R_0}\left[\sum_{k=1}^{N-1}\lambda_k\lambda_{-k} - \sum_{k=1}^{N-1}\sum_{k_1=1}^{N-1}\lambda_{k_1}\lambda_{k-k_1}\lambda_{-k} + \sum_{k=1}^{N-1}\sum_{k_1=1}^{N-1}\sum_{k_2=1}^{N-1}\lambda_{k_2}\lambda_{k-k_1}\lambda_{k_1-k_2}\lambda_{-k} - \ldots\right]$$

6.2.4.3: Exploiting Orthogonality by Adding and Subtracting the Zero Wave Number Term

In order to utilize the orthogonality of the Fourier states and collapse the sums over the Fourier indices, the sums need to be modified such that the index runs from 0 to $N-1$ instead of 1 to $N-1$. This is achieved by adding and then subtracting the zero wave

vector component. To understand this process, we examine the first several terms in turn. First, we examine the term

$$\sum_{k=1}^{N-1}\lambda_k\lambda_{-k}=\sum_{k=1}^{N-1}\left(\frac{1}{N}\sum_{j=0}^{N-1}e^{\frac{-2\pi ik}{N}j}\lambda_j\right)\left(\frac{1}{N}\sum_{j'=0}^{N-1}e^{\frac{2\pi ik}{N}j'}\lambda_{j'}\right)$$

We permute the sums to obtain

$$\sum_{k=1}^{N-1}\lambda_k\lambda_{-k}=\sum_{j=0}^{N-1}\sum_{j'=0}^{N-1}N^{-2}\lambda_j\lambda_{j'}\left[\sum_{k=1}^{N-1}e^{\frac{2\pi ik}{N}(j'-j)}\right]$$

After adding and subtracting the zero wave vector component, this becomes an expression which one may evaluate:

$$\sum_{k=1}^{N-1}\lambda_k\lambda_{-k}=\sum_{j=0}^{N-1}\sum_{j'=0}^{N-1}N^{-2}\lambda_j\lambda_{j'}\left[\sum_{k=0}^{N-1}e^{\frac{2\pi ik}{N}(j'-j)}-1\right]$$

$$=\sum_{j=0}^{N-1}\sum_{j'=0}^{N-1}N^{-2}\lambda_j\lambda_{j'}\left[\delta_{jj'}N-1\right]$$

$$=\frac{q}{N}\sum_{j=0}^{N-1}\lambda_j{}^2-\left(\frac{1}{N^2}\sum_{j=0}^{N-1}\sum_{j'=0}^{N-1}\lambda_j\lambda_{j'}\right)$$

So we see that

$$\sum_{k=1}^{N-1}\lambda_k\lambda_{-k}=\frac{1}{N}\sum_{j=0}^{N-1}\lambda_j{}^2-\left(\frac{1}{N}\sum_{j=1}^{N-1}\lambda_j\right)^2$$

$$=\left\langle\lambda_j{}^2\right\rangle_s-\left\langle\lambda_j\right\rangle_s{}^2$$

where the symbol "*s*" denotes a system average for a static configuration of disorder. The angle brackets lacking an "*s*" indicate an average over disorders, in the manner described prior to the introduction of Padé approximants.

In a similar manner, we examine the term

$$\sum_{k=1}^{N-1}\sum_{k_1=1}^{N-1}\lambda_{k_1}\lambda_{k-k_1}\lambda_{-k}=\sum_{k=1}^{N-1}\sum_{k_1=1}^{N-1}N^{-3}\left(\sum_{j=0}^{N-1}\lambda_j e^{\frac{-2\pi i j k_1}{N}}\right)\left(\sum_{j'=0}^{N-1}\lambda_{j'}e^{\frac{-2\pi i j'[k-k_1]}{N}}\right)\left(\sum_{j''=0}^{N-1}\lambda_{j''}e^{\frac{2\pi i j'' k}{N}}\right)$$

Again, it is advantageous to permute the sums over position and Fourier indices, and the result is:

$$\sum_{k=1}^{N-1}\sum_{k_1=1}^{N-1}\lambda_{k_1}\lambda_{k-k_1}\lambda_{-k}=\sum_{j=0}^{N-1}\sum_{j'=0}^{N-1}\sum_{j''=0}^{N-1}N^{-3}\lambda_j\lambda_{j'}\lambda_{j''}\left(\sum_{k=1}^{N-1}e^{\frac{2\pi i k}{N}[j''-j']}\right)\left(\sum_{k_1=0}^{N-1}e^{\frac{2\pi i k_1}{N}[j'-j]}\right)$$

The Fourier index sums may each be executed independently. The result is

$$\sum_{j_1,j_2j_3=0}^{N-1}N^{-3}\lambda_{j_1}\lambda_{j_2}\lambda_{j_3}\left(\sum_{k=1}^{N-1}e^{\frac{2\pi i k}{N}[j_3-j_2]}\right)\left(\sum_{k_1=1}^{N-1}e^{\frac{2\pi i}{N}k_1[j_2-j_1]}\right)$$

where the symbol $\sum_{j_1,j_2,j_3=0}^{N-1}$ is an abbreviated representation of the triple sum notation $\sum_{j_1=0}^{N-1}\sum_{j_2=0}^{N-1}\sum_{j_3=0}^{N-1}$. Bearing in mind that the "k" indices run from 1 to $N-1$, we write

$$\sum_{k=1}^{N-1}\sum_{k_1=1}^{N-1}\lambda_{k_1}\lambda_{k-k_1}\lambda_{-k}=N^{-3}\sum_{j_1,j_2,j_3=0}^{N-1}\lambda_{j_1}\lambda_{j_2}\lambda_{j_3}\left(\delta_{j_3j_2}-1\right)\left(\delta_{j_2j_1}-1\right)$$

Now the expression can be evaluated directly. We will then consider an alternative technique which leads more succinctly to the same result. We have:

$$\sum_{k=1}^{N-1}\sum_{k_1=1}^{N-1}\lambda_{k_1}\lambda_{k-k_1}\lambda_{-k}=N^{-3}\sum_{j_1,j_2,j_3=0}^{N-1}\lambda_{j_1}\lambda_{j_2}\lambda_{j_3}\left[\delta_{j_3j_2}\delta_{j_2j_1}-\delta_{j_2j_1}-\delta_{j_3j_2}+1\right]$$

$$=N^{-3}\left[\sum_{j=0}^{N-1}\lambda_j{}^3-2N\sum_{j=0}^{N-1}\sum_{j'=0}^{N-1}\lambda_j{}^2\lambda_{j'}+\sum_{j=0}^{N-1}\sum_{j'=0}^{N-1}\sum_{j''=0}^{N-1}\lambda_j\lambda_{j'}\lambda_{j''}\right]$$

$$=\frac{1}{N}\sum_{j=0}^{N-1}\lambda_j{}^3-2\left(\frac{1}{N}\sum_{j=0}^{N-1}\lambda_j{}^2\right)\left(\frac{1}{N}\sum_{j'=0}^{N-1}\lambda_{j'}\right)+\left(\frac{1}{N}\sum_{j=0}^{N-1}\lambda_j\right)^3$$

$$=\left[\left\langle\lambda_j{}^3\right\rangle_s-2\left\langle\lambda_j{}^2\right\rangle\left\langle\lambda_j\right\rangle+\left\langle\lambda_j\right\rangle^3\right]$$

6.2.4.4: A Diagramatic Method to Facilitate the Evaluation of Perturbative Expansion Terms

Although the direct calculation technique has been successfully implemented for the cubic term in λ, it rapidly becomes cumbersome as higher order terms are considered. To organize this process and eliminate mathematically intricate intermediate steps, we introduce a diagrammatic formalism that we now illustrate for the case of the cubic term $\sum_{k=1}^{N-1}\sum_{k_1=1}^{N-1}\lambda_{k_1}\lambda_{k-k_1}\lambda_{-k}$.

Since the term is cubic, there are three nodes as shown below where they are depicted, evenly spaced, in a row:

Without Kronecker Delta symbols, there are no contractions among the indices, and the sums over the positional "j" indices are independent. For each absent Kronecker Delta symbol, we introduce a factor of (-1). Thus, the term represented by the diagram

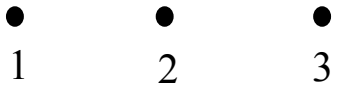

may be expressed as

$$\left(\frac{1}{N}\sum_{j=0}^{N-1}\lambda_j\right)\left(\frac{1}{N}\sum_{j'=0}^{N-1}\lambda_{j'}\right)\left(\frac{1}{N}\sum_{j''=0}^{N-1}\lambda_{j''}\right)=\frac{1}{N^3}\left(\sum_{j=0}^{N-1}\lambda_j\right)^3(-1)^2=\left\langle\lambda_j\right\rangle_s^3$$

Let's suppose that we perform only a single index contraction, which collapses only one of the sums over positional indices. Remembering that the Kronecker Delta symbols may only link adjacent nodes, we see that there are the following possibilities:

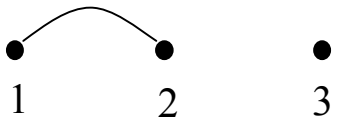

and

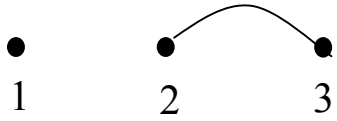

We note that a third "wrap-around" diagram connection the first and third indices is forbidden by the mathematical rules used to craft the perturbative series. Furthermore, we also bear in mind that the terms corresponding to the diagrams will receive a single factor of (-1) since we are excluding only one of the Kronecker Delta symbols.

We then find that the

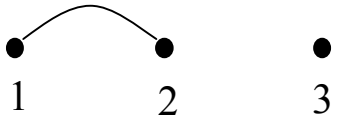

diagram yields

$$\left(\frac{1}{N}\sum_{j=0}^{N-1}\lambda_j{}^2\right)\left(\sum_{j'=0}^{N-1}\lambda_{j'}\right)(-1) = -\left(\left\langle\lambda_j{}^2\right\rangle_s\left\langle\lambda_j\right\rangle_s\right)$$

The second diagram yields $-\left(\frac{1}{N}\sum_{j=0}^{N-1}\lambda_j\right)\left(\frac{1}{N}\sum_{j'=0}^{N-1}\lambda_{j'}{}^2\right)(-1) = -\left(\left\langle\lambda_j\right\rangle_s\left\langle\lambda_j{}^2\right\rangle_s\right)$. So for a single contraction permitted, we find $-2\left\langle\lambda_j{}^2\right\rangle_s\left\langle\lambda_j\right\rangle_s$ and both diagrams yield the same contribution.

Now we examine the case in which two Kronecker Delta functions are selected. There is only a single diagram to describe this situation, with each of the nodes linked together:

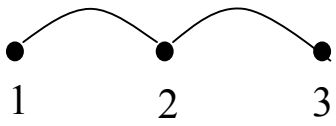

No Kronecker Delta symbols are omitted, so the negative factor -1 is not introduced. The sole contribution, and the evaluation of the diagram shown above is

$$\frac{1}{N}\sum_{j=0}^{N-1}\lambda_j{}^3 = \left\langle \lambda_j{}^3 \right\rangle_s$$

Adding the contributions from each diagram considered for the third order case gives

$$\left[\left(\left\langle \lambda_j \right\rangle_s\right)^3 - 2\left\langle \lambda_j{}^2 \right\rangle_s \left\langle \lambda_j \right\rangle_s + \left\langle \lambda_j{}^3 \right\rangle_s\right] = \sum_{k=1}^{N-1}\sum_{k_1=1}^{N-1}\lambda_{k_1}\lambda_{k-k_1}\lambda_{-k}$$

We now proceed in a similar fashion for the contribution at the fourth order level. For the purpose of brevity, we rely exclusively now on the diagrammatic analysis, and we do not invoke the formal mechanisms. The term we wish to study is

$$\sum_{k=0}^{N-1}\sum_{k_1=0}^{N-1}\sum_{k_2=0}^{N-1}\lambda_{k_2}\lambda_{k-k_1}\lambda_{k_1-k_2}\lambda_{-k}$$

First, we examine the case in which there are no Kronecker Delta symbols. The sole relevant diagram has no contractions:

Including the three corrections, three factors of (-1) appear. The evaluation of the diagram is

$$(-1)^3\frac{1}{N^4}\sum_{j,j',j'',j'''=0}^{N-1}\left[\lambda_j\lambda_{j'}\lambda_{j''}\lambda_{j'''}\right] = (-1)^3\left(\frac{1}{N}\sum_{j=0}^{N-1}\lambda_j\right)^4 = -\left\langle \lambda_j \right\rangle_s^4$$

Next we examine the situation in which a single connection is made, and there is one Kronecker Delta symbol that appears. The three possible diagrams are:

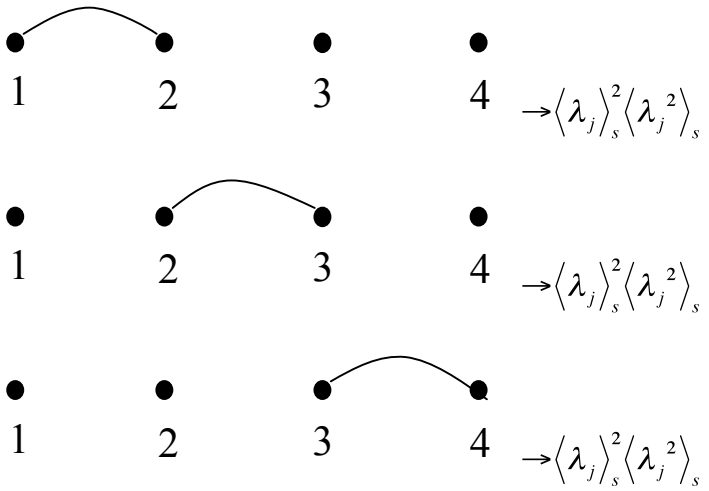

As shown above, the diagrams yield identical contributions. Since two site connections are avoided, there are two negative factors. The result is

$$3\langle \lambda_j \rangle_s^2 \langle \lambda_j^2 \rangle_s$$

If two connections are made, not every diagram yields the same result. The possibilities are:

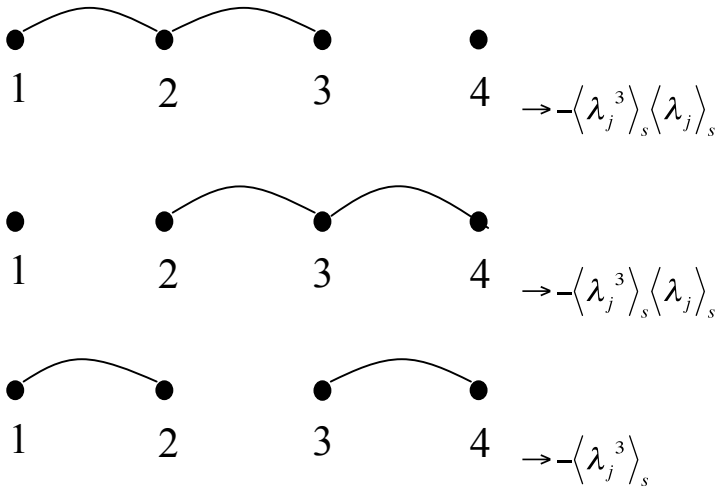

The first two diagrams contain contiguous sets of connected nodes with a single isolated vertex. The last diagram contains two pairs of nodes that are isolated from each other. The total contribution for the case in which there are two contractions is

$$-\left[2\left\langle \lambda_j{}^3\right\rangle_s\left\langle \lambda_j\right\rangle_s+\left\langle \lambda_j{}^2\right\rangle^2\right]$$

If we form connections among each of the nodes, we have the following diagram:

$$\rightarrow\left\langle \lambda_j{}^4\right\rangle_s$$

So, the result for the total fourth order contribution is

$$\sum_{k=1}^{N-1}\sum_{k_1=1}^{N-1}\sum_{k_2=1}^{N-1}\lambda_{k_2}\lambda_{k-k_1}\lambda_{k_1-k_2}\lambda_{-k}=\left[-\left\langle \lambda_j\right\rangle_s^4+3\left\langle \lambda_j{}^2\right\rangle_s\left\langle \lambda_j\right\rangle_s^2-2\left\langle \lambda_j{}^3\right\rangle_s\left\langle \lambda_j\right\rangle_s-\left\langle \lambda_j{}^2\right\rangle_s^2+\left\langle \lambda_j{}^4\right\rangle_s\right]$$

There are several ways to check the validity of one's results. Firstly, the total numerical value of the coefficients should sum to zero. Of considerable utility and importance is the fact that the total number of diagrams for a specific order in λ and number of contractions is actually a binomial coefficient that is given by the formula

$$N_C^M=\frac{(M-1)!}{(C!)(M-C-1)!}$$

For example, in the $M=4$ fourth order case with $C=2$ connections we find

$N_2^4=\frac{3!}{(2!)(1!)}=3$ as we discovered.

We now examine the fifth order case, again using the diagrammatic approach. For the case in which no connections are made, the diagram and its contribution are

$$\rightarrow(-1)^4\left\langle \lambda_j\right\rangle_s^5=\left\langle \lambda_j\right\rangle_s^5$$

Performing a single contraction, we expect to find four contributions. We have the following:

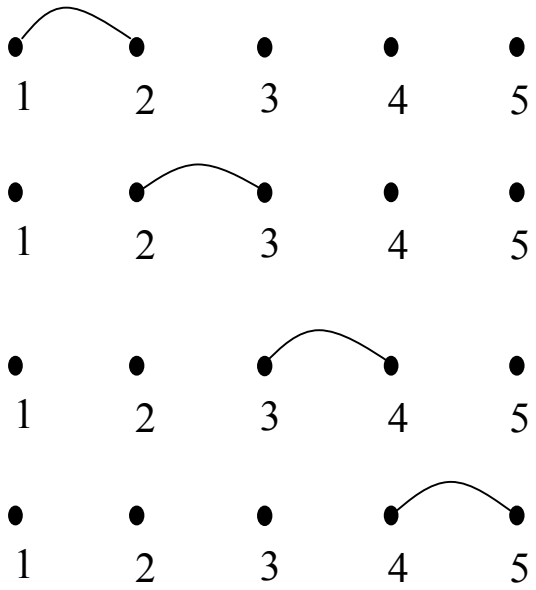

$$\rightarrow 4(-1)^3\left\langle \lambda_j{}^2\right\rangle_s\left\langle \lambda_j\right\rangle_s^3 = -4\left\langle \lambda_j{}^2\right\rangle_s\left\langle \lambda_j\right\rangle_s^3$$

For the case in which two connections are made, the number of expected diagrams is:

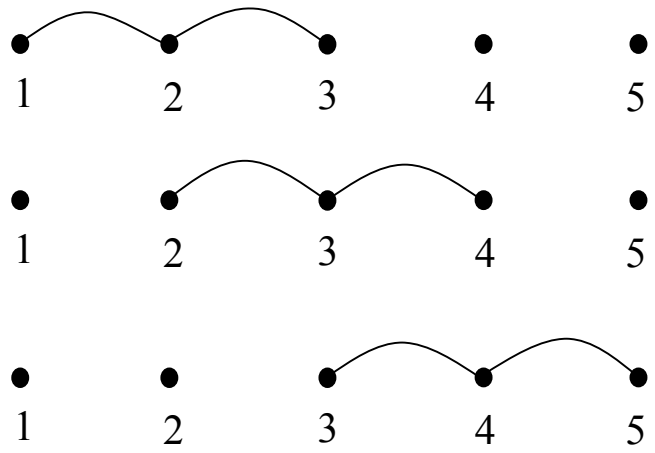

$$\rightarrow 3(-1)^2\left\langle \lambda_j{}^3\right\rangle_s\left\langle \lambda_j\right\rangle_s^2$$

Furthermore,

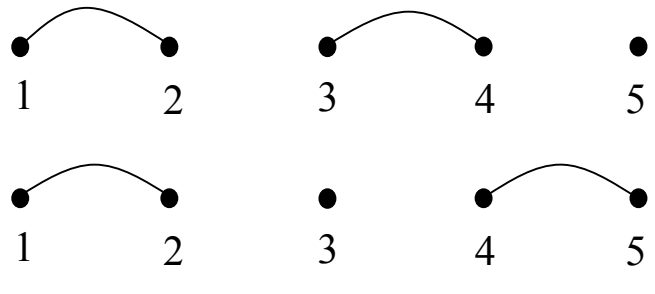

$$\rightarrow 3(-1)^2\left\langle \lambda_j{}^2\right\rangle_s^2\left\langle \lambda_j\right\rangle_s$$

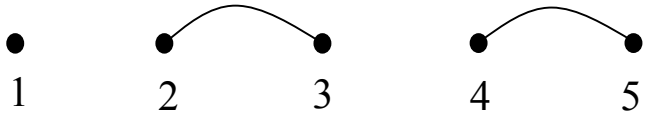

Now, for the fourth order case with two contractions we obtain

$$3\left[\left\langle \lambda_j{}^3 \right\rangle_s \left\langle \lambda_j \right\rangle_s^2 + \left\langle \lambda_j{}^2 \right\rangle_s^2 \left\langle \lambda_j \right\rangle_s^2 \left\langle \lambda_j \right\rangle_s\right]$$

Next, we examine the situation in which there are a total of three connections.

We will be seeking four diagrams, which are:

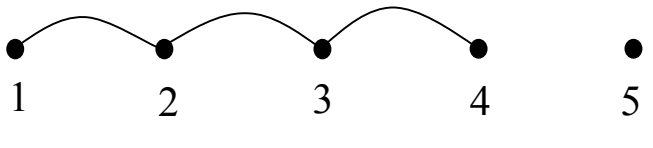

$$\rightarrow (-1)\left\langle \lambda_j{}^4 \right\rangle \left\langle \lambda_j \right\rangle$$

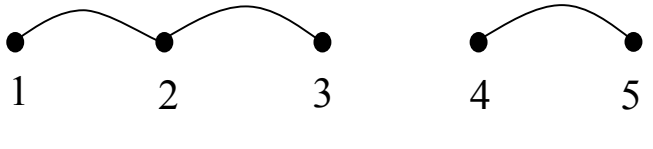

$$\rightarrow (-1)\left\langle \lambda_j{}^3 \right\rangle \left\langle \lambda_j{}^2 \right\rangle$$

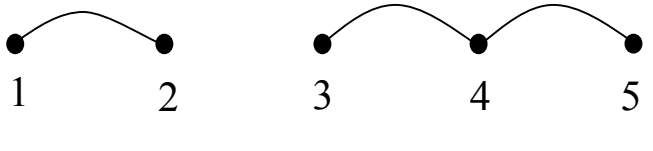

$$\rightarrow (-1)\left\langle \lambda_j{}^2 \right\rangle \left\langle \lambda_j{}^3 \right\rangle$$

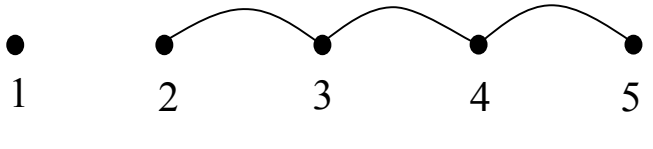

$$\rightarrow (-1)\left\langle \lambda_j \right\rangle \left\langle \lambda_j{}^4 \right\rangle$$

The total contribution in the case of three connections is

$$-2\left[\left\langle \lambda_j{}^4 \right\rangle \left\langle \lambda_j \right\rangle + \left\langle \lambda_j{}^3 \right\rangle \left\langle \lambda_j{}^2 \right\rangle\right]$$

Four connections will link all of the nodes and the contribution is

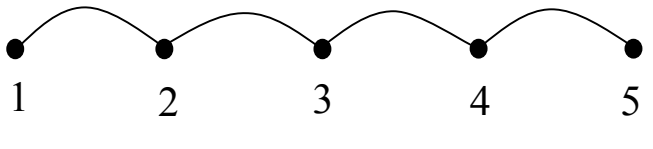

$$\rightarrow \left\langle \lambda_j{}^5 \right\rangle$$

Combining the results yields

$$\sum_{k=1}^{N-1}\sum_{k_1=1}^{N-1}\sum_{k_2=1}^{N-1}\sum_{k_3=1}^{N-1}\lambda_{k_3}\lambda_{k-k_1}\lambda_{k_1-k_2}\lambda_{k_2-k_3}\lambda_{-k} = \begin{bmatrix} \langle\lambda_j^{\,5}\rangle_s - 2\langle\lambda_j^{\,4}\rangle_s\langle\lambda_j\rangle_s - 2\langle\lambda_j^{\,3}\rangle_s\langle\lambda_j^{\,2}\rangle_s + 3\langle\lambda_j^{\,2}\rangle_s^2\langle\lambda_j\rangle_s \\ +3\langle\lambda_j^{\,3}\rangle_s\langle\lambda_j\rangle_s^2 - 4\langle\lambda_j^{\,2}\rangle_s\langle\lambda_j\rangle_s^3 + \langle\lambda_j\rangle_s^5 \end{bmatrix}$$

The sixth order case is handled in the same manner as the previous five cases. If all five contractions are avoided, the contribution is

After examining single and multiple contiguous and noncontiguous contractions as done previously, we find that in total, we have

$$\sum_{k=1}^{N-1}\sum_{k_1=1}^{N-1}\sum_{k_2=1}^{N-1}\sum_{k_3=1}^{N-1}\sum_{k_4=1}^{N-1}\lambda_{k_4}\lambda_{k-k_1}\lambda_{k_1-k_2}\lambda_{k_2-k_3}\lambda_{k_3-k_4}\lambda_{-k} = \begin{bmatrix} \langle\lambda_j^{\,6}\rangle_s - 2\langle\lambda_j^{\,5}\rangle_s\langle\lambda_j\rangle_s - 2\langle\lambda_j^{\,4}\rangle_s\langle\lambda_j^{\,2}\rangle_s - \langle\lambda_j^{\,3}\rangle_s + 3\langle\lambda_j^{\,4}\rangle_s\langle\lambda_j\rangle_s^2 \\ +6\langle\lambda_j^{\,3}\rangle_s\langle\lambda_j^{\,2}\rangle_s\langle\lambda_j\rangle_s + \langle\lambda_j^{\,2}\rangle_s^3 - 4\langle\lambda_j^{\,3}\rangle_s\langle\lambda_j\rangle_s^3 - 6\langle\lambda_j^{\,2}\rangle_s^2\langle\lambda_j\rangle_s^2 \\ +5\langle\lambda_j^{\,2}\rangle_s\langle\lambda_j\rangle_s^4 - \langle\lambda_j\rangle_s^6 \end{bmatrix}$$

Hence, up to sixth order in the perturbation we have:

$$\bar{I} = \frac{v_0 e^{-\frac{a}{l}}}{R_0}\begin{bmatrix} 1+\langle\lambda_j\rangle_s + \left(\langle\lambda_j\rangle_s^2 - \langle\lambda_j^{\,2}\rangle_s\right) - \left(2\langle\lambda_j^{\,2}\rangle_s\langle\lambda_j\rangle_s - \langle\lambda_j\rangle_s^3 - \langle\lambda_j^{\,3}\rangle_s\right) + \begin{pmatrix} \langle\lambda_j\rangle_s^4 - 3\langle\lambda_j^{\,2}\rangle_s\langle\lambda_j\rangle_s^2 \\ +2\langle\lambda_j^{\,3}\rangle_s\langle\lambda_j\rangle_s + \langle\lambda_j^{\,2}\rangle_s^2 - \langle\lambda_j^{\,4}\rangle_s \end{pmatrix} \\ +\left(-\langle\lambda_j^{\,5}\rangle_s + 2\langle\lambda_j^{\,4}\rangle_s\langle\lambda_j\rangle_s + 2\langle\lambda_j^{\,3}\rangle_s\langle\lambda_j^{\,2}\rangle_s - 3\langle\lambda_j^{\,2}\rangle_s^2\langle\lambda_j\rangle_s - 3\langle\lambda_j^{\,3}\rangle_s\langle\lambda_j\rangle_s^2 + 4\langle\lambda_j^{\,2}\rangle_s\langle\lambda_j\rangle_s^3 - \langle\lambda_j\rangle_s^5\right) \\ +\begin{pmatrix} -\langle\lambda_j^{\,6}\rangle_s + 2\langle\lambda_j^{\,5}\rangle_s\langle\lambda_j\rangle_s + 2\langle\lambda_j^{\,4}\rangle_s\langle\lambda_j^{\,2}\rangle_s + \langle\lambda_j^{\,3}\rangle_s - 3\langle\lambda_j^{\,4}\rangle_s\langle\lambda_j\rangle_s^2 - 6\langle\lambda_j^{\,3}\rangle_s\langle\lambda_j^{\,2}\rangle_s\langle\lambda_j\rangle_s - \langle\lambda_j^{\,2}\rangle_s^3 \\ +4\langle\lambda_j^{\,3}\rangle_s\langle\lambda_j\rangle_s^3 + 6\langle\lambda_j^{\,2}\rangle_s^2\langle\lambda_j\rangle_s^2 - 5\langle\lambda_j^{\,2}\rangle_s\langle\lambda_j\rangle_s^4 + \langle\lambda_j\rangle_s^6 \end{pmatrix} \end{bmatrix}$$

6.3: Validating the Analytical Techniqueby Direct Comparison

In the one-dimensional case where nearest neighbor couplings are considered, an alternative approach is possible which is complementary to and distinct from the method of expansion facilitated by diagrammatic analysis. This simpler technique, which

involves summing up resistances to calculate an equivalent resistance, can't be implemented if one generalizes to connections beyond next-nearest neighbors, or if geometries in two or three dimensions are considered, even in the case of conductive links among nearest neighbors. However, for the one-dimensional case it is advantageous to perform the calculation using the simpler approach to check the validity of the more general technique.

As noted earlier, the total resistance is

$$R_{eq} = R_0 e^{\frac{a}{l}} \sum_{j=0}^{N-1} e^{\left[x_{j+1} - x_j\right]}$$

$$= R_0 e^{\frac{a}{l}} \sum_{j=0}^{N-1} \frac{1}{e^{\left[x_j - x_{j+1}\right]/l}}$$

$$= R_0 e^{\frac{a}{l}} \sum_{j=0}^{N-1} \left(\frac{1}{1+\lambda_j} \right)$$

$$= N R_0 e^{\frac{a}{l}} \frac{1}{N} \sum_{j=0}^{N-1} \left[1 - \lambda_j + \lambda_j{}^2 - \lambda_j{}^3 + \lambda_j{}^4 - \ldots \right]$$

$$= N R_0 e^{\frac{a}{l}} \left[1 - \left\langle \lambda_j \right\rangle_s + \left\langle \lambda_j{}^2 \right\rangle_s - \left\langle \lambda_j{}^3 \right\rangle_s + \ldots \right]$$

Although the equivalent resistance has a relatively simple formula, we need to form the reciprocal in order to calculate the total current flowing in the system. This total current should be the same as the quantity $\bar{I}$ calculated using the diagrammatic expansion.

Particularly, we know from Ohm's law that

$$\bar{I} = \frac{V_0}{R_{eq}}$$

$$= \frac{V_0}{N R_0} \left[1 - \left\langle \lambda_j \right\rangle_s + \left\langle \lambda_j{}^2 \right\rangle_s - \left\langle \lambda_j{}^3 \right\rangle_s + \ldots \right]^{-1}$$

$$= \frac{v_0}{R_0}\left[\begin{array}{l} 1 + d_1\left(-\left\langle \lambda_j \right\rangle_s\right) + \left\{ d_1\left\langle \lambda_j^{\,2} \right\rangle_s + \frac{1}{2} d_2\left(-\left\langle \lambda_j \right\rangle_s\right)^2 \right\} + \left\{ d_1\left(-\left\langle \lambda_j^{\,3} \right\rangle_s\right) + d_2\left(-\left\langle \lambda_j \right\rangle_s \left\langle \lambda_j^{\,2} \right\rangle_s\right) + \frac{1}{6} d_3\left(-\left\langle \lambda_j \right\rangle_s\right)^3 \right\} \\ + \left\{ d_1\left\langle \lambda_j^{\,4} \right\rangle_s + d_2\left\langle \lambda_j^{\,3} \right\rangle_s \left\langle \lambda_j \right\rangle_s + \frac{1}{2} d_2\left\langle \lambda_j^{\,2} \right\rangle_s^2 + \frac{1}{2} d_3\left\langle \lambda_j^{\,2} \right\rangle_s \left\langle \lambda_j \right\rangle_s \left\langle \lambda_j \right\rangle_s + \frac{1}{24} d_4\left\langle \lambda_j \right\rangle_s^4 \right\} + \ldots \end{array}\right]$$

Upon further calculation, we find for the current

$$\bar{I} = \frac{v_0}{R_0}\left[\begin{array}{l} 1 + \left\langle \lambda_j \right\rangle_s + \left(-\left\langle \lambda_j^{\,2} \right\rangle_s + \left\langle \lambda_j \right\rangle_s^2\right) + \left(\left\langle \lambda_j^{\,3} \right\rangle_s - 2\left\langle \lambda_j^{\,2} \right\rangle_s \left\langle \lambda_j \right\rangle_s + \left\langle \lambda_j \right\rangle_s^3\right) + \left(\begin{array}{l} -\left\langle \lambda_j^{\,4} \right\rangle_s + 2\left\langle \lambda_j^{\,3} \right\rangle_s \left\langle \lambda_j \right\rangle_s + \left\langle \lambda_j^{\,2} \right\rangle_s^2 \\ -3\left\langle \lambda_j^{\,2} \right\rangle_s \left\langle \lambda_j \right\rangle_s^2 + \left\langle \lambda_j \right\rangle_s^4 \end{array}\right) \\ + \left\{ \begin{array}{l} d_1\left(-\left\langle \lambda_j^{\,5} \right\rangle_s\right) + d_2\left(-\left\langle \lambda_j^{\,4} \right\rangle_s \left\langle \lambda_j \right\rangle_s\right) + d_2\left(-\left\langle \lambda_j^{\,3} \right\rangle_s \left\langle \lambda_j^{\,2} \right\rangle_s\right) + \frac{1}{2} d_3\left(-\left\langle \lambda_j^{\,3} \right\rangle_s \left\langle \lambda_j \right\rangle_s^2\right) + \frac{1}{2} d_3\left(-\left\langle \lambda_j^{\,2} \right\rangle_s^2 \left\langle \lambda_j \right\rangle_s\right) \\ + \frac{1}{6} d_4\left\langle \lambda_j^{\,2} \right\rangle_s \left\langle \lambda_j \right\rangle_s^3 + \frac{1}{120} d_5\left(-\left\langle \lambda_j \right\rangle_s^5\right) \end{array} \right\} \\ + \left\{ \begin{array}{l} d_1\left\langle \lambda_j^{\,6} \right\rangle_s + d_2\left\langle \lambda_j^{\,5} \right\rangle_s \left\langle \lambda_j \right\rangle_s + d_2\left\langle \lambda_j^{\,4} \right\rangle_s \left\langle \lambda_j^{\,2} \right\rangle_s + \frac{1}{2} d_3\left\langle \lambda_j^{\,4} \right\rangle_s \left\langle \lambda_j \right\rangle_s^2 + \frac{1}{2}\left\langle \lambda_j^{\,3} \right\rangle_s^2 + d_3\left\langle \lambda_j^{\,3} \right\rangle_s \left\langle \lambda_j^{\,2} \right\rangle_s \left\langle \lambda_j \right\rangle_s \\ + \frac{1}{6} d_4\left\langle \lambda_j^{\,3} \right\rangle_s \left\langle \lambda_j \right\rangle_s^3 + \frac{1}{6} d_3\left\langle \lambda_j^{\,2} \right\rangle_s^3 + \frac{1}{4} d_4\left\langle \lambda_j^{\,2} \right\rangle_s^2 \left\langle \lambda_j \right\rangle_s^2 + \frac{1}{24} d_5\left\langle \lambda_j^{\,2} \right\rangle_s \left\langle \lambda_j \right\rangle_s^4 + \frac{1}{720} d_6\left\langle \lambda_j \right\rangle_s^6 \end{array} \right\} \\ + \ldots \end{array}\right]$$

After full evaluation of the fifth and sixth order terms, we find

$$\bar{I} = \frac{v_0}{R_0}\left[\begin{array}{l} 1 + \left\langle \lambda_j \right\rangle_s + \left(-\left\langle \lambda_j^{\,2} \right\rangle_s + \left\langle \lambda_j \right\rangle_s^2\right) + \left(\left\langle \lambda_j^{\,3} \right\rangle_s - 2\left\langle \lambda_j^{\,2} \right\rangle_s \left\langle \lambda_j \right\rangle_s + \left\langle \lambda_j \right\rangle_s^3\right) + \left(\begin{array}{l} -\left\langle \lambda_j^{\,4} \right\rangle_s + 2\left\langle \lambda_j^{\,3} \right\rangle_s \left\langle \lambda_j \right\rangle_s + \left\langle \lambda_j^{\,2} \right\rangle_s^2 \\ -3\left\langle \lambda_j^{\,2} \right\rangle_s \left\langle \lambda_j \right\rangle_s^2 + \left\langle \lambda_j \right\rangle_s^4 \end{array}\right) \\ + \left(\left\langle \lambda_j^{\,5} \right\rangle_s - 2\left\langle \lambda_j^{\,4} \right\rangle_s \left\langle \lambda_j \right\rangle_s - 2\left\langle \lambda_j^{\,3} \right\rangle_s \left\langle \lambda_j^{\,2} \right\rangle_s + 3\left\langle \lambda_j^{\,3} \right\rangle_s \left\langle \lambda_j \right\rangle_s^2 + 3\left\langle \lambda_j^{\,2} \right\rangle_s^2 \left\langle \lambda_j \right\rangle_s - 4\left\langle \lambda_j^{\,2} \right\rangle_s \left\langle \lambda_j \right\rangle_s^3 + \left\langle \lambda_j \right\rangle_s^5\right) \\ + \left(\begin{array}{l} -\left\langle \lambda_j^{\,6} \right\rangle_s + 2\left\langle \lambda_j^{\,5} \right\rangle_s \left\langle \lambda_j \right\rangle_s + 2\left\langle \lambda_j^{\,4} \right\rangle_s \left\langle \lambda_j^{\,2} \right\rangle_s - 3\left\langle \lambda_j^{\,4} \right\rangle_s \left\langle \lambda_j \right\rangle_s^2 + \left\langle \lambda_j^{\,3} \right\rangle_s^2 - 6\left\langle \lambda_j^{\,3} \right\rangle_s \left\langle \lambda_j^{\,2} \right\rangle \left\langle \lambda_j \right\rangle_s \\ +4\left\langle \lambda_j^{\,3} \right\rangle_s \left\langle \lambda_j \right\rangle_s^3 - \left\langle \lambda_j^{\,2} \right\rangle_s^3 + 6\left\langle \lambda_j^{\,2} \right\rangle_s^2 \left\langle \lambda_j \right\rangle_s^2 - 5\left\langle \lambda_j^{\,2} \right\rangle_s \left\langle \lambda_j \right\rangle_s^4 + \left\langle \lambda_j \right\rangle_s^6 \end{array}\right) \end{array}\right]$$

which is an exact reproduction of what we obtained in the diagrammatic analysis.

In the one-dimensional case, the current $\bar{I}$ is calculated by forming the reciprocal of the system averaged equivalent resistance R_{eq}. Therefore, it's clear that the

diagrammatic approach is of little computational merit in the context of the one-dimensional case in which nearest neighbors are joined by resistance links. However, the diagrammatic method is much more useful in two and three dimensions where an expression for R_{eq} is not as straightforward to calculate.

CHAPTER 7

RANDOM RESISTOR NETWORKS IN TWO DIMENSIONS: ANALYTICAL AND NUMERICAL RESULTS

We shall find that we may make progress in both two and three dimensions by using a method substantially similar to the reciprocal space perturbative expansion derived for the one-dimensional counterpart. **Figure 46** shows a typical two-dimensional situation:

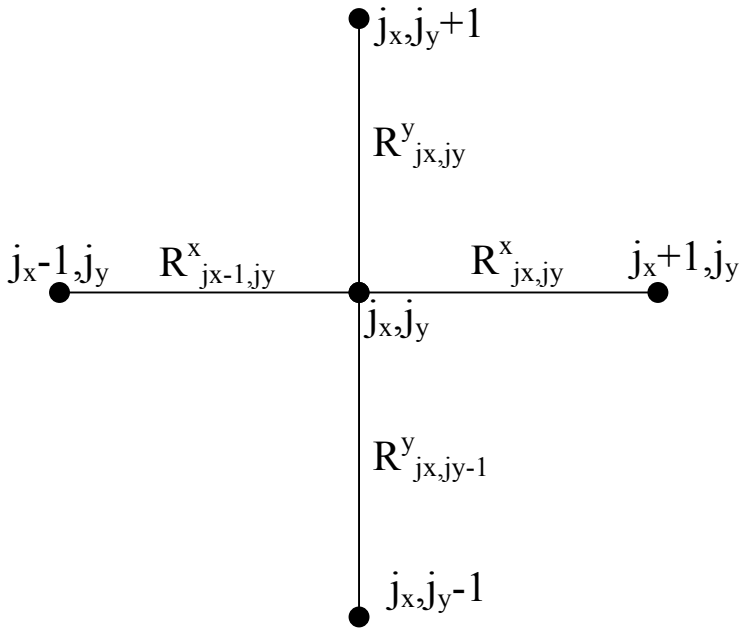

Figure 46: Illustration of the labeling scheme for the nodes and link resistances in the two-dimensional square lattice; connections are confined to nearest neighbors

7.1: Introducing the Conductance of Links

Before we examine the local charge conservation condition, let's revisit Ohm's Law that states that $I = \frac{\Delta V}{R}$. We will gain a measure of convenience by redefining this relation as

$$I = \Delta V \sigma$$

where $\sigma = \frac{1}{R}$ is the conductance. Having assigned a resistance R_{ij}^{x} to the horizontal links and R_{ij}^{y} to their vertical couterparts, we may do the same for conductances: $\sigma_{ij}^{x} = \frac{1}{R_{ij}^{x}}$ and $\sigma_{ij}^{y} = \frac{1}{R_{ij}^{y}}$. In terms of the conductances, the current that flows from the node j_x, j_y to the adjacent node j_{x+1}, j_y to the right is

$$I_{\left[j_x, j_y; j_x+1, j_y\right]} = \sigma_{j_x, j_y}^{x}\left(V_{j_x, j_y} - V_{j_x+1, j_y}\right)$$

Local charge conservation yields the constraint

$$0 = \sigma_{j_x, j_y}^{x}\left(V_{j_x, j_y} - V_{j_x+1, j_y}\right) - \sigma_{j_x-1, j_y}^{x}\left(V_{j_x-1, j_y} - V_{j_x, j_y}\right) + \sigma_{j_x, j_y}^{y}\left(V_{j_x, j_y} - V_{j_x, j_y+1}\right) - \sigma_{j_x, j_y-1}^{y}\left(V_{j_x, j_y-1} - V_{j_x, j_y}\right)$$

$$= \left[V_{j_x, j_y}\left(\sigma_{j_x, j_y}^{x} + \sigma_{j_x, j_y}^{y} + \sigma_{j_x-1, j_y}^{x} + \sigma_{j_x, j_y-1}^{y}\right) - V_{j_x+1, j_y}\sigma_{j_x, j_y}^{x} - V_{j_x-1, j_y}\sigma_{j_x-1, j_y}^{x} - V_{j_x, j_y+1}\sigma_{j_x, j_y}^{y} - V_{j_x, j_y-1}\sigma_{j_x, j_y-1}^{y}\right]$$

This expression becomes tidier and in some ways more transparent when we use the Fourier variables.

7.1.1: Defining the Conductance and the Potential Shifts

It is our goal now to operate in terms of the Fourier variables and obtain a perturbative series in the quantity parameterizing the shifts in conductance values. When introducing the shifts, we use $\sigma_{j_x, j_y}^{x} = \sigma_0 - \lambda_{j_x, j_y}^{x}$ and $\sigma_{j_x, j_y}^{y} = \sigma_0 - \lambda_{j_x, j_y}^{y}$ so the variations

are encoded in $\lambda^x_{j_x,j_y}$ and $\lambda^y_{j_x,j_y}$ for $\sigma^x_{j_x,j_y}$ and $\sigma^y_{j_x,j_y}$ respectively. There will be commensurate changes in the potential values at nodes.

We use $V_{j_x,j_y} = -\frac{V_0}{N} j_x + \Delta V_{j_x,j_y} \equiv -v_0 j_x + \Delta V_{j_x,j_y}$. The current constraint assumes the form

$$0 = \begin{bmatrix} \left(-v_0 j_x + \Delta V_{j_x,j_y}\right)\left(4\sigma_0 - \lambda^x_{j_x,j_y} - \lambda^y_{j_x,j_y} - \lambda^x_{j_x-1,j_y} - \lambda^y_{j_x,j_y-1}\right) - \left(-v_0\left[j_x+1\right] + \Delta V_{j_x+1,j_y}\right)\left(\sigma_0 - \lambda^x_{j_x,j_y}\right) \\ -\left(-v_0\left[j_x-1\right] + \Delta V_{j_x-1,j_y}\right)\left(\sigma_0 - \lambda^y_{j_x-1,j_y}\right) - \left(-v_0 j_x + \Delta V_{j_x,j_y+1}\right)\left(\sigma_0 - \lambda^y_{j_x,j_y}\right) - \left(-v_0 j_x + \Delta V_{j_x,j_y-1}\right)\left(\sigma_0 - \lambda^y_{j_x,j_y-1}\right) \end{bmatrix}$$

After algebraic manipulation, we find

$$\sigma\left(4\Delta V_{j_x,j_y} - \Delta V_{j_x+1,j_y} - \Delta V_{j_x-1,j_y} - \Delta V_{j_x,j_y+1} - \Delta V_{j_x,j_y-1}\right) + v_0\left(\lambda^x_{j_x-1,j_y} - \lambda^x_{j_x,j_y}\right) + \lambda^x_{j_x,j_y}\left(\Delta V_{j_x+1,j_y} - \Delta V_{j_x,j_y}\right)$$
$$+\lambda^y_{j_x,j_y}\left(\Delta V_{j_x,j_y+1} - \Delta V_{j_x,j_y}\right) + \lambda^x_{j_x-1,j_y}\left(\Delta V_{j_x-1,j_y} - \Delta V_{j_x,j_y}\right) + \lambda^x_{j_x,j_y-1}\left(\Delta V_{j_x,j_y-1} - \Delta V_{j_x,j_y}\right) = 0$$

7.1.2: Fourier Analysis of the Charge Conservation Constraint

Once again, we introduce the Fourier variables with $\Delta V_{j_x,j_y} = \sum_{k_x=0}^{N-1}\sum_{k_y=0}^{N-1} \Delta V_{k_x,k_y} e^{\frac{2\pi i}{N}\left[k_x j_x + k_y j_y\right]}$.

Next, we insert the Fourier expansions for ΔV, λ^x, and λ^y into the charge conservation condition and select an individual Fourier component by exploiting the orthogonality of the Fourier states. The result is

$$0 = \sigma_0\left[4 - e^{\frac{2\pi i}{N}k_x} - e^{\frac{-2\pi i}{N}k_y} - e^{\frac{2\pi i}{N}k_y} - e^{\frac{-2\pi i}{N}k_y}\right]V_{k_x,k_y} + v_0\lambda^x_{k_x,k_y}\left[e^{\frac{-2\pi i}{N}k_x} - 1\right]$$
$$+\sum_{k_x'=0}^{N-1}\sum_{k_y'=0}^{N-1}\begin{bmatrix} \Delta V_{k_x',k_y'}\lambda^x_{k_x-k_x',k_y-k_y'}\left(\left[e^{\frac{2\pi i}{N}k_x'} - 1\right] + e^{\frac{-2\pi i}{N}\left(k_x-k_x'\right)}\left[e^{\frac{-2\pi i}{N}k_x'} - 1\right]\right) + \\ \Delta V_{k_x',k_y'}\lambda^y_{k_x-k_x',k_y-k_y'}\left(\left[e^{\frac{2\pi i}{N}k_y'} - 1\right] + e^{\frac{-2\pi i}{N}\left(k_y-k_y'\right)}\left[e^{\frac{-2\pi i}{N}k_y'} - 1\right]\right) \end{bmatrix}$$

This relation may be expressed more succinctly if we use $g^0_{k_x} \equiv \left[e^{\frac{2\pi i}{N} k_x} - 1 \right]$ as well as $g^0_{k_y} \equiv \left[e^{\frac{2\pi i}{N} k_y} - 1 \right]$. In terms of bare propagators $g^0_{k_x}$ and $g^0_{k_y}$ we thus have

$$0 = \sigma_0 \left[g^0_{k_x} g^0_{-k_x} + g^0_{k_y} g^0_{-k_y} \right] V_{k_x,k_y} + v_0 \lambda^x_{k_x,k_y} g^0_{-k_x} - \sum_{k_x'=0}^{N-1} \sum_{k_y'=0}^{N-1} \left[\Delta V_{k_x',k_y'} \lambda^x_{k_x-k_x',k_y-k_y'} g^0_{-k_x} g^0_{k_x'} + \Delta V_{k_x',k_y'} \lambda^y_{k_x-k_x',k_y-k_y'} g^0_{-k_y} g^0_{k_y'} \right.$$

Noting that the expression $\left(g^0_{-k_x} g^0_{k_x'} + g^0_{-k_y} g^0_{k_y'} \right)$ is proportional to the Laplacian in Fourier space, we use $\hat{\Delta}_{\vec{K}} \equiv g^0_{-k_x} g^0_{k_x'} + g^0_{-k_y} g^0_{k_y'}$ where $\vec{K}$ is shorthand for the wave number duo $\left(k_x, k_y \right)$. We also define $\vec{\lambda}_{\vec{K}} \equiv \left[\lambda^x_{k_x,k_y}, \lambda^y_{k_x,k_y} \right]$ and $\vec{\Lambda}_{\vec{K}_1,\vec{K}_2} \equiv \left[g^0_{k_x^1} g^0_{k_x^2}, g^0_{k_y^1} g^0_{k_y^2} \right]$. In terms of these variables, we obtain $0 = \sigma_0 \hat{\Delta}_{\vec{K}} \Delta V_{\vec{K}} + v_0 \lambda^x_{\vec{K}} g^0_{-k_x} - \sum_{\vec{K}'} \Delta V_{\vec{K}'} \vec{\lambda}_{\vec{K}-\vec{K}'} \cdot \vec{\Lambda}_{-\vec{K},\vec{K}'}$ so that we have the means to solve for $\Delta V_{\vec{K}}$. Noting that $\Delta V_0 = 0$, we observe that we must avoid dividing by $\hat{\Delta}_0$ because doing so would be equivalent to dividing by zero. Then we have

$$\hat{\Delta}_{\vec{K}} = \frac{-v_0}{\sigma_0} \frac{\lambda^x_{\vec{K}} g^0_{-k_x}}{\hat{\Delta}_{\vec{K}}} + \frac{1}{\sigma_0 \hat{\Delta}_{\vec{K}}} \sum_{\vec{K}' \neq 0} \Delta V_{\vec{K}'} \vec{\lambda}_{\vec{K}-\vec{K}'} \cdot \vec{\Lambda}_{-\vec{K},\vec{K}'}$$

7.2: Devleoping the Perturbative Series in Fourier Space

Just as we did previously in the one-dimensional case, we use an iterative process to develop a perturbative expansion for $\hat{\Delta}_{\vec{K}}$. This leads to

$$\Delta V_{\vec{K}} = \frac{-v_0 \lambda^x_{\vec{K}} g^0_{-k_x}}{\sigma_0 \hat{\Delta}_{\vec{K}}} + \sum_{\vec{K} \neq 0} \frac{1}{\hat{\Delta}_{\vec{K}}} \left[\frac{-v_0}{\sigma_0} \frac{\lambda^x_{\vec{K}'} g^0_{-k_x'}}{\hat{\Delta}_{\vec{K}'}} + \frac{1}{\sigma_0 \hat{\Delta}_{\vec{K}'}} \sum_{\vec{K}'' \neq 0} \Delta V_{\vec{K}''} \vec{\lambda}_{\vec{K}'-\vec{K}''} \cdot \vec{\Lambda}_{-\vec{K}',\vec{K}''} \right] \left(\vec{\lambda}_{\vec{K}-\vec{K}'} \cdot \vec{\Lambda}_{-\vec{K},\vec{K}'} \right)$$

$$= \frac{-v_0}{\sigma_0}\frac{\lambda^x_{\vec{K}} g^0_{-k_x}}{\hat{\Delta}_{\vec{K}}} - \frac{v_0}{{\sigma_0}^2}\sum_{\vec{K}'\neq 0}\frac{\lambda^x_{\vec{K}'} g^0_{-k_x'}}{\hat{\Delta}_{\vec{K}}\hat{\Delta}_{\vec{K}'}}\left(\vec{\lambda}_{\vec{K}-\vec{K}'}\cdot\vec{\Lambda}_{-\vec{K},\vec{K}'}\right) + \frac{1}{{\sigma_0}^2}\sum_{\vec{K}'\neq 0}\sum_{\vec{K}''\neq 0}\frac{1}{\hat{\Delta}_{\vec{K}}\hat{\Delta}_{\vec{K}'}}\Delta V_{\vec{K}''}\left(\vec{\lambda}_{\vec{K}'-\vec{K}''}\cdot\vec{\Lambda}_{-\vec{K}',\vec{K}''}\right)\left(\vec{\lambda}_{\vec{K}-\vec{K}'}\cdot\vec{\Lambda}_{-\vec{K},\vec{K}'}\right)$$

$$= \frac{-v_0}{\hat{\Delta}_{\vec{K}}}\left[\begin{array}{l}\dfrac{\lambda^x_{\vec{K}} g^0_{-k_x}}{\sigma_0} + \dfrac{1}{{\sigma_0}^2}\displaystyle\sum_{\vec{K}'\neq 0}\frac{\lambda^x_{\vec{K}'} g^0_{-k_x'}}{\hat{\Delta}_{\vec{K}'}}\left(\vec{\lambda}_{\vec{K}-\vec{K}'}\cdot\vec{\Lambda}_{-\vec{K},\vec{K}'}\right) + \dfrac{1}{{\sigma_0}^3}\displaystyle\sum_{\vec{K}'\neq 0}\sum_{\vec{K}''\neq 0}\frac{\lambda^x_{\vec{K}''} g^0_{-k_x''}}{\hat{\Delta}_{\vec{K}'}\hat{\Delta}_{\vec{K}''}}\left(\vec{\lambda}_{\vec{K}'-\vec{K}''}\cdot\vec{\Lambda}_{-\vec{K}',\vec{K}''}\right)\left(\vec{\lambda}_{\vec{K}-\vec{K}'}\cdot\vec{\Lambda}_{-\vec{K},\vec{K}'}\right) \\ + \dfrac{1}{{\sigma_0}^4}\displaystyle\sum_{\vec{K}'\neq 0}\sum_{\vec{K}''\neq 0}\sum_{\vec{K}'''\neq 0}\frac{\lambda^x_{\vec{K}'''} g^0_{-k_x'''}}{\hat{\Delta}_{\vec{K}'}\hat{\Delta}_{\vec{K}''}\hat{\Delta}_{\vec{K}'''}}\left(\vec{\lambda}_{\vec{K}''-\vec{K}'''}\vec{\Lambda}_{-\vec{K}'',\vec{K}'''}\right)\left(\vec{\lambda}_{\vec{K}'-\vec{K}''}\cdot\vec{\Lambda}_{-\vec{K}',\vec{K}''}\right)\left(\vec{\lambda}_{\vec{K}-\vec{K}'}\cdot\vec{\Lambda}_{-\vec{K},\vec{K}'}\right) + \ldots\end{array}\right]$$

This expression is valid in broader generality, and will be applied in the three-dimensional case as well.

7.2.1: Calculating the Current in Fourier Space

Next we will calculate the mean current $\bar{I}$ moving from the nodes in the $\hat{x}$ direction. We will evaluate the contributions order by order in the perturbations λ. We will calculate $\bar{I}$ first, and then perform the average over disorder. For $\bar{I}$ we have

$$\bar{I} = \frac{1}{N^2}\sum_{j_x=0}^{N-1}\sum_{j_y=0}^{N-1}\sigma^x_{j_x,j_y}\left(V_{j_x,j_y} - V_{j_x+1,j_y}\right)$$

$$= \frac{1}{N^2}\sum_{j_x=0}^{N-1}\sum_{j_y=0}^{N-1}\left(\sigma_0 - \lambda^x_{j_x,j_y}\right)\left(\frac{V_0}{N} + \Delta V_{j_x,j_y} - \Delta V_{j_x+1,j_y}\right)$$

$$= \frac{1}{N^2}\left[N^2\left(\frac{V_0\sigma_0}{N}\right) + \sigma_0\sum_{j_x=0}^{N-1}\sum_{j_y=0}^{N-1}\left(\Delta V_{j_x,j_y} - \Delta V_{j_x+1,j_y}\right) - \frac{V_0}{N}\sum_{j_x=0}^{N-1}\sum_{j_y=0}^{N-1}\lambda^x_{j_x,j_y} + \sum_{j_x=0}^{N-1}\sum_{j_y=0}^{N-1}\lambda^x_{j_x,j_y}\left(\Delta V_{j_x+1,j_y} - \Delta V_{j_x,j_y}\right)\right]$$

$$= \left[v_0\sigma_0 + 0 - \frac{v_0}{N^2}\sum_{j_x=0}^{N-1}\sum_{j_y=0}^{N-1}\lambda^x_{j_x,j_y} + \frac{1}{N^2}\sum_{j_x=0}^{N-1}\sum_{j_y=0}^{N-1}\lambda^x_{j_x,j_y}\left(\Delta V_{j_x+1,j_y} - \Delta V_{j_x,j_y}\right)\right]$$

where the second term vanishes due to the periodicity condition.

7.3: Averaging over Disorder

Now, we make the assumption that none of the conductance fluctuations $\lambda^x_{j_x,j_y}$ and $\lambda^y_{j_x,j_y}$ are correlated, and are sampled independently from the same statistical

distribution. Operating in this context, we may average over disorder and thereby obtain specific expressions for the zeroth order and first order terms in λ. Particularly, one finds that

$$\langle \bar{I} \rangle = v_0 \sigma_0 - v_0 \langle \lambda \rangle + \frac{1}{N^2} \sum_{j_x=0}^{N-1} \sum_{j_y=0}^{N-1} \left\langle \lambda^x_{j_x, j_y} \left(\Delta V_{j_x+1, j_y} - \Delta V_{j_x, j_y} \right) \right\rangle$$

The second and higher order terms emerge on the last term in the right side of the expression. Noting that if the conductance shifts λ are as often positive as negative, it's clear that one will have $\langle \lambda \rangle = 0$ so the corrections to the current will be second and higher order in λ. However, a non-vanishing $\langle \lambda \rangle$ will lead to contributions linear in the perturbation which survive the configurational average.

7.3.1: Developing the Perturbative Series for the Current

Now we'll examine and evaluate the term

$$\frac{1}{N^2} \sum_{j_x=0}^{N-1} \sum_{j_y=0}^{N-1} \lambda^x_{j_x, j_y} \left(\Delta V_{j_x+1, j_y} - \Delta V_{j_x, j_y} \right) \equiv I_2$$

Reverting to Fourier components gives

$$I_2 = \frac{1}{N^2} \sum_{\vec{x}} \left(\sum_{\vec{K}} \lambda^x_{\vec{K}} e^{i\vec{K} \cdot \vec{x}} \right) \left(\sum_{\vec{K}'} \Delta V_{\vec{K}'} g^0_{k_x'} e^{i\vec{K}' \cdot \vec{x}} \right)$$

The sum over the positions must vanish unless $\vec{K} = -\vec{K}'$. Hence, a Kronecker Delta symbol $\delta_{\vec{K}, -\vec{K}'}$ arises, and one finds that

$$I_2 = \frac{1}{N^2} N^2 \sum_{\vec{K}} \sum_{\vec{K}} \delta_{\vec{K}, -\vec{K}} \lambda^x_{\vec{K}} g^0_{k_x'} e^{i\left[\vec{K} + \vec{K}'\right] \cdot \vec{x}} \Delta V_{\vec{K}'}$$

$$= \sum_{\vec{K}} \lambda^x_{\vec{K}} g^0_{-k_x} \Delta V_{-\vec{K}}$$

$$= \sum_{\vec{K} \neq 0} \lambda^x_{-\vec{K}} g^0_{k_x} \Delta V_{\vec{K}}$$

In the last step we've relabeled the dummy indices for the sake of future convenience.

Now we examine the term I_2 and evaluate it order by order in λ. Particularly, we find that

$$I_2 \equiv \sum_{\vec{K}\neq 0} \lambda^x_{-\vec{K}} \Delta V_{\vec{K}} g^0_{k_x}$$

$$= \frac{-v_0}{\sigma_0}\left[\begin{array}{l} \displaystyle\sum_{\vec{K}\neq 0} \frac{\lambda^x_{\vec{K}}\lambda^x_{-\vec{K}}}{\hat{\Delta}_{\vec{K}}} g^0_{k_x} g^0_{-k_x} + \frac{1}{\sigma_0}\sum_{\vec{K}\neq 0}\sum_{\vec{K}'\neq 0} \frac{\lambda^x_{\vec{K}'}\lambda^x_{-\vec{K}}\left(\vec{\lambda}_{\vec{K}-\vec{K}'}\cdot\vec{\Lambda}_{-\vec{K},\vec{K}'}\right) g^0_{k_x} g^0_{-k_x'}}{\hat{\Delta}_{\vec{K}}\hat{\Delta}_{\vec{K}'}} \\ \displaystyle + \frac{1}{{\sigma_0}^3}\sum_{\vec{K}\neq 0}\sum_{\vec{K}'\neq 0}\sum_{\vec{K}''\neq 0} \frac{\lambda^x_{\vec{K}''}\lambda^x_{-\vec{K}} g^0_{-k_x''} g^0_{k_x}}{\hat{\Delta}_{\vec{K}}\hat{\Delta}_{\vec{K}'}\hat{\Delta}_{\vec{K}''}}\left(\vec{\lambda}_{\vec{K}'-\vec{K}''}\cdot\vec{\Lambda}_{-\vec{K}',\vec{K}''}\right)\left(\vec{\lambda}_{\vec{K}-\vec{K}'}\cdot\vec{\Lambda}_{-\vec{K},\vec{K}'}\right) + O\left(\lambda^5\right) \end{array}\right]$$

If we evaluate the first three terms shown above, we will have evaluated I_2 up to fourth order in the perturbing influence λ.

7.3.2: Calculating the Second Order Contribution

We will examine each of the terms in succession, beginning with the second order piece. So we consider the term

$$\sum_{\vec{K}\neq 0} \frac{\lambda^x_{\vec{K}}\lambda^x_{-\vec{K}}}{\hat{\Delta}_{\vec{K}}} g^0_{k_x} g^0_{-k_x}$$

which contributes to quadratic order in the perturbing influence.

To calculate the configurational average, one must re-express $\lambda^x_{\vec{K}}$ and $\lambda^x_{-\vec{K}}$ in terms of their counterparts in real space. This is done via

$$\lambda^x_{\vec{K}} = \frac{1}{N^2}\sum_{\vec{x}} e^{-i\vec{K}\cdot\vec{x}}\lambda^x_{\vec{x}}$$

So the term of interest now appears as $\displaystyle\sum_{\vec{K}\neq 0}\sum_{\vec{x}}\sum_{\vec{x}'} N^{-4} \frac{\left(e^{-i\vec{K}\cdot\vec{x}}\lambda^x_{\vec{x}}\right)\left(e^{-i\vec{K}\cdot\vec{x}'}\lambda^x_{\vec{x}'}\right) g^0_{k_x} g^0_{-k_x}}{\hat{\Delta}_{\vec{K}}}$.

7.3.2.1: The Disorder Average in Real Space

Now we are required to average properly over disorder, a step that requires careful consideration. We find

$$\left\langle N^{-4}\sum_{\vec{K}\neq 0}\sum_{\vec{x},\vec{x}'}\frac{e^{i\vec{K}\cdot[\vec{x}'-\vec{x}]}\lambda^x_{\vec{x}}\lambda^x_{\vec{x}'}}{\hat{\Delta}_{\vec{K}}}g^0_{k_x}g^0_{-k_x}\right\rangle = N^{-4}\sum_{\vec{K}\neq 0}\sum_{\vec{x},\vec{x}'}\frac{e^{i\vec{K}\cdot[\vec{x}'-\vec{x}]}}{\hat{\Delta}_{\vec{K}}}g^0_{k_x}g^0_{-k_x}\left\langle\lambda^x_{\vec{x}}\lambda^x_{\vec{x}'}\right\rangle$$

At present, it's not possible to perform any of the indicated sums. However, when we average over disorder it will be possible to evaluate the sums. We will therefore carefully examine the term $\left\langle\lambda^x_{\vec{x}}\lambda^x_{\vec{x}'}\right\rangle$. The situation is simplified if $\vec{x}$ and $\vec{x}'$ represent distinct positions. Discretion is advised for situations in which $\vec{x}$ and $\vec{x}'$ are identical. If $\vec{x}=\vec{x}'$, the averages decouple since $\lambda_{\vec{x}}$ and $\lambda_{\vec{x}'}$ are assumed to fluctuate independently. Then we find that $\left\langle\lambda^x_{\vec{x}}\lambda^x_{\vec{x}'}\right\rangle = \left\langle\lambda^x_{\vec{x}}\right\rangle\left\langle\lambda^x_{\vec{x}'}\right\rangle = \langle\lambda\rangle^2$ for $\vec{x}\neq\vec{x}'$. On the other hand, in the circumstance that $\vec{x}=\vec{x}'$, instead we have $\left\langle\lambda^x_{\vec{x}}\lambda^x_{\vec{x}'}\right\rangle = \left\langle\lambda^{x\,2}_{\vec{x}}\right\rangle = \left\langle\lambda^2\right\rangle$ for $\vec{x}=\vec{x}'$.

This condition may be expressed in explicit mathematical terms with the aid of the Kronecker Delta symbol $\delta_{\vec{x}\vec{x}'}$. Specifically, we may write

$$\left\langle\lambda^x_{\vec{x}}\lambda^x_{\vec{x}'}\right\rangle = \left[\langle\lambda\rangle^2 + \delta_{\vec{x}\vec{x}'}\left(\left\langle\lambda^2\right\rangle - \langle\lambda\rangle^2\right)\right]$$

We now have the means to calculate the second order contribution to the configurationally averaged current. One now has

$$N^{-4}\sum_{\vec{K}\neq 0}\sum_{\vec{x},\vec{x}'}\frac{e^{i\vec{K}\cdot[\vec{x}'-\vec{x}]}}{\hat{\Delta}_{\vec{K}}}g^0_{k_x}g^0_{-k_x}\left\langle\lambda^x_{\vec{x}}\lambda^x_{\vec{x}'}\right\rangle = N^{-4}\sum_{\vec{K}\neq 0}\sum_{\vec{x},\vec{x}'}\frac{e^{i\vec{K}\cdot[\vec{x}'-\vec{x}]}}{\hat{\Delta}_{\vec{K}}}g^0_{k_x}g^0_{-k_x}\left[\langle\lambda\rangle^2 + \delta_{\vec{x}\vec{x}'}\left(\left\langle\lambda^2\right\rangle - \langle\lambda\rangle^2\right)\right]$$

7.3.2.2: Exploiting the Square Symmetry

It is advantageous to exploit the square symmetry of the lattice under consideration. Suppose we impose a potential V_0 across the system in the y direction

instead of the horizontal direction. We would obtain the same configurationally averaged current as in the case in which the potential difference is set up in the x direction.

Hence, we see that

$$N^{-4}\sum_{\vec{K}\neq 0}\sum_{\vec{x},\vec{x}'}\frac{e^{i\vec{K}\cdot[\vec{x}'-\vec{x}]}}{\hat{\Delta}_{\vec{K}}}g^0_{k_x}g^0_{-k_x}\left\langle\lambda^x_{\vec{x}}\lambda^x_{\vec{x}'}\right\rangle=\frac{1}{2}N^{-4}\sum_{\vec{K}\neq 0}\sum_{\vec{x},\vec{x}'}\frac{e^{i\vec{K}\cdot[\vec{x}'-\vec{x}]}}{\hat{\Delta}_{\vec{K}}}g^0_{k_x}g^0_{-k_x}\left[\langle\lambda\rangle^2+\delta_{\vec{x}\vec{x}'}\left(\left\langle\lambda^2\right\rangle-\langle\lambda\rangle^2\right)\right]$$

It's important to note that $\hat{\Delta}_{\vec{K}}=g^0_{k_x}g^0_{-k_x}+g^0_{k_y}g^0_{-k_y}$. Our task now entails calculating

$$\frac{1}{2}N^{-4}\sum_{\vec{K}\neq 0}\sum_{\vec{x},\vec{x}'}e^{i\vec{K}\cdot[\vec{x}'-\vec{x}]}g^0_{k_x}g^0_{-k_x}\left[\langle\lambda\rangle^2+\delta_{\vec{x}\vec{x}'}\left(\left\langle\lambda^2\right\rangle-\langle\lambda\rangle^2\right)\right]=\frac{1}{2}N^{-4}\sum_{\vec{K}\neq 0}\langle\lambda\rangle^2\left(\sum_{\vec{x}}e^{-i\vec{K}\cdot\vec{x}}\right)\left(\sum_{\vec{x}'}e^{i\vec{K}\cdot\vec{x}'}\right)+\frac{1}{2}N^{-2}\sum_{\vec{K}\neq 0}\left(\left\langle\lambda^2\right\rangle-\langle\lambda\rangle^2\right)$$

$$=0+\frac{1}{2}\left(1-N^{-2}\right)\left(\left\langle\lambda^2\right\rangle-\langle\lambda\rangle^2\right)$$

The last step simplifies considerably because of the fact that the independent factors $\left(\sum_{\vec{x}}e^{-i\vec{K}\cdot\vec{x}}\right)$ and $\left(\sum_{\vec{x}'}e^{-i\vec{K}\cdot\vec{x}'}\right)$ in the first term vanish for $\vec{K}\neq 0$. On the other hand, omitting the $\vec{K}=0$ term in the second term yields the $\left(1-N^{-2}\right)$ factor.

Then we have for the second order piece the expression

$$\frac{1}{2}\left(1-N^{-2}\right)\left(\left\langle\lambda^2\right\rangle-\langle\lambda\rangle^2\right)$$

So the second order piece is proportional to the standard deviation of the perturbation λ. So up to second order in the perturbing influence, we have

$$\langle\bar{I}\rangle=v_0\left[\sigma_0-\langle\lambda\rangle-\frac{1}{2}\left(1-N^{-2}\right)\left(\left\langle\lambda^2\right\rangle-\langle\lambda\rangle^2\right)\right]$$

7.3.2.3: Specializing to the Bulk Limit

In the bulk limit, one finds that N^{-2} will tend to zero, and the configurationally averaged current is

$$\left\langle \bar{I} \right\rangle = v_0 \sigma_0 \left[1 - \frac{1}{\sigma_0} \left\langle \lambda \right\rangle - \frac{1}{2\sigma_0^{\,2}} \left(\left\langle \lambda^2 \right\rangle - \left\langle \lambda \right\rangle^2 \right) \right]$$

7.3.3: Calculating the Third Order Contribution

Now we examine the third order piece. To do this, we must evaluate the system average

$$\sum_{\vec{K} \neq 0} \sum_{\vec{K}' \neq 0} \frac{\left\langle \lambda^x_{\vec{K}'} \lambda^x_{-\vec{K}} \left(\vec{\lambda}_{-\vec{K},\vec{K}} \cdot \vec{\Lambda}_{-\vec{K},\vec{K}'} \right) \right\rangle g^0_{k_x} g^0_{-k_{x}'}}{\hat{\Delta}_{\vec{K}} \hat{\Delta}_{\vec{K}'}}$$

Using the fact that $\left(\vec{\lambda}_{-\vec{K},\vec{K}} \cdot \vec{\Lambda}_{-\vec{K},\vec{K}'} \right) = \left[\lambda^x_{\vec{K}-\vec{K}'} g^0_{-k_x} g^0_{k_x'} + \lambda^y_{\vec{K}-\vec{K}'} g^0_{-k_y} g^0_{k_y'} \right]$ we must consider

$$\sum_{\vec{K} \neq 0} \sum_{\vec{K}' \neq 0} \left[\frac{\left\langle \lambda^x_{\vec{K}'} \lambda^x_{-\vec{K}} \lambda^x_{\vec{K}-\vec{K}'} \right\rangle g^0_{k_x} g^0_{-k_x} g^0_{k_x'} g^0_{-k_x'} + \left\langle \lambda^x_{\vec{K}'} \lambda^x_{-\vec{K}} \lambda^y_{\vec{K}-\vec{K}'} \right\rangle g^0_{k_x} g^0_{-k_x} g^0_{-k_y'} g^0_{k_y'}}{\hat{\Delta}_{\vec{K}} \hat{\Delta}_{\vec{K}'}} \right]$$

7.3.3.1: Calculating Triple Product Averages

Now we evaluate the configurational averages. First we examine

$$\left\langle \lambda^x_{\vec{K}'} \lambda^x_{-\vec{K}} \lambda^x_{\vec{K}-\vec{K}'} \right\rangle = N^{-6} \sum_{\vec{x},\vec{x}',\vec{x}''} e^{-i\vec{K}' \cdot \vec{x}} e^{i\vec{K} \cdot \vec{x}'} e^{-i\left[\vec{K}-\vec{K}' \right] \cdot \vec{x}''} \left\langle \lambda^x_{\vec{x}} \lambda^x_{\vec{x}'} \lambda^x_{\vec{x}''} \right\rangle$$

So we need to calculate terms such as $\left\langle \lambda^x_{\vec{x}} \lambda^x_{\vec{x}'} \lambda^x_{\vec{x}''} \right\rangle$. As done previously, our consideration must be nuanced. The simplest case occurs when $\vec{x} \neq \vec{x}' \neq \vec{x}''$, and one has

$$\left\langle \lambda^x_{\vec{x}} \lambda^x_{\vec{x}'} \lambda^x_{\vec{x}''} \right\rangle = \left\langle \lambda^x_{\vec{x}} \right\rangle \left\langle \lambda^x_{\vec{x}'} \right\rangle \left\langle \lambda^x_{\vec{x}''} \right\rangle \quad \left(\vec{x} \neq \vec{x}' \neq \vec{x}'' \right)$$

The other extreme situation is the case in which $\left(\vec{x} = \vec{x}' = \vec{x}'' \right)$ for which $\left\langle \lambda^x_{\vec{x}} \lambda^x_{\vec{x}'} \lambda^x_{\vec{x}''} \right\rangle = \left\langle \lambda_{\vec{x}}{}^3 \right\rangle$. There could also be intermediate situations in which two of the coordinates are the same (e.g. $\vec{x}$ and $\vec{x}'$), and the third coordinate ($\vec{x}''$) is different.

To accommodate all possible cases, we must introduce the Kronecker Delta functions. For example, let $\vec{x} = \vec{x}'$ and $\vec{x}' \neq \vec{x}''$. Then we introduce a term of the form

$\delta_{\bar{x}\bar{x}'}\left[\langle\lambda^2\rangle\langle\lambda\rangle-\langle\lambda\rangle^3\right]$. However, this term must itself be corrected to account for the circumstance in which each of the coordinates are identical. In this case, we introduce the triple Kronecker Delta symbol $\delta_{\bar{x}\bar{x}'\bar{x}''}$ with the characteristic that $\delta_{\bar{x}\bar{x}'\bar{x}''}=1$ for $\vec{x}=\vec{x}'=\vec{x}''$ and zero otherwise. Thus we have

$$\delta_{\bar{x}\bar{x}'}\left[\langle\lambda^2\rangle\langle\lambda\rangle-\langle\lambda\rangle^3\right]\left(1-\delta_{\bar{x}\bar{x}'\bar{x}''}\right)$$

where the factor $\left(1-\delta_{\bar{x}'\bar{x}''\bar{x}'''}\right)$ will eliminate cases where $\vec{x}=\vec{x}'=\vec{x}''$ and confine the contribution to the circumstance in which only $\vec{x}$ and $\vec{x}'$ are the same. If $\vec{x}=\vec{x}''$, then there is a similar factor $\delta_{\bar{x}'\bar{x}''}\left[\langle\lambda^2\rangle\langle\lambda\rangle-\langle\lambda\rangle^3\right]\left(1-\delta_{\bar{x}\bar{x}'\bar{x}''}\right)$. If $\vec{x}=\vec{x}''$, we have the factor $\delta_{\bar{x}\bar{x}''}\left[\langle\lambda^2\rangle\langle\lambda\rangle-\langle\lambda\rangle^3\right]\left(1-\delta_{\bar{x}\bar{x}'\bar{x}''}\right)$.

The last case under consideration is the situation in which each of the three coordinates are the same: $\vec{x}=\vec{x}'=\vec{x}''$. The appropriate term to add in this case is

$$\delta_{\bar{x}'\bar{x}''\bar{x}'''}\left[\langle\lambda^3\rangle-\langle\lambda\rangle^3\right]$$

Incorporating the aforementioned corrections, we find that the average over disorder will yield

$$\langle\lambda_{\bar{x}}\lambda_{\bar{x}'}\lambda_{\bar{x}''}\rangle=\langle\lambda\rangle^3+\left[\delta_{\bar{x}\bar{x}'}+\delta_{\bar{x}'\bar{x}''}+\delta_{\bar{x}''\bar{x}}\right]\left(1-\delta_{\bar{x}\bar{x}'\bar{x}''}\right)\left(\langle\lambda\rangle^2\langle\lambda\rangle-\langle\lambda\rangle^3\right)+\delta_{\bar{x}\bar{x}'\bar{x}''}\left(\langle\lambda^3\rangle-\langle\lambda\rangle^3\right)$$

$$=\langle\lambda\rangle^3+\left[\delta_{\bar{x}\bar{x}'}+\delta_{\bar{x}'\bar{x}''}+\delta_{\bar{x}''\bar{x}}\right]\left(\langle\lambda\rangle^2\langle\lambda\rangle-\langle\lambda\rangle^3\right)-3\delta_{\bar{x}\bar{x}'\bar{x}''}\left(\langle\lambda\rangle^2\langle\lambda\rangle-\langle\lambda\rangle^3\right)+\delta_{\bar{x}\bar{x}'\bar{x}''}\left(\langle\lambda^3\rangle-\langle\lambda\rangle^3\right)$$

The result was simplified by using the property $\delta_{\bar{x}\bar{x}'}\delta_{\bar{x}\bar{x}'\bar{x}''}=\delta_{\bar{x}\bar{x}'\bar{x}''}$. Using a table will help verify that we have obtained the correct result. For the third order case, it is sufficient to operate with the aid of inspection. The possibilities are enumerated in the following table:

Table 1: Special cases and corresponding Expectation values for the products

Case	$\left\langle \lambda_{\vec{x}} \lambda_{\vec{x}'} \lambda_{\vec{x}''} \right\rangle$
$\vec{x} = \vec{x}'$	$\left\langle \lambda^2 \right\rangle \left\langle \lambda \right\rangle$
$\vec{x}' = \vec{x}''$	$\left\langle \lambda^2 \right\rangle \left\langle \lambda \right\rangle$
$\vec{x}'' = \vec{x}$	$\left\langle \lambda^2 \right\rangle \left\langle \lambda \right\rangle$
$\vec{x} = \vec{x}' = \vec{x}''$	$\left\langle \lambda^3 \right\rangle$
$\vec{x} \neq \vec{x}' \neq \vec{x}''$	$\left\langle \lambda \right\rangle^3$

7.3.3.2: Applying the Triple Average Result

Next, this result will used to evaluate the term $\lambda^x_{\vec{K}'} \lambda^x_{-\vec{K}} \lambda^x_{\vec{K}-\vec{K}'}$ as far as possible. Collapsing the Kronecker Delta symbols where they appear will facilitate this. We see that

$$\left\langle \lambda^x_{\vec{K}'} \lambda^x_{-\vec{K}} \lambda^x_{\vec{K}-\vec{K}'} \right\rangle = N^{-6} \sum_{\vec{x},\vec{x}',\vec{x}''} e^{-i\vec{K}'\cdot\vec{x}} e^{i\vec{K}\cdot\vec{x}'} e^{-i\left[\vec{K}-\vec{K}'\right]\cdot\vec{x}''} \left\langle \lambda^x_{\vec{x}} \lambda^x_{\vec{x}'} \lambda^x_{\vec{x}''} \right\rangle$$

$$= N^{-6} \left[\begin{array}{l} \displaystyle\sum_{\vec{x},\vec{x}',\vec{x}''} \left\langle \lambda \right\rangle^3 e^{-i\vec{K}'\cdot\vec{x}} e^{i\vec{K}\cdot\vec{x}'} e^{-i\left[\vec{K}-\vec{K}'\right]\cdot\vec{x}''} + \left(\left\langle \lambda \right\rangle^2 \left\langle \lambda \right\rangle - \left\langle \lambda \right\rangle^3 \right) \left(\begin{array}{l} \left[\displaystyle\sum_{\vec{x}} e^{-i\vec{x}\cdot\left[\vec{K}-\vec{K}'\right]} \right] \left[\displaystyle\sum_{\vec{x}''} e^{-i\vec{x}''\cdot\left[\vec{K}-\vec{K}'\right]} \right] \\ + \left[\displaystyle\sum_{\vec{x}} e^{-i\vec{K}'\cdot\vec{x}} \right] \left[\displaystyle\sum_{\vec{x}'} e^{i\vec{K}'\cdot\vec{x}'} \right] + \left[\displaystyle\sum_{\vec{x}} e^{-i\vec{K}\cdot\vec{x}} \right] \left[\displaystyle\sum_{\vec{x}'} e^{i\vec{K}\cdot\vec{x}'} \right] \end{array} \right) \\ -3N^2 \left(\left\langle \lambda \right\rangle^2 \left\langle \lambda \right\rangle - \left\langle \gamma \right\rangle^3 \right) + N^2 \left(\left\langle \lambda^3 \right\rangle - \left\langle \lambda \right\rangle^3 \right) \end{array} \right]$$

$$= N^{-2} \delta_{\vec{K}\vec{K}'} \left(\left\langle \lambda^2 \right\rangle \left\langle \lambda \right\rangle - \left\langle \lambda \right\rangle^3 \right) - 3N^{-4} \left(\left\langle \lambda \right\rangle^3 \left\langle \lambda \right\rangle - \left\langle \lambda \right\rangle^3 \right) + N^{-4} \left(\left\langle \lambda^3 \right\rangle - \left\langle \lambda \right\rangle^3 \right)$$

In a similar way we examine the term

$$\left\langle \lambda^x_{\vec{K}'}\lambda^x_{-\vec{K}}\lambda^y_{\vec{K}-\vec{K}'}\right\rangle = N^{-6}\sum_{\vec{x},\vec{x}',\vec{x}''} e^{-i\vec{K}'\cdot\vec{x}}e^{i\vec{K}\cdot\vec{x}'}e^{-i\left[\vec{K}-\vec{K}'\right]\cdot\vec{x}''}\left\langle \lambda^x_{\vec{x}}\lambda^x_{\vec{x}'}\right\rangle\left\langle \lambda^y_{\vec{x}''}\right\rangle$$

$$= N^{-6}\sum_{\vec{x},\vec{x}',\vec{x}''} e^{-i\vec{K}'\cdot\vec{x}}e^{i\vec{K}\cdot\vec{x}'}e^{-i\left[\vec{K}-\vec{K}'\right]\cdot\vec{x}''}\left(\langle\lambda\rangle^3 + \delta_{\vec{x}\vec{x}'}\left[\left\langle\lambda^2\right\rangle - \langle\lambda\rangle^2\right]\right)\langle\lambda\rangle$$

$$= N^{-6}\left[\langle\lambda\rangle^3\left(\sum_{\vec{x}} e^{-i\vec{K}'\cdot\vec{x}}\right)\left(\sum_{\vec{x}'} e^{-i\vec{K}\cdot\vec{x}'}\right)\left(\sum_{\vec{x}''} e^{-i\left[\vec{K}-\vec{K}'\right]\cdot\vec{x}''}\right) + \left(\left\langle\lambda^2\right\rangle\langle\lambda\rangle - \langle\lambda\rangle^3\right)\sum_{\vec{x},\vec{x}''} e^{i\left[\vec{K}-\vec{K}'\right]\cdot\vec{x}}e^{-i\left[\vec{K}-\vec{K}'\right]\cdot\vec{x}''}\right]$$

$$= N^{-2}\delta_{\vec{K}\vec{K}'}\left(\left\langle\lambda^2\right\rangle\langle\lambda\rangle - \langle\lambda\rangle^3\right)$$

So we may combine the results and for the third order term we have

$$\sum_{\vec{K}\neq 0}\sum_{\vec{K}'\neq 0}\frac{N^{-4}}{\hat{\Delta}_{\vec{K}}\hat{\Delta}_{\vec{K}'}}\begin{bmatrix} g^0_{k_x}g^0_{-k_x}g^0_{k_x'}g^0_{-k_x'}\left(\left\langle\lambda^3\right\rangle + 2\langle\lambda\rangle^3 - 3\left\langle\lambda^2\right\rangle\langle\lambda\rangle + N^2\delta_{\vec{K}\vec{K}'}\left\{\left\langle\lambda^2\right\rangle\langle\lambda\rangle - \langle\lambda\rangle^3\right\}\right) \\ +N^2\delta_{\vec{K}\vec{K}'}\left(\left\langle\lambda^2\right\rangle\langle\lambda\rangle - \langle\lambda\rangle^3\right)g^0_{k_x}g^0_{-k_x}g^0_{k_y'}g^0_{-k_y}\end{bmatrix}$$

This expression can be split into two terms, one of which is proportional to $\delta_{\nu\nu\nu}_{KK'}$, and one of which is not. We first examine the term containing the Kronecker Delta function, and we have

$$S_1 \equiv \sum_{\vec{K}\neq 0}\sum_{\vec{K}\neq 0}\frac{N^{-2}\delta_{\vec{K}\vec{K}'}}{\hat{\Delta}_{\vec{K}}\hat{\Delta}_{\vec{K}'}}\left(\left\langle\lambda^2\right\rangle\langle\lambda\rangle - \langle\lambda\rangle^3\right)\left[g^0_{k_x}g^0_{-k_x}g^0_{k_x'}g^0_{-k_x'} + g^0_{k_x}g^0_{-k_x}g^0_{k_y'}g^0_{-k_y}\right]$$

$$= \sum_{\vec{K}\neq 0}\frac{N^2}{\left(\hat{\Delta}_{\vec{K}}\right)^2}\left(\left\langle\lambda^2\right\rangle\langle\lambda\rangle - \langle\lambda\rangle^3\right)\left[\left(g^0_{k_x}g^0_{-k_x}\right)^2 + \left(g^0_{k_y}g^0_{-k_y}\right)\left(g^0_{k_x}g^0_{-k_x}\right)\right]$$

7.3.3.3: Taking Advantage of Square Symmetry

Fortunately, we have the opportunity to exploit square symmetry. With no axis preferred in the system, one may map k_x to k_y and vice versa. With this in mind, we re-express S_2 as a symmetric combination of two terms via

$$S_1 = \frac{1}{2}\sum_{\vec{K}\neq 0}\frac{N^{-2}}{\left(\hat{\Delta}_{\vec{K}}\right)^2}\left(\left\langle\lambda^2\right\rangle\langle\lambda\rangle - \langle\lambda\rangle^3\right)\left[\left(g^0_{k_x}g^0_{-k_x}\right)^2 + 2\left(g^0_{k_x}g^0_{-k_x}\right)\left(g^0_{k_y}g^0_{-k_y}\right) + \left(g^0_{k_y}g^0_{-k_y}\right)^2\right]$$

$$= \frac{N^{-2}}{2}\left(\langle\lambda^2\rangle\langle\lambda\rangle - \langle\lambda\rangle^3\right)\sum_{\vec{K}\neq 0}\frac{\left[\left(g^0_{k_x}g^0_{-k_x}\right)+\left(g^0_{k_y}g^0_{-k_y}\right)\right]^2}{\left(\hat{\Delta}_{\vec{K}}\right)^2}$$

Since the numerator and denominator are identical for all values of $\vec{K}$, they cancel. We thus have

$$S_1 = \frac{N^{-2}}{2}\left(\langle\lambda^2\rangle\langle\lambda\rangle - \langle\lambda\rangle^3\right)\sum_{\vec{K}\neq 0}(1)$$

$$= \frac{1}{2}\left[1 - N^{-2}\right]\left(\langle\lambda^2\rangle\langle\lambda\rangle - \langle\lambda\rangle^3\right)$$

We now consider the term S_2 where we will see that the use of square symmetry will again prove useful. We now consider

$$S_2 \equiv N^{-4}\sum_{\vec{K}\neq 0}\sum_{\vec{K}'\neq 0}\frac{1}{\hat{\Delta}_{\vec{K}}\hat{\Delta}_{\vec{K}'}}\left[g^0_{k_x}g^0_{-k_x}g^0_{k_x'}g^0_{-k_x'}\left(\langle\lambda^3\rangle + 2\langle\lambda\rangle^3 - 3\langle\lambda^2\rangle\langle\lambda\rangle\right)\right]$$

$$= N^{-4}\left(\langle\lambda^3\rangle + 2\langle\lambda\rangle^3 - 3\langle\lambda\rangle^2\langle\lambda\rangle\right)\left(\sum_{\vec{K}\neq 0}\frac{g^0_{k_x}g^0_{-k_x}}{\hat{\Delta}_{\vec{K}}}\right)\left(\sum_{\vec{K}'\neq 0}\frac{g^0_{k_x'}g^0_{-k_x'}}{\hat{\Delta}_{\vec{K}'}}\right)$$

Note that the two wave vector sums enclosed in parentheses are independent, a fact that we will use to our advantage. Before proceeding, we note that

$$\sum_{\vec{K}\neq 0}\frac{g^0_{k_x}g^0_{-k_x}}{\hat{\Delta}_{\vec{K}}} = \sum_{\vec{K}\neq 0}\frac{g^0_{k_y'}g^0_{-k_y'}}{\hat{\Delta}_{\vec{K}}}$$

so that we may write

$$\left(\sum_{\vec{K}\neq 0}\frac{g^0_{k_x}g^0_{-k_x}}{\hat{\Delta}_{\vec{K}}}\right)\left(\sum_{\vec{K}'\neq 0}\frac{g^0_{k_x'}g^0_{-k_x'}}{\hat{\Delta}_{\vec{K}'}}\right) = \frac{1}{4}\left(\sum_{\vec{K}\neq 0}\frac{\hat{\Delta}_{\vec{K}}}{\hat{\Delta}_{\vec{K}}}\right)\left(\sum_{\vec{K}'\neq 0}\frac{\hat{\Delta}_{\vec{K}'}}{\hat{\Delta}_{\vec{K}'}}\right)$$

$$= \frac{1}{4}\left(N^2 - 1\right)^2$$

We prove the preceding identity by expanding the $\hat{\Delta}_{\vec{K}}$ and $\hat{\Delta}_{\vec{K}'}$ terms appearing in the numerator. One has

$$\frac{1}{4}\left(\sum_{\vec{K}\neq 0}\frac{\hat{\Delta}_{\vec{K}}}{\hat{\Delta}_{\vec{K}}}\right)\left(\sum_{\vec{K}'\neq 0}\frac{\hat{\Delta}_{\vec{K}'}}{\hat{\Delta}_{\vec{K}'}}\right)=\frac{1}{4}\left(\sum_{\vec{K}\neq 0}\frac{g^0_{k_x}g^0_{-k_x}+g^0_{k_y}g^0_{-k_y}}{\hat{\Delta}_{\vec{K}}}\right)\left(\sum_{\vec{K}'\neq 0}\frac{g^0_{k_x'}g^0_{-k_x'}+g^0_{k_y'}g^0_{-k_y'}}{\hat{\Delta}_{\vec{K}'}}\right)$$

$$=\frac{1}{4}\left(\begin{array}{l}\left[\sum_{\vec{K}\neq 0}\frac{g^0_{k_x}g^0_{-k_x}}{\hat{\Delta}_{\vec{K}}}\right]\left[\sum_{\vec{K}'\neq 0}\frac{g^0_{-k_x}g^0_{-k_x'}}{\hat{\Delta}_{\vec{K}'}}\right]+\left[\sum_{\vec{K}\neq 0}\frac{g^0_{k_y}g^0_{-k_y}}{\hat{\Delta}_{\vec{K}}}\right]\left[\sum_{\vec{K}'\neq 0}\frac{g^0_{k_x'}g^0_{-k_y'}}{\hat{\Delta}_{\vec{K}}}\right]+\left[\sum_{\vec{K}\neq 0}\frac{g^0_{k_x}g^0_{-k_x}}{\hat{\Delta}_{\vec{K}}}\right]\left[\sum_{\vec{K}'\neq 0}\frac{g^0_{k_y}g^0_{-k_y}}{\hat{\Delta}_{\vec{K}'}}\right]\\ +\left[\sum_{\vec{K}\neq 0}\frac{g^0_{k_y}g^0_{-k_y}}{\hat{\Delta}_{\vec{K}}}\right]\left[\sum_{\vec{K}'\neq 0}\frac{g^0_{k_x'}g^0_{-k_x'}}{\hat{\Delta}_{\vec{K}'}}\right]\end{array}\right)$$

$$=\left(\sum_{\vec{K}\neq 0}\frac{g^0_{k_x}g^0_{-k_x}}{\hat{\Delta}_{\vec{K}}}\right)\left(\sum_{\vec{K}'\neq 0}\frac{g^0_{k_x'}g^0_{-k_x'}}{\hat{\Delta}_{\vec{K}'}}\right)$$

$$=\frac{1}{4}\left(N^2-1\right)^2$$

So we see that $S_2=\frac{1}{4}\left(1-N^{-2}\right)^2\left(\langle\lambda^3\rangle+2\langle\lambda\rangle^3-3\langle\lambda^2\rangle\langle\lambda\rangle\right)$. Then the result for the total third order contribution has the form

$$S_1+S_2=\frac{1}{2}\left[1-N^{-2}\right]\left(\langle\lambda^2\rangle\langle\lambda\rangle-\langle\lambda\rangle^3\right)+\frac{1}{4}\left(1-N^{-2}\right)^2\left(\langle\lambda^3\rangle+2\langle\lambda\rangle^3-3\langle\lambda^2\rangle\langle\lambda\rangle\right)$$

In the bulk limit we have

$$S_1+S_2\xrightarrow[N\to\infty]{}\frac{1}{4}\left(\langle\lambda^3\rangle-\langle\lambda^2\rangle\langle\lambda\rangle\right)$$

To summarize, we have found up to third order contributions that the configurational averaged current is of the form

$$\langle I\rangle=v_0\sigma_0\left[1-\frac{1}{\sigma_0}\langle\lambda\rangle-\frac{1}{2\sigma_0^{\,2}}\left(\langle\lambda^2\rangle-\langle\lambda\rangle^2\right)-\frac{1}{4\sigma_0^{\,3}}\left(\langle\lambda^3\rangle-\langle\lambda^2\rangle\langle\lambda\rangle\right)\right]$$

We comment that perturbative treatments have been brought to bear on resistor networks in the past [7,8,9]. However, in earlier treatments, the emphasis has been on

perturbing around around the insulating regime by building up isolated clusters of conducting links. Our approach is in this regard quite distinct. We perturb about the pristine regular network. A salient feature of our approach is that our results will be particularly relevant to a variety of systems which are very tolerant of mild to moderate positional disorder.

7.4: Numerical Monte Carlo Simulations in the Two-Dimensional Case

With the aid of a series of Monte Carlo calculations, we examine our analytical series expansion. Juxtaposition with numerical data is one way to validate the series, by directly checking its accuracy. In the numerical calculation, we operate within the previously discussed iterative scheme. We consider a large resistor network, a square grid containing 10,000 nodes and spanning 100 lattice constants on a side.

7.4.1: A Bond disordered System

We implement bond disorder, and a simple approach is to decrement the conductance by an amount $\varepsilon\sigma_0$, where σ_0 is the unperturbed bond conductance. Hence, if we set ε to $\frac{1}{2}$, then we shall have removed half of the conductance. Equivalently, we will have doubled the resistance. A more drastic step would entail setting ε to 1, such that the entire conductance in a bond is completely eroded away. Then with bond conductances reduced to zero, the link resistance becomes infinite.

The two distinct scenarios, merely attenuated links, and a case in which links are utterly severed, are illustrated in **Figure 47**.

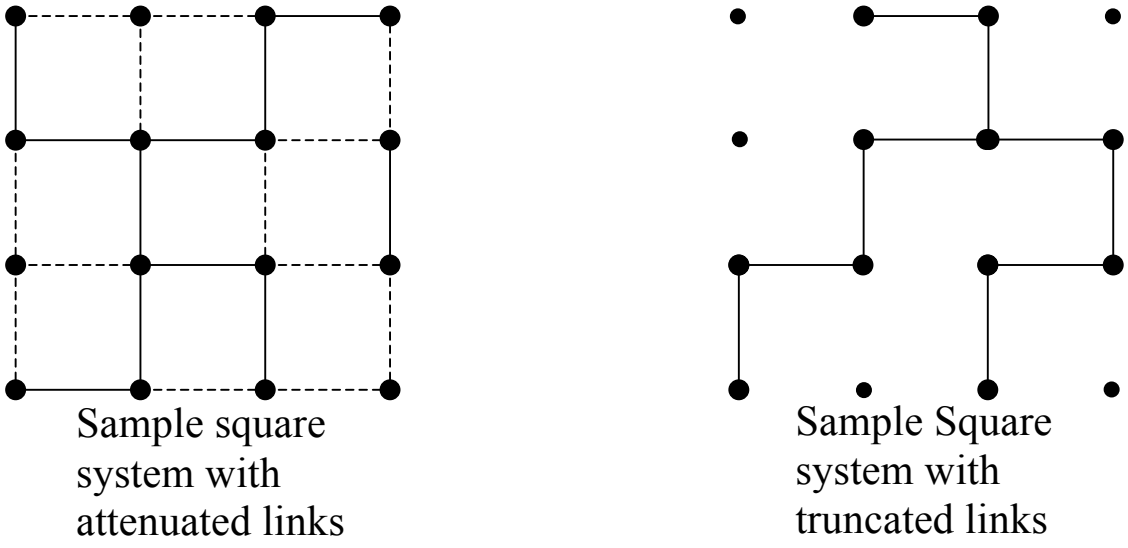

Figure 47: Illustration of system with attenuated links (left) and a case where the conductive bonds are completely sheared away (right)

In this figure, the defects are introduced at the level of 50%. As we approach the situation in which the links are deleted (i.e. where $\varepsilon \approx 1.0$), the analysis of the transport characteristics will encounter a stark difficulty: as the concentration of deleted links is increased, a threshold is eventually attained where current may no longer follow a continuous path through the system. This condition is known as the percolation threshold. In the case of a square lattice with randomly deleted bonds, the percolation threshold is known to occur when precisely 50% of the bonds have been removed, or when $p = \frac{1}{2}$. Thus, while we expect the numerical Monte Carlo simulations to proceed smoothly, we anticipate that our analytical result will break down near the percolation transition where $\varepsilon = 1.0$ and the prevalence of random disorder approaches 50%.

In computer simulations, we do not perform configurational averages. Instead, we find it expedient to use only a single disorder realization. However, the use of a very large system (i.e. the 100 x 100 square grids we consider in the work reported here)

ensures that enough self-averaging occurs to significantly mitigate random statistical fluctuations. Our criterion for convergence of the calculations also is an important feature. We insist that the iterations continue until the residual component has diminished below one part in 10^8 before the iterative sequence is permitted to terminate.

7.4.2: Obtaining the Specific Form of the Perturbative Series

As we specialize to the bond attenuation case examined in the Monte Carlo calculation, we also must calculate the specific form of the perturbative series that we will use to compare with the results of the numerical simulations. To proceed, we must evaluate the first three mements (i.e. $\langle\lambda\rangle$, $\langle\lambda^2\rangle$, and $\langle\lambda^3\rangle$) of the perturbation λ. Noting that with probability p the bond conductance is decreased by $\varepsilon\sigma_0$ and with probability $(1-p)$ no alteration is made to the bond, we may continue.

For the first moment, we have $\langle\lambda\rangle = \varepsilon p\sigma_0$. In a similar manner, $\langle\lambda^2\rangle = \varepsilon^2 p{\sigma_0}^2$ while $\langle\lambda^3\rangle = \varepsilon^3 p{\sigma_0}^3$. Then, to cubic order, the perturbative series has the form

$$\langle\bar{I}\rangle = v_0\sigma_0\left[1-\varepsilon p-\varepsilon^2\left(\frac{p}{2}\right)(1-p)-\frac{\varepsilon^3}{4}p(1-p)\right]$$

We will be interested in the conductance of the disordered system relative to that of the pristine case, where none of the bonds are attenuated. Hence, the series we with to consider is

$$1-\varepsilon p-\varepsilon^2\left(\frac{p}{2}\right)(1-p)-\frac{\varepsilon^3}{4}(1-p)$$

which is parameterized by the bond attenuation probability p and the attenuation magnitude ε.

With the series rendered to cubic order in the perturbation ε, we may also construct an approximant, $P_1^2(\varepsilon)$, to assist in extrapolating the series to larger values of ε. The Padé approximant has the specific form

$$P_1^2(\varepsilon) = \frac{1 + \alpha_1\varepsilon + \alpha_2\varepsilon^2}{1 + \beta_1\varepsilon}$$

where $\beta_1 = -\frac{1}{2}$, $\alpha_1 = -\frac{1}{2} - p$, and $\alpha_2 = \frac{p^2}{2}$. It is our aim to see how the series expansions to first, second, and third order perform relative to results from Monte Carlo simulations. Moreover, we also examine the Padé approximant for its performance relative to the simulations and series expansions that have not been subject to Padé analysis.

7.4.3: Presentation and Discussion of the Monte Carlo Results

Results may be seen in the graphs shown below. Obvious parameters to tune are the strength ε of the perturbation as well as the probability p of perturbing a bond conductance. One might expect the series approximants to the relative conductance to fare best when both ε and p are small, while relatively poor performance is anticipated as p approaches unity, a circumstance tantamount to setting bond resistances to infinity, or deleting the bonds altogether. In large measure, preliminary ideas as to the results are born out. In exploring the available parameter space, we have produced results by holding ε fixed and permitting p to vary.

The Monte Carlo data shows a relative conductivity that decreases monotonically in p. A characteristic that increases with prominence as ε is made larger is the concavity of the curves. The curvature introduces deviations from linearity which are strongest in the vicinity of the bond percolation threshold where $p = 0.50$. As

anticipated, we find better agreement for the perturbative series and the Padé approximant to the cube order series when $\varepsilon << 1$. As ε approaches unity, discrepancies are more pronounced, and can be discerned most readily for the final graph in the series where we have set $\varepsilon = 0.90$.

A consistent feature of the curves is a progressive improvement in the degree of agreement with the Monte Carlo calculations. There is discernable improvement with each successive order, and ultimately the Padé approximant curves (shown in black) provide the best description of the Monte Carlo simulation results; the extent to which the Padé curves serve as the best approximation is most readily seen in the graphs prepared for the larger ε values where, e.g., $\varepsilon = 0.75$ and $\varepsilon = 0.90$ of the last two of the five plots given below.

In developing the perturbation series for the bond-disordered system, we have used an analytical technique to genuinely reach the thermodynamic limit. In previous work, a static configuration of a regular lattice with a single perturbed resistor has been considered [10].

In our calculation, there are numerous conductance links that have been perturbed. However, there is a trade-off: in order to examine a large system with so many individual perturbations, we have found it necessary to calculate an ensemble average over all possible configurations of disorder.

Thus, we lose details of the local lattice structure. Even so, given that we are in pursuit of bulk characteristics anyway, there is no adverse effect in the loss of specific system details.

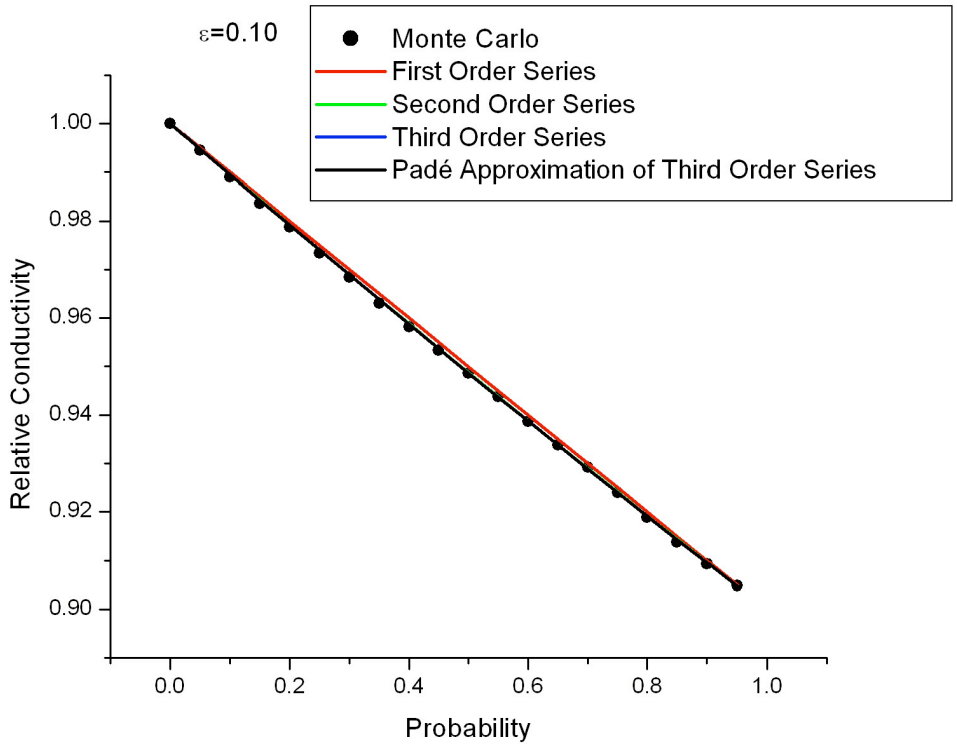

Graph 8: Graph of relative conductivity with respect to the bond attenuation probability for a mild attenuation factor $\varepsilon = 0.10$. The filled symbols represent Monte Carlo numerical results, while solid lines are analytical approximants.

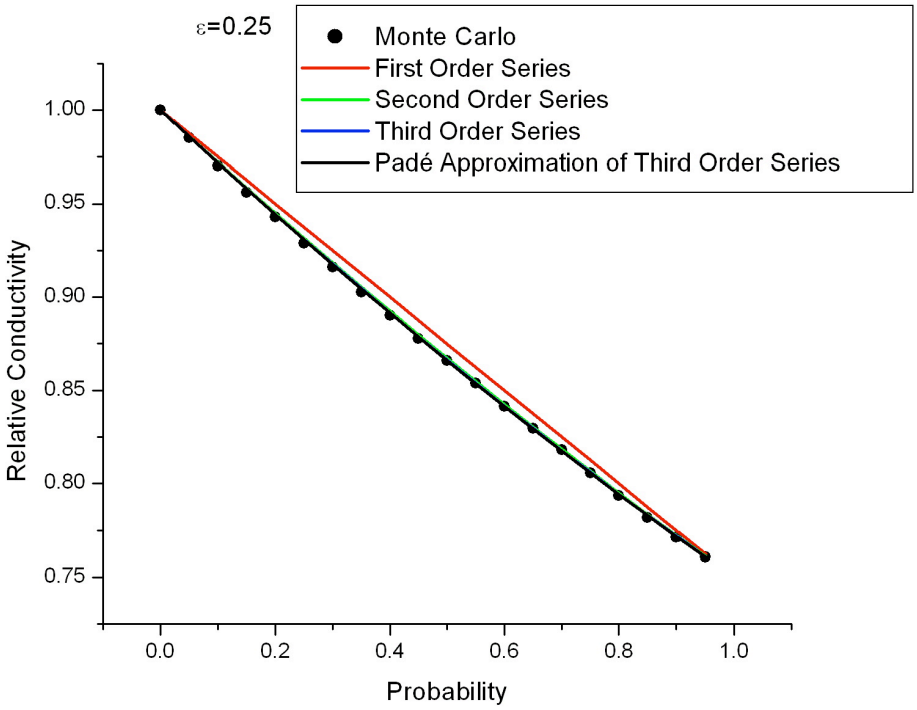

Graph 9: Graph of relative conductivity versus bond attenuation probability for a mild attenuation factor $\varepsilon = 0.25$. Filled symbols are numerial Monte Carlo results, and solid curves are analytical approximants.

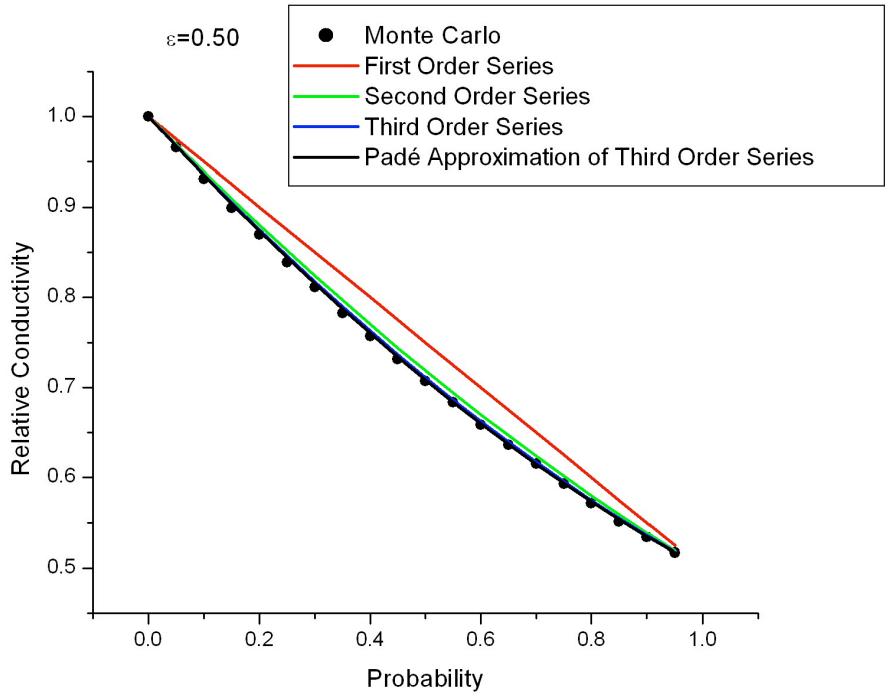

Graph 10: Graph of relative conductivity versus bond attenuation probability for a moderate level of attenuation, $\varepsilon = 0.50$. Filled symbols are numerical Monte Carlo results, and solid curves are analytical approximants.

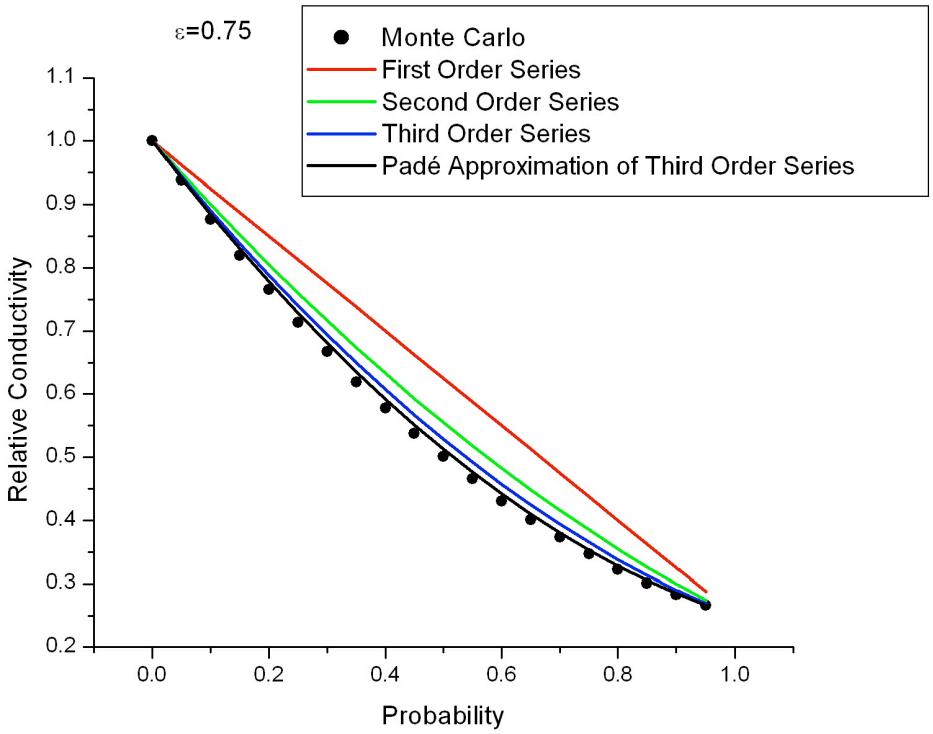

Graph 11: Graph of relative conductivity versus bond attenuation probability for a strong attenuation level, $\varepsilon = 0.75$. Filled symbols are numerical Monte Carlo results, and solid curves are analytical approximants.

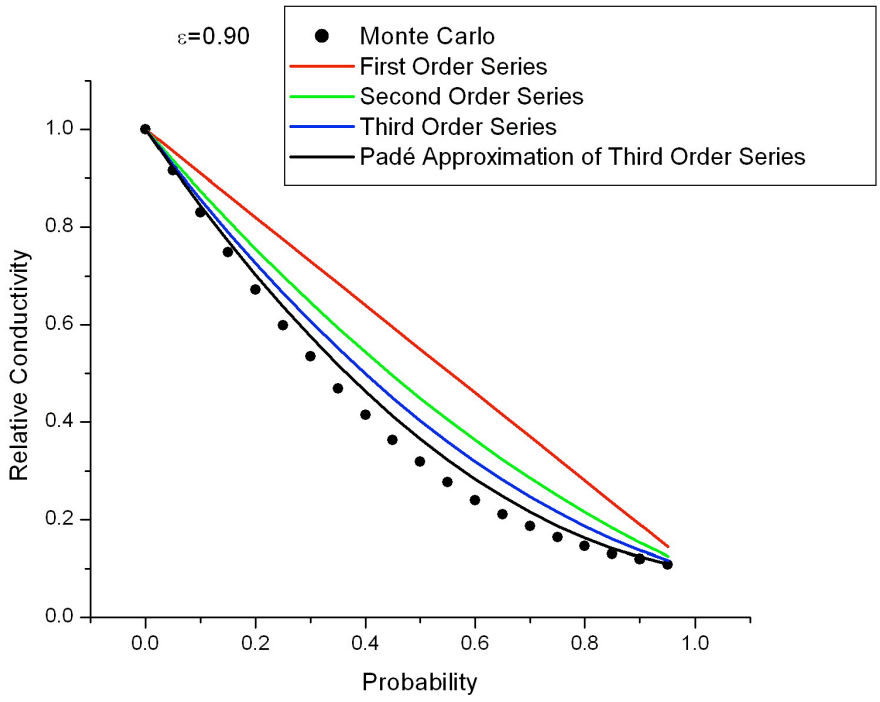

Graph 12: Graph of relative conductivity versus bond attenuation probability for a very strong attenuation factor, $\varepsilon = 0.90$. Filled symbols are numerical Monte Carlo results, and solid curves are analytical approximations

7.5: Logarithmic Bond Disorder for the Two-Dimensional System

We now examine a type of disorder that may be tuned from quite weak to extremely strong. Moreover, the type of disorder we now examine will serve as a closer rendition of the type of disorder that exists in certain types of amorphous conductors. The type of disorder we examine now is spread over a uniform logarithmic range, where for the sake of convenience we operate in terms of base ten logarithms. Bond conductances σ are chosen in such a way that $\log_{10}[\sigma]$ is chosen at random from the interval $[-\eta,0]$ where the right-most value corresponds to the largest conductance values on the order of unity, since $10^0 = 1$. The smallest values of the conductance are of the magnitude $10^{-\eta}$. Hence, if η is relatively large, (e.g. on the order of 5 or so), there will

be an enormously wide range in the variation of bond conductances. In such a regime of strong disorder, the condutances of neighboring bonds may differ by several orders of magnitude.

On the other hand, one may also be in a perturbative regime where $\eta << 1$ and the series expansion we have calculated would be expected to fare best. Nevertheless, in a sense the physics of greatest interest will arise for cases where the lower bound η of the conductance logarithms is relatively large. In such cases, our situation becomes very amenable to description in terms of critical percolation phenomena.

7.5.1: Aspects of Percolation Phase Transitions

In quantitative terms, percolation is simply an objective assessment if a lattice network may be navigated by motion confined strictly to intact lattice conduits [11]. In the illustration below, examples are given of representative cases where percolation does not occur (left), and a lattice exhibiting percolation (right).

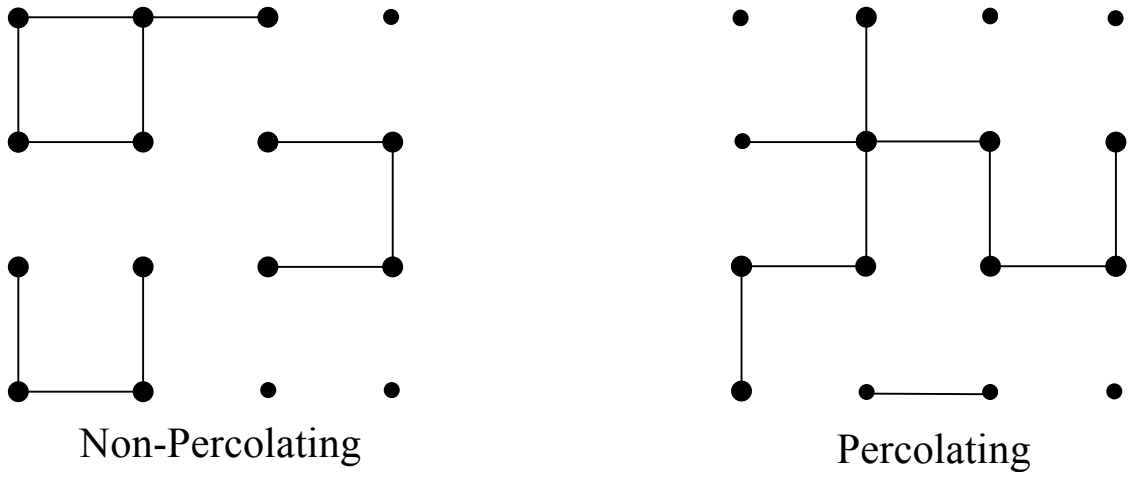

Figure 48: Illustration of percolation behavior (left) and non-percolating behavior (right) in two dimensions

One sees for the lattice on the left that it is not possible, by travelling along intact bonds, to find a way to navigate entirely from left to right or top to bottom. On the other hand, for the case shown on the right, there is a way to move across the system in both the horizontal and vertical directions. In view of these characteristics, we say that there is no percolation in the former case whereas the latter contains a cluster of connected bonds which spans the entire system and therefore exhibits percolation. In practice, as the system size becomes very large, the onset of percolation with increasing lattice connectivity becomes very abrupt. As noted earlier, in the two-dimensional lattice percolation among bonds occurs when the bond occupancy approaches 50%. In terms of our previous model, this situation corresponds to setting ε to 1.0 and p to 0.50.

In the bulk limit, a remarkable thing happens. For an infinite sized system (typical laboraty samples may be considered to lie in this regime due to the enormously large number of atoms contained in a macroscopic sample). The probability of percolation has the form of a step function, being zero below the percolation threshold and exactly 100% immediately above it. Hence, the critical region where percolation just barely occurs is of very small measure in the parameter space.

7.5.2: The Relation of Percolation Transitions to Amorphous Conductors

One might therefore ask what the relevane of the percolation transition may be for practical systems. In fact, as we now discuss, the characteristics of percolation transitions are of broad relevance for amorphous conductions where there is a strong element of disorder. In particular, in our model where the conductances of links are logarithmically dispersed, critical percolation phenomena are of relevance for $\eta >> 1$. To argue for the importance of percolation transition physics for systems in which no bonds are actually

truncated, we reiterate the principle substance of an argument given in a classic work [12].

Consider a system with a wide variation of conductance in the linkds between sites. Now, we assume that such a system has a global potential difference V_0 placed across it. We wish to determine which of the links are absolutely vital for the transport characteristics. To achieve this, we begin by pruning away the weakest links. We continue this process until current no longer flows due to the absence of a connected path which passes through the system.

In this fashion, we arrive at a critical cluster that supports the bulk of the transport of the system. Strong links become isolated by the pruning process, and hence do not make a significant contribution to the conductance of the system. An important question to ask is whether the theoretical Gedanken experiment of pruning away the weakest links is quantitatively valid, though it may seem to be a sound heuristic procedure. Although quantitative tests are most easily performed in the context of numerical Monte Carlo simulations, one may certainly assume that the critical percolation paradigm is more likely to be a reasonable description in a case where the variation of bond conductances is widest. Typically, one envisions cases in which the individual links have conductances that may differ by several orders of magnitude.

7.5.3: The Logarithmic Dispersion Model

Such considerable disorder may nonetheless be envisaged for cases in which there is a significant element of disorder, and where the variable range hopping picture applies. The exponential variation of conductances set up by varying degrees of localized wave function overlap may yield a situation in which the wide variation of conductances

essentially mimics the logarithmically dispersed random resistor network which we now examine. Again, we in previous cases, we seek to evaluate moments of perturbations λ in the bond conductances. The conductance of a specific link will have the form

$$\sigma_0\left[10^{-x}\right]=\sigma$$

where x is a random number chosen uniformly between 0 and η. It is convenient to operate in terms of natural numbers, and one has

$$\sigma=\sigma_0 e^{-x\ln(10)}$$

where "ln" denotes the natural logarithm.

To get a Taylor series in the random numbers x, we use the Taylor series $e^y=1+y+\frac{1}{2}y^2+\frac{1}{6}y^3+\ldots.$ In this fashion, we find

$$\sigma=\sigma_0\left[1-\tau_1 x+\tau_2 x^2-\tau_3 x^3\right]$$

where $\tau_1=\ln(10)$, $\tau_2=\frac{1}{2}\left[\ln(10)\right]^2$, and $\tau_3=\frac{1}{6}\left[\ln(10)\right]^3$. Subsuming the terms in the global perturbation λ gives

$$\sigma=\sigma_0\left[1-\lambda\right];\ \lambda=\tau_1 x-\tau_2 x^2+\tau_3 x^3$$

7.5.3.1: Calculating Moments of the Perturbation

It then becomes our task to calculate the first three moments of λ. For the first moment $\langle\lambda\rangle$, we have

$$\langle\lambda\rangle=\tau_1\langle x\rangle-\tau_2\langle x^2\rangle+\tau_3\langle x^3\rangle$$

It is useful to obtain a formula for a general moment of the random variable x. Hence,

$$\langle x^n\rangle=\frac{1}{n}\int_0^\eta x^n dx=\frac{1}{n+1}\eta^n$$

Thus, we have for the first moment

$$\langle\lambda\rangle = \frac{1}{2}\tau_1\eta - \frac{1}{3}\tau_2\eta^2 + \frac{1}{4}\tau_3\eta^3$$

In a similar way we calculate the higher moments. The second moment may be written as

$$\left\langle\lambda^2\right\rangle = \tau_1{}^2\left\langle x^2\right\rangle - 2\tau_1\tau_2\left\langle x^3\right\rangle$$

$$= \frac{1}{3}\tau_1{}^2\eta^2 - \frac{1}{2}\tau_1\tau_2\eta^3$$

Finally, the third moment is

$$\left\langle\lambda^3\right\rangle = \tau_1{}^3\left\langle x^3\right\rangle = \frac{1}{4}\tau_1{}^3\eta^3$$

If we assemble the results obtained thus far, the series has the form

$$\sigma = \sigma_0\left[1 - \langle\lambda\rangle - \frac{1}{2}\left(\left\langle\lambda^2\right\rangle - \langle\lambda\rangle^2\right) - \frac{1}{4}\left(\left\langle\lambda^3\right\rangle - \left\langle\lambda^2\right\rangle\langle\lambda\rangle\right)\right]$$

$$= \sigma_0\left[1 - \frac{1}{2}\ln(10)\eta + \frac{1}{8}\left[\ln(10)\right]^2\eta^2 - \frac{1}{48}\left[\ln(10)\right]^3\eta^3\right]$$

up to terms cubic in the perturbing influence η.

7.5.3.2: Comparison with Numerical Calculations and Discussion of Results

As before, we also construct the Padé approximant $P_1^2(x) = \dfrac{1 + \alpha_1 x + \alpha_2 x^2}{1 + \beta_1 x}$ appropriate to the third order series expression for the relative conductance. Results appear in **Graph 13** below.

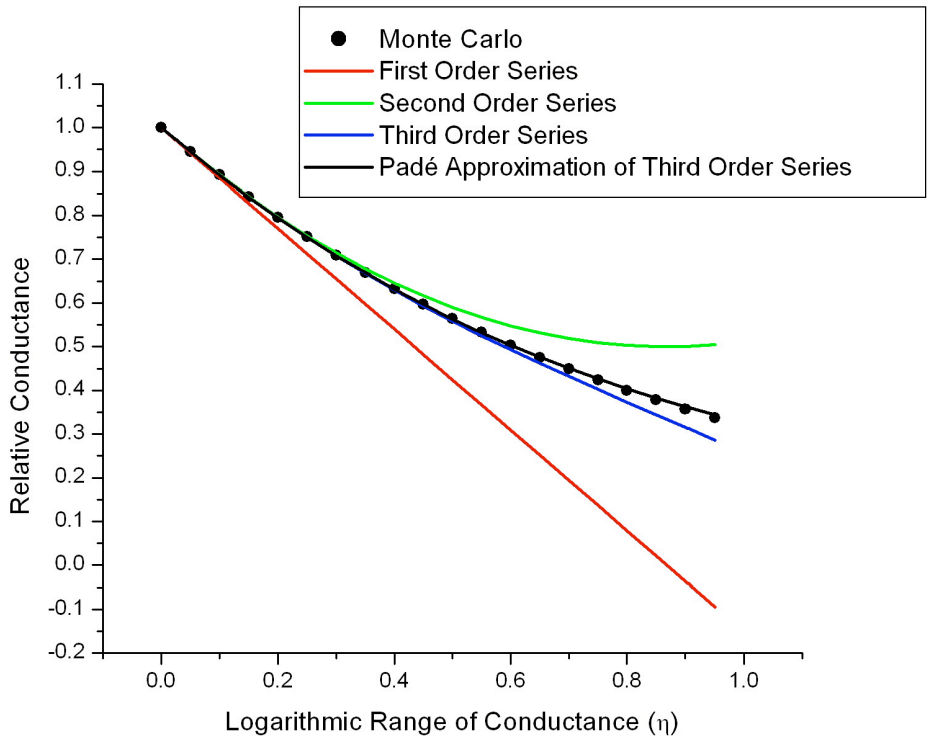

Graph 13: Relative conductance graphed with respect to the logarithmic range of bond conductances for a 100x100 two-dimensional system. Filled symbols are numerical Monte Carlo results, and solid curves are analytical approximations.

Unsurprisingly, the agreement is best for smaller values of η where the variation of conductance values is not as wide ranging. On the other hand, as the parameter η is increased to one, there is a much wider range of conductance values with the possibility for adjacent values to differ by a factor on the order of 10.

The performance of the Padé approximant is significantly better than the simple series approximants. Some of which actually become negative as η approaches unity. Eventually, however, even the Padé curve begins to diverge as η exceeds two or three, and the potential exists for link conductances to vary by several orders of magnitude. Such a regime is better understood in terms of critical percolation phenomena, and the

case in which $\varepsilon >> 1$ is well approximated as a situation in which the bulk of the transport characteristics are determined by a critical percolating cluster.

7.5.3.3: Use of Computational Effort as a Gauge of Criticality

A complementary way to consider the extent to which the critical regime is relevant is to examine the critical slowing down phenomenon and to use it as a gauge of criticality. To this end, we graph the base ten logarithm of the iteration number with respect to the dispersal in the logarithm of the conductance. The graph is given in the figure below. In the plot, there is a monotonic increase in the number of required iterations with respect to the logarithmic dispersal. For small values of the parameter η, the increase is tentative. On the other hand, as η is made larger, in the vicinity of $\eta \approx 1.5$, the curve begins to rise more rapidly, assuming a slope that appears to be asymptotically linear.

A linear slope in $\log_{10}\left[N_I\right]$ where N_I is the number of iterations needed to achieve the desired level of convergence is indicative of an exponential rise of the computational demand with the magnitude of the dispersal parameter η. We interpret this asymptotically exponential rise in N_I as a manifestation of the onset of criticality. In the graph, the dark circles are the actual N_I results while the red line passes through the circles, and is intended as a guide to the eye.

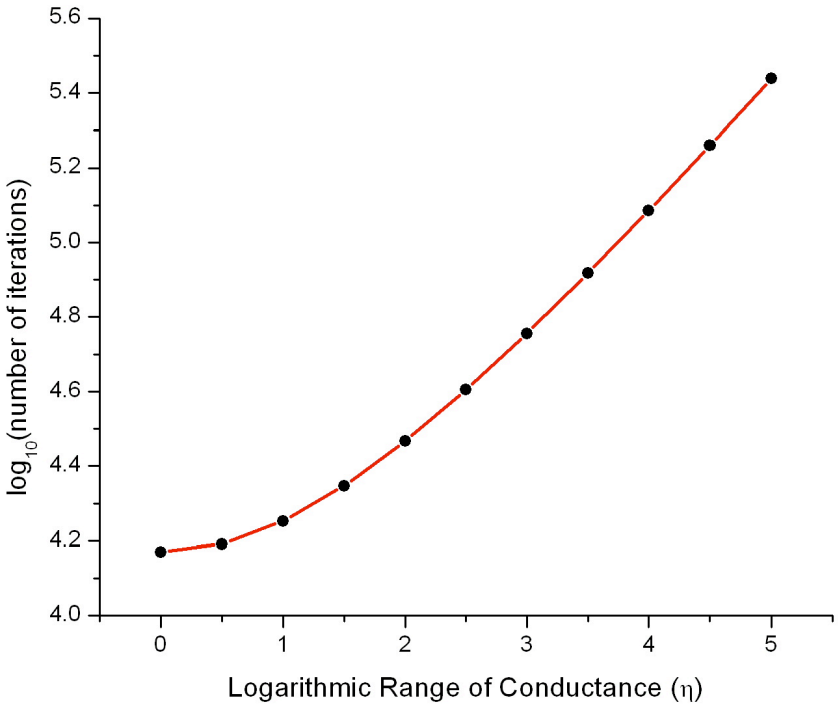

Graph 14: Base ten logarithm of computational cost plotted with respect to the logarithmic range of the conductance for a 100x100 two-dimensional system. Filled symbols are drawn from the simulation and the solid curve is a guide to the eye

7.6: Locating Percolation Transitions

Now, we return to the case of the square lattice where the conductances are degraded by the relative amount ε, with a probability p. We wish to examine the critical regime by using $\log_{10}[N_I]$ as a meter to detect the critical behavior. What has in some cases been a computational inconvenience will now function to our advantage. In fact, our objective is nothing less than to gain an accurate record for the percolation threshold.

7.6.1: Phenomenonology of Percolation

There are three distinct regimes which one may encounter depending on the value of the probability p. For small values of p, the degradation in the lattice is very mild,

and there are many viable conducting pathways. In such a situation, it becomes very easy for the code to redistribute values of the local potential V_{ij}. As a consequence, convergence is very rapid and only a small number of iterations are needed.

On the other hand, suppose that p is quite large, and indeed in the vicinity of 1. In such a situation, there will only exist small isolated networks of conducting links. It will then be easy to move the potential about, and convergence will also be swift. Where N_I will tend to be quite large is near the percolation transition where quite often there is but one viable path through the system, and as a consequence, the redistribution of node potentials to accommodate the complexity of the critical cluster of connected bonds will require a much larger number of iterations than situations where p is either quite small or very near unity, and the calculation is more readily completed.

7.6.2: Using Computational Effort to Locate the Percolation Transition

To determine the maximum number of iterations and hence the location of the percolation transition, we calculate $\log_{10}\left[N_I\right]$ as a function of the bond deletion probability. In the graph shown below, the red curve corresponds to $n = 10$, the green curve is plotted for $n = 20$, or systems twice as large. The blue and black traces correspond, respectively, to the system sizes $n = 40$ and $n = 80$. The purpose for the examination of a variety of system sizes is to determine the extent to which finite size effects influence the determination of the percolation transition threshold. Finite size effects are a consequence of the fact that the percolation transition is a characteristic of the bulk system.

The extrapolation to the infinite size system is known as finite size scaling, and may be a subtle task. In this respect, the percolation transition is a prototypical phas

transition. As the most basic of phase transitions, it nevertheless shares much in common with other types of second order phase transitions such as ferromagnetic phase transitions in which thermal fluctuations disrupt the alignment of the magnetic moments of the atomic species, leading to a disorganized paramagnetic state where the microscopic magnetic moments are oriented in random directions.

7.6.2.1: Percolation Transition in the Nearest Neighbor Square Lattice

We have prepared two graphs. In the first case, the probabilities graphed range from 0.0 to 1.0. However, the second graph displays a tighter range of bond deletion probabilities to make the location of the critical transition easy to discern.

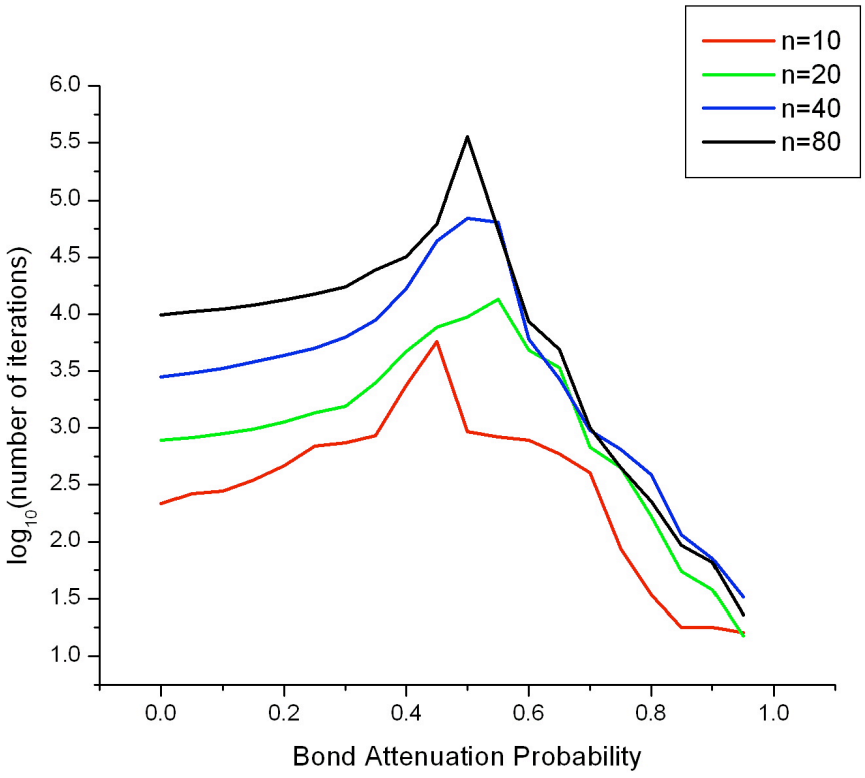

Graph 15: Bas ten logarithm of computational cost plotted versus bond attenuation probability for two-dimensional systems with nearest neighbor connectivity. Results are shown for various system sizes. The bond attenuation factor ε is set to 1.0, so bond attenuation amounts to bond removal.

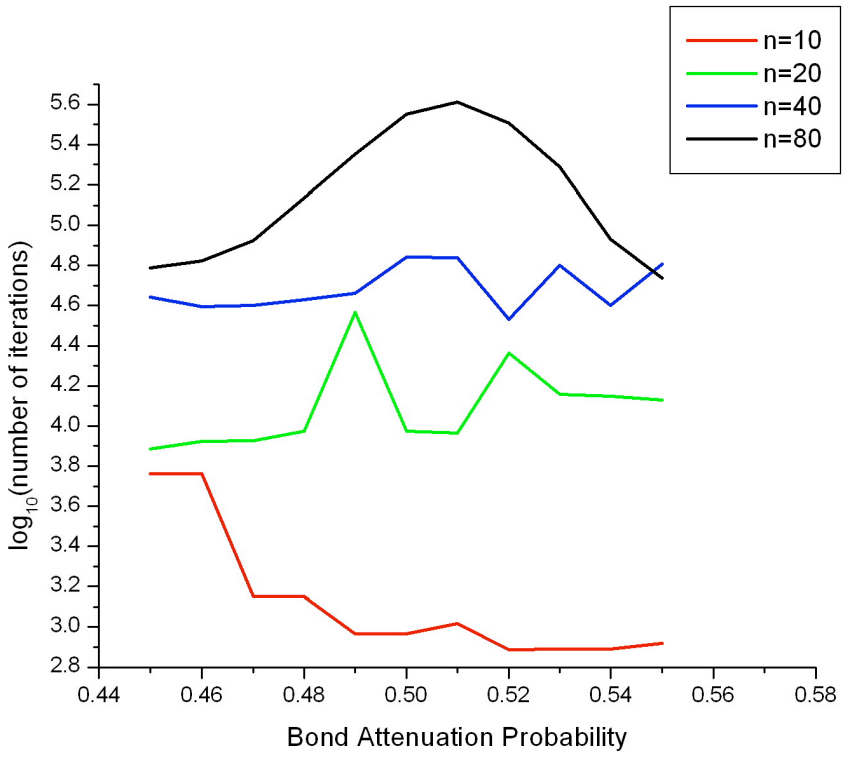

Graph 16: Base ten logarithm of computational cost plotted for a tighter range of bond attenuation probabilities for two-dimensional systems with nearest neighbor connectivity. Results are shown for various system sizes. Since $\varepsilon = 1.0$, bond attenuation amounts to bond removal.

The two-dimensional square lattice with nearest neighbor connectivity is a useful test case since the percolation threshold is known from analytical arguments to be located at precisely $p = \frac{1}{2}$ where exactly half of the bonds are removed.

Hence, we now use the nearest neighbor case to validate another technique. The current approach, in which the number of iterations is used as a gauge of criticality, provides a reliable index of the transition. However, the strength of the method also is its weakness, since the computational overhead will be greater the closer on is to the critical transition, and the larger the system size that is under consideration.

7.6.2.2: Calculating the Percolation Transition with an Extended Coupling Scheme

Regular lattices with nearest neighbor coupling have been examined in both analytical and numerical calculations, but more complicated situations in which, e.g., the connections are made to neighbors more distant than the nearst neighbors have not received as much attention. The methods that we have described in this section nonetheless provide a computationally viable way to determine the percolation threshold.

Accordingly, we examine a more complicated connectivity scheme. In particular, we examine the square lattice geometry with the "union jack" configuration where nodes are connected to nearest neighbors as well as to next-nearest neighbors. The situation is illustrated in the figure below.

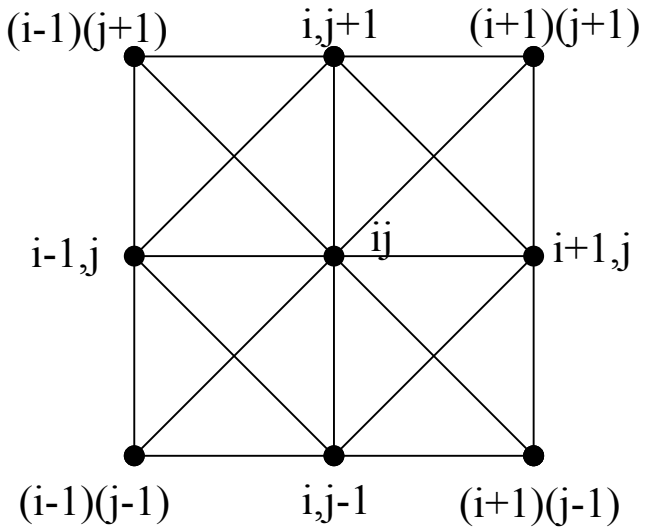

Figure 49: Connectivity pattern for "Union Jack" lattice with bonds to nearest neighbors as well as next-nearest neighbors

For convenience, all bonds are taken to have the same conductance value. In addition, the probability p of bond deletion is the same for horizontal, vertical, and diagonal bonds.

As before, we calculate for a range of probability values p the base ten logarithm of the number of iterations required to reach a tolerance of 10^{-8}. The results are shown in the graph below. As in the case of nearest neighbor connectivity, the computational demand rises significantly in the vicinity of the percolation transition. As a consequence, we consider the alternative, which is not overly encumbered by computational effort.

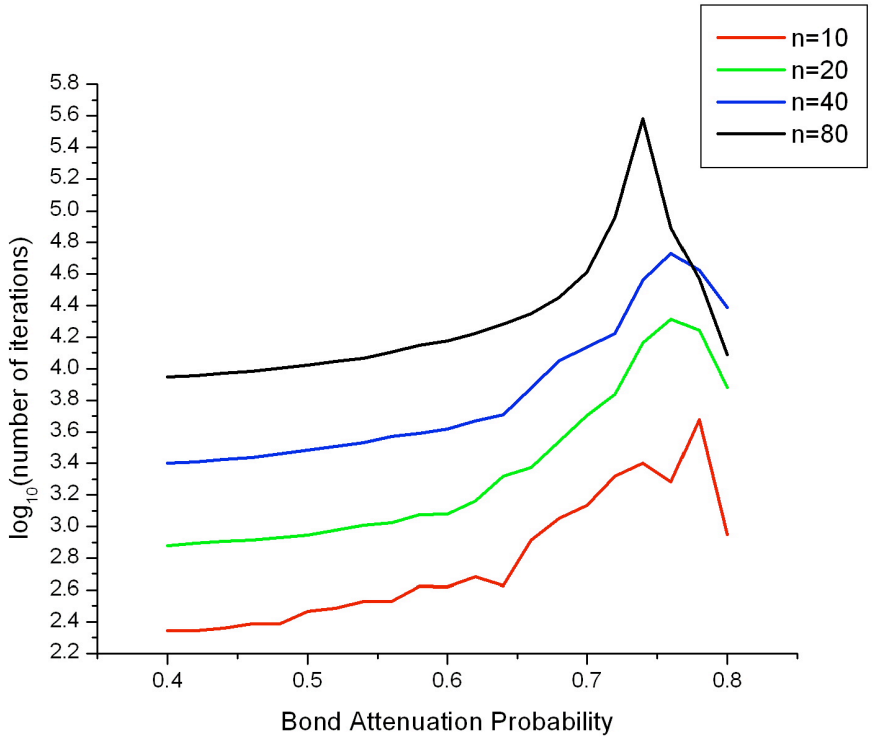

Graph 17: Base ten logarithm of computational cost plotted versus bond attenuation probability for the Union Jack lattice. Results are shown for various system sizes. Since $\varepsilon = 1.0$, bond attenuation amounts to bond removal.

Now we turn our attention to the three-dimensional case, and we also calculate the

disorder averaged current to cubic order. In many respects, the discussion is parallel to that of the two-dimensional case, and to a great extent we will draw on previous results to facilitate the analysis.

CHAPTER 8

THREE-DIMENSIONAL GEOMETRIES: ANALYTICAL PERTURBATIVE CALCULATIONS AND NUMERICAL RESULTS

We now examine three-dimensional geometries, specifically the case of cubic systems. Ultimately we will increase the disorder strength to the extent that the native geometry will be obscured and specializing to the cubic case will not impact the results in the regime of strong disorder. For the cubic lattice there are three indices $\{j_x, j_y, j_z\}$ that specify location. By insisting local charge conservation, we will are again in possession of a means to explicitly calculate the potential shifts at noes in the lattice, and hence any system quantity of interest.

8.1: Nearest Neighbor Geometry and Charge Conservation

Again, we impose a potential difference V_0 across the entire system, and the potential in the unperturbed case has the form $V_{j_x, j_y, j_z} = \frac{-V_0}{n} j_x \equiv -v_0 j_x$ so there is only dependence on the index specifying the location in the "x" direction. **Figure 50** illustrates the geometry for a node in the lattice.

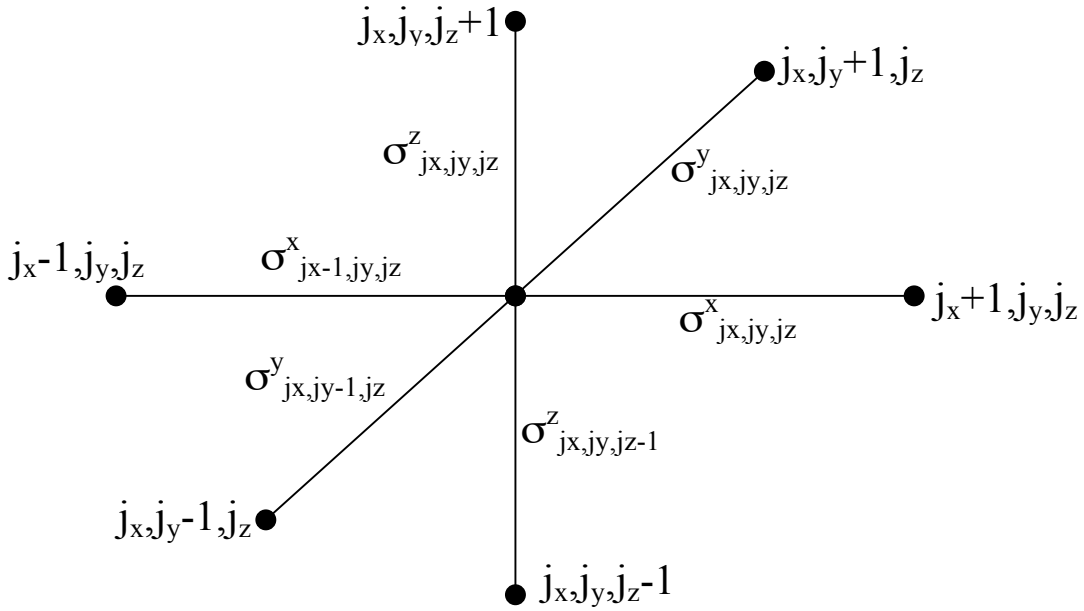

Figure 50: Perspective illustration of the nearest neighbor connectivity scheme and conductance link labeling convention for three-dimensional cubic resistor networks

Insisting on local charge conservation, we find

$$0 = \begin{bmatrix} \left(V_{j_x,j_y,j_z} - V_{j_x+1,j_y,j_z}\right)\sigma^x_{j_x,j_y,j_z} + \left(V_{j_x,j_y,j_z} - V_{j_x-1,j_y,j_z}\right)\sigma^x_{j_x-1,j_y,j_z} + \left(V_{j_x,j_y,j_z} - V_{j_x,j_y+1,j_z}\right)\sigma^y_{j_x,j_y,j_z} \\ +\left(V_{j_x,j_y,j_z} - V_{j_x,j_y-1,j_z}\right)\sigma^y_{j_x,j_y-1,j_z} + \left(V_{j_x,j_y,j_z} - V_{j_x,j_y,j_z+1}\right)\sigma^z_{j_x,j_y,j_z+1} + \left(V_{j_x,j_y,j_z} - V_{j_x,j_y,j_z-1}\right)\sigma^z_{j_x,j_y,j_z-1} \end{bmatrix}$$

The resistance values $\left\{\sigma^x_{j_x,j_y,j_z}, \sigma^y_{j_x,j_y,j_z}, \sigma^z_{j_x,j_y,j_z}\right\}$ occupy the corresponding links.

We consider initial values σ_0 that we take to be the same for each of the links.

Nevertheless, we also introduce perturbations λ so that

$$\sigma^x_{j_x,j_y,j_z} = \sigma_0 - \lambda^x_{j_x,j_y,j_z}$$
$$\sigma^y_{j_x,j_y,j_z} = \sigma_0 - \lambda^y_{j_x,j_y,j_z}$$
$$\sigma^z_{j_x,j_y,j_z} = \sigma_0 - \lambda^z_{j_x,j_y,j_z}$$

The next step is to introduce these expressions into the charge conservation condition for the nodes. Fourier analysis will be used here, as in the one-dimensional case. One finds with the aforementioned substitution and algebraic manipulation that

$$\sigma\left(6\Delta V_{j_x,j_y,j_z} - \Delta V_{j_x+1,j_y,j_z} - \Delta V_{j_x-1,j_y,j_z} - \Delta V_{j_x,j_y+1,j_z} - \Delta V_{j_x,j_y-1,j_z} - \Delta V_{j_x,j_y,j_z+1} - \Delta V_{j_x,j_y,j_z-1}\right)$$
$$+v_0\left(\lambda^x_{j_x-1,j_y,j_z} - \lambda^x_{j_x,j_y,j_z}\right) + \lambda^x_{j_x,j_y,j_z}\left(\Delta V_{j_x+1,j_y,j_z} - \Delta V_{j_x,j_y,j_z}\right) + \lambda^x_{j_x-1,j_y,j_z}\left(\Delta V_{j_x-1,j_y,j_z} - \Delta V_{j_x,j_y,j_z}\right)$$
$$+\lambda^y_{j_x,j_y,j_z}\left(\Delta V_{j_x,j_y+1,j_z} - \Delta V_{j_x,j_y,j_z}\right) + \lambda^x_{j_x,j_y-1,j_z}\left(\Delta V_{j_x,j_y-1,j_z} - \Delta V_{j_x,j_y,j_z}\right) + \lambda^z_{j_x,j_y,j_z}\left(\Delta V_{j_x,j_y,j_z+1} - \Delta V_{j_x,j_y,j_z}\right)$$
$$+\lambda^z_{j_x,j_y,j_z-1}\left(\Delta V_{j_x,j_y,j_z-1} - \Delta V_{j_x,j_y,j_z}\right) = 0$$

8.2: Fourier Analysis of the Charge Conservation Condition

As in the one and two-dimensional cases, we introduce Fourier variables with

$$\Delta V_{j_x,j_y,j_z} = \sum_{k_x=0}^{N-1}\sum_{k_y=0}^{N-1}\sum_{k_z=0}^{N-1}\Delta V_{k_x,k_y,k_z} e^{\frac{2\pi i}{N}\left[k_x j_x + k_y j_y + k_z j_z\right]}$$

After using orthogonality to select an individual Fourier component $\Delta V_{k_x,k_y,k_z}$ for the potential shifts, we again find a more compact notation by using $g^0_{k_x} \equiv \left[e^{\frac{2\pi i}{N}k_x} - 1\right]$, $g^0_{k_y} \equiv \left[e^{\frac{2\pi i}{N}k_y} - 1\right]$, and $g^0_{k_z} \equiv \left[e^{\frac{2\pi i}{N}k_z} - 1\right]$. In terms of these bare propagators we have

$$0 = \sigma_0\left[g^0_{k_x}g^0_{-k_x} + g^0_{k_y}g^0_{-k_y} + g^0_{k_z}g^0_{-k_z}\right]\Delta V_{k_x,k_y,k_z} + v_0\lambda^x_{k_x,k_y,k_z}g^0_{-k_x} - \sum_{k_x'=0}^{N-1}\sum_{k_y'=0}^{N-1}\sum_{k_z'=0}^{N-1}\begin{bmatrix}\Delta V_{k_x',k_y',k_z'}\lambda^x_{k_x-k_x',k_y-k_y',k_z-k_z'}g^0_{-k_x}g^0_{k_x'} \\ +\Delta V_{k_x',k_y',k_z'}\lambda^y_{k_x-k_x',k_y-k_y',k_z-k_z'}g^0_{-k_y}g^0_{k_y'} \\ +\Delta V_{k_x',k_y',k_z'}\lambda^z_{k_x-k_x',k_y-k_y',k_z-k_z'}g^0_{-k_z}g^0_{k_z'}\end{bmatrix}$$

Noting again that the expression $\left(g^0_{k_x}g^0_{-k_x} + g^0_{k_y}g^0_{-k_y} + g^0_{k_z}g^0_{-k_z}\right)$ is proportional to the Laplacian in Fourier space, we use $\hat{\Delta}_{\vec{K}} \equiv \left(g^0_{k_x}g^0_{-k_x} + g^0_{k_y}g^0_{-k_y} + g^0_{k_z}g^0_{-k_z}\right)$ where $\vec{K}$ is

shorthand for the wave number ordered triple $\left(k_x,k_y,k_z\right)$. Again, as a notational convenience, we define $\vec{\lambda}_{\vec{K}} \equiv \left[\lambda^x_{k_x,k_y,k_z},\lambda^y_{k_x,k_y,k_z},\lambda^z_{k_x,k_y,k_z}\right]$. We also use $\vec{\Lambda}_{\vec{K}_1,\vec{K}_2} \equiv \left[g^0_{k_x^1}g^0_{k_x^2},g^0_{k_y^1}g^0_{k_y^2},g^0_{k_z^1}g^0_{k_z^2}\right]$. The expression may be shown more succinctly as

$$0 = \sigma_0\hat{\Delta}_{\vec{K}}\Delta V_{\vec{K}} + v_0\lambda^x_{\vec{K}}g^0_{-k_x} - \sum_{\vec{K}'}\Delta V_{\vec{K}'}\vec{\lambda}_{\vec{K}-\vec{K}'}\cdot\vec{\Lambda}_{-\vec{K},\vec{K}'}$$

which is a formula superficially identical to its counterpart for the two-dimensional system. Again, we note that $\Delta V_0 = 0$ so we are careful to avoid dividing by this vanishing quantity.

8.3: Obtaining a Perturbative Series for Potentials and Currents

As before, an iterated recursive procedure may be applied to develop a perturbative series for the shifts $\Delta V_{\vec{K}}$.

As before, one finds

$$\Delta V_{\vec{K}} = \frac{-v_0}{\hat{\Delta}_{\vec{K}}}\left[\begin{array}{l}\dfrac{\lambda^x_{\vec{K}}g^0_{-k_x}}{\sigma_0} + \dfrac{1}{{\sigma_0}^2}\displaystyle\sum_{\vec{K}'\neq 0}\frac{\lambda^x_{\vec{K}'}g^0_{-k_x'}}{\hat{\Delta}_{\vec{K}'}}\left(\vec{\lambda}_{\vec{K}-\vec{K}'}\cdot\vec{\Lambda}_{-\vec{K},\vec{K}'}\right) \\ + \dfrac{1}{{\sigma_0}^3}\displaystyle\sum_{\vec{K}'\neq 0}\sum_{\vec{K}''\neq 0}\frac{\lambda^x_{\vec{K}''}g^0_{-k_x''}}{\hat{\Delta}_{\vec{K}'}\hat{\Delta}_{\vec{K}''}}\left(\vec{\lambda}_{\vec{K}'-\vec{K}''}\cdot\vec{\Lambda}_{-\vec{K}',\vec{K}''}\right)\left(\vec{\lambda}_{\vec{K}-\vec{K}'}\cdot\vec{\Lambda}_{-\vec{K},\vec{K}'}\right)\end{array}\right]$$

As done for the lower dimensional cases, we calculate the mean current $\bar{I}$ moving from the nodes in the $\hat{x}$ direction. We will evaluate the contributions order by order (i.e. up to cubic order) in the perburbation λ.

We have

$$\bar{I} = \frac{1}{N^3}\sum_{j_x=0}^{N-1}\sum_{j_y=0}^{N-1}\sum_{j_x=0}^{N-1}\sigma^x_{j_x,j_y,j_z}\left(V_{j_x,j_y,j_z} - V_{j_x+1,j_y,j_z}\right)$$

$$= \frac{1}{N^3} \sum_{j_x=0}^{N-1} \sum_{j_y=0}^{N-1} \sum_{j_x=0}^{N-1} \left(\sigma_0 - \lambda^x_{j_x, j_y, j_z} \right) \left(\frac{V_0}{N} + \Delta V_{j_x, j_y, j_z} - \Delta V_{j_x+1, j_y, j_z} \right)$$

After expanding the expression and exploiting periodicity, one finds

$$\bar{I} = \left[v_0 \sigma_0 - \frac{v_0}{N^3} \sum_{j_x=0}^{N-1} \sum_{j_y=0}^{N-1} \sum_{j_z=0}^{N-1} \lambda^x_{j_x, j_y, j_z} + \frac{1}{N^3} \sum_{j_x=0}^{N-1} \sum_{j_y=0}^{N-1} \sum_{j_z=0}^{N-1} \lambda^x_{j_x, j_y, j_z} \left(\Delta V_{j_x+1, j_y, j_z} - \Delta V_{j_x, j_y, j_z} \right) \right]$$

8.4: Calculating a Perturbative Series for the Conductivity by Averaging over Disorder

When we average over disorder, we assume that the perturbations $\lambda^x_{j_x, j_y, j_z}$ and $\lambda^y_{j_x, j_y, j_z}$, while sampled from the same distribution, are not correlated in a statistical sense. Similar to the two-dimensional case, we find that

$$\langle I \rangle = v_0 \left[\sigma_0 - \frac{\langle \lambda \rangle}{\sigma_0} + \frac{1}{N^3} \sum_{j_x=0}^{N-1} \sum_{j_y=0}^{N-1} \sum_{j_z=0}^{N-1} \left\langle \lambda^x_{j_x, j_y, j_z} \left(\Delta V_{j_x+1, j_y, j_z} - \Delta V_{j_x, j_y, j_z} \right) \right\rangle \right]$$

As before, the second and higher order terms emerge from the right-most term. Furthermore, if the shifts λ are as negative as they are positive, then one will find $\langle \lambda \rangle = 0$ and contributions first order in the perturbing influence will not appear.

8.4.1: Calculating the Second Order Contribution

Now we endeavor to calculate the term

$$I_2 = \frac{1}{N^3} \sum_{j_x=0}^{N-1} \sum_{j_y=0}^{N-1} \sum_{j_z=0}^{N-1} \lambda^x_{j_x, j_y, j_z} \left(\Delta V_{j_x+1, j_y, j_z} - \Delta V_{j_x, j_y, j_z} \right)$$

Reverting to Fourier components gives

$$I_2 = \frac{1}{N^3} \sum_{\vec{x}} \left(\sum_{\vec{x}} \lambda^x_{\vec{K}} e^{i\vec{K} \cdot \vec{x}} \right) \left(\sum_{\vec{K}'} \Delta V_{\vec{K}'} g^0_{k_x'} e^{i\vec{K}' \cdot \vec{x}} \right)$$

As before, orthogonality indicates that the sum will vanish unless $\vec{K} = -\vec{K}'$. Ultimately, one has

$$I_2 = \sum_{\vec{K}\neq 0} \lambda^x_{-\vec{K}} g^0_{k_x} \Delta V_{\vec{K}}$$

As seen in the two-dimensional case, second order contributions will emerge from the term

$$I_{22} \equiv \sum_{\vec{K}\neq 0} \frac{\lambda^x_{\vec{K}} \lambda^x_{-\vec{K}}}{\hat{\Delta}_{\vec{K}}} g^0_{k_x} g^0_{-k_x}$$

To calculate the configurational average, the Fourier components must be expressed in terms of the real space counterparts. For example, we use $\lambda^x_{\vec{K}} = \frac{1}{N^3} \sum_{\vec{x}} e^{-i\vec{K}\cdot\vec{x}} \lambda^x_{\vec{K}}$. Then the term of interest becomes

$$I_{22} = N^{-6} \sum_{\vec{K}\neq 0} \sum_{\vec{x},\vec{x}'} \frac{e^{i\vec{K}\cdot[\vec{x}'-\vec{x}]}}{\hat{\Delta}_{\vec{K}}} g^0_{k_x} g^0_{-k_x} \left\langle \lambda^x_{\vec{x}} \lambda^x_{\vec{x}'} \right\rangle$$

Noting that $\left\langle \lambda^x_{\vec{x}} \lambda^x_{\vec{x}'} \right\rangle = \left[\langle \lambda \rangle^2 + \delta_{\vec{x}\vec{x}'} \left(\langle \lambda^2 \rangle - \langle \lambda \rangle^2 \right) \right]$, we find that

$$I_{22} = N^{-6} \sum_{\vec{K}\neq 0} \sum_{\vec{x},\vec{x}'} \frac{e^{i\vec{K}\cdot[\vec{x}'-\vec{x}]}}{\hat{\Delta}_{\vec{K}}} g^0_{k_x} g^0_{-k_x} \left[\langle \lambda \rangle^2 + \delta_{\vec{x}\vec{x}'} \left(\langle \lambda^2 \rangle - \langle \lambda \rangle^2 \right) \right]$$

It's beneficial to note that $\hat{\Delta}_{\vec{K}} \equiv g^0_{k_x} g^0_{-k_x} + g^0_{k_y} g^0_{-k_y} + g^0_{k_z} g^0_{-k_z}$. So our task entails calculating

$$\frac{1}{3} N^{-6} \sum_{\vec{K}\neq 0} \sum_{\vec{x},\vec{x}'} e^{i\vec{K}\cdot[\vec{x}'-\vec{x}]} \left[\langle \lambda \rangle^2 + \delta_{\vec{x}\vec{x}'} \left(\langle \lambda^2 \rangle - \langle \lambda \rangle^2 \right) \right]$$

In the bulk limit where $N \to \infty$ we ultimately obtain

$$I_{22} = \frac{1}{3} \left(\langle \lambda^2 \rangle - \langle \lambda \rangle^2 \right)$$

Up to second order in the perturbation we have

$$\left\langle \bar{I} \right\rangle = v_0 \sigma_0 \left[1 - \frac{\langle \lambda \rangle}{\sigma_0} - \frac{1}{\sigma_0^{\,2}} \left(\left\langle \lambda^2 \right\rangle - \langle \lambda \rangle^2 \right) \right]$$

8.4.2: Calculating the Third Order Contribution

Next, the goal is to calculate the third piece. To do this, we must evaluate the term

$$I_{23} = \sum_{\vec{K} \neq 0} \sum_{\vec{K}' \neq 0} \frac{\left\langle \lambda^x_{\vec{K}'} \lambda^x_{-\vec{K}} \left(\vec{\lambda}_{\vec{K}-\vec{K}'} \cdot \vec{\Lambda}_{-\vec{K},\vec{K}'} \right) \right\rangle g^0_{k_x} g^0_{-k_x'}}{\hat{\Delta}_{\vec{K}} \hat{\Delta}_{\vec{K}'}}$$

So we need to consider the expression

$$\sum_{\vec{K} \neq 0} \sum_{\vec{K}' \neq 0} \left[\begin{array}{l} \left\langle \lambda^x_{\vec{K}'} \lambda^x_{-\vec{K}} \lambda^x_{\vec{K}-\vec{K}'} \right\rangle g^0_{k_x} g^0_{-k_x} g^0_{k_x'} g^0_{-k_x'} + \left\langle \lambda^x_{\vec{K}'} \lambda^x_{-\vec{K}} \lambda^y_{\vec{K}-\vec{K}'} \right\rangle g^0_{k_x} g^0_{-k_x} g^0_{k_y'} g^0_{-k_y'} \\ + \left\langle \lambda^x_{\vec{K}'} \lambda^x_{-\vec{K}} \lambda^z_{\vec{K}-\vec{K}'} \right\rangle g^0_{k_x} g^0_{-k_x} g^0_{k_z'} g^0_{-k_z'} \end{array} \right] \frac{1}{\hat{\Delta}_{\vec{K}} \hat{\Delta}_{\vec{K}'}}$$

8.4.2.1: Adapting Triple Average Results from the Two-Dimensional Case

There are three configurational averages to evaluate, but in doing so we will make extensive use of logic previously developed in the contextof two-dimensional systems. First we examine $\left\langle \lambda^x_{\vec{K}'} \lambda^x_{-\vec{K}} \lambda^x_{\vec{K}-\vec{K}'} \right\rangle$. We immediately appropriate the result gleaned for two-dimensional systems, and hence we find that

$$\left\langle \lambda^x_{\vec{K}'} \lambda^x_{-\vec{K}} \lambda^x_{\vec{K}-\vec{K}'} \right\rangle = N^{-3} \delta_{\vec{K}\vec{K}'} \left(\left\langle \lambda^2 \right\rangle \langle \lambda \rangle - \langle \lambda \rangle^3 \right) - 3N^{-6} \left(\left\langle \lambda^2 \right\rangle \langle \lambda \rangle - \langle \lambda \rangle^3 \right) + N^{-6} \left(\left\langle \lambda^3 \right\rangle - \langle \lambda \rangle^3 \right)$$

In the same way we discovered in the case of the square system, we also have

$$\left\langle \lambda^x_{\vec{K}'} \lambda^x_{-\vec{K}} \lambda^y_{\vec{K}-\vec{K}'} \right\rangle = N^{-3} \delta_{\vec{K}\vec{K}'} \left(\left\langle \lambda^2 \right\rangle \langle \lambda \rangle - \langle \lambda \rangle^3 \right)$$

From symmetry principles, the argument can be made that

$$\left\langle \lambda^x_{\vec{K}'} \lambda^x_{-\vec{K}} \lambda^z_{\vec{K}-\vec{K}'} \right\rangle = N^{-3} \delta_{\vec{K}\vec{K}'} \left(\left\langle \lambda^2 \right\rangle \langle \lambda \rangle - \langle \lambda \rangle^3 \right)$$

Combining the the results for the three averages, we find

$$I_{23} = \sum_{\vec{K}\neq 0}\sum_{\vec{K}'\neq 0} \frac{N^{-6}}{\hat{\Delta}_{\vec{K}}\hat{\Delta}_{\vec{K}'}} \begin{bmatrix} g^0_{k_x} g^0_{-k_x} g^0_{k_x'} g^0_{-k_x'} \left(\langle\lambda^3\rangle + 2\langle\lambda\rangle^3 - 3\langle\lambda^2\rangle\langle\lambda\rangle\right) \\ +N^3\left(\langle\lambda^2\rangle\langle\lambda\rangle - \langle\lambda\rangle^3\right)\left(g^0_{k_x} g^0_{-k_x}\right)\left(g^0_{k_x'} g^0_{-k_x'} + g^0_{k_y'} g^0_{-k_y'} + g^0_{k_z'} g^0_{-k_z'}\right) \end{bmatrix}$$

We split the calculation into two pieces S_2 and a term S_1 proportional to $\delta_{\vec{K}\vec{K}'}$.

Evaluating the S_1 term gives

$$N^{-6}\sum_{\vec{K}\neq 0}\frac{N^3}{\left(\hat{\Delta}_{\vec{K}}\right)^2}\left(\langle\lambda^2\rangle\langle\lambda\rangle - \langle\lambda\rangle^3\right)\left[\left(g^0_{k_x} g^0_{-k_x}\right)^2 + \left(g^0_{k_x} g^0_{-k_x}\right)\left(g^0_{k_y} g^0_{-k_y}\right) + \left(g^0_{k_x} g^0_{-k_x}\right)\left(g^0_{k_z} g^0_{-k_z}\right)\right]$$

8.4.2.2: Exploiting Cubic Symmetry

The advantage gained using cubic geometry is similar to the advantage gained with square geometry used previously. We note that S_1 is invariant with respect to cyclic permutations of k_x, k_y, and k_z as depicted in **Figure 51**.

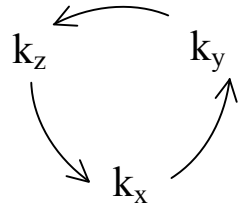

Figure 51: Illustration of a cyclic permutation of wave numbers

Designating the wave number operator as $\hat{\Omega}_{k_x,k_y,k_z}$, we see that

$$\left(s_1+\hat{\Omega}_{k_x,k_y,k_z}S_1+\hat{\Omega}_{k_x,k_y,k_z}\left[\hat{\Omega}_{k_x,k_y,k_z}S_1\right]\right)=\sum_{\bar{K}\neq 0}\frac{N^{-3}}{\left(\hat{\Delta}_{\bar{K}}\right)^2}\left(\left\langle\lambda^2\right\rangle\langle\lambda\rangle-\langle\lambda\rangle^3\right)\begin{bmatrix}\left(g^0_{k_x}g^0_{-k_x}\right)^2+2\left(g^0_{k_x}g^0_{-k_x}\right)\left(g^0_{k_y}g^0_{-k_y}\right)+\left(g^0_{k_y}g^0_{-k_y}\right)^2\\+2\left(g^0_{k_y}g^0_{-k_y}\right)\left(g^0_{k_z}g^0_{-k_z}\right)+\left(g^0_{k_z}g^0_{-k_z}\right)^2\\+2\left(g^0_{k_z}g^0_{-k_z}\right)\left(g^0_{k_x}g^0_{-k_x}\right)\end{bmatrix}$$

Noting that the expression in the squre brackets is precisely the perfect square $\left(\hat{\Delta}_{\bar{K}}\right)^2$, we see that

$$3S_1=N^{-3}\left(N^3-1\right)\left(\left\langle\lambda^2\right\rangle\langle\lambda\rangle-\langle\lambda\rangle^3\right)$$

Therefore we see that $S_1=\frac{1}{3}\left(\left\langle\lambda^2\right\rangle\langle\lambda\rangle-\langle\lambda\rangle^3\right)$ in the bulk limit.

Now we consider the S_2 term where the cubic symmetry proves useful again. One needs to evaluate

$$S_2\equiv N^{-6}\left(\left\langle\lambda^3\right\rangle+2\langle\lambda\rangle^3-3\left\langle\lambda^2\right\rangle\langle\lambda\rangle\right)\left(\sum_{\bar{K}\neq 0}\frac{g^0_{k_x}g^0_{-k_x}}{\hat{\Delta}_{\bar{K}}}\right)\left(\sum_{\bar{K}'\neq 0}\frac{g^0_{k_x'}g^0_{-k_x'}}{\hat{\Delta}_{\bar{K}'}}\right)$$

The wave vector sums are independent, and this will be advantageous. We find that

$$\left(\sum_{\bar{K}\neq 0}\frac{g^0_{k_x}g^0_{-k_x}}{\hat{\Delta}_{\bar{K}}}\right)\left(\sum_{\bar{K}'\neq 0}\frac{g^0_{k_x'}g^0_{-k_x'}}{\hat{\Delta}_{\bar{K}'}}\right)=\frac{1}{9}\left(N^3-1\right)^2$$

We see that in the bulk limit $S_2=\frac{1}{9}\left(\left\langle\lambda^3\right\rangle+2\langle\lambda\rangle^3-3\left\langle\lambda^2\right\rangle\langle\lambda\rangle\right)$. Combining the two contributions gives

$$\begin{aligned}S_1+S_2&=\frac{1}{3}\left(\left\langle\lambda^2\right\rangle\langle\lambda\rangle-\langle\lambda\rangle^3\right)+\frac{1}{9}\left(\left\langle\lambda^3\right\rangle+2\langle\lambda\rangle^3-3\left\langle\lambda^2\right\rangle\langle\lambda\rangle\right)\\&=\frac{1}{9}\left(\left\langle\lambda^3\right\rangle-\langle\lambda\rangle^3\right)\\&=I_{23}\end{aligned}$$

The coefficient $\frac{1}{9}$ is quite small, and significantly suppresses the cubic term. Thus, to cubic order, one has

$$\langle \bar{I} \rangle = v_0 \sigma_0 \left[1 - \frac{1}{\sigma_0} \langle \lambda \rangle - \frac{1}{3\sigma_0^{\,2}} \left(\langle \lambda^2 \rangle - \langle \lambda \rangle^2 \right) - \frac{1}{9\sigma_0^{\,3}} \left(\langle \lambda^3 \rangle - \langle \lambda \rangle^3 \right) \right]$$

8.5: Numerical Calculations of Three-Dimensional Transport Characteristics

As in the case of the square lattice, we perform computer simulations for the three-dimensional case to validate the analytical results. Instead of a 100x100 lattice, we consider a 30x30x30 lattice containing a total of 27,000 nodes. Again, as in the two-dimensional square geometry, our system will be large enough that statistical fluctuations are suppressed and self-averaging effects provide a suitable approximation to the bulk limit. Again, we ensure suitable convergence of the iterative calculations by insistingthat the residual component decrease below on part in 10^8.

8.5.1: Obtaining the Perturbative Series for the Bond Disordered Cubic Lattice

We now specialize to the bond attenuation scheme analogous to the model examined for the square system. As before, the first, second, and third moments are of the form $\langle \lambda \rangle = \varepsilon p \sigma_0$, $\langle \lambda^2 \rangle = \varepsilon^2 p \sigma_0^{\,2}$, and $\langle \lambda^3 \rangle = \varepsilon^3 p \sigma_0^{\,3}$. Then, to cubic order the relative conductance has the form

$$1 - \varepsilon p - \varepsilon^2 \left(\frac{p}{3} \right) (1 - p) - \varepsilon^3 \left(\frac{p}{9} \right) (1 - p^2)$$

where again p is the bond attenuation probability and ε is the attenuation magnitude. As before, we also construct a Padé approximant $P_1^2(\varepsilon)$ to assist with the extrapolation to

values of ε in the vicinity of 1. We have $P_1^2(\varepsilon) = \dfrac{1+\alpha_1\varepsilon+\alpha_2\varepsilon^2}{1+\beta_1\varepsilon}$, and the coefficients are

$\beta_1 = -\dfrac{1}{3}(1+p);\ \alpha_1 = -\dfrac{1}{3}(1+4p);\ \alpha_2 = \dfrac{2p}{9}(1+p)(1+2p).$

8.5.2: Presentation and Discussion of the Three-Dimensional Numerical Results

As in the two-dimensional case, we show on the same graph the first, second, and third order series results as red, green, and blue curves respectively. Also graphed are the Padé approximant results, plotted as black curves. The Monte Carlo results are shown as dark filled circles. As in the case of the square lattice, the Monte Carlo data shows a monotonically decreasing conductivity in the bond attenuation probability p. Again, the trend with increasing ε is for concavity to develop in the Monte Carlo data. Although the concave upward profile is mirrored in the series approximations, higher order series invariably provide better approximations, and the Padé approximant results are in closest agreement with the Monte Carlo data points.

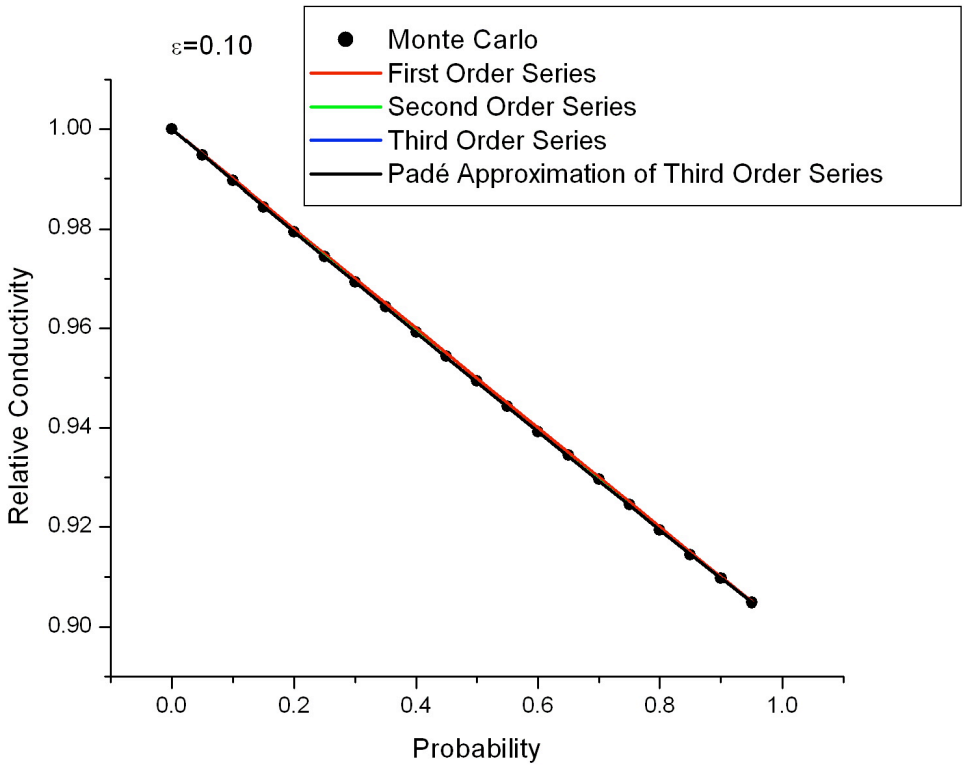

Graph 18: Graph of relative conductivity with respect to the bond attenuation probability for a mild attenuation factor, $\varepsilon = 0.10$. Filled symbols represent Monte Carlo numerical results, while solid lines are analytical approximations; system is three-dimensional cubic with nearest neighbor connectivity.

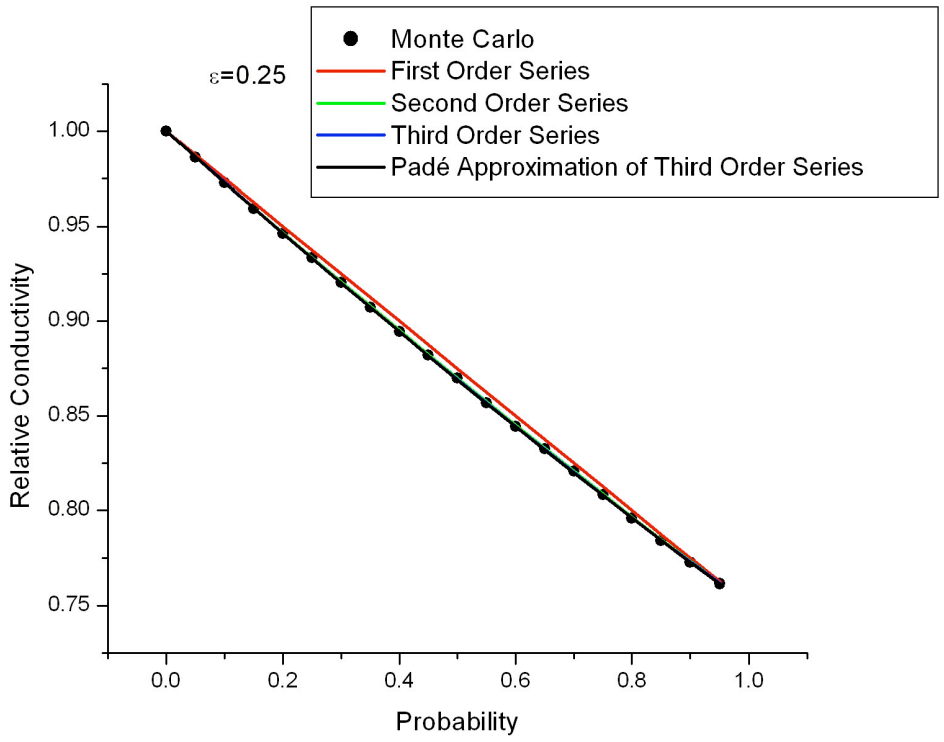

Graph 19: Graph of relative conductivity with respect to the bond attenuation probability for a mild attenuation factor, $\varepsilon = 0.25$. Filled symbols represent Monte Carlo numerical results, while solid lines are analytical approximations; three-dimensional cubic geometry with nearest neighbor connectivity scheme applies.

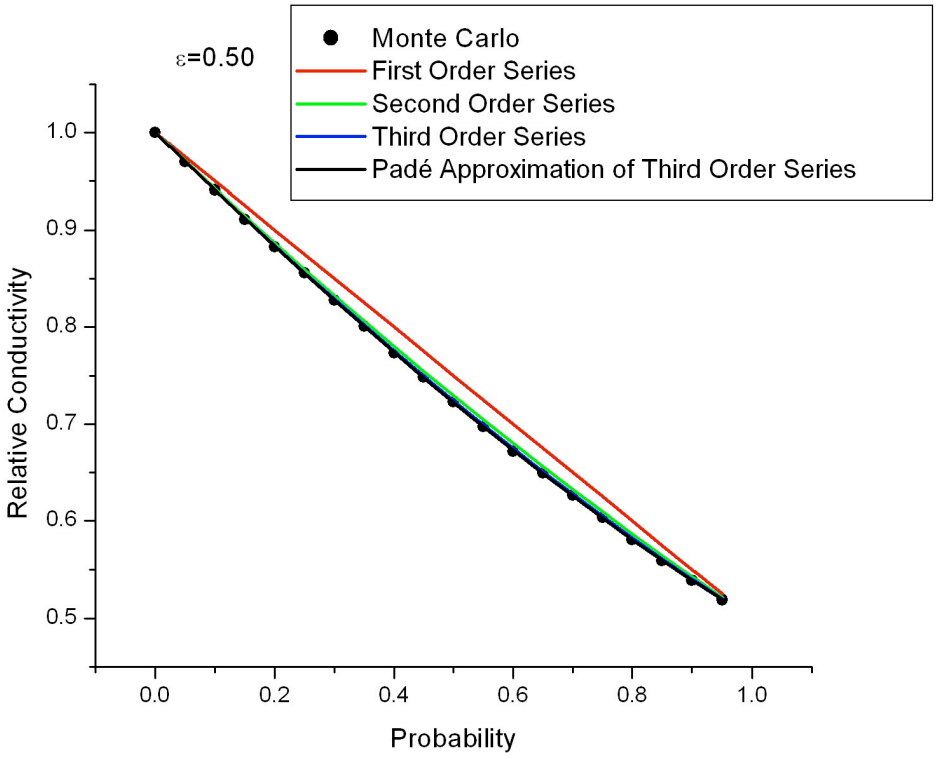

Graph 20: Graph of relative conductivity with respect to the bond attenuation probability for a moderate attenuation factor, $\varepsilon = 0.50$. Filled symbols represent Monte Carlo numerical results, while solid lines are analytical approximations. The system is in three dimensions with nearest neighbor connectivity.

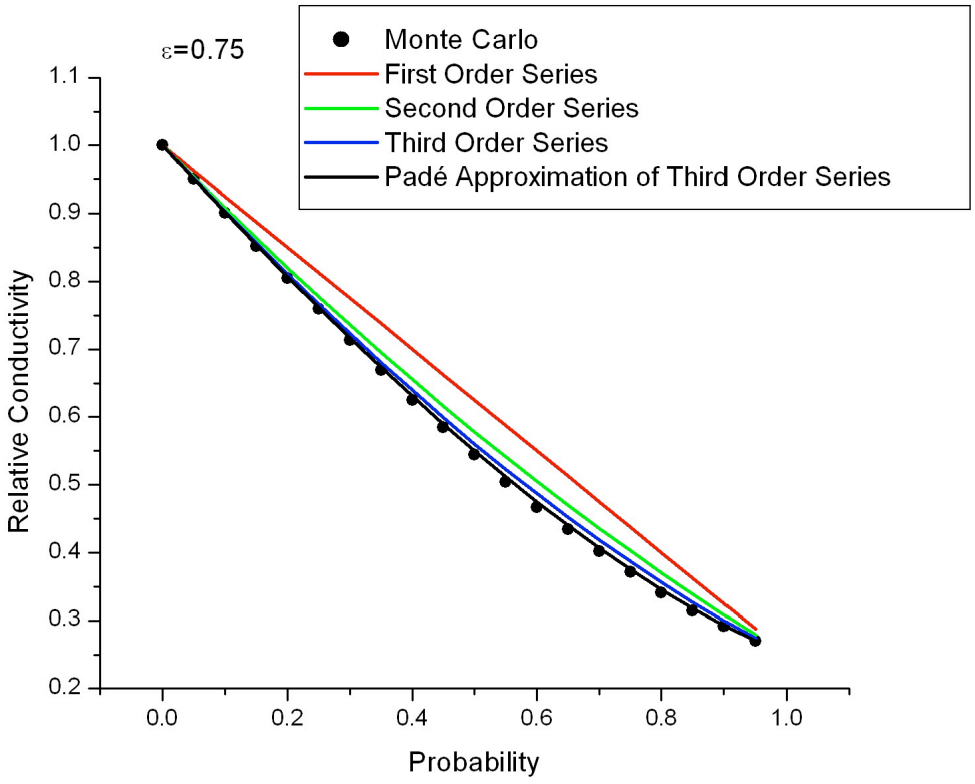

Graph 21: Graph of relative conductivity with respect to the bond attenuation probability for a strong attenuation factor, $\varepsilon = 0.75$. Filled symbols represent Monte Carlo numerical results, while solid lines are analytical approximations. The system is cubic with nodes connected to nearest neighbors.

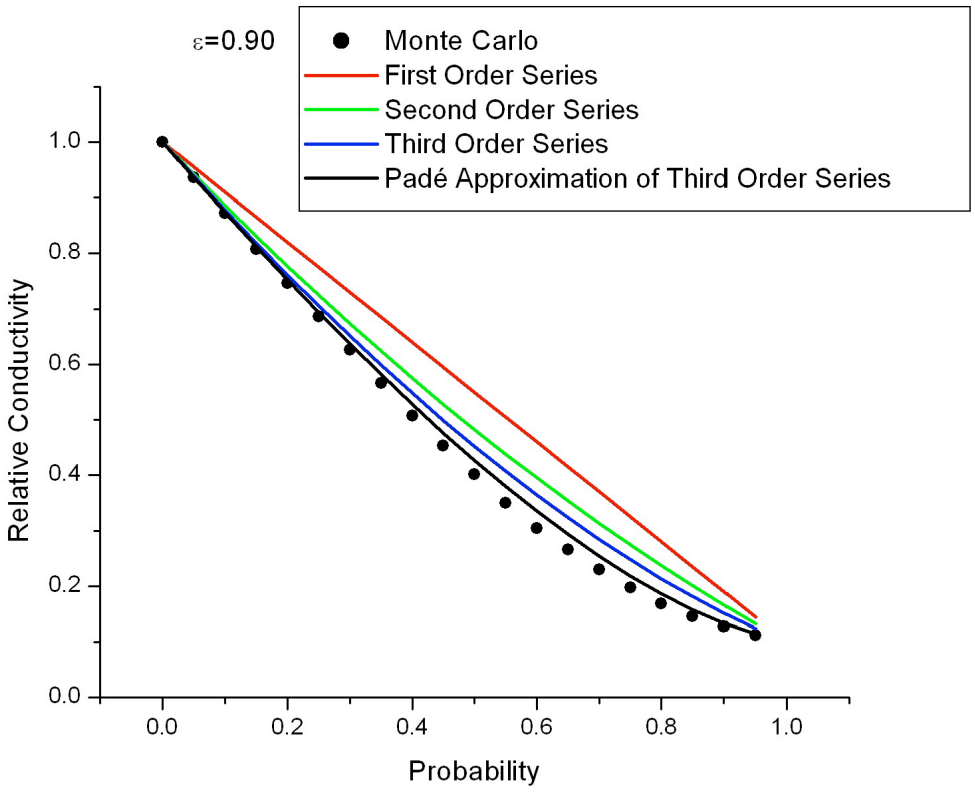

Graph 22: Graph of relative conductivity with respect to the bond attenuation probability for a very strong attenuation factor, $\varepsilon = 0.90$. Filled symbols represent Monte Carlo numerical results, while solid lines are analytical approximations. The system is three-dimensional cubic with connections between nearest neighbors.

8.6: Logarithmic Bond Disorder for the Three-Dimensional System

As for the square geometry in two dimensions, we consider a type of disorder that may readily be tuned from mild to quite strong, a logarithmic distribution in the values of the conductances of the link between neighboring nodes in the cubic lattice. Again, bond conductances σ are chosen in such a way that $\log_{10}[\sigma]$ is selected randomly, and with uniform probability from the interval $[-\eta,0]$ where the magnitude of the perturbations in conductance values is set by the upper bound η of the logarithmic range.

Again, if $\eta >> 1$ there will be a considerable range in the variation of bond conductances. In such a regime of strong disorder, the bond conductance will span a very broad range with the smallest values on the order of $10^{-\eta}$; the opposite regime, with $\eta << 1$, corresponds to a case in which disorder is relatively weak and perturbative expansions are anticipated to fare well. As in the two-dimensional system, there are similarities to a critical system at the brink of percolation, which became increasingly quantitatively correct as η is made larger, and one arrives at a regime in which nearby links may differ by several orders of magnitude in the values of their conductance.

8.6.1: Calculating Moments of the Perturbation

It is our task now to calculate the appropriate series for the relative conductance in terms of the perturbing influence η. Again, we write $\sigma = \sigma_0 e^{-x\ln(10)} = \sigma_0\left[1-\lambda\right]$ where $\lambda \equiv \left[1-e^{-x\ln(10)}\right]$. The expectation values $\langle\lambda\rangle$, $\langle\lambda^2\rangle$, and $\langle\lambda^3\rangle$ are precisely what we calculated for the two-dimensional case. Hence, the relative conductance has the form

$$1-\langle\lambda\rangle-\frac{1}{3}\left(\langle\lambda^2\rangle-\langle\lambda\rangle^2\right)-\frac{1}{9}\left(\langle\lambda^3\rangle-\langle\lambda\rangle^3\right)$$

Ultimately, after substituting the previously obtained results for the first three moments of λ, we have

$$\sigma = 1-\frac{1}{2}\ln(10)\eta+\frac{5}{36}\left[\ln(10)\right]^2\eta^2-\frac{1}{36}\left[\ln(10)\right]^3\eta^3$$

up to terms cubic in the perturbing parameter η. We again also obtain the companion Padé approximant $P_1^2(\varepsilon) = \dfrac{1+\alpha_1\eta+\alpha_2\eta^2}{1+\beta_1\eta}$ corresponding to the third order series for the relative conductance.

8.6.2: Presentation and Discussion of Results

The analytical and Monte Carlo results may be seen in **Graph 23**.

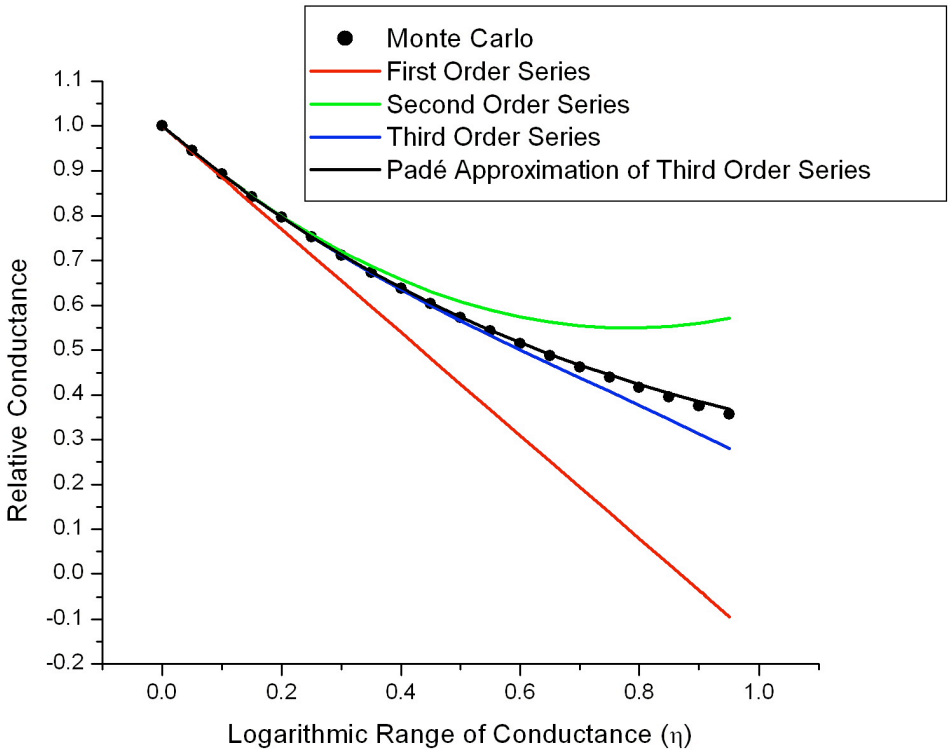

Graph 23: Relative conductance graphed versus logarithmic dispersal in the bond conductance for a cubic nearest neighbor geometry in three dimensions. Filled symbols represent Monte Carlo data, and solid curves represent analytical results.

While there is reasonably good agreement of the analytical results with the Monte Carlo data for smaller η values, deviations increase significantly as η approaches 1 and the range of random variation among the conductances becomes appreciable.

8.6.3: Use of Computational Effort as a Gauge of Criticality

As we did in the two-dimensional case, we examine the critical slowing down effect more specifically by seeking its manifestations in the number of iterations needed

to achieve the required level of convergene as quantified by the residual number. Hence, we again graph the base ten logarithm of the iteration number with respect to the dispersal η in the logarithm of the link conductances. As seen for the case of the square lattice, there is a monotonic increase in the number of iterations required which initially rises slowly, but then increases in slope with respect to η. Ultimately, the slope becomes asymptotically linear, which we again interpret as an exponential rise in the number of iterations needed to achieve the desired level of convergence.

The linear profile for sufficiently large η, as before, is a phenomenon that we regard as a sign that the critical regime has been reached. In the graph below, the dark circles are the N_I results while the red line passes through the filled symbols, and is intended as a guide to the eye.

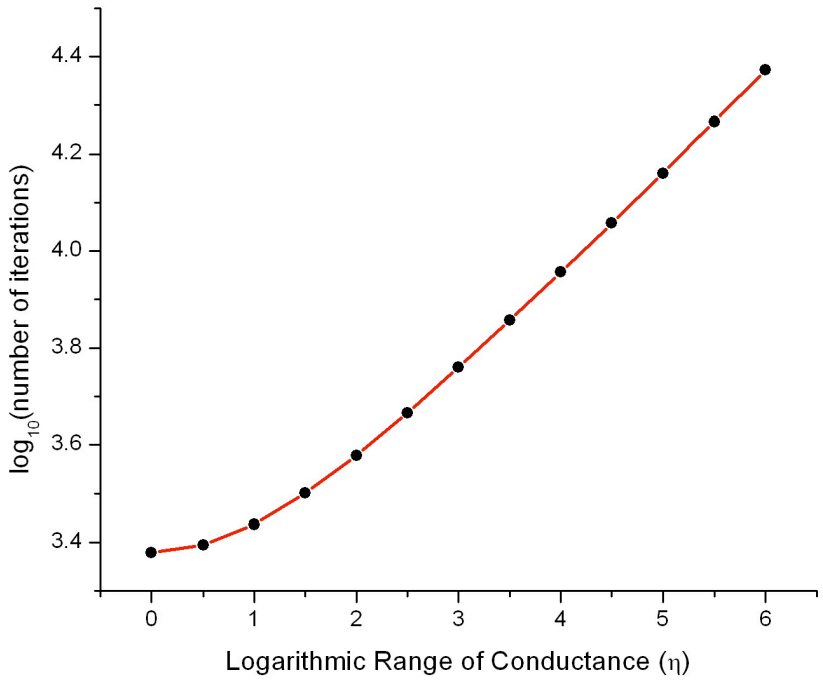

Graph 24: Base ten logarithm of the computational effort plotted versus the logarithmic dispersal of the bond conductances for a three-dimensional cubic system with nearest neighbor connectivities. Filled symbols represent simulation data and the solid curve is a guide to the eye.

8.7: Locating the Percolation Transition for the Bond Truncated Cubic Lattice

We return to the bond attenuated system where the removal of conductance links altogether is achieved by setting ε to 1. We intend, as we did for the square lattice geometry, to use the critical slowing down effect in the iterative numerical calculations as a tool to locate the percolation transition. First, we vary the bond deletion probability over a broad range to locate the percolation transition in a general sense. Results appear in the graph shown below, where again results are displayed for a range of system sizes. The red trace corresponds to the case $n = 4$, the green curve is plotted for $n = 8$, the blue curve corresponds to $n = 16$, and the black curve is graphed for $n = 32$.

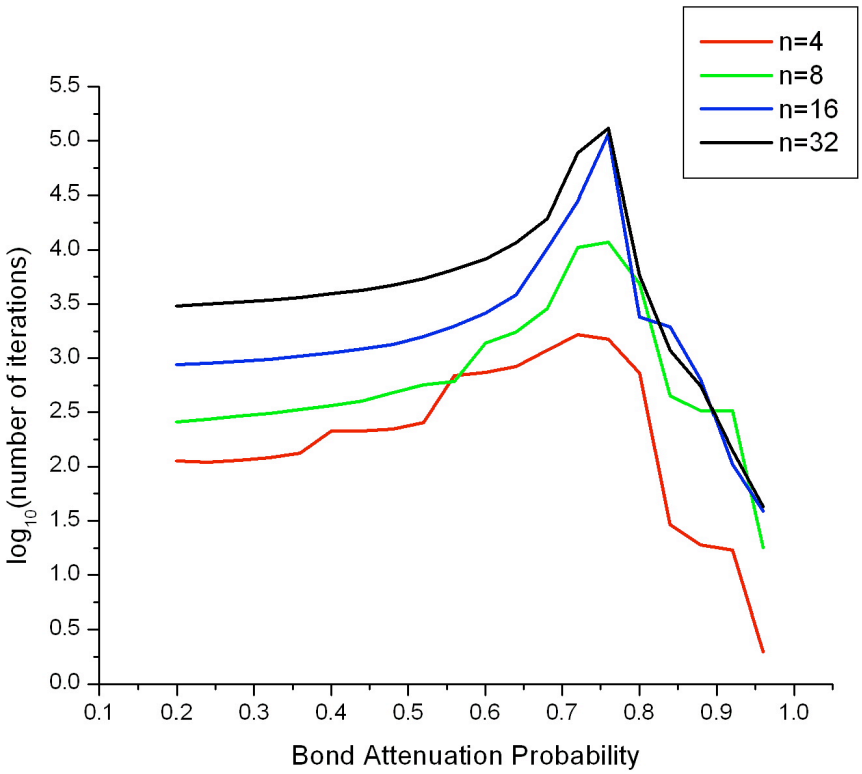

Graph 25: Computational effort as a base ten logarithm plotted versus the bond attenuation probability for the simple cubic geometry in three dimensions with connections between nearest neighbors. Curves for several system sizes are plotted, and the attenuation factor is set to 1.0, so bond attenuation amounts to bond removal.

Now, our attention will be focused on physical systems of interest. Initially, we operate in the iso-energetic regime.

8.8: Calculating Transport Characteristics in the Iso-Energetic Regime

Consider two nodes i and j separated by a distance d_{ij}, as shown in **Figure 52**.

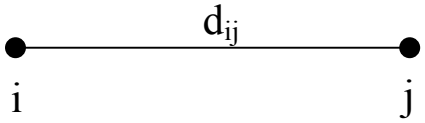

Figure 52: Representation of bond between sits i and j with the length shown as d_{ij}

In the iso-energetic case, following Pike and Seager, the conductance of a link spanning nodes i and j is $\sigma_0 e^{-\alpha d_{ij}}$ where $e^{-\alpha d_{ij}}$ is the suppression due to the wave function overlap. We again adopt the cubic system as the native unperturbed lattice geometry and introduce shifts in the locations of the lattice nodes.

8.8.1: Specifying the Positional Perturbations

The position deviations will be random and chosen with uniform probability from the interval $[-\varepsilon a, \varepsilon a]$ where ε parameterizes the perturbation and a is the lattice constant. Then a specific position would have the form

$$[x,y,z] = \left[j_x a + \delta^x_{j_x,j_y,j_z}, \quad j_y a + \delta^y_{j_x,j_y,j_z}, \quad j_z a + \delta^z_{j_x,j_y,j_z} \right]$$

where, e.g., $\delta^x_{j_x,j_y,j_z} = \eta^x_{j_x,j_y,j_z}$. The η variables are random and range between $[-1 \; and \; +1]$.

We now examine the implications of the local charge conservation condition. It is useful to note that link conductances are of the general form $\sigma_0 e^{-\alpha d_{ij}}$. The distance formula d_{ij} is written as $d_{ij} = \sqrt{\left(x_i - x_j\right)^2 + \left(y_i - y_j\right)^2 + \left(z_i - z_j\right)^2}$, which is the standard Cartesian formula for distance.

In the cubic lattice, let us consider the distance between the points indexed by j_x, j_y, j_z and $j_x + 1, j_y j_z$. In the absence of the perturbing influence, the distance is a. However, we now incorporate the random shifts and expand the radical with respect to

the perturbing influence ε. We will label this distance $d\left(\left[j_x, j_y, j_z\right];\left[j_x+1, j_y, j_z\right]\right)$. In the radical, one has terms such as $\left(-x_{j_x, j_y, j_z}+x_{j_x+1, j_y, j_z}\right)^2=\left(a+a\varepsilon\left[\eta^x_{j_x+1, j_y, j_z}-\eta^x_{j_x, j_y, j_z}\right]\right)^2$.

8.8.2: Calculating Bond Conductances to Cubic Order in the Perturbation ε

When terms such as these are inserted into the radical and expanded to quadratic order in ε the result is:

$$d\left(\left[j_x, j_y, j_z\right];\left[j_x+1, j_y, j_z\right]\right)=a\sqrt{1+f_1\varepsilon+f_2\varepsilon}$$

The f_1 and f_2 coefficients are given by

$$f_1=2\left[\left(\eta^x_{j_x+1, j_y, j_z}-\eta^x_{j_x, j_y, j_z}\right)+\left(\eta^y_{j_x+1, j_y, j_z}-\eta^y_{j_x, j_y, j_z}\right)+\left(\eta^z_{j_x+1, j_y, j_z}-\eta^z_{j_x, j_y, j_z}\right)\right]$$
$$f_2=\left[\left(\eta^x_{j_x+1, j_y, j_z}-\eta^x_{j_x, j_y, j_z}\right)^2+\left(\eta^y_{j_x+1, j_y, j_z}-\eta^y_{j_x, j_y, j_z}\right)^2+\left(\eta^z_{j_x+1, j_y, j_z}-\eta^z_{j_x, j_y, j_z}\right)^2\right]$$

At present, we do not evaluate or analyze f_1 and f_2 further. We will give a more detailed treatment of the coefficients as we calculate the configurational averages. If we use the labels

$$\Delta_{xx}=\eta^x_{j_x+1, j_y, j_z}-\eta^x_{j_x, j_y, j_z}$$
$$\Delta_{yx}=\eta^y_{j_x+1, j_y, j_z}-\eta^y_{j_x, j_y, j_z}$$
$$\Delta_{zx}=\eta^z_{j_x+1, j_y, j_z}-\eta^z_{j_x, j_y, j_z}$$

we find that $f_1=2\left[\Delta_{xx}+\Delta_{yx}+\Delta_{zx}\right]$ and $f_2=\left(\Delta_{xx}{}^2+\Delta_{yx}{}^2+\Delta_{zx}{}^2\right)$; if one expands $\sigma^x_{j_x, j_y, j_z}=\sigma_0 e^{-\alpha a\sqrt{1+f_1\varepsilon+f_2\varepsilon^2}}$ up to terms cubic in the perturbation ε, we have

$$\sigma^x_{j_x, j_y, j_z}=\sigma_0 e^{-\alpha a}\left[\begin{array}{l}1-\varepsilon\left(\alpha a\left[\Delta_{xx}+\Delta_{yx}+\Delta_{zx}\right]\right)+\varepsilon^2\left(\alpha a\left[\frac{\alpha a}{2}\left(\Delta_{xx}+\Delta_{yx}+\Delta_{zx}\right)^2+\left(\Delta_{xx}\Delta_{yx}+\Delta_{yx}\Delta_{zx}+\Delta_{zx}\Delta_{xx}\right)\right]\right) \\ -\frac{\varepsilon^3}{6}\left(\alpha a\left[\Delta_{xx}+\Delta_{yx}+\Delta_{zx}\right]\left[\alpha^2 a^2\left[\Delta_{xx}+\Delta_{yx}+\Delta_{zx}\right]^2+6\left[1+\alpha a\right]\left[\Delta_{xx}\Delta_{yx}+\Delta_{yx}\Delta_{zx}+\Delta_{zx}\Delta_{xx}\right]\right]\right)\end{array}\right]$$

Then we see that we may write the conductance as a nunperturbed term plus a shift caused by the presence of disorder in the system, so

$$\sigma^{x}_{j_x,j_y,j_z} = \sigma_0 e^{-\alpha a}\left(1 - \lambda^{x}_{j_x,j_y,j_z}\right)$$

where $\lambda^{x}_{j_x,j_y,j_z}$ contains terms of disorder ε and higher.

8.8.3: Evaluating Moments of the Master Perturbation λ

To determine the effect of disorder on the conductivity in the bulk limit, we will need to calculate various moments of the perturbations $\lambda^{x}_{j_x,j_y,j_z}$ and the counterparts in the y and z directions. From cubic symmetry we know that

$$\left\langle \lambda^{x}_{j_x,j_y,j_z} \right\rangle = \left\langle \lambda^{y}_{j_x,j_y,j_z} \right\rangle = \left\langle \lambda^{z}_{j_x,j_y,j_z} \right\rangle$$

with similar relations holding for the higher moments.

The task now is to calculate the various moments of $\lambda^{x}_{j_x,j_y,j_z}$. To facilitate this calculation, we introduce the identities $S_3 = \Delta_{xx} + \Delta_{yx} + \Delta_{zx}$ and $S_{cyc} = \Delta_{xx}\Delta_{yx} + \Delta_{yx}\Delta_{zx} + \Delta_{zx}\Delta_{xx}$. In terms of these abbreviations, we find a more compact expression for $\lambda^{x}_{j_x,j_y,j_z}$, namely:

$$\lambda^{x}_{j_x,j_y,j_z} = \varepsilon\left[\alpha a S_3\right] - \varepsilon^2\left[\frac{a^2\alpha^2}{2} S_3{}^2 + \alpha a S_{cyc}\right] + \frac{\varepsilon^3}{6}\left[\alpha^3 a^3 S_3{}^3 + 6\left(\alpha a + \alpha^2 a^2\right) S_3 S_{cyc}\right]$$

This is our more compact rendition, which will facilitate the calculation of the moments $\langle\lambda\rangle$, $\langle\lambda^2\rangle$, and $\langle\lambda^3\rangle$. The aim ultimately is to calculate a perturbative series up to cubic order in ε.

First, we determine

$$\langle\lambda\rangle = \left\langle \lambda^{x}_{j_x,j_y,j_z} \right\rangle = \alpha a \varepsilon \langle S_3\rangle - \varepsilon^2\left[\frac{a^2\alpha^2}{2}\langle S_3{}^2\rangle + \alpha a \langle S_{cyc}\rangle\right] + \frac{\varepsilon^3}{6}\left[\alpha^3 a^3 \langle S_3{}^3\rangle + 6\left(\alpha a + \alpha^2 a^2\right)\langle S_3 S_{cyc}\rangle\right]$$

The first moment of S_3 is $\langle S_3 \rangle = \langle \Delta_{xx} \rangle + \langle \Delta_{yx} \rangle + \langle \Delta_{zx} \rangle = 0$. Even without averaging disorder, the periodicity condition is enough to cause each term to vanish, and there is no contribution to linear order in ε.

Next we calculate

$$\langle {S_3}^2 \rangle = \langle \Delta_{xx}^2 \rangle + \langle \Delta_{yx}^2 \rangle + \langle \Delta_{zx}^2 \rangle + 2\langle \Delta_{xx} \rangle \langle \Delta_{yx} \rangle + 2\langle \Delta_{yx} \rangle \langle \Delta_{zx} \rangle + 2\langle \Delta_{zx} \rangle \langle \Delta_{xx} \rangle$$

where the cross terms factor into separate expectation values due to the fact that Δ_{xx}, Δ_{yx}, and Δ_{zx} are not statistically correlated. From previous logic, one then asserts that the cross terms will vanish. Then we see that

$$\langle {S_3}^2 \rangle = \langle \Delta_{xx}^2 \rangle + \langle \Delta_{yy}^2 \rangle + \langle \Delta_{zz}^2 \rangle$$
$$\langle \Delta_{xx}^2 \rangle = \left\langle \left(\eta^x_{j_x+1, j_y, j_z} \right)^2 \right\rangle + \left\langle \left(\eta^x_{j_x, j_y, j_z} \right)^2 \right\rangle - 2 \left\langle \left(\eta^x_{j_x+1, j_y, j_z} \right)^2 \right\rangle \left\langle \left(\eta^x_{j_x, j_y, j_z} \right)^2 \right\rangle$$

where in the cross term we have again used the fact that $\eta^x_{j_x+1, j_y, j_z}$ and $\eta^x_{j_x, j_y, j_z}$ are statistically uncorrelated to write

$$\left\langle \eta^x_{j_x+1, j_y, j_z} \eta^x_{j_x, j_y, j_z} \right\rangle = \left\langle \eta^x_{j_x+1, j_y, j_z} \right\rangle \left\langle \eta^x_{j_x, j_y, j_z} \right\rangle$$

Since $\eta^x_{j_x, j_y, j_z}$ varies between (-1) and $(+1)$ and is as often positive as negative, we see that first moments vanish. Then the moment $\langle \Delta_{xx}^2 \rangle$ becomes $\langle \Delta_{xx}^2 \rangle = 2 \left\langle \left(\eta^x_{j_x, j_y, j_z} \right)^2 \right\rangle$ where we have exploited periodicity to combine the two second moments.

$$\left\langle \left({\eta^x_{j_x, j_y, j_z}}^2 \right) \right\rangle = \frac{\int_{-1}^{+1} \eta^2 d\eta}{\int_{-1}^{+1} d\eta} = \frac{1}{3}$$

so that $\langle \Delta_{xx}^2 \rangle = \frac{2}{3}$. Similarly, $\langle \Delta_{yx}^2 \rangle = \langle \Delta_{zx}^2 \rangle = \langle \Delta_{xx}^2 \rangle = \frac{2}{3}$ so $\langle {S_3}^2 \rangle = 2$. Now we examine the first moment of the cyclic term: $\langle S_{cyc} \rangle = \langle \Delta_{xx} \rangle \langle \Delta_{yx} \rangle + \langle \Delta_{yx} \rangle \langle \Delta_{zx} \rangle + \langle \Delta_{zx} \rangle \langle \Delta_{xx} \rangle = 0$.

Finally, in order to compute $\langle\lambda\rangle$, we need to evaluate $\langle {S_3}^3 \rangle$ as well as $\langle S_3 S_{cyc} \rangle$:

$$\langle S_3 \rangle = \begin{bmatrix} \langle \Delta_{xx}^3 \rangle + \langle \Delta_{yx}^3 \rangle + \langle \Delta_{zx}^3 \rangle + 3\langle \Delta_{xx}^2 \rangle \langle \Delta_{yx} \rangle + 3\langle \Delta_{xx} \rangle \langle \Delta_{yx}^2 \rangle + 3\langle \Delta_{yx}^2 \rangle \langle \Delta_{zx} \rangle + 3\langle \Delta_{yx} \rangle \langle \Delta_{zx}^2 \rangle + 3\langle \Delta_{zx}^2 \rangle \langle \Delta_{xx} \rangle \\ +3\langle \Delta_{zx} \rangle \langle \Delta_{xx}^2 \rangle + 6\langle \Delta_{xx} \rangle \langle \Delta_{yx} \rangle \langle \Delta_{zx} \rangle \end{bmatrix}$$

However, all terms involving linear moments vanish and one has

$$\langle {S_3}^3 \rangle = \langle \Delta_{xx}^3 \rangle + \langle \Delta_{yx}^3 \rangle + \langle \Delta_{zx}^3 \rangle$$

Let us examine the first term, the third moment of Δ_{xx}.

$$\langle \Delta_{xx}^3 \rangle = \left\langle \left(\eta^x_{j_x+1, j_y, j_z} - \eta^x_{j_x, j_y, j_z} \right)^3 \right\rangle$$

$$= \left\langle \left(\eta^x_{j_x+1, j_y, j_z} \right)^3 \right\rangle + \left\langle \left(\eta^x_{j_x, j_y, j_z} \right)^3 \right\rangle - 3\left\langle \eta^x_{j_x+1, j_y, j_z} \right\rangle \left\langle \left(\eta^x_{j_x, j_y, j_z} \right)^2 \right\rangle - 3\left\langle \left(\eta^x_{j_x+1, j_y, j_z} \right)^2 \right\rangle \left\langle \eta^x_{j_x, j_y, j_z} \right\rangle$$

Since all odd moments vanish, we see that $\langle \Delta_{xx}^3 \rangle = 0$. Thus $\langle {S_3}^3 \rangle = 0$. Finally we calculate

$$\langle S_3 S_{cyc} \rangle = \left\langle \left(\Delta_{xx}\Delta_{yx} + \Delta_{yx}\Delta_{zx} + \Delta_{zx}\Delta_{xx} \right)\left(\Delta_{xx} + \Delta_{yx} + \Delta_{zx} \right) \right\rangle$$

$$= \langle \Delta_{xx}^2 \rangle \langle \Delta_{yx} \rangle + \langle \Delta_{xx} \rangle \langle \Delta_{yx} \rangle \langle \Delta_{zx} \rangle + \langle \Delta_{xx}^2 \rangle \langle \Delta_{zx} \rangle + \langle \Delta_{xx} \rangle \langle \Delta_{yx}^2 \rangle + \langle \Delta_{yx}^2 \rangle \langle \Delta_{zx} \rangle$$
$$+ \langle \Delta_{xx} \rangle \langle \Delta_{yx} \rangle \langle \Delta_{zx} \rangle + \langle \Delta_{xx} \rangle \langle \Delta_{yx} \rangle \langle \Delta_{zx} \rangle + \langle \Delta_{yx} \rangle \langle \Delta_{zx}^2 \rangle + \langle \Delta_{xx} \rangle \langle \Delta_{zx}^2 \rangle$$
$$= 0$$

since each of the nine terms in the expansion of $\langle S_3 S_{cyc} \rangle$ involve vanishing first moments.

Thus, in the average $\langle\lambda\rangle$, only the quadratic term survives, and we find

$$\left\langle \lambda^x_{j_x, j_y, j_z} \right\rangle = \langle\lambda\rangle = -\varepsilon^2 \left[\frac{a^2\alpha^2}{2} \langle {S_3}^2 \rangle \right] = -a^2\alpha^2\varepsilon^2$$

Now our task is to calculate the second moment of λ. To cubic order in ε, the square of $\lambda^x_{j_x, j_y, j_z}$ is

$$\left(\lambda^{x}_{j_x,j_y,j_z}\right)^2 = \varepsilon^2\left[\alpha^2 a^2 {S_3}^2\right] + \varepsilon^3\left[-a^3\alpha^3 {S_3}^3 - 2\alpha^2 a^2 S_3 S_{cyc}\right] + O\left(\varepsilon^4\right)$$

With the results of earlier calculations, we may evaluate $\langle\lambda^2\rangle$, and we find that

$$\begin{aligned}\langle\lambda^2\rangle &= \left\langle\left(\lambda_{j_x,j_y,j_z}\right)^2\right\rangle \\ &= \varepsilon^2\alpha^2 a^2\langle {S_3}^2\rangle + -\varepsilon^3\left[a^3\alpha^3\langle {S_3}^2\rangle + 2\alpha^2 a^2\langle S_3 S_{cyc}\rangle\right] \\ &= \varepsilon^2\left[2\alpha^2 a^2\right] + 0\end{aligned}$$

since $\langle {S_3}^3\rangle = \langle S_3 S_{cyc}\rangle = 0$. Then $\langle\lambda^2\rangle = \left(2a^2\alpha^2\right)\varepsilon^2$.

Finally, we evaluate $\langle\lambda^3\rangle$, and we have $\langle\lambda^3\rangle = \left\langle\left(\lambda^{x}_{j_x,j_y,j_z}\right)^3\right\rangle = \varepsilon^3\alpha^3 a^3\langle {S_3}^3\rangle = 0$. So to cubic order in the perturbing influence ε, the third moment $\langle\lambda^3\rangle$ vanishes. Let us tabulate a summary of our findings:

Table 2: Moments of the subsuming perturbation λ

Term	**Result**
$\langle\lambda\rangle$	$\left(-a^2\alpha^2\right)\varepsilon^2$
$\langle\lambda^2\rangle$	$\left(2\alpha^2 a^2\right)\varepsilon^2$
$\langle\lambda^3\rangle$	0

So up to cubic order in ε, the shifts are purely quadratic in the perturbation ε. We will see that the conductivity is also only affected to second order in ε with no linear shift.

8.8.4: Calculating Transport Characteristics for the Nearest Neighbor Three Dimensional Model

8.8.4.1: Geometric Considerations

Now we will calculate up to cubic order in the perturbation ε the current set up in large three-dimensional systems. When the perturbations involve shifts in locations of the lattice nodes, one has an additional consequence not observed for lattices in which only the bond conductances were manipulated with the lattice geometry unchanged. The new complication is illustrated in **Figure 53** that contrasts a pristine case where the regular lattice geometry is retained, and a perturbed lattice with geometric disorder introduced. The result of the lattice distortions will be currents set up beyond those between nodes and the forward nearest neighbors.

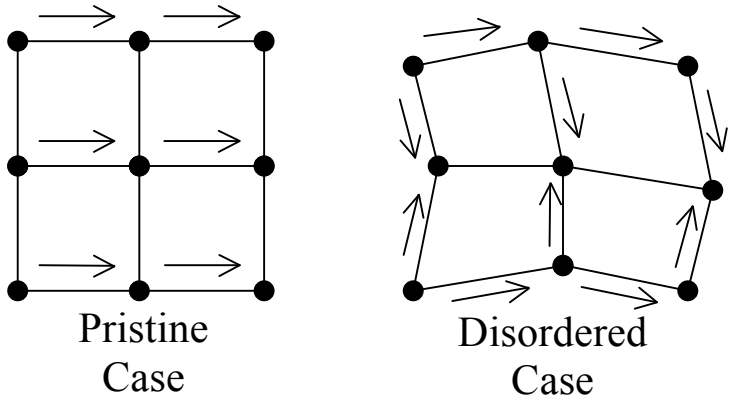

Figure 53: Illustration of a portion of the unperturbed lattice (left), and a case where positional disorder is present (right)

Note that the main contrast among the regular and distorted lattices is current that appears in conductance links that formerly were oriented in directions perpendicular to the imposed potential difference. Although in principle one would need to take into account the contributions from links that previously were perpendicular, a simple

illustration, rendered in **Figure 54**, reveals that we need only concern ourselves with currents moving to the forward nodes.

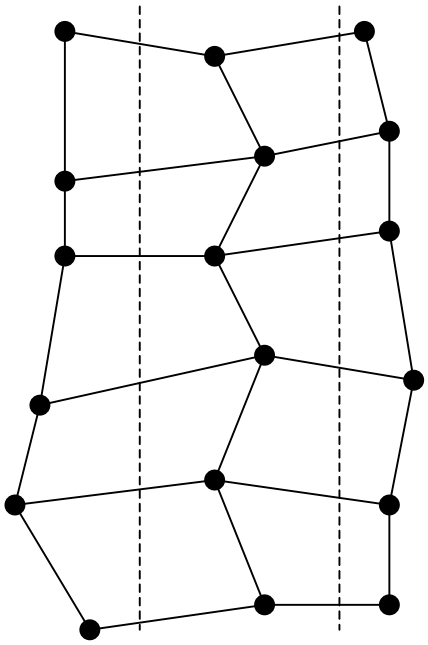

Figure 54: Illustration of strongly disordered systems where the dashed lines are theoretical constructs used to intercept and calculate the total current

Note that the dashed lines only intersect the links that are forwardly directed. As a result, we may use the formulas we have obtained for the three dimensional geometry to determine the conductivity.

8.8.4.2: Collecting Results and Obtaining the Current

We found earlier that

$$\langle \bar{I} \rangle = v_0 \sigma_0 \left[1 - \frac{1}{\sigma_0} \langle \lambda \rangle - \frac{1}{3\sigma_0^{\,2}} \left(\langle \lambda^2 \rangle - \langle \lambda \rangle^2 \right) - \frac{1}{9\sigma_0^{\,3}} \left(\langle \lambda^3 \rangle - \langle \lambda \rangle^3 \right) + \ldots \right]$$

In the present context, σ_0 needs to be modified. Moreover, in our calculation we had factored the expressin for $\sigma_0 e^{-\alpha a}$ out of the λ parameters, so what we must calculate is instead

$$v_0\sigma_0\left[1-\langle\lambda\rangle-\frac{1}{3}\left(\langle\lambda^2\rangle-\langle\lambda\rangle^2\right)\right]=\langle\bar{I}\rangle$$

where we have taken note of the fact that $\left(\langle\lambda^3\rangle-\langle\lambda\rangle^3\right)$ vanishes to cubic order in the perturbing influence ε. Inserting results for $\langle\lambda\rangle$ and $\langle\lambda^2\rangle$ gives

$$\langle\bar{I}\rangle=v_0\sigma_0\left[1+\left(a^2\alpha^2\right)\varepsilon^2-\frac{2}{3}\left(a^2\alpha^2\right)\varepsilon^2\right]e^{-\alpha a}$$

So we actually see a slight enhancement in the current caused by the disorder. This has been observed in numerical simulations by [ ], but here we have shown analytically to cubic order in ε that

$$\langle\bar{I}\rangle=v_0\sigma_0 e^{-\alpha a}\left[1+\frac{1}{3}\left(a^2\alpha^2\right)\varepsilon^2+O\left(\varepsilon^4\right)\right]$$

In the two-dimensional case, there is a precise cancellation of the quadratic contribution, so

$$\langle\bar{I}\rangle=v_0\sigma_0 e^{-\alpha a}\left[1+\textit{quartic corrections in }\varepsilon\right]$$

So in the two-dimensional case we anticipate finding a current robust (up to terms fourth order in the perturbing influence) with respect to disorder.

CHAPTER 9

CONCLUSIONS AND SUGGESTIONS FOR FUTURE RESEARCH

9.1: Overview of Results and Primary Perpsectives

In our consideration of resistor networks, we have revived a notion that random resistor networks are best understood in terms of their scheme of connectivity to near neighbors. The node connectivity perspective is a more general point of view than the mesh current analysis, which often is applied in the case of regular lattices. While even regular lattices with conductance links extended to next-nearest neighbors may confound the mesh current techniques, arbitrary connectivity schemes (i.e. even such cases where each node is connected to every other site in the lattice) are readily managed in the node connectivity point of view we have adopted in this thesis.

At the heart of the node-connectivity picture is the current conservaton condition, also known as Kirchhoff's First Rule. We have seen that the charge conservation condition is not merely a physical constraint, but it also may be pressed into service as a tool for calculating any physical observable that one wishes to determine in relation to the transport characteristics of a random resistor network.

In the case of numerical calculations, the constraint that no current either depart from a node or enter it is part of an algorithm that may be used to calculate the node potentials, and thus any other germane transport characteristic. We have seen, in this vein, that one may transform the charge conservation into an iterative scheme for successively improving an initial guess for the voltages at the lattice nodes.

Whereas the charge conservation condition is the core of a variety of numerical algorithms which circumvent a direct matrix solution, Kirchhoff's First Rule also serves

as the basis for analytical calculations. The latter have an iterative character not unlike the numerical counterparts. Nonetheless, the analytical methods differ from the numerical Monte Carlo calculations in that an average over disorder is performed to strip away a specific configuration of disorder to yield a closed form expression for the conductance as a closed form perturbative series in the influence setting up the positional disorder and eliminating the possibility of a simple exploitation of discrete translational invariance.

As in the numerical calculations, the analytical results benefit from the use of special periodic boundary conditions where an infinite number of system replicas are fused together to allow for an uninterrupted increase of the potential in the direction of the imposed bias. While the potential raises steadily, all physical observables, quantities that must each be constructed from potential differences, are strictly periodic. In this manner, it never becomes necessary to set aside portions of the system to be given over as part of an electrode. In addition, the bulk limit is more readily and more naturally addressed; we have argued that the bulk case is in most instances a desirable regime to seek to consider in theoretical calculations.

In any analytical calculation where the unperturbed system is a regular crystal lattice, the prospect of conveniently obtaining closed form results is greatly improved if one from the outset avoids the introduction of electrode plates, which would spoil the translational invariance of the unperturbed case.

9.2: Summary of Regular Lattice Results

Although a large part of our program in this dissertation has been to take into consideration the effect of sidorder, we nonetheless have found utilityin the theoretical

study of regular lattices where no positional perturbations have been introduced. For these types of pristine lattices, we have been able to work out closed form relations for the bulk conductivity in a variety of situations. For the one-dimensional case, we found an exact relation for an extended scheme in the variable range hopping picture where the hopping frequency is taken to decrease exponentially in the distance separating lattice sites among which hopping occurs.

In the two and three-dimensional geometries where square and cubic geometries were examined, we gleaned conductance formulas expressed as infinite sums. In addition, in both the two and three-dimensional systems we specialized to the limit where the length scale of the exponential decay of the hopping frequency is large in relation to the lattice constant; we found in such instances that the infinite sum for the conductivity goes over to an intergral readily evaluated for a simple closed form expression for the conductivity.

Finally, in the case of the square lattice, we posed the question as to what would happen with a potential bias not aligned with either principal Cartesian axis, but directed along a diagonal. We proved, first in a scheme connecting nearest neighbors, and then in an extended scheme that the current set up in a bulk system does not depend on the orientation of the potential bias with respect to crystallographic axes, but is instead isotropic in the imposed potential. We determined through rigorous argument that the isotropy characteristic holds when the hopping scheme is extended to an infinite range (i.e. in a situaion where in principal carriers may hop from a paticular site to any other location in the crystal lattice) provided that the hopping frequency is itself dependent only on the physical distance between two sites.

We did not pursue similar logic for the case of the cubic lattice in three dimensions. Even so, we anticipate that one may readily generalize our arguments and carry out the calculation appropriate to the cubic system. We expect isotropy of the conductivity to hold in the three-dimensional case as well.

Finally, we offer one more observation that extends considerably the likely relevance of the calculations of transport characteristics for the regular lattice geometries. Our comment, articulated in this conducting segment, benefits from hindsight in an important sense. We have found in the case of numerical and analytical calculations of transport characteristics that for some types of disorder, the conductivity is robust with respect to small, or even moderate, values of the perturbing parameter.

From the results of calculations reported on in this dissertation, we conclude that where disorder is most likely to be tolerated is in the case of positional disorder where there are fluctuations in the locations of atomic species that lead to perturbations that vanish to first order. Hence, we anticipate that the regular lattice results will be relevant for many cases in which disorder levels are mild to moderate in extend.

9.3: The Relevance of Percolation Phenomena

Elsewhere, as well as within this thesis, a variety of arguments (some heuristic and some based on calculations) have been used to argue for the relevance of physics near the percolation transition where a system with a large portion of truncated links is at the boundary separating systems which percolate, and those which have lost enough bridges among nodes that an uninterrupted path spanning the entire system does not exist.

One the other hand, a case in which many links have been sheared completely away may seem to be very distinct from a resistor network for which the conductance of

links has merely been degraded but not altogether removed. Nevertheless, if the conduits joining the nodes are left intact, but are sufficiently diverse in their conductance values, then the transport of charge may occur mainly through a critical cluster formed by pruning away the weaker links until the system is at the verge of a percolation transition. Thus, critical behavior associated with percolation transitions may be of surprisingly broad relevance for strongly disordered amorphous materials.

A salient phenomenon associated with criticality is a marked deceleration of many algorithmsused to calculate transport characteristics. By using the number of iterations required to achieve convergence as a gauge of critical behavior, we found that increasing the spread in the resistance of lattice bonds eventually leads to a regime in which the required computational effort rises exponentially with the logarithm of the dispersal of the conductance. The transition to this asymptotic scaling of the number of iterations occurs when the variation of the conductances spans about an order of magnitude in both two and three-dimensional geometries, and we interpret the shift as the onset of the critical regime where characteristics of the percolation transition are an important determinant of the transport characteristics of the system. As another test of the use of the computational effort as a meter to detect critical behavior, we considered simple scenarios where percolation characteristics were well understood and found peaks in the number of iterations for parameter settings where the percolation transition is known to occur.

9.4: Comments on the Analytical Calculations

In using analytical arguments to express the transport characteristics as a perturbative series in a parameter governing the strength of random perturbations, we have fashioned a technique distinct from previous methods in several respects.

First, by using periodic boundary conditions for the unperturbed system and avoiding cathode and anode geometry, we simplified the calculation and facilitated the calculation of system characteristics to third order in the perturbing influence. Second, by subsuming the details of the perturbation parameter λ, we are able to treat a detailed perturbation in a simple and compact way, and the task is reduced to calculating moments of a more detailed perturbation which may then be inserted into the master series, which has the same form irrespective of the complexities of the specific perturbation.

Finally, our perspective is complementary to previous efforts in that the unperturbed state is a pristine system with no interruption to the global transport of charge. In this sense, the starting point of our calculation differs from that of other efforts where finite clusters are built up in an insulating medium. Hence, whereas we work from the conductive side, other efforts to build up a high order perturbative series begin in the opposite regime where the native system does not permit the flow of charge through the material.

Analytical and numerical results suggest there are many types of systems that are robust with respect to the introduction of positional disorder. Thus, we argue that treatments that begin with a regular crystal lattice may offer a more rapid convergence and a more realistic model for the transport characteristics of such systems.

9.5: Directions for Future Efforts

For both the analytical and the numerical calculations, there are avenues for extending the research we have reported on in this dissertation. For the numerical Monte Carlo calculations of the conductance, critical slowing down will plague the analysis of very strongly disordered systems modeled with random resistor networks where adjacent resistances may vary by several orders of magnitude. By examing large systems containing at least on the order of 10^4 nodes, we have been able to reduce the importance of finite size effects and fluctuations due to random variations from specific disorder configurations which are muted byt not entirely suppressed by self-averaging.

The examination of larger systems will require the availability of more efficient algorithms, and one possibility are iterative calculations based on the conjugate gradient technique often used to solve systems of sparse matrices. In cases where critical slowing down due to percolation threshold effects is not a significant concern, the conjugate gradient calculations usually converge very rapidly, often in just a handful of iterations.

The effort to repair iterative methods for calculating the conductance of critical networks is an old problem that is rooted in a fundamental incompatibility between simple iterative methods and the percolation transition. Both the iterative scheme that we have used in the context of this thesis and more intricate methods have a common feature: these numerical approaches are local, in that each iteration only redistributes voltage values among nodes and nearest neighbors. On the other hand, a percolation transition involves correlation effects that span the entire system.

Local moves are best at responding to disturbances on a small scale, but are much less effective in the analysis of cooperative phenomena where global effects are at work. Global moves such as the Swendsen-Wang algorithm are used in a different context, the study of ferromagnetic phase transitions where local Monte Carlo moves also break down. The Swendsen-Wang technique is an excellent example of a global update technique that is efficiently implemented, and to a great extend resolves the problem of critical slowing down. At the heart of the Swendsen-Wang technique is an algorithm called the Hoshen-Kopelman method that is used to identify clusters of sites connected by intact bonds. The task, in the context of random resistor networks, then becomes a matter of finding a way to construct a counterpart to the Swendsen-Wang method that would be effective in mitigating critical slowing down in charge transport calculations.

Finally, we comment on the analytical calculations and consider how improving the accuracy of the numerical calculations is a relevant consideration. In fact, we envision that explicit numerical calculations and the theoretical analysis leading to a perturbative series will continue to operate in tandem. The availability of more accurate numerical data will provide an independent means for validating the closed form analytical results. In turn, a more powerful and higher order perturbative result will encourage the improvement of the numerical calculations.

There are a number of challenges involved in extending the analysis to higher order contributions. Salient among these, the number of terms to be considered will nominally grow expontially in the orderof the perturbation. As an example, at tenth order the number of terms to separately consider and calculate is at least 256. However, this number may overestimate the amount of effort that may be involved.

A judicious and prudent calculation would identify and combine together identical terms and thereby mitigate the effort involved at each order. Ultimately, the strongest hope would be to arrive at an analytical technique which would not grow exponentially with the order as is true of many types of perturbative calculations, but would instead scale as some polynomial in the order of the term. The latter prospect would allow a detailed interrogation of critical behavior on extremely high order series.

BIBLIOGRAPHY

[1] Haliday, D., Resnick, R., and Walker, J., *Fundamentals of Physics*, 7th Ed. Wiley (2004).

[2] Morita, T. and Horiguchi, T., *Journal of Mathemaitical Physics*, **12** (1971) 986.

[3] Atkinson, D. and Van Steenwijk, F.J., *Americal Journal of Physics*, **67** (1999) 486.

[4] Press, W.H., Teukolsky, S.A., and Vatterling, W.T., *Numerical Recipes 3rd Edition: The Art of Scientific Computing*. Cambridge University Press (2007).

[5] Seager, C.H. and Pike, G.E., *Phys. Rev. B*. **10** (1974) 1435.

[6] Miller, A. and Abrahams E., *Phys. Rev*. **120** (1960) 745.

[7] Risch, R. and Harris, A.B., *Phys. Rev. B*. **18** (1978) 416.

[8] Meir, Y., Aharony A., and Harris, A.B., *Phys. Rev. B*. **41** (1990) 9183.

[9] Adler, J., Aharony A., Blumenfeld, R., Harris, A.B., and Meir, Y., *Phys. Rev. B*. **47** (1993) 5770.

[10] Scerti, J., David, G., and Piróth, A., *American Journal of Physics*. **70** (2002) 153-159.

[11] Stauffer, D. and Ahrony, A., *Introduction to Percolation Theory, Revised 2nd Edition*. CRC Press (1994).

[12] Ambegaokar, V., Halperin, B.I., and Langer, J.S., *Phys. Rev. B*. **4** (1971) 2612.

VITA

Benjamin A. Walker was born in Kansas City, Missouri on September 23, 1980. He attended Truman High School in Independence Missouri, where he graduated in 1999. In 2004, he earned his B.S. in Computer Science from the University of Missouri-Kansas City. In 2008 he entered graduate school to obtain his M.S. in Physics.